The In Vivo Evaluation of Coronary Atheroma and Endothelium-Dependent Vasomotor Reactivity in Humans with Coronary Artery Disease: Studies Utilizing Intravascular Ultrasound

A thesis submitted by

Dr. Rishi Puri

M.B.,B.S., F.R.A.C.P.

For the degree of

Doctor of Philosophy

Discipline of Medicine

University of Adelaide

June 2014

TABLE OF CONTENTS

THESIS SUMMARY

Although many consider plaque burden and vasoconstriction as critical components of 'vulnerable' coronary atheroma, their intrinsic relationship *in vivo* remains relatively unexplored. This thesis, presented as a series of experiments conducted in intact humans with coronary artery disease, explores the fundamental *in vivo* relationships between coronary atheroma volume, composition and topography in relation to underlying segmental epicardial coronary endothelium-dependent vasomotor reactivity. The contributions of segmental wall shear stress (WSS), and the first-in-man assessment of left main coronary arterial endothelium-dependent vasomotor reactivity and its determinants, are also explored. A novel feature was the utility of intravascular ultrasound (IVUS) for all coronary structural and functional assessments. In these experiments, IVUS was pivotal in enabling the first-in-man validation of intracoronary salbutamol as a novel epicardial endothelium-dependent stimulus.

Of the 3 introductory chapters, chapters 1 and 2 outline the utility of IVUS for exploring coronary atherosclerosis and 'vulnerable' plaques. Chapter 3 draws specific attention to the nature of endothelium-dependent stimulus required to safely explore, with greater precision, the coronary structure-function relationship in humans *in vivo*.

Chapters 4-9 comprise the results sections of this thesis. Chapter 4 outlines the utility of 'provocation intravascular imaging' [IVUS-upon-Doppler Flowire imaging during simultaneous intracoronary (IC) infusions] to validate IC salbutamol as a novel endothelium-dependent epicardial coronary and microvascular stimulus.

Chapter 5 describes the coronary structure-function relationship in patients with stable, minimally diseased coronary arteries (i.e. the population studied in chapter 4) compared with patient with non ST-segment elevation myocardial infarction (NSTEMI). Irrespective of the nature of clinical presentation, the magnitude of segmental lumen vasoreactivity, controlled for by the degree of atheroma volume, did not differ. Our results also suggested possible interactions between systemic inflammation and coronary atheroma in mediating coronary vasomotor reactivity.

Utilizing a custom-built IVUS console to deliver radio-frequency IVUS signals, Chapter 6 outlines the relationship between plaque composition and segmental vasomotor reactivity in the NSTEMI population evaluated in chapter 5. Both the volumes of lipidic and necrotic core composition predicted vasoconstriction, whereas greater fibrotic plaque predicted vasodilatation.

Chapter 7 describes a unique investigation into *in vivo* relationships between segmental WSS, arterial remodeling and vasomotor function in paients with stable, minimally diseased coronaries (population studied in chapter 4). Independent of plaque burden, WSS directly related to vasomotor reactivity, and inversely to arterial remodeling. Regions of high plaque burden associated with lower WSS, expansive remodeling and greater plaque eccentricity, thus providing a novel link between these known individual features of plaque vulnerability.

Chapter 8 outlines the first-in-man description of left main coronary arterial (LMCA) vasomotor reactivity, in comparison to downstream epicardial segments. The study population comprised of all patients across study protocols who underwent left-

sided coronary imaging with evaluable matched LMCA images. LMCA and proximal epicardial segments were least reactive, compared to more distal conduit segments, which may relate to higher WSS in smaller caliber distal segments. These results may also explain the propensity for culprit plaques to cluster proximally in humans.

Chapter 9 describes a unique comparison of *in vivo* lumen dimensions measured with IVUS, Fourier-domain optical coherence tomography (FD-OCT) and 3D quantitative coronary angiography (3D-QCA). Lumen dimensions were greater with IVUS compared to FD-OCT and 3D-QCA, and were magnified within smaller coronary segments. We concluded that specific cut-off values validated with IVUS should not be arbitrarily translated into the OCT hemisphere for clinical decision making.

DECLARATION

Name: Rishi Puri Program: Doctor of Philosophy

I certify that this work contains no material which has been accepted for the award of any other degree or diploma in my name, in any university or other tertiary institution and, to the best of my knowledge and belief, contains no material previously published or written by another person, except where due reference has been made in the text. In addition, I certify that no part of this thesis will, in the future, be used in a submission in my name, for any other degree or diploma in any university or other tertiary institution without the prior approval of the University of Adelaide and where applicable, any partner institution responsible for the joint-award of this degree. I give consent to this copy of my thesis when deposited in the University Library, being made available for loan and photocopying, subject to the provisions of the Copyright Act 1968. The author acknowledges that copyright of published works contained within this thesis resides with the copyright holder(s) of those works. I also give permission for the digital version of my thesis to be made available on the web, via the University's digital research repository, the Library catalogue, and also through web search engines, unless permission has been granted by the University to restrict access for a period of time.

Signature: Date: 3rd Dec 2013

ACKNOWLEDGEMENTS

Seduced by the field of Interventional Cardiology during my first year of Cardiology training, the concept of undertaking PhD research was the farthest thing from my mind. Following a few months involving countless discussions with numerous colleagues, mentors and family, I eventually embraced the concept of a PhD program. Little did I realize the enormous future impact this would make on my life, both professionally, and personally.

A fundamental reason for the success of my PhD program has been the superb nature and quality of academic mentorship that I have received during this time. Associate Professor Matthew Worthley and Professor Stephen Worthley were instrumental in guiding me along this career path. Each had a genuine vision for my academic development and for eventual transition back to the cath lab as a well-trained academic Interventional Cardiologist. I especially want to single out Matthew Worthley, who not only conceptualized the general topic of my PhD, but has been there for me on a night and day basis, throughout this entire PhD journey and beyond. I wish that all PhD students would be so lucky as to experience the caliber and nature of supervisor that is Matt! Matt was also instrumental in fostering an early collaboration with Professor Stephen Nicholls, who at the time, directed the IVUS Core Laboratory and co-directed clinical research at the Cleveland Clinic Coordinating Center for Clinical Research. It was indeed Matt's vision for me to complete a hybrid PhD and Post-Doctoral Fellowship program between the University of Adelaide, and the Cleveland Clinic. This key collaboration with Steve Nicholls and other senior academic

cardiologists here at the Cleveland Clinic (most notably Professors Steven E. Nissen, E. Murat Tuzcu and Samir R. Kapadia) has been fundamental in enabling me to thrive here in Cleveland as a post-doctoral Fellow. I am truly grateful to each of these named individuals for their mentorship over the last two-and-a-half years here in Cleveland. In particular, the mentorship, friendship, and ongoing guidance of Stephen Nicholls and his family has been truly special, and one that I will continue to cherish for many years to come.

My PhD journey has enabled me to collaborate with many exceptional individuals both in Adelaide and in Cleveland. I would particularly like to thank Professor John Beltrame for his additional PhD supervision, Dr Gary Liew, Dr Adam Nelson, Mr Angelo Carbone, Mrs Barbara Copus (and all nursing staff of the Cardiovascular Investigation Unit, Royal Adelaide Hospital), Dr Dennis Wong, Dr Darryl Leong, Mr Claudio LaPosta (and Radiography staff at the Cardiovascular Investigation Unit, Royal Adelaide Hospital), and all of the staff Interventional Cardiologists of the Cardiovascular Investigation Unit, Royal Adelaide Hospital. In Cleveland, I have been honored to work with the likes of Mrs Kathy Wolski, Mrs Danielle Brennan and Mr Craig Balog from the C5R statistical team, Ms Jordan Andrews, Mrs Karilane King, Mr William Magyar and Mr Tim Crowe from the IVUS Core Laboratory, and Mrs Suzanne Turner, Mrs Mary Ann Citraro and Ms Charlene Surace from the graphics team who've all offered their kind support at various times.

I am who I am, and what I am, because of my parents, Vinod and Veena, and my sister Richa. Their undivided love and support has strengthened me enormously, and

whatever success I achieve in life has largely been due to the sacrifices my parents have made to provide my sister and me with a better opportunity to succeed than they ever had.

And last but not least, I wanted to thank all of the patients who participated in these research studies. Throughout this journey in research, I have never forgotten the kindness and co-operation of patients that consent for clinical research protocols. All of the findings listed in this thesis, their clinical and scientific implications, and the personal accolades I attained from publishing such data, are because of them!

PUBLICATIONS ARISING FROM THIS THESIS

1. Puri R, Worthley MI, Nicholls SJ: Intravascular Imaging of Vulnerable Coronary Plaque: Current and Future Concepts. Nat Rev Cardiol. 2011;8:131-9

2. Puri R, Liew GY, Nicholls SJ, Nelson AJ, Leong DP, Carbone A, Copus B, Wong DTL, Beltrame JF, Worthley SG, Worthley MI: Coronary β_2-adrenoreceptors Mediate Endothelium-Dependent Vasoreactivity in Humans: Novel Mechanistic Insights from an In Vivo Intravascular Ultrasound Study. Eur Heart J. 2012;33(4):495-504

3. Puri R, Nelson AJ, Liew GY, Nicholls SJ, Carbone A, Wong DTL, Harvey JE, Uno K, Copus B, Leong DP, Beltrame JF, Worthley SG, Worthley MI: Variations In Human Coronary Lumen Dimensions Measured *In Vivo*. J Am Coll Cardiol Cardiovasc Imaging. 2012;5(1):123-24

4. Puri R, Tuzcu EM, Nissen SE, Nicholls SJ. Exploring Coronary Atherosclerosis with Intravascular Imaging. Int J Cardiol. 2013;168(2):670-9

5. Puri R, Leong DP, Nicholls SJ, Liew GY, Nelson AJ, Carbone A, Copus B, Wong DT, Beltrame, Worthley SG, Worthley MI. Coronary Artery Wall Shear Stress Is Associated with Endothelial Dysfunction and Expansive Arterial Remodeling In Patients with Coronary Artery Disease. EuroIntervention. 2014 [Epub ahead of print Jan 15]

6. Puri R, Nicholls SJ, Nissen SE, Brennan DM, Andrews J, Liew GY, Nelson AJ, Carbone A, Copus B, Tuzcu EM, Beltrame JF, Worthley SG, Worthley MI. Coronary Endothelium-Dependent Vasoreactivity an Atheroma Volume in Subjects with Stable, Minimal Angiographic Disease versus Non-ST Segment Elevation Myocardial Infarction: An Intravascular Ultrasound Study. Circ Cardiovasc Imaging. 2013;6(5):674-82

7. Puri R, Nicholls SJ, Brennan DB, Andrews J, King KL, Liew GY, Carbone A, Copus B, Nelson AJ, Kapadia SR, Tuzcu EM, Beltrame JF, Worthley SG, Worthley MI. Left main Coronary Arterial Endothelial Function and Heterogeneous Segmental Epicardial Vasomotor Reactivity In Vivo: Insights from Intravascular Ultrasonography. Eur Heart J Cardiovasc Imaging. 2014 [Accepted In Press]

8. Puri R, Nicholls SJ, Brennan DB, Andrews J, Liew GY, Carbone A, Copus B, Nelson AJ, Kapadia SR, Tuzcu EM, Beltrame JF, Worthley SG, Worthley MI. Coronary Atheroma Composition and its Association with Segmental Endothelial Dysfunction in Non-ST Segment Elevation Myocardial Infarction: Novel Insights with Radiofrequency (iMAP) Intravascular Ultrasonography. Int J Cardiol. 2014 [Accepted In Press]

ABSTRACTS ARISING FROM THIS THESIS

1. Puri R, Liew G, Nelson AJ, Das R, Carbone AJ, Copus B, Nicholls SJ, Beltrame J, Worthley SG, Worthley MI: Comparison of intravascular ultrasound assessment of segmental coronary vasomotor responses with quantitative coronary angiography. Heart, Lung and Circulation. 20010;19(suppl 2):s53

2. Puri R, Liew GYH, Nicholls SJ, Nelson AJ, Carbone A, Copus B, Wong DTL, Anderson TJ, Beltrame JF, Worthley SG, Worthley MI. Intracoronary Salbutamol is a Novel Endothelium-Dependent Coronary Vasodilator – Mechanistic Insights From an in vivo Intravascular Ultrasound (IVUS) Study. Circulation. 2010;122:A14843

3. Puri R, Liew GY, Nicholls SJ, Nelson AJ, Leong DP, Carbone A, Copus B, Wong DT, Beltrame JF, Worthley SG, Worthley MI. Intracoronary Salbutamol, Segmental Plaque Burden and Focal Coronary Endothelial Function: Novel Mechanistic Insights from an In Vivo Intravascular Ultrasound Study. J Am Coll Cardiol. 2011;57(14, Supplement A):0410-08,133

4. Puri R, Nelson AJ, Liew GY, Nicholls SJ, Carbone A, Wong DT, Copus B, Leong DP, Beltrame JF, Worthley SG, Worthley MI. Variations in Coronary Lumen Dimensions Measured In Vivo: Quantitative Comparisons Between Intravascular Ultrasound, Fourier Domain Optical Coherence Tomography and Three Dimensional Quantitative Coronary Angiography. Heart Lung and Circulation. 2011;20S:S155.

5. Puri R, Nicholls S, Liew G, Brennan D, Andrews J, Nelson A, Carbone A, Copus B, Kapadia S, Tuzcu EM, Beltrame J, Worthley S, Worthley M. Comparison of Endothelial Function In the Left Main Coronary Artery and Epicardial Arterial Segments. J Am Coll Cardiol 2012:60(17):TCT-226

6. Puri R, Leong D, Nicholls S, Liew G, Nelson A, Carbone A, Copus B, Wong D, Beltrame J, Worthley S, Worthley M. Low Coronary Arterial Wall Shear Stress Is Associated with Endothelial Dysfunction and Expansive Arterial Remodeling In Vivo: Implications for Plaque Vulnerability. Heart, Lung and Circulation 2012;21:S43

7. Puri R, Nicholls SJ, Brennan DB, Andrews J, Liew G, Carbone A, Copus B, Nelson AJ, Kapadia SR, Tuzcu EM, Beltrame JF, Worthley SG, Worthley MI. Coronary Atheroma Composition Predicts Endothelial Dysfunction in Non-ST Segment Elevation Myocardial Infarction: Novel Insights with Radiofrequency (iMAP) Intravascular Ultrasonography. J Am Coll Cardiol. 2013;62(18_S1);B197-B197

PRIZES AWARDED FROM THIS THESIS

1. FINALIST (and 2nd place) Young Investigator Awards Competition, American College of Cardiology Annual Scientific Sessions, New Orleans, Louisiana, USA, April 2011

2. Cardiac Society of Australia & New Zealand Travelling Fellowship (American College of Cardiology Meeting, New Orleans, Louisiana, USA), April 2011

3. National Heart Foundation of Australia Overseas Travelling Fellowship (American College of Cardiology, New Orleans, Louisiana, USA), April 2011

4. Cardiac Society of Australia & New Zealand Travelling Fellowship (American Heart Association Meeting, Chicago, Illinois, USA), November 2010

5. 1st Prize (Best Poster Prize), Pfizer Cardiovascular Lipid Annual Symposium, July 2010

CHAPTER 1: EXPLORING CORONARY ATHEROSCLEROSIS WITH INTRAVASCULAR IMAGING

Adapted from PURI, R., TUZCU, E.M., NISSEN S.E., NICHOLLS, S.J. 2013. Exploring coronary atherosclerosis with intravascular imaging. *Int J Cardiol*. 168(2):670-9

Key words

Imaging; coronary artery disease; atherosclerosis; risk factors; allograft vasculopathy; neointimal hyperplasia

Abbreviations and acronyms

PROSPECT: Providing regional observations to study predictors of events in the coronary tree

IBIS: Integrated biomarker and imaging study

PREDICTION: Prediction of progression of coronary artery disease using vascular profiling of shear stress and wall morphology

MAIN-COMPARE: Revascularization for Unprotected Left Main Coronary Artery Stenosis: Comparison of Percutaneous Coronary Angioplasty vs. Surgical Revascularization

ABSTRACT

Coronary angiography has been widely used for five decades to evaluate a range of vascular pathologies and triage patients to therapeutic interventions. The inability to directly visualize the artery wall with conventional angiographic techniques has stimulated development of a number of intravascular imaging modalities. These approaches have the potential to provide a more comprehensive characterization of the burden, composition and functionality of atherosclerotic plaque, neointimal hyperplasia and allograft vasculopathy that develops within coronary arteries. The ability to use these modalities *in vivo* and in a serial fashion has provided a greater insight into the factors that underlie the disease process and guide therapeutic interventions.

Introduction

Coronary artery disease remains the leading cause of morbidity and mortality in the Western world (Roger et al., 2012). While public health initiatives focus on the need for disease prevention, many patients present to catheterization laboratories for evaluation of their coronary arteries as part of the diagnostic evaluation of their symptoms. Coronary angiography has been widely used in clinical practice for five decades, by virtue of its ability to detect and quantify obstructive disease. During this time however, it has been recognized that angiography, which visualizes the lumen, does not directly image the vessel wall, the site at which disease accumulates. As a result, there has been considerable effort to develop a range of intravascular modalities that image the arterial wall and potentially provide a more comprehensive characterization of the extent, composition and functionality of disease. Accordingly, intravascular imaging-based clinical trials are providing unique opportunities to assess the efficacy and mechanisms of novel anti-atherosclerotic therapies, prior to establishing clinical efficacy. As such, these modalities are increasingly being utilized in the drug development process. The development of these modalities and their implications for the clinical management of patients will be reviewed.

Coronary angiography

Increasing recognition that obstruction to myocardial blood flow underlies the majority of symptomatic episodes of myocardial ischemia stimulated the development of approaches to identify stenotic lesions within the epicardial coronary tree, and it remains fundamental for clinical decision making in patients with symptomatic

coronary artery disease. Coronary angiography has provided important insights into the temporal behavior of complex coronary lesions identified during acute infarct angioplasty (Goldstein et al., 2000). Clinical trials that employed serial quantitative coronary angiography demonstrated that medical therapies targeting major cardiovascular risk factors slowed the progression of obstructive disease (Ballantyne, 1998). The clinical implications of these findings were based on observations that these therapies also reduce clinical event rates in outcome trials and that earlier studies demonstrated a direct association between the overall burden of angiographic disease and adverse cardiovascular outcomes (1983).

Subsequent studies, however, demonstrated that the relationship between the severity of angiographic disease at focal sites and development of acute ischemic syndromes is limited, with most cases of acute myocardial infarction attributed to culprit lesions that are only mild to moderately stenotic (Falk et al., 1995, Naghavi et al., 2003). These observations fueled increasing interest in the importance of plaque composition, rather than burden, in the pathogenesis of acute ischemic syndromes. At the same time it was also recognized that angiography provides a suboptimal characterization of the full extent of atherosclerotic plaque. Angiography generates a two-dimensional silhouette of the arterial lumen and does not image the vessel wall. As a result, it demonstrates lumen stenoses, a complication of advanced atherosclerosis, as opposed to directly visualizing the entire burden of atherosclerotic plaque with wall-based imaging modalities (Topol and Nissen, 1995).

Further advances have sought to generate three-dimensional (3D) quantitative coronary angiographic (QCA) reconstruction, using images from at least two orthogonal two-dimensional angiographic views. An immediate clinical application lies in the ability to more accurately image coronary bifurcations in order to optimize procedural strategy. Tu et al. have recently shown the utility of (3D) QCA to display the optimal viewing angle of coronary bifurcations which are often not attainable due to the mechanical constraints of current X-Ray viewing systems (Tu et al., 2012). Some investigators have reported on the utility of 3DQCA measurements of coronary bifurcations angles prior to coronary stenting to predict changes in bifurcation geometry, whereby a decrease in bifurcation angle post-stenting was shown to associate with less favorable clinical outcomes (Hassoon et al., 2011). Other than the evaluation of complex, bifurcating coronary anatomy, 3D QCA creates the angiographic backbone for the undertaking of advanced computational fluid dynamics processing for evaluation of *in vivo* coronary arterial wall shear stress patterns.

Gray-scale intravascular ultrasonography

Intravascular ultrasound (IVUS) is a high-frequency imaging modality that generates high-resolution, cross-sectional, topographic images of the vascular lumen and vessel wall. Early enthusiasm for the use of IVUS was based on its ability to facilitate percutaneous coronary interventions and understanding the responses within the vessel wall (Mintz et al., 1994). Subsequent studies affirmed the role of IVUS in the guidance of optimal stent deployment in a manner to improve procedural and longer-term clinical outcomes (Roy et al., 2008, Claessen et al., 2011). The early experience of IVUS in the setting of PCI enabled use of more aggressive approaches to management of obstructive

lesions within the coronary vasculature. Colombo et al. were the first to show that IVUS-guided PCI enabled the interventionalist to achieve adequate stent expansion, which obviated the need for systemic anticoagulation to limit stent thrombosis rates (Colombo et al., 1995). This landmark IVUS study paved the way for antiplatelet therapies to become the standard of care following PCI and stent implantation. Serial imaging with IVUS has been widely used to evaluate novel intracoronary devices (Serruys et al., 2009). Ultrasonic imaging within the coronaries has also been of utility to the interventional cardiologist for the evaluation of ambiguous lesions on angiography, particularly those within the left main coronary artery. As a result, IVUS has been adopted within many cardiac catheterization laboratories for the evaluation and management of patients with coronary artery disease.

In parallel to its role in facilitating coronary interventions, IVUS has provided a unique insight into the natural history of atherosclerotic disease. Early studies confirmed autopsy observations of the diffuse and extensive distribution of atherosclerotic plaque, even in regions that appear normal on angiography (Mintz et al., 1995) (Figure 1). This discordance between lumen and wall based imaging approaches reflects the degree of arterial wall remodeling that occurs in association with accumulation of atherosclerotic plaque. Intravascular ultrasound studies have demonstrated a typical pattern of vascular expansion, followed by constriction in association with plaque deposition. The remodeling pattern may be an important factor in determining the clinical expression of a lesion, with expansive remodeling more commonly encountered in culprit lesions of patients with acute coronary syndromes (Smits et al., 1999, Varnava et al., 2002, Schoenhagen et al., 2000); associated with

higher circulating matrix metalloproteinase levels (Schoenhagen et al., 2002). Observations of multiple sites of plaque rupture in patients with acute coronary syndromes further supports the concept of pan-coronary arterial instability (Rioufol et al., 2002, Hong et al., 2004, Maehara et al., 2002), highlighting the systemic nature of the disease process.

The ability to generate images continuously during catheter withdrawal permits quantification of atherosclerotic plaque burden in anatomically matched arterial segments. As a result, serial IVUS imaging has been integrated into a number of clinical trials that have evaluated the impact of medical therapies upon progression of coronary atherosclerosis. These studies have emphasized the importance of modifying established cardiovascular risk factors in slowing disease progression. Early statin studies have demonstrated the benefits of more intensive LDL-C lowering, with evidence of regression at levels below 70 mg/dL (Nissen et al., 2006a, Nissen et al., 2004b, Okazaki et al., 2004) (Figure 2). Most recently, administration of high dose therapy with atorvastatin or rosuvastatin was demonstrated to produce disease regression (Nicholls et al., 2011). However, the finding that 20% of patients achieving very low LDL-C levels continue to progress is largely due to the presence of other uncontrolled risk factors (Bayturan et al., 2010), highlighting the multifactorial nature of atherosclerotic disease.

Serial IVUS studies have been pivotal in enabling a greater understanding the complexity of HDL-targeted therapies. A potential role for HDL-targeted therapies is supported by observations that modest elevations of HDL-C associate with the ability of statins to slow disease progression (Nicholls et al., 2007b), and that infusing lipid-

deplete forms of HDL promote rapid plaque regression (Nissen et al., 2003, Tardif et al., 2007, Waksman et al., 2010). Lowering blood pressure to levels beyond the pre-hypertensive range is associated with less disease progression (Nissen et al., 2004a), although its impact on clinical events remains to be elucidated. Favorable effects of LDL-C lowering and the multiple metabolic benefits of pioglitazone have been demonstrated in patients with type 2 diabetes (Nissen et al., 2008), a cohort with accelerated disease progression and adverse arterial wall remodeling on serial coronary IVUS imaging (Nicholls et al., 2008). A beneficial impact on emerging risk factors, with evidence of potential anti-inflammatory effects of statins correlating with slowing of disease progression (Nissen et al., 2005), highlights the potential impact of additional therapeutic targets for novel anti-atherosclerotic therapies.

Serial IVUS imaging has been integrated into the early stages of clinical development of new therapies, demonstrating the lack of benefit or potential adverse effects of ACAT inhibitors (Nissen et al., 2006b, Tardif et al., 2004), and the CETP inhibitor, torcetrapib (Nissen et al., 2007). Further analysis of these studies may provide additional mechanistic insights that may be of use in developing other agents. Subsequent analysis of torcetrapib treated patients demonstrated disease regression in those achieving the highest HDL-C levels, consistent with the ongoing ability to mobilize lipid from the vessel wall and supporting intact HDL functionality in CETP inhibitor treated patients (Nicholls SJ, 2007). When combined with evidence that torcetrapib possesses off-target toxicities, there remains hope that alternative CETP inhibitors may be of potential clinical benefit. Accordingly, early findings from these imaging studies may be of utility in determining whether to proceed with more

advanced form of clinical evaluation of these therapies. The clinical implications of these findings are based on observations of a direct association between both disease burden and progression with adverse cardiovascular events (Nicholls et al., 2010, von Birgelen et al., 2003). Ultimately, whether a new agent comes to clinical practice will continue to be determined by its proven efficacy and safety in large outcome trials. As such, IVUS is therefore likely to play an ongoing role in evaluating the mechanistic efficacy of novel anti-atherosclerotic drug platforms, with data obtainable in advance of larger clinical endpoint trials.

Intravascular ultrasound has provided important insights into the pathogenesis and modulation of cardiac allograft vasculopathy, the single greatest determinant of allograft failure and mortality in heart transplant recipients. In parallel, serial IVUS imaging has been employed to assess the progression of cardiac allograft vasculopathy (Kapadia et al., 1999). Everolimus-based immunosuppressive therapy following cardiac transplantation has been demonstrated to have a beneficial impact upon the rate of progression of coronary intimal thickening in cardiac allograft recipients (Eisen et al., 2003). This was associated with fewer episodes of rejection and the need for repeat transplantation when compared to the previous standard azathioprine-based immunosuppressive regimen. The clinical implications of these findings are further supported by observations that the rate of intimal thickening seen on IVUS at the 1 year mark following cardiac transplantation predicts 5 year mortality rates (Kobashigawa et al., 2005).

Ultrasonic radiofrequency analysis

In contrast to its ability to measure disease burden, conventional IVUS imaging is limited in its ability to reliably characterize plaque composition, beyond attempts to measure plaque echogenicity (Schartl et al., 2001, Tardif et al., 2007). More comprehensive analysis of reflected IVUS signals has the potential to provide a more detailed evaluation of plaque. Grey-scale IVUS images are formed only by the envelope (amplitude) of the radiofrequency (RF) backscatter signal. Autoregressive spectral analysis of generated IVUS RF backscatter data has facilitated the image interpretation of different tissue components. This algorithm generates tissue-color maps that classify plaque into fibrous, fibro-fatty, necrotic and calcific components (Figure 3), with a high degree of correlation and predictive accuracies with *ex-vivo* histological findings in some reports (Nair et al., 2001, Nair et al., 2002, Nair et al., 2007), while others have reported variable associations (Thim et al., 2010). Alternative algorithms have been developed that analyze the average power of the RF backscatter signal to generate tissue color maps (Kawasaki et al., 2001), or use a spectral similarity algorithm (Sathyanarayana et al., 2009).

In addition to reporting individual plaque components as a percentage of total plaque burden, radiofrequency analysis can also classify plaques by phenotype, ranging from pathological intimal thickening through to IVUS-derived thin-cap fibroatheroma (IDTCFA), based on correlation with *ex vivo* histological analysis (Rodriguez-Granillo et al., 2005). Due to the resolution limitations to detect a thin fibrous cap (of ≤65 μm thickness), an IDTCFA has been formally defined as a lesion containing a necrotic core of ≥10% without obvious overlying fibrous tissue and a total plaque burden ≥40% in

three consecutive images (Figure 3b) (Rodriguez-Granillo et al., 2005). Numerous investigators have reported a greater prevalence of IDTCFA or necrotic core volume in patients with multiple cardiovascular risk factors, diabetes or acute coronary syndromes. The PROSPECT study performed a comprehensive ultrasonic and radiofrequency analysis of lesions throughout the coronary vasculature in patients who underwent PCI after an acute coronary syndrome. Plaque sub-typing demonstrated that 22% of lesions were classified as an IDTCFA. The major imaging predictors of subsequent cardiovascular events during the next 3.4 years included plaque burden, lumen size and the presence of an IDTCFA (Stone et al., 2011). The implications of these findings remain uncertain, given that the definition of an IDTCFA includes the presence of a large atherosclerotic plaque. Accordingly, it remains to be elucidated whether radiofrequency analysis of atherosclerotic lesions provides independent information beyond that obtained from angiographic and ultrasonic evaluation of the coronary arteries. Furthermore, there is currently no evidence to suggest that radiofrequency analysis of atherosclerotic plaque be utilized for clinical decision making.

Given the importance of plaque composition in determining its propensity to rupture and promoting acute ischemic events, there is increasing interest in the ability to evaluate changes in plaque composition in response to novel anti-atherosclerotic therapies. The combination of increasing data from clinical trials with acquisition at the time of conventional ultrasonic imaging has permitted radiofrequency analysis in small clinical trials of medical therapies. The IBIS-2 trial reported that administration of the lipoprotein-associated phospholipase A_2 inhibitor, darapladib, had no impact on plaque burden but attenuated accumulation of necrotic tissue (Serruys et al., 2008). The

potential impact of these findings is currently being evaluated in large clinical outcome trials of this agent (O'Donoghue et al., 2011, 2011c). The effect of open-labeled treatment with rosuvastatin is currently being assessed in the IBIS-3 trial (2011a). Given that high-dose rosuvastatin promotes plaque regression (Nicholls et al., 2011), it will be of interest to observe whether this is accompanied by favorable changes in plaque composition.

A number of caveats however, provide potential limitations to the use of radiofrequency analysis in the evaluation of new therapies. Gating acquisition of images according to the R-wave of the ECG signal introduces the potential for heart-rate variability at different time points to limit precise matching. This is further complicated by the observation that many IDTCFAs spontaneously resolve upon follow-up evaluation (Kubo et al., 2010b), limiting potential interpretation of serial changes with new therapies. Analysis artifacts, particularly in regions surrounding calcific deposits, and classification of thrombus, provide further potential pitfalls that contribute to the reports by some investigators of limited correlation between radiofrequency and histology findings in animal models of atherosclerosis (Thim et al., 2010). Despite these limitations, the technique is based on a fundamental observation that all tissues emit radiofrequency signals and that composition patterns should be quantifiable. Accordingly, with ongoing validation, it is possible that this technique may be of potential utility for the development of new therapies and guidance of percutaneous coronary interventions in the catheterization laboratory. As a result, ongoing clinical research of this tool should be undertaken.

Intravascular imaging, in particular IVUS, currently accompanies approximately 10% of all coronary interventions undertaken in the United States (Riley et al., 2011). The uptake of adjunctive intracoronary imaging in mainstream clinical practice has been tempered by increased procedural times, the need for operational expertise, added costs to the invasive procedure coupled with a lack of physician reimbursement from health insurance bodies. This occurs despite the known clinical benefits of IVUS-guided percutaneous coronary interventions (Roy et al., 2008, Claessen et al., 2011). More recently, a meta-analysis of data involving 1 randomized trial and 10 registries found that IVUS-guided drug-eluting stent implantation was associated with a significant reduction in the hard clinical endpoint of death, the combined endpoint of major adverse cardiovascular events, and stent thrombosis, compared with angiography-guidance (Zhang et al., 2012). The net benefit of an IVUS-guided approach became apparent when a more complex 2-stent strategy is employed for intervening for bifurcation stenoses. Chen et al. recently demonstrated the clinical superiority of IVUS-guided drug-eluting stenting, compared to angiography-guided drug-eluting stenting, in 628 patients undergoing a 2-stent strategy for bifurcation stenoses (Chen et al., 2012c). At 12 months, and after propensity matching, stent thrombosis and ST-segment elevation myocardial infarction were lower in the IVUS-guided group. Similar benefits were noted in a larger Korean multicenter bifurcation registry (Kim et al., 2011).

We have recently reviewed and presented the rationale for the liberal use of IVUS during the assessment of left main coronary disease, and for the performance and optimization of left main coronary stenting (Puri et al., 2012a). The most comprehensive evidence of the clinical benefit of IVUS-guided left main coronary

stenting stems from the MAIN-COMPARE registry (Park et al., 2009). Despite the known caveats of interpreting non-randomized data, out of 975 patients involved in this registry, 201 pairs of patients were propensity matched to show that the 3-year Kaplan-Meier incidence of mortality was significantly lower in the group receiving IVUS-guided drug-eluting stents compared to the angiography-guided group (4.7% vs. 16%, p=0.048). The recommended approach is to use IVUS to achieve a minimum stent area of >8.5mm^2 for the main branch, and >5.5mm^2 for the origins of each daughter branch, in order to minimize restenosis rates (Kim et al., 2006, Leon, February 14-16, 2011, Puri et al., 2012a).

Clinical risks associated with routine intravascular imaging are believed to be modest, with a 2.9% risk of coronary spasm being the most commonly encountered adverse event (Hausmann et al., 1995). More serious events (vessel dissection, myocardial infarction) have been reported in patients presenting with unstable coronary syndromes. In the PROSPECT study, routine 3-vessel IVUS resulted in a 1.6% complication rate, including a 0.4% rate of non-fatal myocardial infarction (Stone et al., 2011). From an economic standpoint, there is a paucity of data on the cost-effectiveness of embarking upon an IVUS-guided strategy for percutaneous coronary intervention. Aside from time-constraints, many practitioners still feel that the additional expense of an IVUS catheter during coronary intervention may outweigh the clinical benefits of such a strategy. Mueller et al. undertook a cost-effectiveness analysis of (provisional) IVUS-guided coronary stenting, by evaluating 269 consecutive patients who were randomly assigned to receive an angiography only versus IVUS-guided approach (Mueller et al., 2003). Although the rate of coronary stenting was equal in both

treatment groups, the 2 year event free survival in the IVUS-guided group was significantly lower than the angiography-only group (p=0.04). While immediate in-hospital costs were higher for IVUS, during the 2 years of clinical follow-up, cardiac hospitalizations were lower in the IVUS-group, resulting in no net difference in total costs. An IVUS-guided approach appeared more economical in 55% of bootstrapping simulations. Analogous to the demonstrable cost-effectiveness of a physiological-guided approach for managing obstructive multi-vessel coronary artery disease (Fearon et al., 2010), further studies with IVUS, involving current generation drug-eluting stents and contemporary pharmacotherapy's, will be needed to ascertain the true cost effectiveness of IVUS-guided coronary intervention.

Optical coherence tomography

Optical coherence tomography (OCT) processes backscattered reflections of light to generate axial topographic images. Low coherence interferometry generates real-time, two-dimensional, high resolution (10-20 μm) images. This major advance in resolution permits imaging of microstructures including fibrous cap thickness, neo-adventitial vessels (Moreno et al., 2006, Vorpahl et al., 2010), macrophages (Tearney et al., 2003), and endothelial coverage of stent struts (Prati et al., 2010) (Figure 6). In addition, OCT is able to accurately depict the thickness of superficial calcium deposits, superior to IVUS, assisting the coronary interventionalist in deciding on the most appropriate strategy for lesion preparation prior to stent insertion. However, greater imaging resolution comes at the expense of much poorer penetration through blood and tissue. Therefore, deeper arterial structures other than those based at the lumen-intima (or lumen-plaque) interface are much less well visualized, therefore limiting the ability of

OCT to evaluate larger caliber coronary arteries and the true extent of the plaque volume within the vessel wall in all patients. In addition, the technique of OCT imaging makes it difficult to image lesions at the ostia of the right or left coronary systems. Given its ability to image superficial elements with high resolution, OCT has been primarily used in the clinical setting to evaluate dissections, stent apposition, endothelialization and subsequent development of neointimal hyperplasia in patients undergoing PCI (Finn et al., 2007, Sawada et al., 2008). OCT has been integrated into an increasing number of clinical trials that evaluate novel devices (Serruys et al., 2009, Barlis et al., 2010).

First-generation time-domain OCT (TD-OCT) required balloon occlusion proximal to the target segment of interest, in order to displace blood from the lumen during image acquisition. TD-OCT utilizes a broadband light source and performs multiple scanning of the reference delay distance, directly measuring the amplitude of the electrical field (Ferrante et al., 2013). Slower pullback speeds and subsequent longer imaging times could however result in the triggering of transient myocardial ischemia and electrocardiographic changes during imaging (Prati et al., 2007). Recent technological advancements resulted in the development of Fourier domain (FD) OCT, which uses a monochromatic laser of variable wavelength over time, a constant reference delay distance, and computation of the electrical field amplitude through Fourier transformation undertaken simultaneously at all detectable depths. Image acquisition speeds 15-50 times faster than TD-OCT, wider fields of view, improved lateral resolution, without the need for balloon occlusion, has resulted in the widespread uptake of this latest generation of OCT imaging. Different names have been given this

more recent OCT technology, however optical frequency domain imaging (OFDI) is the commonest term and type of OCT imaging now utilized in interventional cardiology.

Enhanced near-field resolution with OCT imaging has the potential to permit characterization of features of plaque vulnerability. Early reports demonstrate a greater rate of detection of plaque rupture and thrombus (Kubo et al., 2007), in association with thin fibrous caps (≤65 μm) (Jang et al., 2005) in patients with ACS compared with patients with stable angina pectoris. Further attempts to classify plaque composition have yielded conflicting results (Kawasaki et al., 2006, Manfrini et al., 2006). In addition to variable tissue penetrance, OCT characterization of lipid-rich pools, macrophage deposits and fibrous cap thickness remains subjective, with need for further validation and standardization of definitions (van Soest et al., 2011, Radu and Falk, 2012). This will be of particular importance if serial OCT is going to be integrated into evaluation of novel anti-atherosclerotic therapies. While early reports suggest that statin therapy might result in greater fibrous cap thickness (Takarada et al., 2009), it is unknown whether relatively small changes will be reliably detected, even with better imaging resolution.

More advanced image processing from OFDI has enabled the 3D reconstruction of stented coronary bifurcations. This has allowed investigators to accurately assess the extent of apposition and performance of stents within side branches (Okamura et al., 2010), as means to evaluate mechanisms behind the occurrence of focal restenosis in coronary bifurcation stenting (Foin et al., 2011). Perhaps the most pertinent role and future for OCT is its superior ability to assess the vascular response of following stent

implantation. There are now more than 30 studies that utilized OCT to assess the performance of coronary stents. In particular, OCT has been useful in demonstrating the unique vascular response and backscattering of bioabsorbable vascular scaffolds, with disappearance of one third of originally identified stent struts, otherwise difficult to discern with IVUS (Serruys et al., 2009). High image resolution has enabled the potential for the creation of new standards for reporting on the performance of novel coronary stents and scaffolds, including measuring strut apposition, strut coverage, neo-intimal tissue volumes, tissue characterization around stent struts, *in vivo* thrombosis and stent-healing. It is likely that OCT will become the standard imaging modality used to assess the performance of novel intravascular devices, and what is needed is the standardization of imaging analysis from which to objectively base our assessments.

At present, there appears limited evidence to suggest that the routine use of OCT during coronary stenting results in improved clinical outcomes. Despite the frequent finding of vessel injury following stent implantation, these observations were not found to be associated with clinical events during hospitalization (Gonzalo et al., 2009b). Moreover, a recent randomized study evaluated the results of 70 patients involved a cross-over design, whereby 35 patients who underwent OCT-guided coronary stenting had post-procedural stent expansion measured with IVUS, and those who underwent IVUS-guided coronary stenting had post-procedural stent expansion measured with FD-OCT (Habara et al., 2012). FD-OCT-guided coronary stent implantation resulted in significantly smaller stent expansion and more frequent significant reference segment stenosis compared with conventional IVUS-guided coronary stenting. A more recent case-control study did however demonstrate the first suggestive evidence of the clinical

benefit of an OCT-guided approach to coronary stent implantation in 335 patients (Prati et al., 2012). Whenever post-procedure OCT showed evidence of stent malapposition, dissection or under-expansion, corrective measures were performed, which usually involved iterative post-dilatation or additional stent implantation. Although there are several caveats to consider in the design and methods of this study (Räber and Radu, 2012), following the adjustment of baseline differences in clinical characteristics between the groups, there was a reported reduction in the primary endpoint of cardiac death or myocardial infarction, in favor of an OCT-guided approach compared with angiography alone. Much larger, randomized studies (including possibly an IVUS-guided stent arm) will be needed to either confirm or refute that superior imaging resolution of FD-OCT in the immediate post-procedural assessment of coronary stent implantation translates into clinical benefit.

Near-infrared spectroscopy

Photonic spectroscopy is based on the premise that molecules within biological tissue can absorb, scatter and emit light. The light–tissue interaction can be employed to determine chemical composition by analyzing the resulting light spectra. Near-infrared (NIR) spectroscopy utilizes near-infrared light (780–2,500 nm) to illuminate tissue. Given that various types of chemical bonds absorb light with differing wavelengths, a unique absorbance spectrum reflecting the chemical composition of the tissue is generated. The early clinical application has been based on the ability to detect and quantify lipid within atherosclerotic plaque (Cassis and Lodder, 1993, Gardner et al., 2008, Waxman et al., 2009) (Figure 5), although there is considerable potential to characterize other molecular components of plaque that increases its propensity to

rupture. Clinical studies are ongoing to evaluate the role of NIRS-guided utilization of an embolic protection device to prevent peri-procedural myocardial infarction in patients undergoing PCI, as well as the use of NIRS to determine changes in plaque lipid content with lipid-modifying therapies (Goldstein et al., 2011, 2011b, 2011a). Further studies will also be required to determine the relationship between plaque lipid and cardiovascular outcomes, beyond conventional risk factor scores and measures of plaque burden.

Endothelial shear stress

Endothelial shear stress (ESS) is thought to play an important role in atherosclerosis, with evidence that plaque typically originates in regions of low shear stress (Gibson et al., 1993). The fusion of IVUS and bi-plane coronary angiographic images with computational fluid dynamics and finite element analysis enables mapping of ESS patterns along the human coronary vasculature (Slager et al., 2000, Krams et al., 1997) (Figure 6). A recent study in humans has demonstrated that regions with low baseline ESS are more likely to develop ongoing accumulation of plaque and necrotic core, in association with constrictive remodeling on serial IVUS imaging (Samady et al., 2011). In the PREDICTION study, 506 Japanese patients undergoing percutaneous coronary intervention in the setting of hospitalization for an acute coronary syndrome underwent vascular profiling of an average of 2.7 vessels. Approximately three-quarters of patients underwent repeat imaging 6-10 months later, with nearly complete clinical follow-up of all patients over the next 12 months. The investigators reported that a greater plaque burden at baseline was associated with more disease progression and that both plaque burden and low ESS were associated with reductions in lumen dimensions. This

translated into these factors being associated with a greater likelihood for the need for coronary revascularization (Stone et al., 2012). It remains to be determined whether pre-emptive therapies (local and/or systemic) that favorably modulate local ESS patterns will alter the natural history of atherosclerosis progression and improve clinical outcomes. Investigators have already demonstrated the utility of assessing changes in localized WSS patterns following differing coronary bifurcation stenting techniques, in order to predict the incidence of in-stent restenosis (Chen et al., 2012a). Further studies in this area will shed more light on the predictive value of optimizing local WSS values to lower clinical event rates.

Thermography

The premise that vulnerable plaques possess a greater inflammatory component, potentially producing more heat within the vessel wall, compared with stable plaques, promoted interest in the measurement of catheter-based thermography (Madjid et al., 2006). Greater thermal heterogeneity, with a difference between plaque and normal vessel up to 1.5^{0}C, has been demonstrated in patients with acute coronary syndromes (Verheye et al., 2002, Verheye et al., 2004). The impact of circulating blood on the accuracy and reproducibility of measurements, potentially necessitating evaluation during interruption of blood flow has limited the uptake and development of this approach (Rzeszutko et al., 2006).

Angioscopy

Angioscopy involves direct visualization of luminal surface and endothelium, and has been largely used to characterize the color appearance of atherosclerotic plaque and

detection of thrombus. Yellow plaque on angioscopy is associated with greater lipid content (Ueda et al., 2004), and histological features of plaque vulnerability, whereas white plaques typically reflect a more fibrosed and stable lesion (Thieme et al., 1996, Takano et al., 2001b) (Figure 7). Serial angioscopic evaluation has demonstrated reductions in the appearance of yellow plaque in statin treated patients (Takano et al., 2003). More recently, angioscopy was used to compare neointimal coverage of sirolimus-eluting stents with or without a biodegradable polymer (Chen et al., 2012b), demonstrating that the presence of a biodegradable polymer improves neointimal coverage of stent struts, resulting in less plaque and thrombus. However the need to image in the absence of blood, coupled with the subjective nature of assessment has limited the use of angioscopy largely to the research setting.

Intravascular molecular imaging

Elucidation of the molecular factors involved in the formation, propagation and ultimate rupture of atherosclerotic plaque provides additional opportunities for arterial wall imaging. Administration of specific epitopes directed against specific factors within the atherosclerotic plaque represent potential targets for label-based approaches to imaging that provide additional information beyond anatomical characterization of size and broad composition. Such approaches can span from targeting the inflammatory pathways involved in the early formation of atherosclerotic plaque, through to factors involved in breakdown of the fibrous cap and thrombus formation. Accordingly, such molecular techniques permit a functional assessment of underlying disease. While there is considerable interest in molecular imaging of atherosclerosis using non-invasive techniques such as computed tomography, magnetic resonance and nuclear-based

modalities, several groups have investigated the ability to integrate molecular imaging with catheter based imaging, with good histological correlation in animal models (Hamilton et al., 2004).

Future directions and conclusions

Ongoing advances in intravascular imaging have enhanced the ability to characterize underlying vascular disease, beyond the traditional assessment of lumen obstruction. The ability to image from within the arterial lumen presents a considerable advantage in terms of resolution. Accordingly, a number of important insights have been made with regard to our understanding of the disease in patients, who have presented for a clinically indicated invasive procedure. While it is unlikely that these invasive approaches will have much utility in the asymptomatic patient, they are likely to play an important role in the ongoing validation of non-invasive imaging modalities. Ultimately, to what degree any of these novel invasive imaging approaches are used by the interventional cardiologist will be determined by clinical trials that demonstrate that their use modifies patient management and outcome. While the last three decades have witnessed considerable advances in our ability to visualize the disease process, the challenge moving forward remains how to determine the optimal way to use these modalities to improve patient care.

The authors of this manuscript have certified that they comply with the Principles of Ethical Publishing in the International Journal of Cardiology (Coats and Shewan, 2011).

Figure legends

Figure 1: Plaque burden on IVUS vs. angiography

A coronary angiogram showing minor atherosclerotic disease within the mid portion of the left circumflex artery. Inset shows the corresponding IVUS cross-sectional view highlighting significant plaque burden

Figure 2: The relationship between plaque regression and achieved LDL-C levels in clinical trials

Line of regression highlighting the on-treatment mean LDL-C vs. median change in atheroma volume. [**Adapted from: Nicholls SJ, Ballantyne CM, Barter PJ, et al. Effect of two intensive statin regimens on progression of coronary disease. The New England journal of medicine 2011;365:2078-87.]**

Figure 3: VH-IVUS definitions of plaque morphology

Plaque classification by VH-IVUS. (A) Pathological intimal thickening (B) Thin-capped fibroatheroma (VH-IVUS derived) (C) Thick-capped fibroathroma (D) Fibrotic plaque (E) Fibrocalcific plaque. [**Adapted from: Kubo T, Maehara A, Mintz GS, et al. The dynamic nature of coronary artery lesion morphology assessed by serial virtual histology intravascular ultrasound tissue characterization. J Am Coll Cardiol 2010;55:1590-7.]**

Figure 4: Insights from optical coherence tomography

OCT images of proposed markers of plaque vulnerability. (A) Thin-capped fibroatheroma, white arrows depicting narrowest portion of fibrous cap overlying a lipid-rich area of plaque (B) Macrophage density of a lipid rich plaque (LP). The * represents guide wire shadow artifact, and a 500 μm scale bar is shown. The darker areas represent macrophages [**Adapted from MacNeill BD, Jang IK, Bouma BE et al. JACC.**

2004 44(5):972-9]. (C) Neo-adventitial vessel, as depicted by white arrow. (D) Optical coherence tomography cross section corresponding to a patient treated with drug-eluting stent implantation during primary percutaneous coronary intervention in the right coronary artery for an inferior ST-segment elevation myocardial infarction 9 months before. The **red arrows** indicate incomplete stent apposition, whereas the white arrows show some struts not covered by tissue. From 12 to 5 an irregular material suggestive of organized thrombus can be observed behind the struts. *Guidewire artefact. **[Adapted from Gonzalo N, Barlis P, Serruys PW et al. JACC Cardiovasc Inter. 2009;2(5):445-52]**

Figure 5: Near-infrared spectroscopy

Near-infrared spectroscopy. Top row shows a chemogram (color scale identifies high probability of lipid as bright yellow, and lesser degrees of yellow towards orange identifying lower probability of lipid, with red corresponding to no detectable lipid) with corresponding co-registered longitudinal gray-scale IVUS pullback sequence immediately below. Depicted below this on the left, is a cross-sectional frame of a calcified plaque with signal drop-out, and no lipid (lack of yellow). In the centre, is a cross-sectional frame of plaque containing calcium (signal drop-out), however with a lipid rich component. On the right is a cross-sectional frame of a section of vessel with minimal disease, and no detectable lipid. The bottom section depicts the histology truth, with good correlation with NIRS findings.

Figure 6: Endothelial shear stress profiling

Example of a 3D reconstructed coronary arterial segment (B) Example of endothelial shear stress profiling along a 3D reconstructed left anterior descending artery. **[Adapted from Chatzizisis YS, Coskun AU, Jonas M, et al. JACC, 2007;49(25):2379-93]**

Figure 7: Coronary angioscopy

Coronary angioscopy. A representative case with no yellow plaque (A) and a representative case with multiple yellow plaques (B). **[Adapted from Ohtani T, Ueda Y, Mizote I et al. JACC 2006. 47(11):2194-200]**

Figures

Figure 1

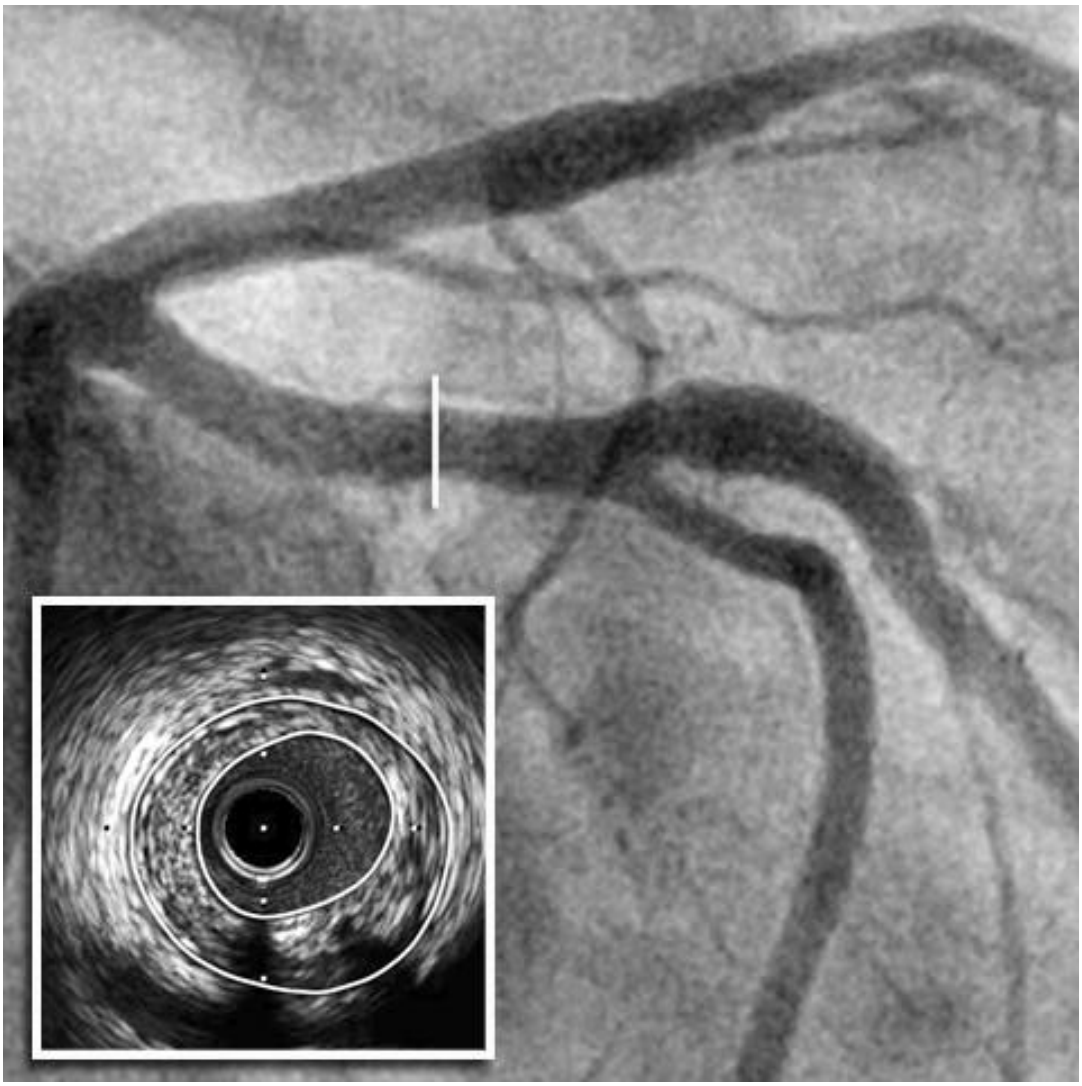

Figure 2

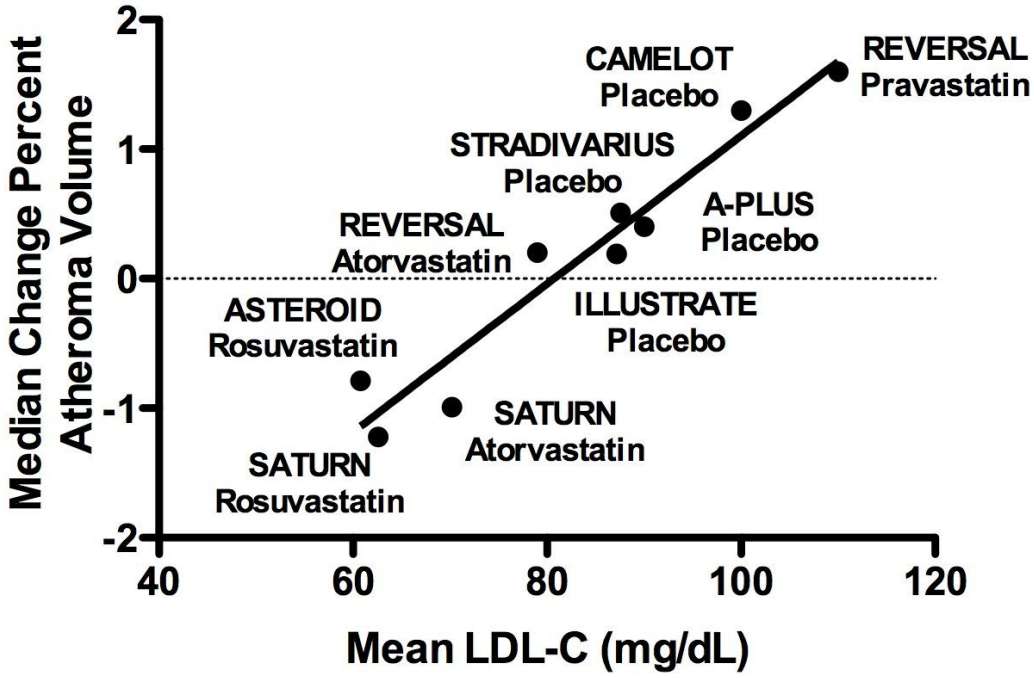

Figure 3

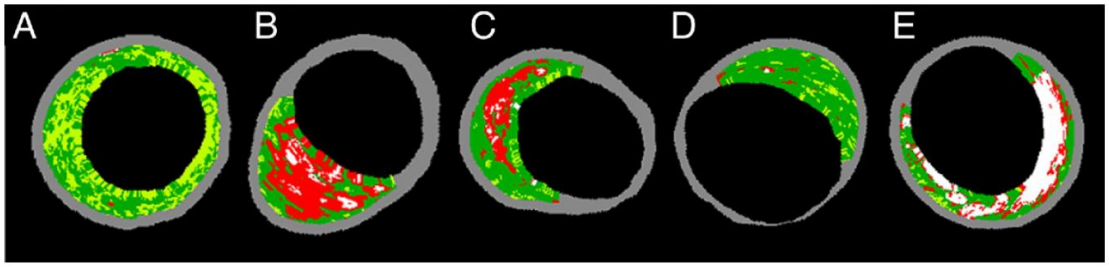
A
B
C
D
E

Figure 4

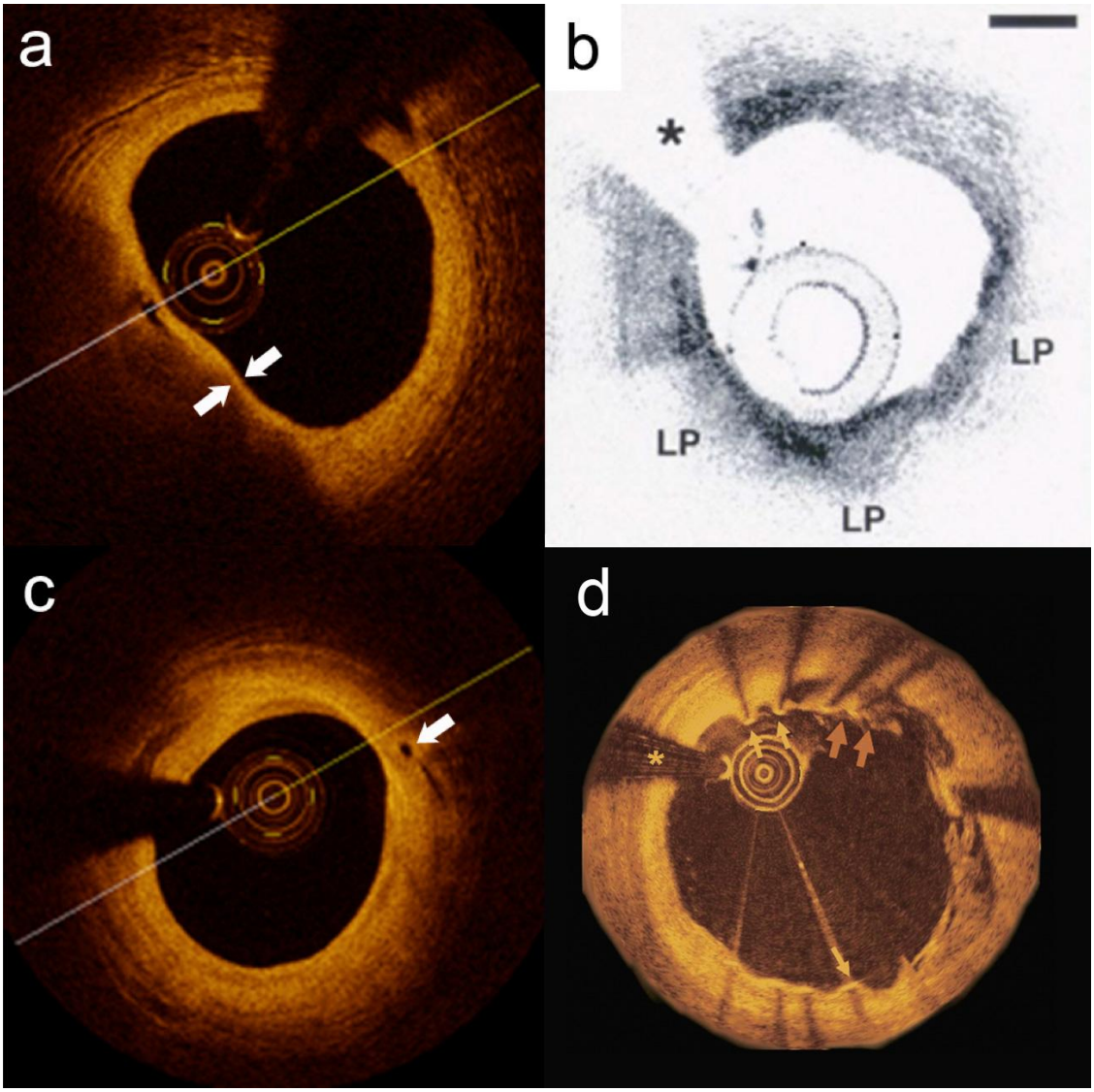

Figure 5

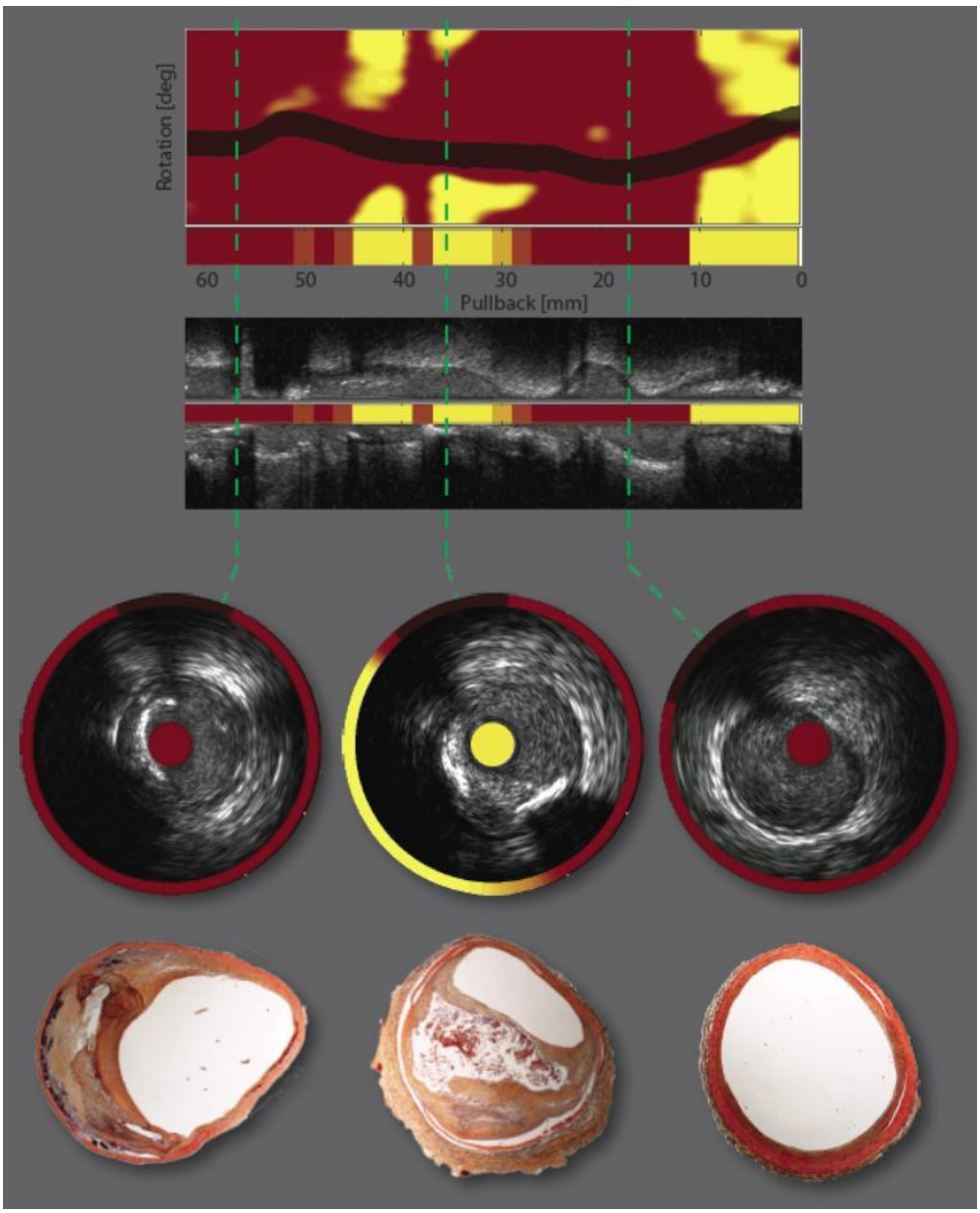

Figure 6

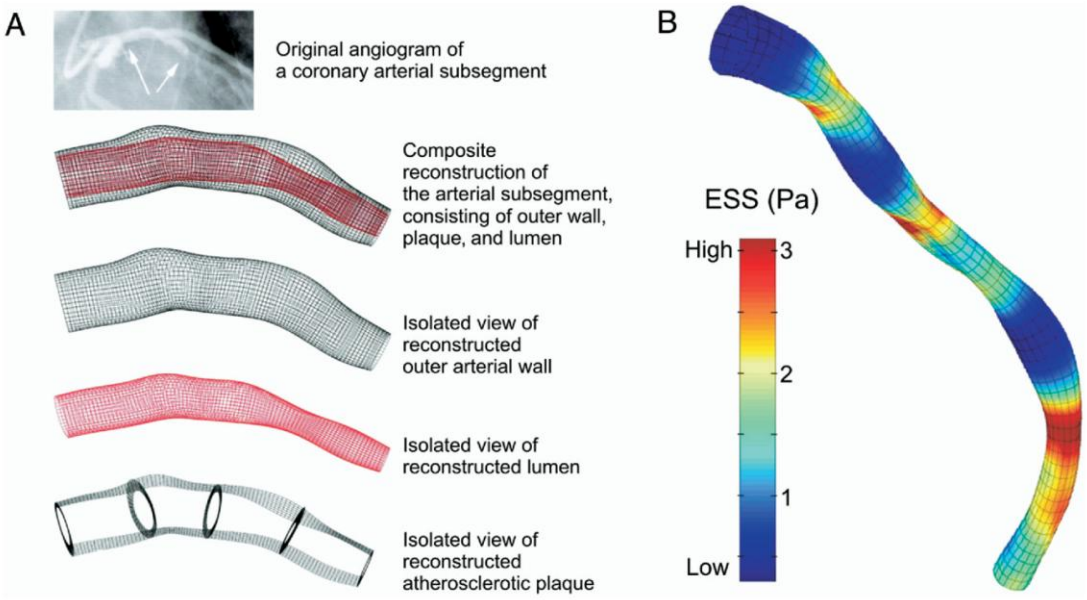
A
Original angiogram of
a coronary arterial subsegment
Composite
reconstruction of
the arterial subsegment,
consisting of outer wall,
plaque, and lumen
Isolated view of
reconstructed
outer arterial wall
Isolated view of
reconstructed lumen
Isolated view of
reconstructed
atherosclerotic plaque
B
ESS (Pa)
High
3
2
1
Low

Figure 7

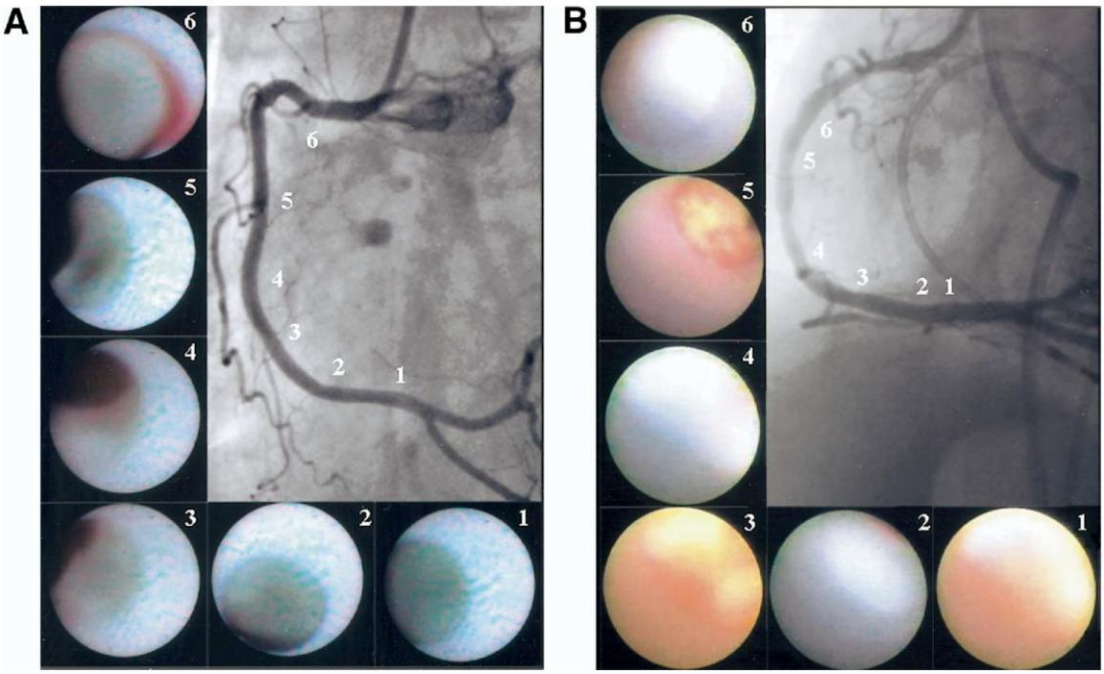

Author contributions:

Dr Rishi Puri – Preparation of manuscript

Professor E. Murat Tuzcu - Correction and critical review of manuscript

Professor Steven E. Nissen - Correction and critical review of manuscript

Professor Stephen J. Nicholls - Correction and critical review of manuscript

I hereby give permission for this published review article to be included in this thesis submission:

Dr Rishi Puri

Professor E. Murat Tuzcu

Professor Steven E. Nissen

Professor Stephen J. Nicholls

CHAPTER 2: INTRAVASCULAR IMAGING OF VULNERABLE CORONARY PLAQUE: CURRENT AND FUTURE CONCEPTS

Adapted from PURI, R., WORTHLEY M.I., NICHOLLS, S.J. 2011. Intravascular imaging of vulnerable coronary plaque: current and future concepts. *Nat Rev Cardiol*. 8(3):131-9

ABSTRACT

Advances in coronary imaging are needed to enable the early detection of plaque segments considered to be ‘vulnerable’ for causing clinical events. Pathological studies have contributed to our current understanding of these vulnerable or unstable segments of plaque. Intravascular ultrasonography (IVUS) has provided insights into the morphology of atherosclerosis, the mediators of plaque progression and the factors associated with acute coronary syndrome (ACS). In addition, the demonstration of pan coronary arterial instability has highlighted that ACS involves a multifocal disease process. Various second-generation intravascular imaging technologies - employing advanced processing of ultrasound radiofrequency backscatter signals, light-based imaging, spectroscopic imaging and molecular targeting - possess inherent advantages for the identification of meaningful surrogates of plaque instability. The fusion of these imaging technologies within a single imaging catheter is likely to allow for greater synergism in image quality and early disease detection. However, natural-history studies to validate the use of these novel imaging tools for enhanced risk prediction are needed prior to the incorporation of these strategies into mainstream clinical practice.

Since the first autopsy report of plaque rupture mediating catastrophic intracoronary thrombosis, in 1844, intense debate regarding the substrate responsible for causing acute myocardial infarction (AMI) has taken place (Herrick, 1983). Seminal pathological observations by Davies & Thomas (Davies and Thomas, 1984) confirmed that features of plaque disruption (rupture and erosion) mediate intracoronary thrombosis. Although DeWood *et* al. (DeWood et al., 1980) highlighted angiographic evidence of the causal role of intracoronary thrombosis in AMI, an ongoing discord remained between the burden of disease, as observed with coronary angiography, and the subsequent clinical events (Ambrose et al., 1988). Glagov et al.(Glagov et al., 1987) gave a description of vessel remodeling whereby coronary arterial segments were able to harbor considerable amounts of plaque burden before overt lumen compromise, thereby providing the first mechanistic explanation of this apparent discord. Intravascular ultrasonography (IVUS) has provided important insights into the extent of plaque burden *in vivo*, and has allowed for the characterization of the vessel wall, plaque morphology and vessel remodeling (Nicholls et al., 2006). These imaging capabilities have, therefore, enabled a thorough assessment of the potential plaque segments that are responsible for ACS, a disorder in which plaque rupture is known to be a major cause of AMI.

The term ‘vulnerable plaque’ was first coined by Muller *et al.* in 1989 (Muller et al., 1989), who proposed the concept of non-flow-limiting stenoses undergoing acute changes that result in sudden plaque rupture or erosion, acute coronary thrombosis and subsequent AMI (Finn et al., 2010). Although a cause- and-effect relationship between vulnerable plaque and clinical events has not been confirmed, factors promoting

vulnerability for plaque rupture are thought to include: the presence of lipid pools and necrotic core with an overlying thin fibrous cap; increased macrophage activity; and the neoadventitial proliferation of leaky vasa vasorum causing intraplaque hemorrhage and plaque progression. Such features are observed within plaques that are modest in terms of angiographic stenosis severity within positively remodeled arterial segments. The thin-cap fibroatheroma (TCFA), therefore, is currently considered the prototypic vulnerable plaque phenotype that precedes plaque rupture (Burke et al., 1997). These markers of vulnerability provide potential targets for vulnerable plaque imaging.

Data from various catheter-based imaging technologies that attempt to profile vulnerable plaques *in vivo* have generated enormous interest and debate within the medical community. A number of such vulnerable plaques are thought to exist within both culprit and nonculprit vessels in patients with ACS and AMI, making attempts to detect isolated vulnerable plaques in these patients a somewhat inefficient process (Rioufol et al., 2002, Hong et al., 2004). Furthermore, it is difficult to reliably predict which segments of plaque are likely to undergo transformation and culminate in a substrate for an acute clinical event. Despite contemporary medical therapies, a substantial residual incidence of morbidity and mortality is associated with both primary and secondary acute coronary events. An improved understanding of the important pathobiological processes that drive pan coronary arterial instability *in vivo* will be fundamental in our attempts for enhanced risk prediction strategies. Indeed, these processes might ultimately result in novel imaging end points and future therapeutic targets. In the interim, however, the definition of ‘vulnerable plaque’ will continue to reflect the plaque phenotype observed following an ACS event or from

pathological comparator data. The aim of this Review is to summarize the role of imaging modalities in the assessment of vulnerable coronary plaque. Rapid advances in technology, particularly the advent of fusion imaging modalities, and the future characterization of the vessel wall *in vivo* will likely improve the understanding of what constitutes a vulnerable segment of plaque.

Intravascular ultrasonography (IVUS)

IVUS has provided a unique insight into the burden and distribution of atherosclerotic plaque, allowing for a comprehensive characterization of the vessel wall (Nicholls et al., 2006). IVUS has also demonstrated the ubiquitous presence of plaque in regions that seem normal on quantitative coronary angiography (Mintz et al., 1995). This phenomenon has been explained by the ability of the artery (as determined by IVUS) adapt to plaque accumulation within the vessel wall in order to preserve lumen encroachment—termed 'adaptive' or 'positive' remodeling (Porter et al., 1993, Schoenhagen et al., 2001). The dynamic nature of the arterial wall in response to atheroma burden might have an important role in the propensity of particular plaque segments to undergo biological transformations that result in a corresponding clinical syndrome. Both histopathological findings and *in vivo* IVUS studies have demonstrated that culprit lesions resulting in ACS are more likely to be harbored within positively remodeled coronary arterial segments in patients with unstable coronary syndromes than in those with stable coronary syndromes (Smits et al., 1999, Varnava et al., 2002, Schoenhagen et al., 2000, Naghavi et al., 2003). The identification of multiple ruptured plaques (with or without overlying thrombus) within culprit and nonculprit vessels in patients with ACS suggests that atherosclerosis and its associated complications are

features of an underlying systemic disorder in patients with multifocal disease activation (Maehara et al., 2002, Rioufol et al., 2002, Hong et al., 2004). In addition, patients with ACS were found to have culprit lesions that showed positive remodeling and had greater distensibilty indices compared with lesions that showed negative remodeling in patients with stable angina (Jeremias et al., 2000). Another study showed that plaques causing ACS were visualized as yellow on angioscopy, and using IVUS these yellow plaques had greater distensibility than white plaques found in patients with stable coronary syndromes (Takano et al., 2001a). Furthermore, IVUS analysis highlights the greater amount of plaque burden within culprit lesion segments, in comparison with non-culprit coronary lesions, which create the substrate for plaque rupture and subsequent thrombus formation (Fujii et al., 2003, Fujii et al., 2006).

IVUS imaging radiofrequency analysis

The vulnerability of specific plaque components is a growing field of inquiry. Although echogenicity analysis of conventional ultrasonography has been reported to associate with plaque composition (Schartl et al., 2001, Tardif et al., 2007), this approach provides a suboptimal characterization of the individual components within a plaque. Images obtained by grayscale IVUS are formed only by the envelope (amplitude) of the radiofrequency backscatter signal (Figure 1a). Autoregressive spectral analysis is applied to IVUS radiofrequency backscatter data to facilitate the interpretation of the images of different tissue components. As a result, the first commercially available IVUS radiofrequency backscatter image analysis system was named Virtual Histology™ (VH-IVUS; Volcano, Rancho Cordoba, USA). This system is currently

available on a 20 MHz steady-state (non-rotational) IVUS catheter and will be available with the use of a 45 MHz rotational catheter in the future. The VH-IVUS algorithm generates tissue–color maps that classify plaque into four major subtypes: fibrous, fibrofatty, necrotic core and calcium (Figure 1b). These tissue–color maps have a high degree of correlation and predictive accuracies with *ex vivo* histological findings (Nair et al., 2001, Nair et al., 2002, Nair et al., 2007). An alternative algorithm characterizes tissue plaque composition using the average power of the radiofrequency backscatter signal (Integrated Backscatter; IB-IVUS) to generate tissue–color maps (Wickline SA, 1994, Okubo et al., 2008, Kawasaki et al., 2001). In addition, Boston Scientific (Natick, Massachusetts, USA) have released proprietary software (iMap) to characterize plaque composition using full spectral information and spectral similarity (pattern recognition) (Figure 1c) (Sathyanarayana et al., 2009). *Ex vivo* histological validation has demonstrated a high degree of accuracy for this technique although the quantitative data is yet to be reported (Sathyanarayana et al., 2009). This iMap technique is available on a 40 MHz rotational catheter.

IVUS-derived TCFA

A definition of an IVUS-derived TCFA (IDTCFA) has been proposed to evaluate the *in vivo* incidence of vulnerable plaque (when using VH-IVUS imaging) that closely matches *ex vivo* pathological observations (Rodriguez-Granillo et al., 2005). As the resolution of VH-IVUS is insufficient to directly image a thin fibrous cap (diameter ≤65 μm), IDTCFA has been defined as the presence of ≥10% of necrotic core volume without obvious overlying fibrous tissue and a total plaque burden of ≥40% observed within three consecutive VH-IVUS frames. Based on this definition, a three-vessel VH-

IVUS study found that patients with ACS have a greater incidence of IDTCFA than patients with stable coronary artery disease, with a clustering of plaques within the proximal 20–40 mm of the coronary arterial tree (Hong et al., 2008). A study of the longitudinal behavior of nonobstructive coronary atheroma utilizing VH-IVUS imaging found that approximately 75% of IDTCFAs spontaneously resolved over a 12 month period (potentially evolving into other plaque subtypes) (Kubo et al., 2010b). Spontaneous IDTCFAs might also arise from other plaque subtypes, notably those involving pathological intimal-thickening and fibroatheromas with superimposed thick fibrous caps. In addition, a variety of specific plaque subtypes (characterized by pathological intimal thickening, thick-capped fibroatheroma, and IDTCFA) underwent an increase in overall atheroma burden (or transformation to another plaque subtype), whereas fibrotic and fibrocalcific plaques did not show evidence of disease progression or plaque modification (Kubo et al., 2010b). Overall, baseline VH-IVUS characteristics (and plaque subtypes) were not predictive of the dynamic, serial behavior of IDTCFAs; however, the underlying plaque burden was found to be a major predictor of serial IDTCFA behavior.

Although the results are yet to be officially published, the Providing Regional Observations to Study Predictors of Events in the Coronary Tree (PROSPECT) study was another attempt to identify the influence of baseline plaque composition, and particularly the presence of IDTCFA, on future coronary events (Stone, 2009). Although the baseline presence of an IDTCFA in PROSPECT was shown to be an independent predictor of future coronary events, an analysis revealed that all of the significant multivariate predictors of future coronary events in this study were

intrinsically related to plaque burden and lesion size (Stone, 2009). Approximately 600 IDTCFAs were identified at baseline. At least 50% of all hard and soft clinical events, however, were found not to be related to the presence of a baseline IDTCFA (Stone, 2009). These findings might be attributable to inherent limitations of the current VH-IVUS algorithm (as described in a following section). Another limitation of this study was the lack of serial VH-IVUS imaging (only event-led repeat coronary angiographic imaging and intervention were utilized), which failed to allow for a genuine observation of the natural history of coronary atheroma.

IVUS and arterial wall elasticity

The elastic properties of the coronary arterial walls can be assessed using IVUS, and these properties have been proposed to be predictive of plaque vulnerability (de Korte et al., 1998). The mechanical strain of the arterial wall is measured and local tissue deformation is determined by cross-correlation analysis of radiofrequency signals to derive strain maps of the arterial wall. The calculated local radial strain is displayed in a color-coded fashion in areas where plaque rupture can occur - either within the plaque area (elastography) or at the luminal boundary to a depth of 450 μm (palpography). Although plaque and lumen dimensions remained static with optimal medical therapy at 6 months of follow-up, the Integrated Biomarker and Imaging Study (IBIS)-1 trial highlighted a significant reduction in the density of abnormal high-strain areas over this time period (density high strain areas per centimeter: 1.6 ± 1.5 versus 1.2 ± 1.4, P = 0.023) (Van Mieghem et al., 2006); such changes were predominantly found in patients presenting with AMI. High-strain areas have been found in morphologically high-risk plaques (Schaar et al., 2004b). The IBIS-2 trial utilized IVUS-palpography to detect

changes in plaque deformability in response to darapladib, a lipoprotein-associated phospholipase A_2 inhibitor (Serruys et al., 2008). The expectation was that darapladib would lower the deformability of atherosclerotic plaques. However, the results of this trial failed to show any effect of darapladib upon plaque mechanical strain, despite an increase in the necrotic core volume in the placebo group compared with the darapladib group (as derived by Virtual Histology™) (Serruys et al., 2008). Total atheroma burden remained unchanged between the darapladib and placebo groups. Palpography, therefore, remains an experimental tool and has not yet been established as a valid surrogate end point.

Limitations of IVUS

Although the characterization of human plaque composition *in vivo* is relevant for the identification of plaque vulnerability, there remain some limitations to the current generation of radiofrequency backscatter signal-based IVUS technologies. The acquisition of VH-IVUS images are gated at the R-wave of the electrocardiography signal, which fails to allow for VH-IVUS imaging upon a number of frames acquired within each R–R interval. Variability in a patient's heart rate at different time points results in a degree of horizontal bias during serial VH-IVUS imaging. This bias can reduce the accuracy of volumetric estimations of serial variations in specific plaque subtypes in predefined plaque segments or lesions over time. Furthermore, the validation of VH-IVUS (in *ex vivo* and *in vivo* studies involving human coronary arteries) has predominantly focused on the qualitative validation of particular plaque subtypes, as opposed to their quantitative burden. One study found a lack of correlation

between the necrotic core size derived from VH-IVUS and that found from histology (Thim et al., 2010). Moreover, the current VH-IVUS algorithm has difficulty distinguishing necrotic core from calcification and has a tendency to display tissue within the halo surrounding the calcium as necrotic core. Any superficial calcification, therefore, will invariably be displayed as an IDTCFA, resulting in false positive results (Nair et al., 2002). In addition, current generation radiofrequency-based IVUS algorithms are unable to identify thrombi *in vivo*, which commonly form in patients with ACS (Kubo et al., 2007). Although limited to the rotational catheter systems, guide wire-induced artefact is currently another source of error during radiofrequency-based plaque phenotyping. Both VH-IVUS and iMap are available in most cardiac catheterization laboratories worldwide that have regular Volcano and/or Boston Scientific IVUS imaging consoles. Despite the widespread dissemination of such technology, it is important to note that, to date, there is no data that supports a clinical indication to promote the use of VH-IVUS (or affiliated technologies that process the radiofrequency backscatter signal) to guide percutaneous coronary interventions.

At present, an *in vivo* 'gold-standard' of the key features of plaque substrates responsible for an acute coronary event is lacking. As a result, the current definitions of vulnerable plaque segments are predominantly derived from *ex vivo* pathological data. A further complexity is that there are currently no reliable models of experimental atherosclerosis that produce plaque rupture. Alterations in tissue architecture as a result of fixation methods, together with difficulties in *in vivo* and *ex vivo* frame-matching for image comparison, ensures that histological validation of intravascular imaging modalities remains challenging. The development of an experimental model of plaque

rupture and of imaging modalities that provide us with accurate, reliable, reproducible and serial data of the biological processes within the vessel wall deemed responsible for ACS are needed. Indeed, these developments will ultimately enable the creation of an *in vivo* gold-standard definition of a vulnerable segment of coronary plaque. Following the prospective validation of this definition in serial natural-history studies in humans, further serial *in vivo* trials will be required to assess the effect of novel anti-atherosclerotic therapies on plaque vulnerability and subsequent clinical outcomes.

Spectroscopic plaque imaging

Photonic spectroscopy requires that various molecules within biological tissue to be able to absorb, scatter and emit light. The light–tissue interaction determines the chemical composition of a structure by analyzing the spectra of light induced by its interaction with tissue material. Both near-infrared spectroscopy (NIRS) and Raman spectroscopy (RS) have been validated to characterize the chemical composition of plaque. Near-infrared absorption utilizes near-infrared light (780–2,500 nm) to illuminate tissue. Various types of chemical bonds absorb this light with differing wavelengths, creating a unique absorbance spectrum that reflects the chemical composition of the tissue. This technique is well-suited for the detection of lipid-laden atherosclerotic plaque (Cassis and Lodder, 1993, Jaross et al., 1999).

The potential of *in vivo* spectroscopic signal analysis as an index of plaque vulnerability is also of interest. Catheter-based NIRS imaging specifically identifies lipid pools within autopsy specimens of human coronary plaques that accurately correlate with histological analysis (Figure 2) (Gardner et al., 2008). The Spectroscopic

Assessment of Coronary Lipid (SPECTACL) trial was the first attempt to demonstrate whether the *in vivo* spectroscopic signals obtained from living patients with lipid-core coronary plaques (undergoing percutaneous coronary intervention) were spectrally similar to those obtained from prior autopsy studies with pathologic validation of lipid-core presence and burden (Figure 2) (Waxman et al., 2009). This trial suggested that the current generation of catheter-based NIRS imaging is safe, feasible and enables high-quality spectroscopic images to be taken through blood and during coronary motion. In addition, the spectroscopic data proved to be relatively concordant with previously derived *ex vivo* data (Gardner et al., 2008). However, the reproducibility of spectroscopic data from repeated catheter imaging is yet to be reported, and the ability to detect and differentiate biological signals from various other pathological features of plaque vulnerability (such as thrombus, intraplaque hemorrhage and inflammation) remains to be determined. The Study of NIRS and IVUS Combination Coronary Catheter (SAVOIR) trial is currently recruiting patients to evaluate the performance and handling of an IVUS catheter with NIRS imaging capabilities (Serruys, 2010). This multimodality imaging catheter will not only enable topographical and structural information of *in vivo* plaque burden, but should also facilitate the selective identification of lipid pools within the vessel wall (Figure 3).

The Raman effect involves the scattering of light between molecules, which can change the energy level of the scattering photon and shift the scattered light to another frequency (Raman scattering) (Bruggink et al., 2010). The Raman spectrum of a given molecule is unique and provides direct information regarding the characteristics of the molecule within tissue. Raman scattering, therefore, is capable of discriminating various

lipid subclasses within an atherosclerotic plaque (Nazemi and Brennan, 2009). An *ex vivo* study demonstrated the synergism between RS and IVUS coronary imaging to accurately identify and quantify calcium salts and cholesterol deposits within areas of plaque that had been structurally identified with IVUS (Romer et al., 2000, Buschman et al., 2001). RS imaging techniques will eventually enable *in vivo* metabolomic profiling of the vessel wall and the ability to directly map important pathological and molecular processes implicated in the pathogenesis of atherosclerosis. RS imaging, therefore, has great potential for the future research of *in vivo* human vascular biology (Bruggink et al., 2010).

Optical coherence tomography

Optical coherence tomography (OCT) processes backscattered reflections of infrared light to generate real-time tomographic images (Figure 4a). This technique allows for a vastly superior axial and lateral resolution than IVUS-based approaches, and facilitates the imaging of microstructures such as thin fibrous cap and endothelium. However, this improvement comes at the expense of poor penetration through blood and tissue. Deeper arterial structures (other than those at the lumen–intima or lumen–plaque interface), therefore, are poorly visualized and limit the ability of OCT to evaluate large-caliber coronary arteries and the extent of plaque volume at the vessel wall (Prati et al., 2010).

The introduction into clinical practice of nonocclusive optical frequency domain imaging has considerably reduced procedural time and increased safety (Prati et al., 2007). To date, the chief application of OCT has been the visualization of the

interaction between stent struts and the endothelium (Figure 4b). OCT has been fundamental in highlighting the mechanisms of the novel bioabsorbable everolimus-eluting stent platform (Serruys et al., 2009). Furthermore, OCT has been used to assess potential mechanisms of stent thrombosis by quantifying the degree of stent strut apposition and endothelial strut coverage following drug-eluting stent implantation (Cook et al., 2007, Finn et al., 2007, Joner et al., 2006).

OCT has a considerably higher sensitivity in detecting culprit lesion morphology in patients with AMI than IVUS. Indeed, the incidence of plaque rupture (73%) and thrombus formation (100%) detected by OCT in 30 patients with AMI was greater than the equivalent detections by IVUS (40% and 33%, respectively) (Kubo et al., 2007). This finding highlights the unique ability of OCT to determine the fibrous-cap thickness of culprit lesions in patients with AMI to be 49 ± 21 μm (Kubo et al., 2007). From the perspective of the current plaque–rupture hypothesis (a TCFA undergoing plaque rupture), therefore, the major strength of OCT lies in its ability to accurately image *in vivo* fibrous cap thickness. Another study revealed that patients with both AMI and ACS had a considerably higher frequency of thinner fibrous caps in regions of lipid-rich plaque than was observed in patients with stable angina pectoris (Jang et al., 2005). By applying a cut-off value of ≤65 μm for a lipid-rich plaque to be identified as a TCFA, the incidence of OCT-derived TCFA was also considerably greater in patients with AMI (72%) and ACS (50%) than in patients with stable coronary syndromes (20%). Using a similar methodology to this study, but also applying OCT imaging within nonculprit vessels in patients with either AMI or stable angina, a separate study found that multiple OCT-derived TCFAs were more prevalent in both target and nontarget

lesion vessels in the setting of AMI (38%) compared with stable angina (0%) (Kubo et al., 2010a), highlighting the concept of pan coronary arterial instability in the setting of AMI.

The utility of OCT in assessing macrophage infiltration within fibrous caps as a marker of lesion instability has also been investigated. OCT images (standard deviation of signal intensity) of lipid-rich arterial segments obtained at autopsy correlated highly with histological analysis of macrophage cap density (MacNeill et al., 2004); various systemic markers of inflammation also correlated with fibrous cap macrophage density and thickness (Raffel et al., 2007, Li et al., 2010a). Furthermore, OCT imaging has been used to speculate about the mechanisms of fibrous cap rupture in patients with AMI (Tanaka et al., 2008). However, to date, the ability of OCT to accurately classify plaque composition has yielded conflicting results (Kawasaki et al., 2006, Manfrini et al., 2006). This discrepancy might be attributable to the inefficient tissue penetrance and subsequent poor imaging capabilities of light-based imaging modalities compared with those involving ultrasonography. The combination of OCT with fluorescent molecular imaging, therefore, will enable synergistic structural and molecular information to be obtained during intravascular imaging (Yuan et al., 2010). Enhancing OCT imaging with molecular sensitivity or spectroscopic techniques will likely facilitate a greater understanding of *in vivo* atheroma biology, and perhaps of plaque vulnerability.

Novel intravascular imaging methods

The optimum tool for intravascular imaging to assess plaque and/or vessel instability is yet to be formally defined. Each candidate imaging modality possesses unique features

that yield important information and, therefore, a synergistic approach in combination with other imaging modalities seems favorable. IVUS, for example, allows for ideal tissue penetration to accurately assess plaque burden and vessel remodeling, but lacks the resolution to directly image fibrous cap thickness. The SAVOIR trial is expected to provide information regarding the benefit of the fusion of IVUS with both NIRS and RS capabilities *in vivo* (Serruys, 2010). Furthermore, intravascular imaging catheters with dual IVUS and OCT capabilities have been developed and tested in animal models of atherosclerosis (Li et al., 2010b), although further validation of these catheters in humans is needed. The optimum intravascular imaging technique would combine the spectroscopic imaging capabilities of tissue composition, the near-field resolution of OCT and the far-field tissue penetration of IVUS to accurately image the entire vessel wall. Further advances in microelectromechanical systems will yield multimodality imaging sensors in small-caliber catheter-based systems to, ultimately, allow for fusion intravascular imaging capabilities to become a mainstream reality.

An advanced technique that produces an accurate three-dimensional (3D) reconstruction of human coronary arteries *in vivo*, termed ANGUS (angiography and IVUS), has been achieved by the fusion of information from both biplane coronary angiography and IVUS (Slager et al., 2000). This technique of coronary 3D reconstruction allows for the evaluation of endothelial shear stress *in vivo* using advanced computational fluid dynamic and finite element models (Krams et al., 1997, Coskun et al., 2003). This attribute of ANGUS is of clinical importance as endothelial shear stress has a fundamental role in the initiation and evolution of atherosclerosis. Regions of low endothelial shear stress have been shown to contribute to the

atherogenic endothelial phenotype (Gibson et al., 1993). Furthermore, local endothelial shear stress and remodeling had a synergistic effect in determining the natural history of individual coronary lesions in an *in vivo* pig model of atherosclerosis (Koskinas et al., 2010).

Experimental atherosclerosis models and pathologic investigations of human atherosclerotic plaque highlight the important role of plaque neovascularisation in promoting plaque progression and mediating plaque instability (Kolodgie et al., 2003). Intravascular imaging has allowed for the detection of plaque neovascularisation in humans (Vavuranakis et al., 2008, Prati et al., 2010). IVUS has offered the greatest hope in this area owing to the advantage of accurate far-field imaging. The ongoing refinement of IVUS transducers (using either single-crystal technology or dual-frequency elements) and improvements in signal processing methods (including pulse-inversion strategies for second harmonics or sub harmonics) will overcome the current limitations with respect to signal-to-noise ratio and resolution (Goertz et al., 2007). The challenge will be to incorporate the presence of plaque neovessels into appropriately designed natural-history studies to determine the prospective role of plaque neovessel imaging in identifying future coronary risk.

Ultrasonographic molecular imaging uses microbubbles, microparticles (such as echogenic liposomes) or nanoparticles as acoustic tracers (Kaufmann, 2009). After intravenous or direct intra-arterial injection, these microparticles bind to disease-specific epitopes that can be imaged in real time. Given the intrinsic role that inflammation has in the initiation and progression of atherosclerosis, inflammatory

markers that are expressed on the endothelial cell surface early in the course of atherogenesis might be potential targets for imaging. The field of targeted molecular ultrasonography is still in its infancy, and much remains to be accomplished in order to develop the clinical relevance of this approach. However, once the technological challenges have been met, intravascular-based targeted molecular-imaging technologies are likely to feature prominently in future clinical trials. The destruction of microbubble or nanoparticle agents by ultrasonography results in local bio-effects that have the capacity to alter the biologic activity of the microenvironment (Lindner, 2009). The ability to favorably modulate and enhance these local bio-effects will allow the exciting concept of therapeutic intravascular imaging to be realized.

Conclusions

Attempts to identify vulnerable plaques *in vivo* have stimulated the development of a variety of intravascular imaging modalities. These tools will be used to define the natural history of coronary atherosclerosis and determine specific plaque and vessel features that can be used to predict intracoronary thrombosis and subsequent clinical events. Given the multifocal nature of coronary lesion instability and propensity for plaque rupture, the ideal therapeutic regimen will involve the systemic delivery of anti-atherosclerotic therapies. Nevertheless, the need for accurate and prospective risk stratification of coronary lesions will continue to drive emerging imaging technologies and, ultimately, local and systemic therapeutic strategies. The immediate challenge is to develop a reliable animal model of plaque rupture to facilitate further validation of imaging modalities, and to initiate well-designed natural-history studies to employ these modalities.

There is hope that the clinical utility of intravascular imaging will be enhanced with fusion imaging technologies and with the potential feasibility of targeted therapeutic imaging. Nevertheless, the definitive test of a developing imaging modality will be its ability to change patient management. Accordingly, large prospective clinical trials are urgently required to determine whether the utilization of a novel imaging modality will change clinical practice and, ultimately, disease outcomes. Unequivocal evidence from these clinical trials is needed to define the optimum approach with respect to imaging for the presence of vulnerable plaques.

Figure legends

Figure 1

Images obtained using various IVUS techniques. a | Grayscale IVUS coronary imaging of the left anterior descending artery in a patient with chest pain and angiographically minor coronary artery disease. b | VH-IVUS coronary imaging of the left anterior descending artery in a patient with chest pain and angiographically minor coronary artery disease. Grayscale coronary image shown on left, with corresponding VH-IVUS image seen on right. Note the color-coding of the four histological tissue subtypes: fibrous (green); fibrofatty (yellow); necrotic core (red); and calcium (white). c | iMap coronary imaging of the non-culprit vessel (left anterior descending artery) in a patient with ACS within the right coronary artery. The four tissue subtypes are shown with slightly different color-coding to VH-IVUS: lipidic tissue (green); necrotic core (magenta); and calcium (blue). Abbreviations: IVUS, intravascular ultrasonography; VH-IVUS, Virtual Histology™ IVUS.

Figure 2

The correlation between catheter-based NIRS imaging and histology. The upper panel depicts the chemogram (false color map) which displays the probability of an LCP at each location along the horizontal pullback (x-axis) and circumference (y-axis). Red coloration indicates a low probability of an LCP, while yellow coloration represents a high probability. The middle panel depicts a ‘block chemogram’ that summarizes the presence of LCP probability at 2 mm intervals. The lower panel shows the correlation of NIRS imaging and histology, with the strongest signal and, therefore, the highest

probability of an LCP at 32 mm and 34 mm of pullback. The four lower images represent movat cross-sections of the artery at the indicated positions (sections illustrated within white lines in the NR chemogram). The chemogram shows prominent lipid core signal at 29–37 mm and 41–47 mm. The block chemogram shows the strongest LCP signals at 29–35 mm and 41–47 mm. Histology shows that the greatest LCP signal at 31–35 mm and 46–48 mm. Abbreviations: LCBt, lipid core burden index; LCP, lipid core-containing plaque; LRP, lipid-rich plaque; NIR, near-infrared; NIRS, NIR spectroscopy.

Figure 3

The combination of NIRS technology with an IVUS catheter. A cross-sectional IVUS frame with circumferential chemogram is displayed on the left, with a corresponding block chemogram with horizontal IVUS pullback on the right. Red coloration indicates a low probability of an LCP, while yellow coloration represents a high probability. Abbreviations: IVUS, intravascular ultrasonography; LCP, lipid core-containing plaque; NIRS, near-infrared spectroscopy.

Figure 4

Images obtained using OCT coronary imaging. a | OCT coronary imaging highlighting diffuse intimal thickening. A guidewire artifact can be seen at the base of the artery. b | OCT image in a bare-metal-stented coronary segment highlighting complete apposition of the stent struts to the intima. A guidewire artifact can be seen at the base of the artery. Abbreviation: OCT, optical coherence tomography.

Figure 1

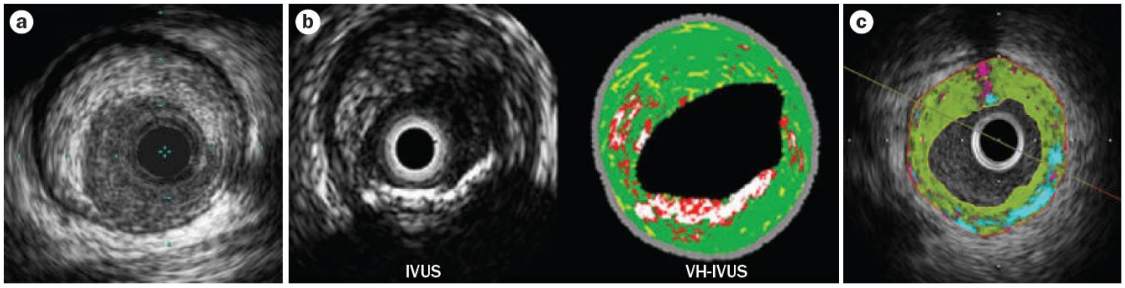

Figure 2

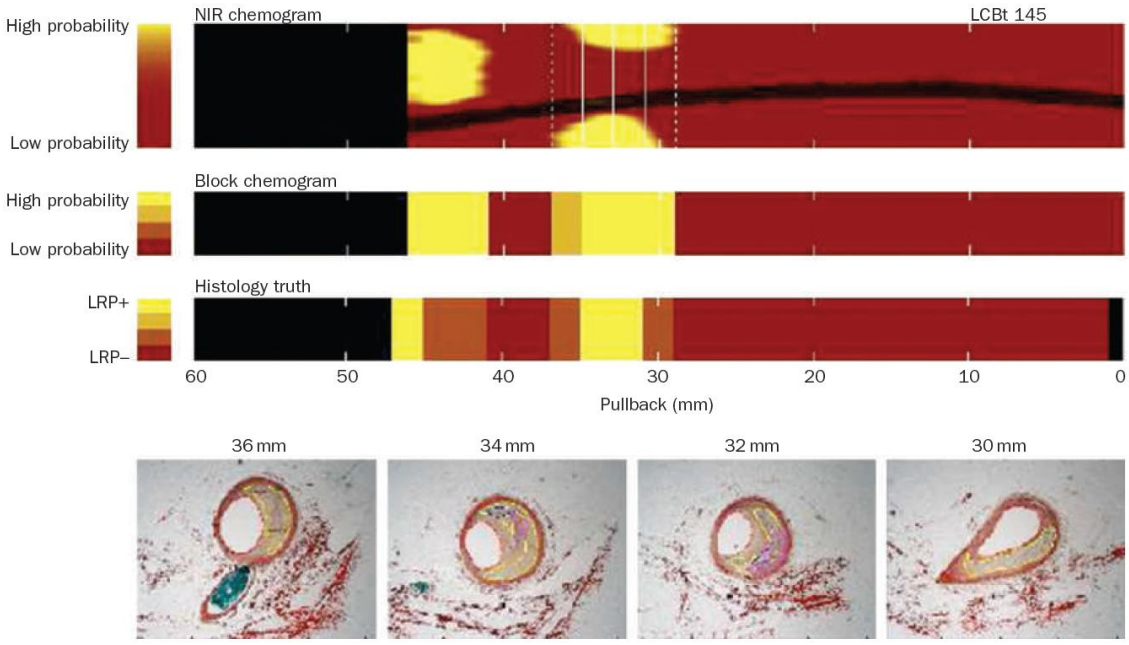
High probability
Low probability
NIR chemogram
LCBt 145
High probability
Low probability
Block chemogram
LRP+
LRP–
Histology truth
60
50
40
30
20
10
0
Pullback (mm)
36 mm
34 mm
32 mm
30 mm

Figure 3

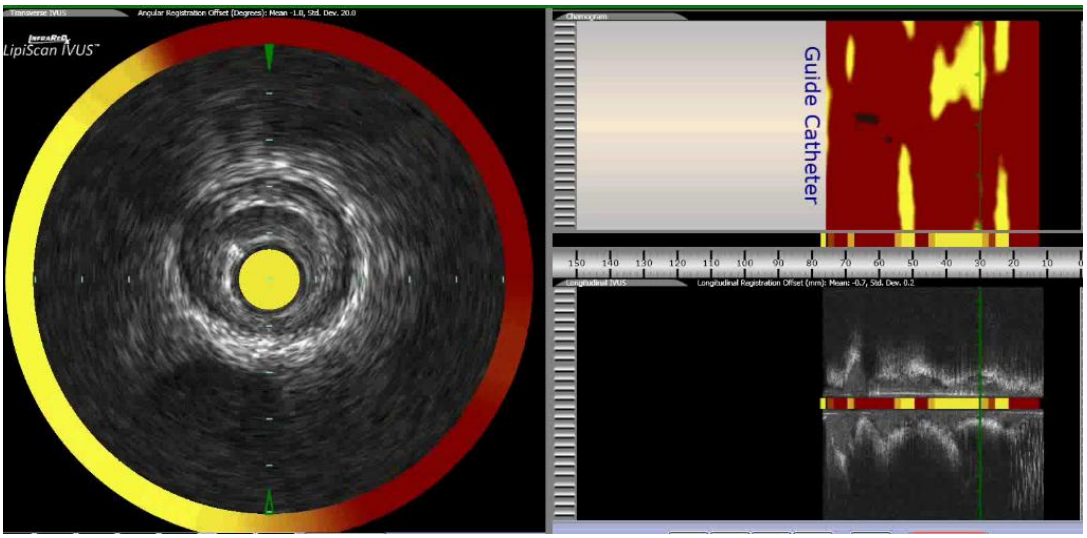

Figure 4

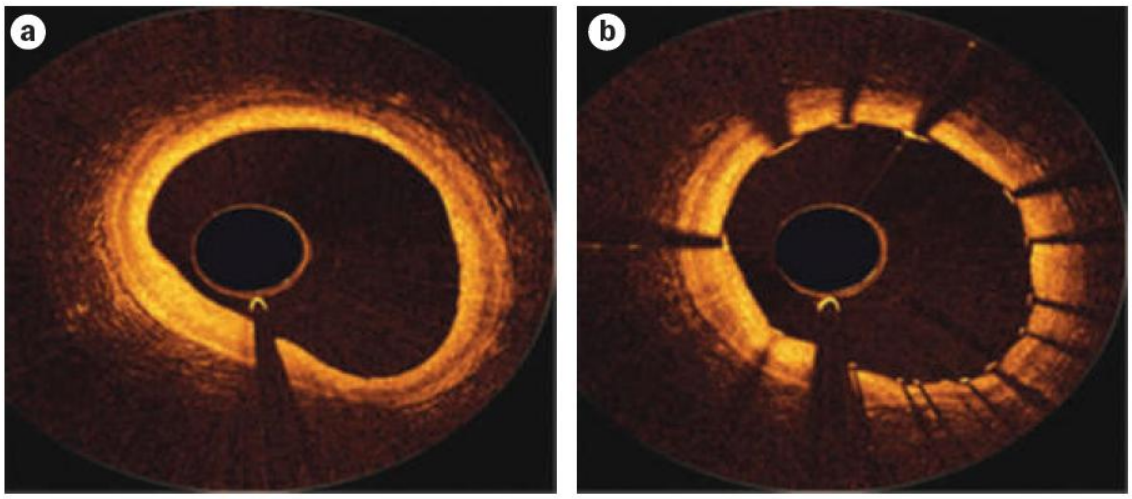

Author contributions:

Dr Rishi Puri – Preparation of manuscript

Associate Professor Matthew I. Worthley - Correction and critical review of manuscript

Professor Stephen J. Nicholls - Correction and critical review of manuscript

I hereby give permission for this published review article to be included in this thesis submission:

Dr Rishi Puri

Associate Professor Matthew I. Worthley

Professor Stephen J. Nicholls

CHAPTER 3: INVASIVE IMAGING OF CORONARY ENDOTHELIAL VASOMOTOR REACTIVITY – WHAT IS THE RATIONALE AND OPTIMAL REQUIREMENTS?

Imaging requirements

Although candidate mechanisms for the development of acute coronary syndrome (ACS) are complex and multi-factorial (Libby, 2013), it is widely accepted that a large volume of atheroma within an expansively remodeled conduit segment, vasoconstriction and platelet-rich thrombosis (Falk et al., 1995, Naghavi et al., 2003) are fundamental pathophysiological requirements for an ACS to occur.

Very little *in vivo* work has been done to demonstrate the link between various structural pre-requisites of 'vulnerable' plaque and segmental endothelial dysfunction. Although many believe that endothelial dysfunction is the earliest manifestation of atherosclerosis, its relationship with various structural and compositional measurements of coronary plaque has not been directly ascertained in culprit coronary segments in humans. Intravascular ultrasound (IVUS) is currently best positioned to evaluate the direct relationships between various plaque structural and compositional characteristics to underlying segmental vasomotor reactivity in humans.

Traditional methods of invasive coronary endothelial function testing have been comprehensively reviewed by others (Farouque and Meredith, 2001). These angiographic based methodologies however, are somewhat limited in their ability to quantify and co-register focal plaque burden and corresponding vasomotor reactivity.

Until now, the only demonstration of culprit segment vasoreactivity was undertaken in 7 patients with unstable angina using coronary angiography, ergometric bicycle exercise and cold pressor testing (Bogaty et al., 1994). This elegant, yet small study revealed enhanced culprit segment vasoreactivity, but preserved vasoreactivity in non-culprit vessels. These findings led the study authors to hypothesize that local, rather than systemic mechanisms were responsible for culprit lesion pathophysiology. However the use of coronary angiography failed to allow the authors to directly ascertain various plaque structural and compositional features and their relationship to segmental endothelial function. Other investigators relied on offline co-registration techniques in an attempt to match stimulated lumen responses on angiography to plaque measurements on IVUS (Nishimura et al., 1995, Lavi et al., 2009, Zeiher et al., 1994, Zeiher et al., 1991b, Manginas et al., 1998). In each of these studies, volumetric measurements of lumen response and plaque were not ascertained, resulting in conflicting observations of the coronary structure-function relationship (Nishimura et al., 1995). Other limitations common to these studies was the assessment of single, focal regions within the epicardial coronary tree, rather than appraising the entire imaged conduit vessel. Furthermore, some investigators limited their evaluations within individuals who displayed regions of conduit vasoconstriction, rather than an all-comers approach to patient inclusion (Lavi et al., 2009).

With these limitations in mind, a more comprehensive imaging approach for directly assessing the coronary structure-function relationship *in vivo* would ideally involve the volumetric appraisal of lumen response across multiple, non-overlapping, contiguous conduit segments during intracoronary provocation, and to directly evaluate

these responses with measures of plaque volume, vessel remodeling, plaque eccentricity and plaque composition. Ideally, a single imaging tool such as IVUS should be used to measure each of these components, avoiding the requirement of offline image co-registration.

Intracoronary stimuli

Despite optimizing the imaging methodology as described above, an appropriate, safe endothelium-dependent vasomotor stimulus during IVUS also warrants consideration. In considering the choice of stimulus, an important caveat for assessing endothelial function is the need to perform IVUS during/immediately following intracoronary (IC) infusions, and without pre-treatment with exogenous nitroglycerin (NTG). Pretreatment with NTG would likely cause significant vasodilation and therefore limit the assessment of significant, but subtle vasodilator changes in response to an endothelium-dependent stimuli. Consequently, the nature of the stimulus should be such that it has the capacity to cause endothelium-dependent vasodilatation, or only mild amounts of vasoconstriction during live IVUS imaging, to minimize the possibility of epicardial spasm and dissection.

Extending the earlier *in vitro* work performed by Furchgott and Zawadzki (Furchgott and Zawadzki, 1980), the initial demonstration of endothelial dysfunction (endothelium-dependent vasoconstriction) following IC acetylcholine (ACh) infusion within diseased human epicardial coronary arteries *in vivo* was made by Ludmer and colleagues in 1986 (Ludmer et al., 1986). ACh acts on muscarinic receptors to stimulate endothelial nitric oxide (NO) release, and subsequent endothelium-dependent

vasodilatation of both the coronary epicardial and microcirculation. In patients with preserved endothelial function, the normal response following IC ACh provocation is mild vasodilatation. Paradoxical vasoconstriction is observed in individuals with endothelial dysfunction. A number of agents other than ACh have been used to assess vasomotor reactivity, including IC bradykinin (Kato et al., 1997, Aptecar et al., 2000), substance P (Quyyumi et al., 1997b) and serotonin (McFadden et al., 1991). In the coronary microcirculation, IC infusions of ACh, substance P and bradykinin all have the capacity to augment coronary blood flow via vasodilatation of the myocardial resistance vessels (Drexler et al., 1989, Zeiher et al., 1991a). Endothelial shear stress caused by augmented arterial blood flow (following pharmacological stimuli, or tachycardia) results in a physiologic release of endothelial NO, and subsequent upstream epicardial (flow-mediated) vasodilatation. Mental stress also provokes endothelium-dependent flow-mediated vasodilatation (Yeung et al., 1991). Coronary microvascular endothelial dysfunction is thought to be present if an attenuated hyperemic response is demonstrated following provocation.

Endothelial adrenoreceptor stimulation

Activation of the sympathetic nervous system (mental stress or cold pressor testing) results in neuronal release of noradenaline, which further acts on conduit vessel α-adrenoreceptors to cause vasoconstriction (Zeiher et al., 1989). In individuals with preserved endothelial function, the α-adrenoreceptor-mediated effects are thought to be offset by flow-mediated dilatation secondary to sympathetic nervous system activation, whereas in diseased vessels, the net response is vasoconstriction (Farouque and

Meredith, 2001). These epicardial responses are believed correlate closely with ACh-induced changes.

The original observation that endothelial denudation significantly reduces β-adrenergic agonist-induced coronary arterial relaxation in canines (Rubanyi and Vanhoutte, 1985), provided evidence for the concept of β-adrenergic-mediated NO-dependent vasomotion. Within the human forearm, the vasodilator response to β_2-adrenoreceptor agonists was reduced by N^G-monomethyl-L-arginine (L-NMMA), the inhibitor of NO synthase (Dawes et al., 1997, Majmudar et al., 1999, Wilkinson et al., 2002). Although demonstrable within the intact human coronary microcirculation, Barbato and colleagues were not able to quite elucidate NO-dependent vasomotor reactivity within the human epicardial system *in vivo* (Barbato et al., 2005). Part of this may relate to a limited sample size of this study, but also the choice of coronary angiography to assess disease burden and lumen response. It is well accepted that angiography offers a 2-dimensional silhouette of blood flow within the arterial lumen, failing to provide a true appreciation of the amount of disease within the vessel wall (Topol and Nissen, 1995), as well as a complete 3-dimensional response the lumen following IC provocation. Importantly however, the Barbato study was the first to compare the epicardial and microvascular responses of the β_2-adrenoreceptor agonist, salbutamol, with achieved responses following IC ACh. Within normal coronary segments, IC salbutamol resulted in a significant degree of vasodilatation from baseline, comparable to the magnitude of responses achieved within normal segments with IC ACh. Within mildly diseased epicardial segments, IC salbutamol still caused reduced, yet preserved vasodilatation, whereas mild epicardial constriction was noted with IC

salbutamol in stenotic segments. In comparison, IC ACh caused significant vasoconstriction in both mildly diseased and stenotic epicardial segments. Infusions of IC phentolamine (α_1-adrenergic antagonist) followed by IC salbutamol in a subgroup of patients with stenotic lesions demonstrated complete abrogation of the salbutamol-induced vasoconstrictive response. These observations prompted the conclusion that within angiographically normal coronary arteries, there appears an important role for β_2-adrenergic receptor-mediated coronary vasomotion that is partially endothelium-mediated, but more so within the coronary microcirculation. Within stenotic segments however, there appeared to be impaired β_2-adrenergic receptivity with evidence of subsequent enhanced α-adrenoreceptor receptivity, with resultant vasoconstriction.

More recently, Jensen and colleagues provided the seminal identification of adrenergic receptor subtypes located within human epicardial coronary arteries (Jensen et al., 2009). Using mRNA assays and quantitative real-time reverse transcription polymerase chain reaction, this group identified that the predominant α-adrenoreceptor found within the human epicardial tree is the α1D subtype, with the α1A- and α1B-adrenoreceptors being present at very low levels. In contrast, the α1D subtype was present in very low amounts within the human myocardium. Importantly, coronary α1-adrenoreceptor levels totaled a mere one third the quantity of β-adrenoreceptors demonstrated within human coronaries, 99% of which were found to be of the β_2 subtype. The clinical implications of these findings therefore lie within the realm of possible pharmacological manipulation of arterial adrenoreceptors (i.e. a combined α1D antagonist and β_2 agonist) to selectively achieve arterial vasodilatation, without significant off-target myocardial or chronotropic effects. This theoretical possibility

could ultimately be positioned to treat systemic hypertension, coronary artery disease or the no-reflow phenomenon that occasionally occurs following percutaneous coronary intervention.

Hence, the findings of Jensen et al., in addition to those of Barbato et al., provided impetus for us to conduct a series of experiments to elucidate potential endothelium-dependent epicardial vasomotor effects of IC salbutamol. The nature of vasomotor response (equivalent vasodilatation to IC ACh, yet limited constriction compared with IC ACh), the potential of the endothelial adrenergic system as a therapeutic target, as well as the possibility of the non-invasive delivery of salbutamol, stimulated our interest in elucidating potential NO-dependent effects of IC salbutamol. With the enhanced resolution and topographic imaging capabilities of IVUS, it was felt that the potential coronary NO-dependent effects of IC salbutamol, stratified according to segmental plaque burden, would be readily ascertained.

CHAPTER 4: CORONARY β_2-ADRENORECEPTORS MEDIATE ENDOTHELIUM-DEPENDENT VASOREACTIVITY IN HUMANS: NOVEL INSIGHTS FROM AN *IN VIVO* INTRAVASCULAR ULTRASOUND STUDY

Adapted from PURI, R., LIEW, G.Y., NICHOLLS, S.J., NELSON, A.J., LEONG, D.P., CARBONE, A., COPUS, B., WONG, D.T., BELTRAME, J.F., WORTHLEY, S.G., WORTHLEY, M.I. 2012. Coronary β_2-adrenoreceptors mediate endothelium-dependent vasoreactivity in humans: novel insights from an in vivo intravascular ultrasound study. *Eur Heart J*. 33(4):495-504

Key words: salbutamol, β_2-adrenoreceptors, IVUS, endothelial function, atherosclerosis

ABSTRACT

Aims: The interaction between coronary β_2-adrenoreceptors and segmental plaque burden is complex and poorly understood in humans. We aimed to validate intracoronary (IC) salbutamol as a novel endothelium-dependent vasodilator utilizing intravascular ultrasound (IVUS), and thus assess relationships between coronary β_2-adrenoreceptors, regional plaque burden and segmental endothelial function.

Methods and Results: In 29 patients with near-normal coronary angiograms, IVUS-upon-Doppler Flowire imaging protocols were performed. Protocol 1: incremental IC salbutamol (0.15, 0.30, 0.60 μg/min) infusions (15 patients, 103 segments); Protocol 2: salbutamol (0.30μg/min) infusion before and after IC administration of N^G-monomethyl-L-arginine (L-NMMA) (10 patients, 82 segments). Vehicle infusions (IC dextrose) were performed in 4 patients (21 segments). Macrovascular response [% change segmental lumen volume (ΔSLV)] and plaque burden [percent atheroma volume (PAV)] were studied in 5 mm coronary segments. Microvascular response [percent change in coronary blood flow (ΔCBF)], was calculated following each infusion. Intracoronary salbutamol demonstrated significant dose-response ΔSLV and ΔCBF from baseline respectively (0.15μg/min: 3.5±1.3%, 28±14%, p=0.04, p=NS; 0.30μg/min: 5.5±1.4%, 54±17%, p=0.001, p<0.0001; 0.60μg/min: 4.8±1.6%, 66±15%, p=0.02, p<0.0001), with ΔSLV responses further exemplified in low versus high plaque burden groups. Salbutamol vasomotor responses were suppressed by L-NMMA, supporting nitric oxide-dependent mechanisms. Vehicle infusions resulted in no significant ΔSLV or ΔCBF. Multivariate analysis including conventional cardiovascular risk factors, PAV, segmental remodeling and plaque eccentricity indices identified PAV

as the only significant predictor of a ΔSLV to IC salbutamol (coefficient -0.18, 95% CI -0.32 to -0.044, p=0.015).

Conclusions: Intracoronary salbutamol is a novel endothelium-dependent epicardial and microvascular coronary vasodilator. IVUS-derived regional plaque burden is a major determinant of segmental coronary endothelial function.

The *in vivo* evaluation of the human coronary adrenergic system is complex (Barbato, 2009), whereby the significant interspecies and inter-territory variability of adrenoreceptor sub-type expression has resulted in numerous prior conflicting observations (Braun and Insel, 2009, Ferro et al., 1999, Bea et al., 1994, Macdonald et al., 1987). Specifically, the *in vivo* functional role of human coronary β_2-adrenoreceptors (β_2AR) in eliciting nitric-oxide (NO)-dependent vasoreactivity in varying stages of atherosclerosis remains unclear. Endothelial dysfunction is a systemic process shown to be an independent predictor of major cardiac events (Suwaidi et al., 2000, Schachinger et al., 2000, Halcox et al., 2002). Conduit vessel endothelial dysfunction has been recently shown to occur in a segmental fashion (Lavi et al., 2009), and thought to play a mechanistic role in mediating focal plaque disruption (Bogaty et al., 1994). Additionally, the intravascular ultrasound (IVUS)-derived burden of coronary atherosclerosis has been shown to be a strong predictor of future cardiac events (Nicholls et al., 2010). However, the fundamental *in vivo* relationship between segmental coronary endothelial function and regional plaque burden in humans is unknown. Defining this dynamic relationship might provide incremental information regarding plaque stability, progression and relationship to future coronary events.

The present study was designed to (1) assess the safety and physiologic responses of selective coronary β_2AR stimulation [with intracoronary (IC) salbutamol delivery] during IVUS and Doppler Flowire imaging, and (2) test that the coronary arterial salbutamol response is NO-dependent, (3) utilize this validated stimulus and IVUS imaging to investigate the fundamental determinants of segmental coronary

endothelial function in humans, with a particular emphasis upon this dynamic relationship with corresponding regional plaque burden.

METHODS

Study subjects

This study enrolled 29 patients (aged ≥18 years) electively referred to the Royal Adelaide Hospital Cardiac Catheterization Laboratories for the investigation of chest pain. Informed consent was obtained >48 hours prior to the procedure and all vasoactive medications were held for 24 hours prior to the study. All procedures were performed on a morning list following an overnight fast. Patients with significant valvular heart disease, left ventricular dysfunction, prior percutaneous or surgical coronary revascularization, recent acute coronary syndrome (within 4 weeks), known predilection to coronary artery spasm, calculated creatinine clearance of ≤60 mL/min, chronic β-blocker therapy or the use of short or long acting β_2-agonists within the previous 12 hours were excluded. Target vessels with visual angiographic stenoses of >30% were excluded. Fasting blood samples for serum lipids, high sensitivity C-reactive protein (hsCRP), and biochemistry were obtained at angiography. This study was approved by the Royal Adelaide Hospital Human Research Ethics Committee.

Catheterization, imaging and coronary endothelial function testing protocols

Coronary angiography was performed via a standard 6 French technique. Intravenous heparin (70 IU/kg) was administered for the research protocol. Following intubation of the left (or right) coronary system, a 0.014 inch Doppler guide wire (Flowire; Volcano Therapeutics, Rancho Cordova, CA, USA) was placed into the target vessel within its

mid-segment away from major side-branches. This wire was also used to monorail a 2.5 French 40 MHz Atlantis SR Pro IVUS catheter (Boston Scientific, Natick, MA, USA) into the study artery. This technique allowed for the dual and simultaneous assessment of macro- and microvascular coronary responses to IC infusions. All IC infusions were administered through a Medrad infusion pump at 2ml/min via the coronary guiding catheter for a period of 5 minutes. Intravascular ultrasound was performed in the usual fashion, but *without* pre-treatment of the target vessel with IC nitroglycerin. After 3 minutes of IC infusion, the instantaneous average peak velocity (APV) was recorded, followed by the guide wire being repositioned into the distal vessel and IVUS pullback commenced at 0.5 mm/sec. The infusions continued for the remaining 2-minutes during which IVUS acquisition/pullback was undertaken. All IVUS images were saved and recorded on a DVD for off-line analysis.

Infusion protocols

This study involved two main active infusion protocols summarized in Figure 1. Protocol 1 assessed the safety and efficacy of the imaging methodology with incremental IC salbutamol doses. Concentrations of IC salbutamol previously shown not to significantly affect heart rate and blood pressure were evaluated (Barbato et al., 2005). Following a baseline 5-minute period of 5% IC dextrose infusion, 15 patients underwent sequential 5-minute infusions of IC salbutamol at doses of 0.15, 0.30 and 0.60 μg/min respectively, with APV measurements and the initiation of the IVUS pullback performed at the 3 minute mark (Figure 1a). The second protocol was designed to assess the endothelium-dependent nature of IC salbutamol upon the epicardial coronary conduit vessel. An additional 10 patients underwent a 5 minute IC salbutamol

infusion at 0.30 μg/min (selected upon the findings from protocol 1) both before and after NO synthase inhibition with N^G-monomethyl-L-arginine (L-NMMA, Bachem Distribution Services GmbH, Weil am Rhein, Switzerland) given at 20 μmol/min for 5 minutes (Anderson et al., 2005, Seddon et al., 2009) (Figure 1b). All patients received IC nitroglycerin at the completion of the protocol, and cine angiography was performed to confirm the absence of coronary spasm or local dissection.

In order to determine the variation in segmental coronary lumen measurements and coronary blood flow over time, another 4 patients underwent IVUS and Doppler Flowire imaging following each of 4 consecutive IC dextrose (vehicle) infusions.

Data acquisition and analysis

Hemodynamics: Hemodynamic data (aortic pressure) and ECG was digitally recorded and printed at the end of each step of the infusion protocol.

Intravascular ultrasound: All IVUS data was analyzed using echoPlaque 3.0.53 (Indec Systems, Santa Clara, CA, USA). From the initial IVUS run, the common most distal and proximal fiducial markers (anatomical side-branches) were chosen to define the region of vessel to be analyzed. Cross-sectional images were selected every 30 frames (0.5 mm) apart. Each IVUS run was precisely divided into pre-defined 5 mm segments comprising of 10 cross-sectional frames spaced 0.5 mm apart (Figure 2). Due to angiographically proven heterogeneity of coronary vasodilator function (Penny et al., 1995), each segment was evaluated separately. Using MIB software (Indec Medical Systems, Santa Clara, CA, USA), the baseline IVUS run (with numbered frames) was simultaneously played with each subsequent IVUS run in order to precisely frame

match anatomical fiducial markers between each run. This technique ensured that the same arterial segments were consistently analyzed for each infusion. The leading edges of the lumen and external elastic membrane (EEM) were traced by manual planimetry. Plaque area was defined as the area occupied between these leading edges. Only cross-sectional images deemed acceptable for complete lumen and EEM analysis were included. Percent atheroma volume (PAV) was chosen as our determinant of segmental plaque burden (Nicholls et al., 2010). This was calculated as the proportion of the entire vessel cross-sectional area of that segment occupied by atherosclerotic plaque:

$\mathbf{PAV} = \sum [(EEM_{area} - Lumen_{area}) / \sum EEM_{area}] \text{ X } 100$

Segmental lumen volumes (SLV) were calculated as the summation of lumen area in each measured image. The SLV for each 5 mm segment was normalized to account for differences in the number of analyzable frames within each pre-defined segment:

$\mathbf{SLV_{normalised}} = \sum [(Lumen_{area}) / \text{number of images in segment}] \text{ X } 10.$

Percentage changes in SLV (ΔSLV) were used as the primary analysis of segmental vasomotor response. Low and high plaque burden groups were defined around the mean PAV for respective analysis regarding plaque burden. Segmental remodeling indices (RI) were determined by calculating the average segmental EEM_{area} dividing this by a reference EEM_{area} taken from either a proximal or distal reference point located within 10 mm from the index segment with the least plaque burden. Segmental eccentricity indices (EI) were determined by calculating the average of all EI's of each analyzable frame within a coronary segment (EI= ratio of maximal to minimal plaque thickness) (Mintz et al., 1996). All measurements were performed with the analyst blinded to the

specific segment, and the degree of plaque burden and lumen response from preceding infusion sequences.

Coronary Blood Flow: A Doppler flowire-derived APV was determined from instantaneous velocity signals from the Doppler wire by an online fast Fourier transform. Coronary blood flow (CBF) was calculated from the product of IVUS-derived average segmental cross-sectional area (CSA) and Doppler flowire-derived APV using the equation: CBF = CSA x APV/2 (Lavi et al., 2009). Percent change in CBF (ΔCBF) from baseline was assessed for each patient for each run in all infusion protocols.

Statistical analysis

Data are expressed as mean ± SEM or median (IQR) as appropriate. The effect of salbutamol dose and covariates upon ΔSLV was evaluated by mixed effects modeling. To identify univariate predictors of SLV and SLV response to salbutamol, the covariate of interest and salbutamol dose, and the covariate*dose interaction were modeled as fixed effects, with subject identity and arterial segment modeled as random effects to account for repeated measures within arterial segments within patients. For significant covariate*dose interactions, *post hoc* testing was performed at each dose. Two multivariate models were then constructed. First, any covariate with significant dose-dependent association with SLV on univariate analysis and second, any covariate whose main effect on SLV independent of salbutamol dose exhibited a p-value <0.2 was included. Independent predictors of change in SLV were then identified by multivariate mixed-effects modeling using backward elimination. In the second analysis, we determined whether incremental predictive value for change in SLV was added by the

stepwise inclusion of covariates found to or previously reported to influence SLV, using the likelihood-ratio test. Intra- and inter-observer variability analysis was performed following planimetry of lumen and plaque areas from 20 randomly selected IVUS frames by 2 independent observers and by 1 observer at 2 separate time points. All statistical tests were two-sided and a p-value <0.05 considered significant. Statistical analysis was performed with STATA 11 (Stata Corp, College Station, Texas).

RESULTS

Clinical, hemodynamic and observer variability data

Baseline demographics of the study cohort are shown in Table 1. Two patients experienced transient coronary spasm during instrumentation, prior to IC infusions (one during Flowire manipulation and second with the IVUS catheter), both responding promptly to IC nitroglycerin. These patients were excluded from the research protocol, and data not included in the analysis. In protocol 1, successive doses of IC salbutamol, and in protocol 2, the infusion of L-NMMA each had no significant effect upon baseline blood pressure or heart rate respectively. For coronary lumen measurements, the intra-observer coefficient of variation was 1.1%, and inter-observer coefficient of variation was 2.6%. For plaque measurements, the intra-observer coefficient of variation was 1.8%, and the inter-observer coefficient of variation was 3.8%.

IVUS and CBF results (Protocol 1)

Analysis from protocol 1 (n=103 segments) suggests a dose-dependent increase in SLV across all segments from baseline (ΔSLV: 0.15 μg/min: 3.5±1.3%, p=0.04; 0.30 μg/min: 5.5±1.4%, p=0.001; 0.60 μg/min: 4.8±1.6%, p=0.02) (Figure 3a). Absolute variations of

mean SLV values across all segments (including for stratification of plaque burden) at various time points are shown in Table 2 and largely reflect the corresponding percent changes in SLV that were observed from baseline. Segmental plaque burden was dichotomized into low (mean PAV 15±0.6%) and high (mean PAV 38±1.5%) plaque burden groups using the mean sample PAV as the cut-off. The vasodilator properties of IC salbutamol were observed at all doses within the low plaque burden group (ΔSLV: 0.15 μg/min: 5.8±1.8%, p=0.015; 0.30 μg/min: 9.1±1.9%, p<0.0001; 0.60 μg/min: 8.8±2.1%, p=0.001) but were no longer significant in the high plaque burden group (ΔSLV: 0.15 μg/min: 1.2±1.8%, p=0.25; 0.30 μg/min: 1.8±1.8%, p=0.2; 0.60 μg/min: 0.7±2.2%, p=0.5), with significant differences seen between low and high plaque burden groups noted at both the 0.3 and 0.6 μg/min doses (p<0.01 respectively).

There was a progressive and significant ΔCBF from baseline with escalating doses of IC salbutamol (ΔCBF: 0.15 μg/min: 28±14%, p=0.04; 0.30 μg/min: 54±17%, p<0.0001; 0.60 μg/min: 66±15%, p<0.0001) (Figure 3b).

Based upon the results of Protocol 1, a salbutamol dose was chosen to resemble a sub maximal 'EC50' dose, in order to provide the optimal chance of differentiating subtle changes in vasomotor reactivity according to varying degrees of plaque burden for the planned L-NMMA infusion in Protocol 2. While changes (percent change from baseline and absolute change) in conduit vessel volumes were similar between the 0.30 and 0.60 μg/min salbutamol doses, microvascular effects were less when comparing the effects of the 0.30 μg/min with the 0.60 μg/min dose of salbutamol from Protocol 1

respectively (Figure 3). Hence, for Protocol 2, the 0.30 μg/min of salbutamol was chosen (with L-NMMA) to evaluate its NO-dependent vasomotor properties.

IVUS and CBF results (Protocol 2)

The infusion sequence in Protocol 2 was designed to assess the potential endothelium-dependent effects of IC salbutamol within the epicardial coronary vasculature (n=82 segments). In all segments (irrespective of plaque burden), salbutamol produced a significant increase in ΔSLV compared to baseline (4.7±1.6%, p=0.03). Following IC L-NMMA, repeat IC salbutamol infusion no longer caused a significant increase in ΔSLV (0.03±1.4%, p=0.78) (Figure 4a), and this response was significantly impaired compared with the vasomotor changes observed from the initial salbutamol infusion (p = 0.03). Absolute variations of mean SLV values (including for stratification of plaque burden) across all segments at various time points are shown in Table 2 and largely reflect the corresponding percent changes in SLV that were observed from baseline. Conduit segments were further stratified according to low (mean PAV 19±1.3%) and high (mean PAV 41±1.0%) plaque burden groups. In the low plaque burden group, salbutamol infusion resulted in a significant ΔSLV of 7.0±1.5% from baseline (p<0.0001). The addition of L-NMMA resulted in a significant blunted salbutamol response, however with incomplete vasodilator abolishment noted (ΔSLV of 3.8±1.9%, p=0.09 vs. baseline). In the high plaque burden group, salbutamol infusion resulted in an insignificant degree of vasodilatation from baseline (ΔSLV 0.74±2.0%, p=0.9). The addition of L-NMMA resulted in a net degree of vasoconstriction compared to baseline (ΔSLV -3.8±1.9%, p=0.09), which was significant lower compared to the initial salbutamol infusion (p<0.01).

In protocol 2, ΔCBF significantly increased from baseline following the first infusion of salbutamol (ΔCBF 56±22%, p<0.01). Following IC L-NMMA, repeat IC salbutamol infusion no longer caused a significant increase in ΔCBF (5.5±12, p=0.9) (Figure 4b), and this response was also significantly impaired compared with the vasomotor changes observed from the initial salbutamol infusion (p < 0.01).

IVUS and CBF results (Repeated IC vehicle infusions)

In the 4 patients (21 segments) who underwent 4 consecutive vehicle (IC dextrose) infusions, there was no significant variation in ΔSLV (Run 2: -2.3±1.9%, p=0.24; Run 3: 2.7±2.1%, p=0.20; Run 4: -0.38±2.7%, p=0.73) and ΔCBF (Run 2: 6.4±1.6%, p=0.20; Run 3: 7.8±2.1%, p=0.15; Run 4: 1.4±7.3%, p=0.85) following each infusion compared to baseline (Run 1). These experiments confirm no impact of intracoronary vehicle infusion or coronary instrumentation on dynamic vascular measurements over time. Mean absolute SLV values at each time pint are depicted in Table2.

Determinants of segmental coronary endothelial function

Systemic patient factors (age, hypertension, smoking, LDL, HDL, hsCRP) and local plaque/vessel factors (segmental PAV, RI, EI) were each evaluated as univariate predictors of segmental endothelial function. Segmental plaque burden (PAV) was found to be the only significant univariate predictor (coefficient -0.18, 95% CI -0.32 to -0.044, p=0.009) of ΔSLV (Table 3). Age and LDL were forced into a multivariate model with PAV to identify independent predictors of ΔSLV response to salbutamol. PAV was found to be the sole independent predictor of ΔSLV from baseline (p=0.015).

Likelihood ratio testing was performed to determine the predictive capacity of cardiovascular risk factors (age, hypertension, smoking, LDL, HDL, hsCRP - each of which have been previously shown to influence coronary vasoreactivity) (Vita et al., 1990, Schindler et al., 2004, Lavi et al., 2007), and plaque burden (PAV) in determining a change in the salbutamol-endothelial conduit vessel response. As observed in Figure 5, each risk factor imparted a significant, individual effect upon the salbutamol-endothelial conduit vessel response, when assessed in a stepwise manner. For example, age was a significant predictor of the change in the salbutamol-endothelial vasomotor response, however the combination of age and hypertension was more predictive of the salbutamol-endothelial response than age alone, and so on. Furthermore, plaque burden remained a major predictor of the segmental-endothelial conduit vessel response, above and beyond the cumulative predictive effect of all cardiovascular risk factors summated in the model.

DISCUSSION

We have successfully described the physiological role of coronary β_2AR's in mediating endothelium-dependent vasoreactivity across various stages of atherosclerotic disease within the *in vivo* human epicardial coronary circulation. The study achieved its objectives demonstrating that IC salbutamol mediates its vasoactive effects via NO within both the coronary macro- and microvasculature, supporting earlier *in vitro* (Molenaar et al., 1988, Rubanyi and Vanhoutte, 1985, Gray and Marshall, 1992), and human *in vivo* observations within the peripheral vasculature (Dawes et al., 1997, Wilkinson et al., 2002). Furthermore, we also show for the first time the incremental

predictive capacity of regional plaque burden in determining corresponding segmental coronary endothelial responses, above and beyond that of the cumulative burden of traditional cardiovascular risk factors. These insights provide an explanation of the observed heterogeneity in vasomotor response within an epicardial coronary artery in a majority of our patients, which has been elusive with conventional quantitative coronary angiographic (QCA) assessment.

Beta$_2$ – adrenoreceptors, salbutamol and human coronary arteries

Although the presence of β_2AR's upon human coronary vascular endothelial cells has been well described (Molenaar et al., 1988), their physiological responses within an intact human coronary arterial system are complex (Whalen et al., 2000, Stein et al., 1995), with such responses being further susceptible to a number of genetic polymorphisms that result in functional alterations of the receptor complex and subsequent vascular response (Dishy et al., 2001). Since the original finding that removal of endothelium reduces βAR-agonist induced vasorelaxation of canine coronary arteries (Rubanyi and Vanhoutte, 1985), accumulating evidence has suggested that endothelium mediated β-adrenergic induced vasorelaxation is impaired by endothelial removal or inhibition of NO synthesis (Gray and Marshall, 1992, Graves and Poston, 1993, Toyoshima et al., 1998, Parent et al., 1993, Gardiner et al., 1991).

Very few studies have investigated the *in vivo* function of endothelial β_2AR's in humans. The direct infusion of salbutamol into the intact human brachial artery or inhaled salbutamol, have each been shown to posses endothelium-dependent properties within the peripheral vasculature (Dawes et al., 1997, Wilkinson et al., 2002). The only

prior study conducted within intact human coronary arteries was undertaken by Barbato *et al*., who utilized QCA and Flowire methodology to elegantly show a microvascular endothelium-dependent vasomotor effect of salbutamol, as well as impaired β_2AR responsiveness coupled with enhanced αAR tone in angiographically stenotic conduit segments, which together mediated a constrictive effect of salbutamol in these segments (Barbato et al., 2005). Similar mechanisms were observed in our experiments when subgroup analysis was done according to the degree of plaque burden present. Although it may be possible that the residual degree of salbutamol-mediated vasodilatation observed in the low plaque burden group following L-NMMA may be due to salbutamol-mediated smooth muscle cell effects (Sun et al., 2002), it is more likely that our findings are a result of the variability in L-NMMA-mediated NOS inhibition in relation to the degree of plaque burden present. It is also likely that low atheroma burden segments require higher doses of L-NMMA for complete NOS inhibition, which may reflect the residual endothelium-dependent vasodilating effects of salbutamol observed. In contrast, higher atheroma burden segments may release much less NO, and thus require lower doses of L-NMMA to completely inhibit the residual amount of NOS present. This was evident with complete abolition of NOS resulting in net coronary vasoconstriction, due to impaired β_2AR responsiveness and enhanced αAR tone, as described by Barbato et al (Barbato et al., 2005).

Utilizing IVUS, a more a sensitive imaging methodology, our study shows that IC salbutamol (and epicardial β_2AR stimulation) possesses NO-dependent properties within the intact human coronary vasculature, synonymous with acetylcholine-induced muscarinic receptor stimulation mediating NO-dependent vasoreactivity. Moreover, the

magnitude of segmental coronary vasomotor reactivity observed within our study are consistent with responses observed in some prior studies evaluating the dose-response effects of IC acetyl choline (Newman et al., 1990, Hollenberg et al., 1999), and similar in magnitude to the IC salbutamol responses reported by Barbato et al.(Barbato et al., 2005). However from a mechanistic viewpoint, unlike acetylcholine, βAR-agonists are not known to activate the inositol 1,4,5 triphosphate signalling pathway. Therefore alternative mechanisms are likely to explain our observations. These may include (a) synergism between the actions upon adenylate cyclase of exogenous βAR-agonists and endothelium derived prostaglandins (Rubanyi and Vanhoutte, 1985) ; (b) inhibition of cyclic adenosine monophosphate (cAMP) phosphodiasterase by cyclic guanosine monophosphate (cGMP) (produced within vascular smooth muscle cells) in response to basal endothelium-NO release (Miyata et al., 1992) ; (c) β_2AR-mediated endothelial cAMP synthesis to directly stimulate NO synthase and subsequent release of endothelial NO (Gray and Marshall, 1992, Ferro et al., 1999) and/or (d) activation of potassium channel-induced endothelial hyperpolarization and subsequent NO-synthase activation via Ca^{2+}/calmodulin (Graier et al., 1993). Despite these postulated mechanisms, the functional significance of β_2AR's within the human coronary arterial system however cannot be understated. Adrenergic stimulation plays an important role in the regulation of coronary vasomotor tone, whereby both endothelial β_1 and β_2 AR's contribute towards vasodilatory drive, opposing the vasoconstrictive effects of endothelial αAR's, particularly within atherosclerotic coronary arteries (Baumgart et al., 1999, Heusch et al., 2000). A recent characterization of the relative expression of α and βAR-subtypes within human epicardial coronary arteries has uncovered that two-thirds of all such

AR's are of the βAR type, of which 99% are of the β_2AR sub-type (Jensen et al., 2009). Given the recent discovery of the α_1DAR being the predominant αAR responsible for epicardial coronary vasoconstriction (Heusch et al., 2000, Jensen et al., 2009), the interplay between coronary β_2 and α_1D AR function will therefore be important for the selective modulation of coronary vasomotor tone as a potential novel therapeutic strategy.

Plaque burden and vessel function seen with IVUS

The discrepancy between findings on coronary angiography (or 'lumenography') and IVUS in the assessment of plaque burden has been well documented (Topol and Nissen, 1995). Intravascular ultrasound frequently demonstrates the ubiquitous presence of plaque within angiographically normal coronary arterial segments. Prior attempts to characterize the structure-function relationship between plaque burden and epicardial coronary vasoreactivity failed to systematically evaluate volumetric indices of plaque burden, and at best relied upon the off-line matching of QCA-derived lumen diameter responses with plaque topography measured separately with IVUS (Manginas et al., 1998, Nishimura et al., 1995, Schachinger and Zeiher, 1995, Lavi et al., 2009). The comprehensive method of assessing pan-segmental volumetric endothelial luminal response with IVUS has confirmed the heterogeneous dynamic properties of the human epicardial coronary vasculature, with all but 3 patients exhibiting both segmental vasodilatation and vasoconstriction in adjacent segments. Our data supports the heterogeneity of segmental lumen vasoreactivity to be intrinsically related to plaque burden, not detected angiographically (Penny et al., 1995).

Recent analysis has demonstrated a significant relationship between the baseline extent and progression of disease, as determined by IVUS, with the prospective risk of major adverse cardiac events (Nicholls et al., 2010). These observations were made in stable patients within non-critically diseased vessels. The mean baseline PAV value of 38.6 % in these trial patients compared similarly with the mean PAV within segments that were stratified as having high plaque burden in our protocols. Most of the segments with this extent of PAV exhibited blunted vasomotor (or mild vasoconstrictive) responses to IC salbutamol. We also found that PAV provides a significant and incremental prediction of focal coronary endothelial function beyond what the cumulative burden of atherosclerosis risk factors provide. This strengthens the validity of PAV as an important biomarker of coronary risk. It remains unclear from the large collection of patients in the various atheroma progression–regression trials as to whether plaque burden itself, component risk factors or localized endothelial dysfunction, mediates further disease progression.

Clinical and future implications

Further work is required in this area to evaluate the impact of segmental coronary endothelial function upon atheroma progression, plaque instability and ultimately clinical outcomes. It is increasingly apparent that plaque burden is an important biomarker of future coronary risk. Factors linking plaque burden to vessel function may therefore be pivotal in determining the likelihood of a clinical event from a given atheromatous coronary arterial segment. This will require future coronary imaging modalities to incorporate not only structural, but also vascular dynamic information when risk-assessing potentially high-risk plaque segments. Furthermore, there exists a

unique opportunity to selectively modulate coronary endothelial function as a method to alter the natural progression of coronary atherosclerosis via the coronary endothelial adrenergic system (Maseri et al., 2009).

Limitations

Additional infusion sequences to the current experimental protocols would allow for further exploration of the underlying mechanisms involved in the salbutamol-mediated human coronary vasomotor response. However, the practicality of doing this are limited by ethical concerns of infusing novel, vasoconstricting substances *in vivo* within human coronary arteries during a prolonged and highly invasive protocol. Nevertheless, such limitations of our experimental protocols include the inability to entirely exclude a non-specific vasoconstrictive effect of IC L-NMMA. Further infusions to evaluate the effects of concomitant dosing of a selective β_2AR antagonist acting as an endothelium-independent vasoconstrictor (i.e. butoxamine) with progressive doses of IC salbutamol could be performed, as has been the case within the *ex vivo* human coronary arterial setting (Sun et al., 2002), to address this issue. To the best of our knowledge, our study is the first to utilize IVUS to evaluate *in vivo* lumen responses to IC L-NMMA. However it is known that while L-NMMA blocks the oxidation of L-arginine, it fails to inhibit the formation of superoxide anions from molecular oxygen, and thus may have provided incomplete NOS inhibition in our low atheroma burden group. Therefore, although rarely used during *in vivo* human experimentation, L-N^G-Nitroarginine (L-NNA) is considered to be a more ideal inhibitor of NO synthase. However its safety of administration within the human *in vivo* intracoronary setting is uncertain. Time constraints also limited the further evaluation of the impact of segmental plaque burden

upon assessing endothelium-independent vasomotion following IC nitroglycerin administration, which would have provided incremental mechanistic information to the above findings.

We also cannot reliably exclude a concomitant direct salbutamol-induced smooth muscle vasorelaxation effect as shown by Sun et al. (Sun et al., 2002), nor can we exclude an upstream flow-mediated effect due to the observed changes in coronary blood flow. Although the use of state-of-the-art imaging software enabled a precise degree of real-time frame matching for segmental analysis with multiple IVUS runs, subtle degrees of horizontal bias due to subtle variations in actual catheter pullback speeds between different runs may result in slight variations in repeated measurements over multiple IVUS runs. We however feel this has not significantly impacted upon our results. Finally, true mechanistic studies involving the determination of segmental tissue expression of various effector molecules, and the contribution of genetic polymorphisms, are unable to be achieved during human *in vivo* studies, and further human *ex vivo* or *in vitro* studies will need to be conducted to explore the underlying molecular mechanisms of our findings.

CONCLUSIONS

We provide important insights into the functional role of coronary β_2AR's in varying degrees of health and segmental atherosclerotic coronary disease, and outline the NO-dependent properties of these receptors within human coronary arteries *in vivo*. This study has shown that IC salbutamol is both a macro- and microvascular coronary endothelium-dependent vasodilator. These findings within the macrovasculature have

been demonstrated using a novel IVUS-based methodology, which has further shown segmental plaque burden to be a strong independent predictor of endothelium-dependent coronary conduit vessel vasodilatation.

FIGURE LEGENDS

Figure 1: Infusion protocols

(a) Incremental salbutamol dose response protocol (Protocol 1) (b) salbutamol and L-NMMA protocol (Protocol 2).

Figure 2: Segmental volumetric lumen & plaque analysis with IVUS

IVUS pullback divided into 5-mm segments (denoted by red lines on longitudinal view). Within each segment, plaque and lumen volumes were calculated upon sequential numbered frames spaced 0.5 mm apart, numbered 1-10 (cross-sectional views).

Figure 3: Salbutamol dose-responses: macro- and microvasculature (Protocol 1)

(a) All segments. * $p < 0.05$ vs. baseline (b) CBF response to incremental salbutamol dosing. * $p < 0.0001$ vs. baseline, # $p < 0.05$ vs. low dose salbutamol

Figure 4: Salbutamol & L-NMMA responses: macro- and microvasculature (Protocol 2)

(a) All segments. * $p < 0.05$ salbutamol vs. baseline, # $p < 0.05$ salbutamol vs. salbutamol + L-NMMA. (b) CBF responses. * $p < 0.01$ salbutamol vs. baseline, # $p < 0.01$ salbutamol vs. salbutamol + L-NMMA

Figure 5: Cumulative value of cardiovascular risk factors and plaque burden in predicting segmental endothelial function

Each nested model's ability to predict segmental coronary endothelial function is compared with the adjacent model using the likelihood ratio test

TABLES

TABLE 1: Clinical characteristics

	Entire cohort n=29
Age, years	58 ± 3
Male, n (%)	13 (45)
Smoking, n (%)	16 (55)
Hypertension, n (%)	10 (34)
Diabetes, n (%)	4 (14)
Family History CAD, n (%)	4 (14)
Medications, n (%)	
Aspirin	15 (52)
Statin	9 (31)
ACEI/ARB	8 (26)
Calcium channel blocker	3 (10)
Lipids, mg/dL	
total cholesterol	176 ± 4
TGL	62(45,98)
HDL	50 ± 11
LDL	112 ± 6
hsCRP, mg/L	2.5(1.6,4.6)
Artery Investigated, n (%)	
LAD	24 (83)
LCx	4 (14)
RCA	1 (3)

ACEI = angiotensin converting enzyme inhibitor; ARB = angiotensin receptor blocker; CAD = coronary artery disease; HDL = high-density lipoprotein; LAD = left anterior descending artery; LCx = left circumflex artery; LDL = low-density lipoprotein; RCA = right coronary artery; TGL = triglycerides

TABLE 2: Mean absolute SLV values at each time point per infusion protocol

Protocol	**Mean SLV at each time point (mm^3)**			
Protocol 1	**Baseline**	**Salb low dose**	**Salb mod dose**	**Salb high dose**
All segments	101.4±4.0	103.4±3.9	106.3±4.2†	104.7±4.0
Low PAV	119.5±5.6	123.7±5.3	127.9±5.4‡	127.2±5.2*
High PAV	82.2±4.4	81.9±3.9	83.4±4.6	80.9±4.1
Protocol 2	**Baseline**	**Salb dose # 1**	**L-NMMA**	**Salb dose # 2**
All segments	83.4±3.4	87.2±3.3†	81.6±3.3‡	82.5±3.3$^{\wedge}$
Low PAV	88.1±5.2	93.1±5.2$^{\#}$	89.6±4.7	90.3±5.0
High PAV	78.7±4.3	78.2±4.2	73.6±4.5**	74.7±4.0
Control	**Run 1**	**Run 2**	**Run 3**	**Run 4**
All segments	79.7±7.2	77.9±7.3	81.7±4.9	80.4±8.1

PAV = percent atheroma volume, SLV = segmental lumen volume
$^{\#}$ p=0.02, * p<0.01, † p<0.001, ‡ p<0.0001 (all vs. baseline)
$^{\wedge}$ p=0.03 vs. salb dose # 1, ** p<0.01 vs. baseline and salb dose # 1

TABLE 3: Univariate and multivariate predictors of salbutamol-induced SLV

Variable	Univariate			Multivariate		
	Coefficient (95% CI)		p-value	Coefficient (95% CI)		p-value
EI	-0.021	(-0.34 to 0.29)	0.9			
HDL	-0.30	(-9.1 to 8.5)	0.9			
Smoker	0.69	(-5.7 to 7.1)	0.8			
hsCRP	-0.17	(-0.53 to 0.19)	0.4			
RI	-7.0	(-19 to 5.2)	0.3			
Hypertension	3.7	(-2.0 to 9.4)	0.21			
Age*	-0.20	(-0.43 to 0.033)	0.1	-0.16	(-0.38 to 0.060)	0.3
LDL*	-2.1	(-4.8 to 0.50)	0.1	-1.4	(-1.9 to 1.1)	0.2
PAV*	-0.18	(-0.32 to -0.044)	0.01	-0.17	(-0.31 to -0.03)	0.02

* represents univariate predictors entered into multivariate model
EI = eccentricity index; HDL = high-density lipoprotein; hsCRP = high sensitivity C-reactive protein; RI = remodeling index; LDL = low-density lipoprotein; PAV = percent atheroma volume

FIGURES

Figure 1

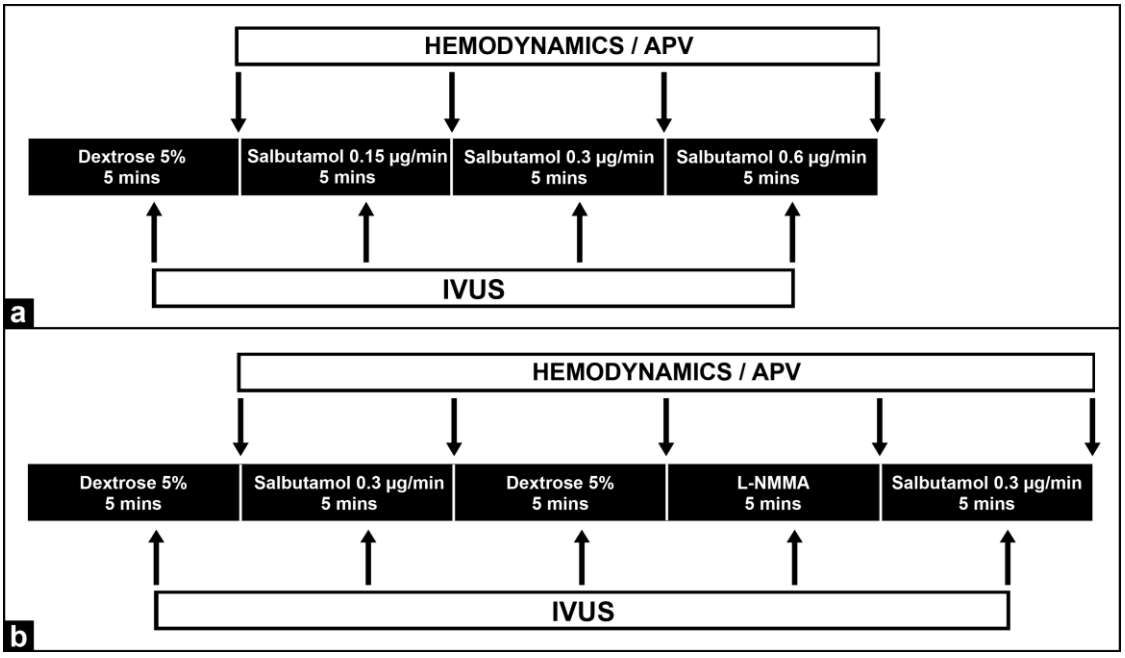

Figure 2

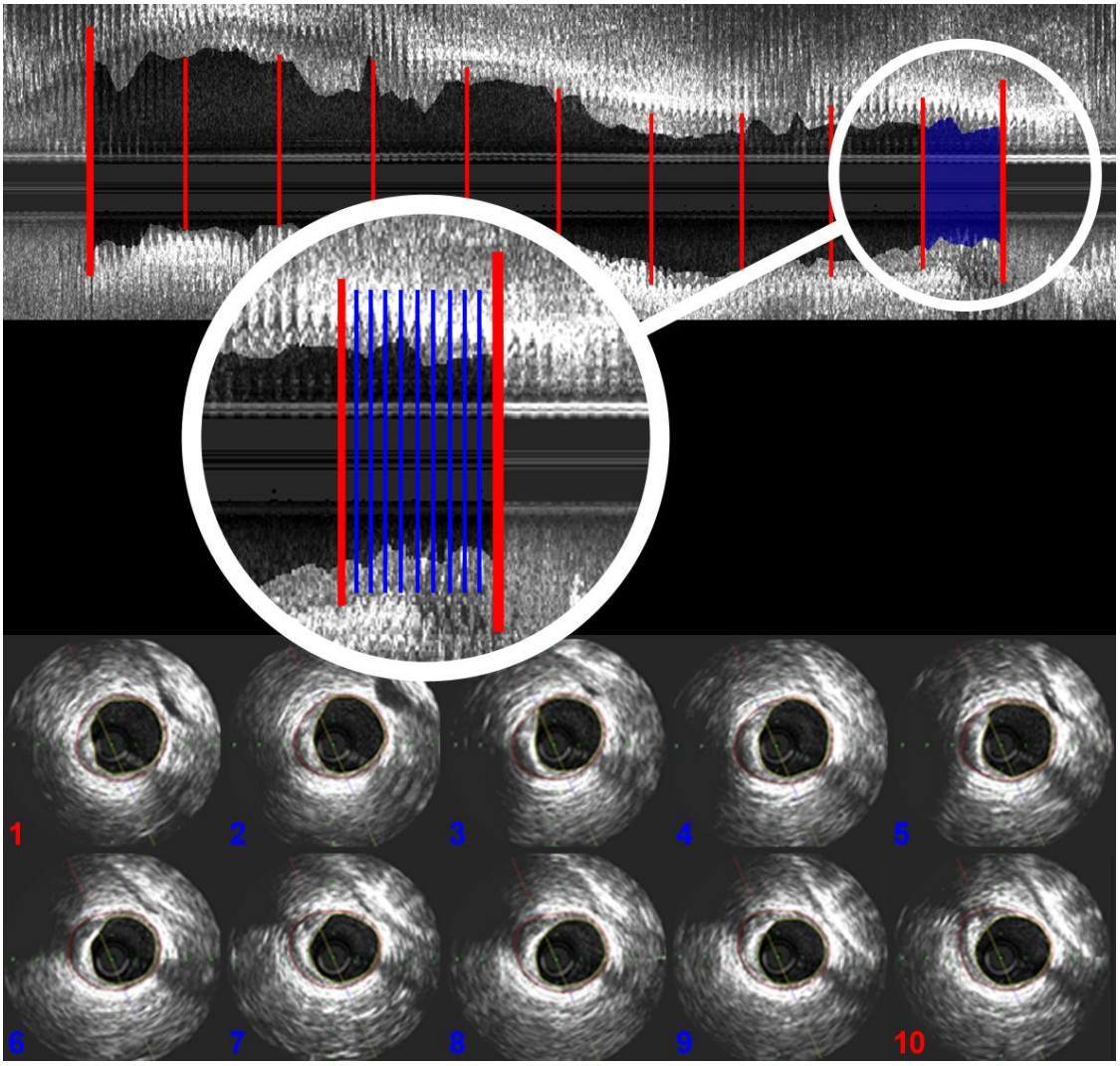

Figure 3

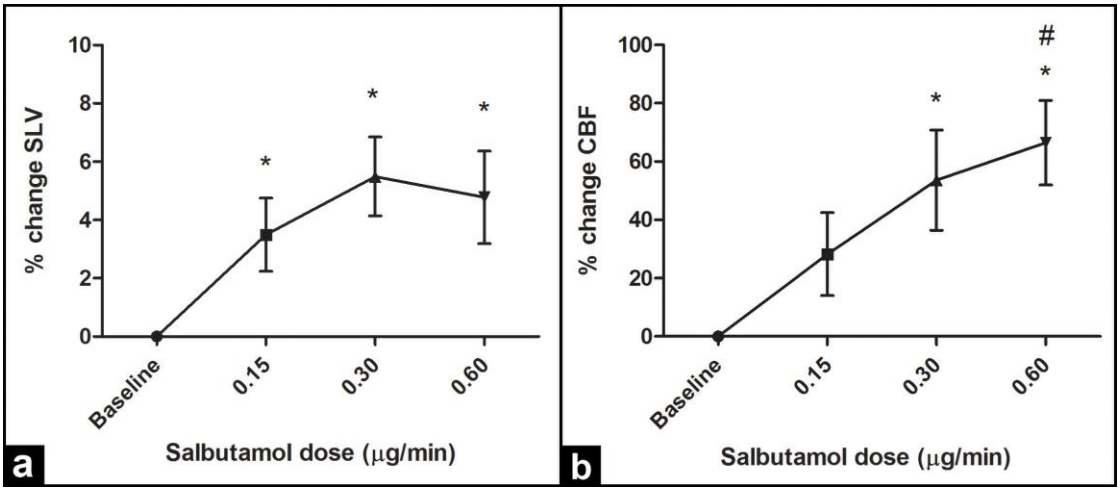
% change SLV
10
8
6
4
2
0
*
*
*
Baseline
0.15
0.30
0.60
Salbutamol dose (μg/min)
a
% change CBF
100
80
60
40
20
0
#
*
*
Baseline
0.15
0.30
0.60
Salbutamol dose (μg/min)
b

Figure 4

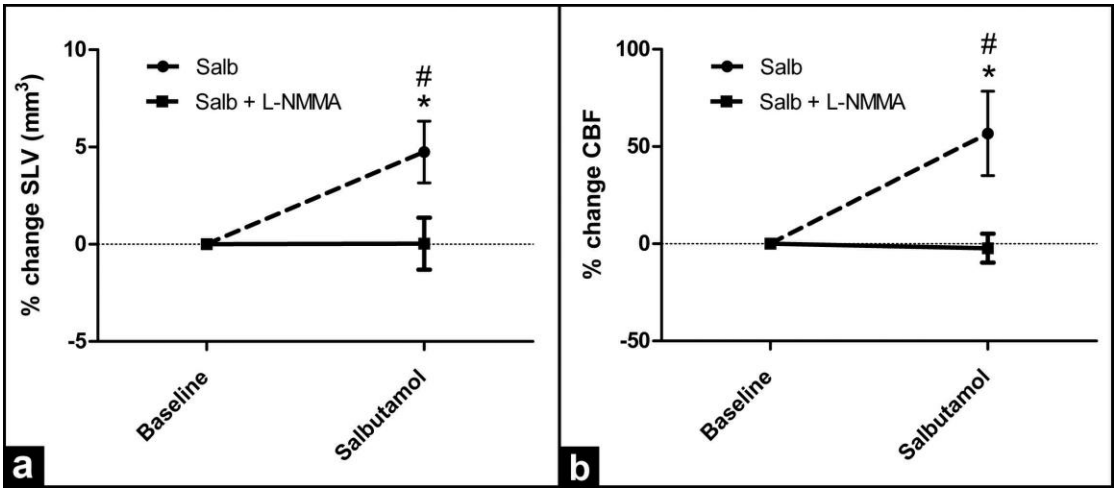
10
5
0
-5
% change SLV (mm3)
Salb
Salb + L-NMMA
#
*
Baseline
Salbutamol
a
100
50
0
-50
% change CBF
Salb
Salb + L-NMMA
#
*
Baseline
Salbutamol
b

Figure 5

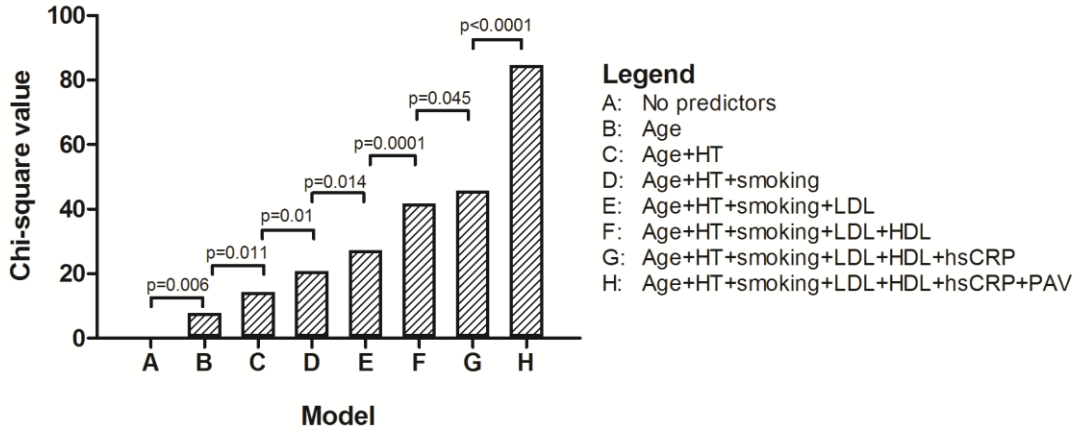
100
80
60
40
20
0
Chi-square value
p=0.006
p=0.011
p=0.01
p=0.014
p=0.0001
p=0.045
p<0.0001
A
B
C
D
E
F
G
H
Model
Legend
A: No predictors
B: Age
C: Age+HT
D: Age+HT+smoking
E: Age+HT+smoking+LDL
F: Age+HT+smoking+LDL+HDL
G: Age+HT+smoking+LDL+HDL+hsCRP
H: Age+HT+smoking+LDL+HDL+hsCRP+PAV

Author contributions:

Dr Rishi Puri – Study design, patient recruitment, analysis, preparation of manuscript

Dr Gary Liew – Cath lab procedures, analysis, correction and critical review of manuscript

Professor Stephen J. Nicholls - Correction and critical review of manuscript

Dr Adam Nelson - Correction and critical review of manuscript

Dr Darryl Leong - Analysis, correction and critical review of manuscript

Mr Angelo Carbone – Record keeping, critical review of manuscript

Ms Barbara Copus – Cath lab procedures, critical review of manuscript

Dr Dennis Wong - Correction and critical review of manuscript

Professor John Beltrame – Supervision, correction and critical review of manuscript

Professor Stephen Worthley – Supervision, cath lab procedures, critical review of manuscript

Associate Professor Matthew I. Worthley – Primary Supervision, study design, cath lab procedures, correction and critical review of manuscript

I hereby give permission for this published original manuscript to be included in this thesis submission:

Dr Rishi Puri

Dr Gary Y. Liew

Professor Stephen J. Nicholls

Dr Adam J. Nelson

Mr Angelo Carbone

Ms Barbara Copus

Dr Dennis T. Wong

Professor John F. Beltrame

Professor Stephen G. Worthley

Dr Darryl P. Leong

Associate Professor Matthew I. Worthley

CHAPTER 5: CORONARY ENDOTHELIUM-DEPENDENT VASOREACTIVITY AND ATHEROMA VOLUME IN SUBJECTS WITH STABLE, MINIMAL ANGIOGRAPHIC DISEASE VERSUS NON-ST SEGMENT ELEVATION MYOCARDIAL INFARCTION: AN INTRAVASCULAR ULTRASOUND STUDY

Adapted from PURI, R., NICHOLLS, S.J., NISSEN, S.E., BRENNAN, D.B., ANDREWS, J.A., LIEW, G.Y., NELSON, A.J., CARBONE, A.J., COPUS, B., TUZCU E.M., BELTRAME, J.F., WORTHLEY, S.G., WORTHLEY, M.I. 2013. Coronary endothelium-dependent vasoreactivity and atheroma volume in subjects with stable, minimal angiographic disease versus non-ST-segment-elevation myocardial infarction: an intravascular ultrasound study. *Circ Cardiovasc Imaging*, 6(5):674-82

Key words: plaque burden; endothelial function; intravascular ultrasound; salbutamol; adrenergic receptor; NSTEMI

Puri, R., Nicholls, S.J., Nissen, S.E., Brennan, D.B., Andrews, J.A., Liew, G.Y., Nelson, A.J., Carbone, A.J., Copus, B., Tuzcu, E.M., Beltrame, J.F., Worthley, S.G. & Worhtley, M.I. (2013) Coronary endothelium-dependent vasoreactivity and atheroma volume in subjects with stable, minimal angiographic disease versus non-st segment elevation myocardial infarction: an intravascular ultrasound study.
Circulation, Cardiovascular Imaging, v. 6, pp. 674-682

Author contributions:

Dr Rishi Puri – Study design, patient recruitment, analysis, preparation of manuscript

Professor Stephen Nicholls - Correction and critical review of manuscript

Professor Steven Nissen - Correction and critical review of manuscript

Mrs Danielle Brennan – Analysis, correction and critical review of manuscript

Ms Jordan Andrews - Analysis, correction and critical review of manuscript

Dr Gary Liew – Cath lab procedures, analysis, correction and critical review of manuscript

Dr Adam Nelson - Correction and critical review of manuscript

Mr Angelo Carbone – Record keeping, critical review of manuscript

Ms Barbara Copus – Cath lab procedures, critical review of manuscript

Professor E. Murat Tuzcu - Correction and critical review of manuscript

Professor John Beltrame – Supervision, correction and critical review of manuscript

Professor Stephen Worthley – Supervision, cath lab procedures, critical review of manuscript

Associate Professor Matthew Worthley – Primary Supervision, study design, cath lab procedures, correction and critical review of manuscript

I hereby give permission for this published original manuscript to be included in this thesis submission:

Dr Rishi Puri Professor Stephen J. Nicholls

Professor Stephen E. Nissen

Mrs Danielle M. Brennan

Ms Jordan Andrews

Dr. Gary Y. Liew

Dr Adam J. Nelson

Mr Angelo Carbone

Ms Barbara Copus

Professor E. Murat Tuzcu

Professor John F. Beltrame

Professor Stephen G. Worthley

Associate Professor Matthew I. Worthley

CHAPTER 6: CORONARY ATHEROMA COMPOSITION AND ITS ASSOCIATION WITH SEGMENTAL ENDOTHELIAL DYSFUNCTION IN NON-ST SEGMENT ELEVATION MYOCARDIAL INFARCTION: NOVEL INSIGHTS WITH RADIOFREQUENCY (iMAP) INTRAVASCULAR ULTRASONOGRAPHY

Adapted from PURI, R., NICHOLLS S.J., BRENNAN, D.M., ANDREWS, J.A., LIEW, G.Y., CARBONE, A., COPUS, B., NELSON, A.J., KAPADIA, S.R., TUZCU, E.M., BELTRAME, J.F., WORTHLEY, S.G., WORTHLEY, M.I. 2013. Coronary atheroma composition and its association with segmental endothelial dysfunction in non-ST-segment elevation myocardial infarction: novel insights with radiofrequency (iMap) intravascular ultrasonography. *Int J Cardiol* 2014 [Accepted In Press]

Keywords: Endothelial function; Atherosclerosis; Intravascular ultrasound; iMAP; Salbutamol

ABSTRACT

Little is known of the relationship between coronary atheroma composition and corresponding endothelial dysfunction. We tested the hypothesis that segmental epicardial vasoreactivity relates to atheroma composition in patients with non-ST segment elevation myocardial infarction (NSTEMI) *in vivo*. In 23 NSTEMI patients referred for coronary angiography, a non-culprit vessel underwent intracoronary salbutamol (0.30 mcg/min) provocation during automated IVUS pullback. A 40 MHz rotational IVUS catheter delivered radiofrequency signals at constant 67 micron intervals via a custom-built IVUS console (iMAP, iLAB, Boston Scientific). Macrovascular response [change in segmental lumen volume (SLV) at baseline and following salbutamol], percent atheroma volume (PAV) and tissue composition was evaluated in 187 contiguous non-overlapping 5 mm coronary segments. Compared with segments that dilated, constrictive segments showed similar SLV, but greater vessel volumes and PAV at baseline. The extent of necrotic and lipidic plaque was significantly greater in constrictive segments, whereas fibrotic plaque content was significantly greater in segments that dilated. Calcific plaque content did not relate to endothelium-dependent vasoreactivity. The change in SLV correlated inversely with the amount of lipidic and necrotic plaque (both r = -0.23, p=0.002), and directly with fibrotic plaque content (r= 0.23, p=0.002). In a multivariable model, the extent of both lipidic and necrotic plaque independently associated with segmental vasoconstriction (β =1.2, p=0.023; β =0.66, p=0.027). In conclusion, following NSTEMI, both lipidic and necrotic plaque content each associate with segmental endothelial dysfunction. The link

between plaque composition and vessel reactivity provides a mechanistic basis of the pathogenesis associated with vulnerable plaque in humans *in vivo.*

While atherosclerosis is systemic disease, a focalized milieu within the arterial wall promotes regions of atheroma progression and instability, predisposing an individual to an athero-thrombotic clinical event. The vascular endothelium, a monolayer of cells separating the lumen from the vessel wall, serves to regulate vascular tone and various homeostatic mechanisms promoting vascular health (Celermajer, 1997). Numerous *in vitro* (Steinberg, 1987) and animal studies (Moore, 1973) highlight strong mechanistic links between dysfunctional endothelium and atherogenesis. This led many to postulate that endothelial dysfunction *per se*, in the presence of systemic cardiovascular risk factors, precedes atheroma formation (Celermajer et al., 1994), stimulating its progression, instability and thus propensity for causing a clinical event (Ross and Glomset, 1973, Williams and Tabas, 1995, Lerman and Zeiher, 2005). However to date, direct invasive interrogations of the epicardial coronary vasculature in humans has failed to confirm these hypotheses *in vivo* (Reddy et al., 1994, Nishimura et al., 1995).

Imaging studies utilizing coronary angiography demonstrated an association between epicardial coronary endothelial dysfunction and incident clinical events (Suwaidi et al., 2000, Schachinger et al., 2000, Halcox et al., 2002). Similarly, serial coronary intravascular ultrasonography (IVUS) highlighted prognostic associations between baseline coronary atheroma burden, and its rate of progression, with incident clinical events (Nicholls et al., 2010, Puri et al., 2013c, Puri et al., 2013b). More recently, via processing the spectral analysis of the radiofrequency (RF) backscatter IVUS signal, studies have elucidated the prognostic significance of coronary atheroma composition and phenotype (Stone et al., 2011, Calvert et al., 2011, Kim et al., 2013). Yet there is a paucity of direct *in vivo* human observations outlining the dynamic

interplay between segmental coronary endothelial function and underlying plaque composition, as a potential means of identifying segments of coronary atheroma with a heightened risk for causing a future coronary event.

This study tested the hypothesis that the degree of segmental coronary endothelium-dependent vasomotor reactivity relates to the composition of underlying atheroma. A novel imaging approach employing intracoronary stimulation during coronary IVUS acquisition was utilized. This enabled direct *in vivo* volumetric appraisals of lumen response and plaque composition in contiguous, non-overlapping whole epicardial coronary segments of patients presenting with non-ST segment elevation myocardial infarction (NSTEMI).

METHODS

Study subjects

We enrolled twenty-three patients (aged ≥18 yrs) referred for coronary angiography following admission to hospital with NSTEMI. A clinical presentation with chest discomfort in concert with a significant Troponin T elevation with or without ST-segment depression and/or T-wave inversion, was classified as NSTEMI (Cannon et al., 2013), and consecutive patients meeting this criteria were considered for study enrolment. Following initial medical stabilization and informed consent, vasoactive medications were held for at least 24 hrs prior to the planned invasive study. Only those patients who were pain-free following hospitalization and initial medical stabilization, and had no form of nitrate therapy in the 12 hours prior to their coronary angiogram were recruited. All procedures were performed in the morning prior to an overnight fast.

The invasive research protocol was performed in a non-critically diseased (<30% angiographic stenosis), non-culprit ('study') vessel, prior to percutaneous coronary intervention within the culprit vessel. All procedures were performed in the morning prior to an overnight fast. Exclusion criteria included significant valvular heart disease, left ventricular dysfunction (known ejection fraction ≤40%), prior percutaneous or surgical coronary revascularization, acute coronary syndrome within the preceding 4 weeks, known coronary spasm, severe obstructive lung disease, creatinine clearance ≤60 mL/min, β-blocker use in the preceding 24 hours, or the use of short or long acting β_2 agonists within the previous 24 hours. This study was approved by the Royal Adelaide Hospital Human Research Ethics Committee.

Cardiac catheterization and intravascular imaging protocols

Coronary angiography was performed via a standard 6-French technique. Intravenous heparin (70 IU/kg) was administered for the research protocol. A 0.014 inch coronary guide wire was placed into the study vessel within its mid-segment away from major side-branches. This wire was also used to deliver a 3.2 French 40 MHz Atlantis SR Pro IVUS catheter (Boston Scientific, Natick, MA, USA) into the study artery. This was undertaken without pre-treatment with IC nitroglycerin. All IC infusions were administered through an infusion pump at 2 mL/min via the coronary guiding catheter for a period of 5 minutes. During the final 2 minutes of IC infusion (of either vehicle solution or salbutamol), the IVUS catheter was then moved from within the guiding catheter into the distal conduit vessel and images were acquired during automated catheter withdrawal at 0.5 mm/sec. Our previous validation studies have shown that repeated, consecutive, IC vehicle infusions over 5 minutes during IC instrumentation

with IVUS has no significant impact on changes in lumen measurements over time (Puri et al., 2012b). The IVUS images were recorded on a DVD for off-line analysis.

Coronary infusion and endothelial function testing protocols

The infusion protocols that were performed for the validation of IC salbutamol as an endothelium-dependent coronary vasomotor stimulus have been previously described in detail (Puri et al., 2012b, Barbato et al., 2005). A series of *in vivo* human observations have implicated coronary β_2-adrenoreceptor stimulation to cause NO-mediated peripheral and coronary arterial vasomotor responses (Dawes et al., 1997, Wilkinson et al., 2002, Barbato et al., 2005, Puri et al., 2012b). Our endothelial function testing protocol involved [following baseline IC 5% dextrose (vehicle) infusion] a 5-minute infusion of IC salbutamol (0.30 μg/min). The IC salbutamol vasomotor responses have been found to be similar magnitude to those evoked following IC acetyl choline (Newman et al., 1990, Barbato et al., 2005, Puri et al., 2012b, Puri et al., 2013a).

Data acquisition and analysis

A custom built IVUS console (iLAB) was provided by Boston Scientific (Fremont, CA, USA), capturing ultrasonic RF signals on every 4th IVUS frame during an automated transducer pullback speed of 0.5 mm/sec. Hence, tissue compositional data was available at regular 67 micron intervals of the entire IVUS pullback. This enabled a consistent ability to provide near-identical amounts of tissue compositional data per 5 mm coronary segment, unaffected by heart rate variability, thus negating the issue of horizontal bias that occurs during gated acquisition of the RF signal. This, in turn allowed for a more robust volumetric assessment of tissue composition in relation to

lumen response in each of the studied epicardial segments. The more recently developed iMAP-IVUS (Boston Scientific, Fremont, CA, USA) RF imaging system for tissue characterization was utilized, which uses a pattern recognition algorithm from spectra obtained from fast-Fourier transformation of a human autopsy database of coronary atheroma (Sathyanarayana et al., 2009). Using a color-code, iMAP depicts fibrotic tissue as light green, lipidic tissue as yellow, necrotic tissue as pink, and calcified tissue as blue based on geometrically traced contours (Figure 1). On each frame displaying tissue composition, the acoustic shadow imparted by the rotational IVUS catheter had a mask assigned to it, and this area was excluded from all tissue compositional analyses.

Analysis of IVUS data was performed by the Atherosclerosis Imaging Core Laboratory of the Cleveland Clinic Coordinating Center for Clinical Research, according to prior experience and published guidelines (Mintz et al., 2001, Nicholls et al., 2010), using dedicated software (echoPlaque 4.0, Indec Systems, Santa Clara, CA, USA). Technicians were blinded to clinical details and infusion sequence. Proximal and distal fiduciary markers (anatomical side-branches) were chosen to define the overall region of vessel to be analyzed, as well as for segment matching. Cross-sectional images were selected every 60 frames (1 mm apart). As per the IVUS Core Laboratory protocols, frames that precluded complete lumen or vessel wall planimetry were excluded from analysis, as were segments that involved major branch points. Each IVUS pullback was divided into 5 mm segments comprising of 6 frames taken at 5 evenly spaced cross-sectional (1 mm) intervals (Figure 2). Given the known segmental heterogeneity of coronary vasomotor reactivity (el-Tamimi et al., 1994, Tousoulis et al.,

1996, Lavi et al., 2009), each segment was thus analyzed separately as an individual entity, with appropriately utilized statistical methods to account for clustering. Matching frames of anatomical side-branches from the baseline and post-salbutamol stimulation IVUS runs were co-registered to ensure accurate segment matching between runs. Leading edges of the lumen and external elastic membrane (EEM) were manually planimetered. Percent atheroma volume (PAV) was calculated to determine segmental plaque burden (Nicholls et al., 2010):

$$\mathbf{PAV = \sum [(EEM_{area} - Lumen_{area}) / \sum EEM_{area}] \; X \; 100}$$

Segmental lumen volumes (SLV) were calculated as the summation of lumen area in each measured image. As some frames were deemed technically inadequate by the IVUS Core Laboratory for complete IVUS analysis, the SLV for each 5 mm segment was normalized to account for differences in the number of analyzable frames within each pre-defined segment, as previously described (Puri et al., 2012b):

$$\mathbf{SLV_{normalised} = \sum [(Lumen_{area}) / number\ of\ analyzable\ images\ in\ segment] \; X \; 5}$$

Fibrous, lipidic, necrotic and calcified plaque volumes per 5 mm coronary segment were calculated based on Simpsons rule, and expressed as a percentage of total segmental atheroma volume. A previous analysis outlined the acceptable reproducibility of iMAP tissue compositional areas (Heo et al., 2014). For grey-scale IVUS measurements in the present analysis, the intra- and inter-observer coefficients of variation for lumen area were 1.1% and 2.6% respectively. For plaque area, the intra- and inter-observer coefficients of variation were 1.8% and 3.8% respectively.

Statistical analysis

Continuous data are expressed as mean ± standard deviation (SD) or median and 25th and 75th percentiles, when appropriate. Categorical data are presented as a percent of non-missing data. Absolute and percent change in SLV was calculated for each segment. Segments were categorized as constrictors (absolute change in SLV ≤0) and dilators (absolute change in SLV >0). Comparisons between segments that constricted and dilated were made using Student's t-test for continuous data (or Wilcoxon-rank sum for non-normally distributed data) and chi-square tests for categorical data. Correlations between absolute and percent change in SLV and tissue composition were performed and are represented by Spearman correlation coefficients and their 95% confidence intervals.

Multivariable models were created to determine independent predictors of change in SLV. Mixed models were used to account for multiple segment measurements within a patient. All variables that were univariately associated with change in SLV (p-value <0.20) were considered for multivariable adjustment. Variables were then kept in the final model if they reached statistical significance (p-value <0.05). Baseline lumen volume was forced into the model as an adjustment variable. Variables that remained in the final model were age, smoking and the log-transformation of hsCRP. Each tissue composition variable was entered separately in the model, and the Aikake Information Criteria (AIC) was used to determine the strongest independent predictor of change in SLV. A separate generalized linear model was created to assess the relationship of each plaque composition variable to segmental vasoconstriction (change in SLV ≤0). The same methods as described above were used for model

development. The Quasi-likelihood Information Criteria (QIC) was used to determine the strongest independent predictor of each tissue composition variable on vasoconstriction. All analyses were performed using SAS version 9.2 (SAS Institute, Cary, NC). P values of less than 0.05 were considered statistically significant.

RESULTS

Clinical and IVUS data

Table 1 summarizes baseline clinical, biochemical and angiographic characteristics of the study cohort. Of the 23 coronary arteries interrogated, 11 (48%) involved the left anterior descending artery, 9 (39%) involved the circumflex artery, and 3 (13%) involved the right coronary. Overall, 960.9 mm of epicardial coronary artery was analyzed, comprising 187 contiguous 5 mm segments that were deemed technically suitable for volumetric lumen, plaque and tissue compositional (iMAP) analysis. This equated to a median of 8 contiguous non-overlapping epicardial segments analyzed per patient. Following IC salbutamol, there were no significant changes from baseline of heart rate ($p=0.16$), systolic ($p=0.99$) or diastolic ($p=0.91$) blood pressure.

Segmental grey-scale and tissue compositional data according to pattern of endothelium-dependent function

Table 2 describes baseline segmental ultrasonic grey-scale and (iMAP) tissue compositional volumes according to the presence of endothelium-dependent vasomotor dysfunction (defined as change from baseline SLV ≤ 0 following IC salbutamol, or vasoconstriction), or segmental vasodilatation (change from baseline SLV >0) (Schachinger et al., 2000). Of the analyzed 187 epicardial segments, 78 displayed a vasoconstrictor response to IC salbutamol. Overall, these segments underwent a relative

-3.1±2.8% (or absolute -7.4±6.0 mm^3) change from baseline ($p<0.001$) in SLV. The corresponding relative and absolute values of change from baseline in SLV in segments that vasodilated were +3.4±3.5% and +10.0±10.4 mm^3 respectively. Compared with segments that vasodilated, constrictive segments had greater PAV (42.5±1.4 vs. 38.6±1.1%, p=0.029) and EEM volume (72.5±2.6 vs. 61.9±2.2 mm^3, p=0.002), but no significant differences in baseline lumen volume (40.7±1.7 vs. 37.5±1.4 mm^3, p=0.15) were observed. Additionally, compared with segments displaying vasodilatation, constrictive segments contained significantly greater amounts of necrotic (18.3±1.2 vs. 14.9±0.98%, p=0.029) and lipidic tissue (9.2±0.45 vs. 7.9±0.37%, p=0.039), similar amounts of calcific tissue (1.5±0.21 vs. 1.58±0.18%, p=0.72), yet significantly less fibrotic tissue (71.0±1.6 vs. 75.6±1.3%, p=0.026).

Correlations between coronary vasomotor responses and tissue composition

Table 3 outlines correlations between segmental coronary vasomotor reactivity (relative and absolute changes in SLV) and underlying segmental tissue composition. Changes in SLV correlated inversely with the amount of necrotic and lipidic tissue, such that greater volumes of these tissue components were associated with segmental vasoconstriction. On the other hand, changes in SLV correlated directly with the extent of fibrotic tissue, such that greater volume of fibrous tissue associated with segmental vasodilatation (Figure 3). No correlation was observed between the extent of calcific tissue and changes in SLV, consistent with the proposition that calcified tissue may not significantly affect segmental epicardial coronary vasoreactivity *in vivo*.

Multivariable predictors of segmental epicardial vasomotor reactivity

Table 4 summarizes 2 multivariable models. In a multivariable model assessing the independent vessel-based predictors of any change in SLV, based on the lowest significant AIC value, the amount of fibrotic tissue was the strongest independent predictor of change in SLV, found to promote segmental epicardial vasodilatation (β-coefficient 3.9±1.7, p=0.027, AIC 1021.8). In a multivariable model specifically assessing the vessel-based predictors of segmental vasoconstriction (endothelial dysfunction), based on the lowest significant QIC value (a modification of the AIC applied to models fit by generalized estimates equations), the amount of lipidic tissue was the strongest, independent predictor of segmental epicardial endothelial dysfunction (β-coefficient 1.2±0.51, p=0.023, QIC 229.5).

DISCUSSION

Intracoronary imaging has played a fundamental role in enhancing our understanding of factors promoting the progression and instability of coronary atheroma *in vivo* (Puri et al., 2011). The present analysis demonstrates novel *in vivo* associations between volumetric measures of atheroma composition and segmental epicardial endothelium-dependent vasoreactivity in non-culprit vessels of patients with NSTEMI; a patient population thought to harbor the most 'vulnerable' form of coronary plaque throughout the coronary tree. Greater amounts of lipidic and necrotic tissue were associated with segmental endothelial dysfunction, whereas epicardial segments containing a greater extent of fibrotic tissue were more likely associated with the tendency to vasodilate. Such associations appeared independent of the overall burden of plaque in a multivariable model, after controlling for baseline lumen volume and a number of known systemic risk factors for endothelial dysfunction.

Necropsy findings of lipid pools and necrotic core within disrupted coronary plaques causing fatal myocardial infarction underscores the contemporary ideology of vulnerable plaque phenotype (Kolodgie et al., 2004, Schaar et al., 2004a), which has been proposed to be identifiable *in vivo* using RF-IVUS (Rodriguez-Granillo et al., 2005). Accordingly, there has been a major focus on the predictive capacity of RF-IVUS-derived necrotic core tissue as an imaging biomarker of coronary risk (Stone et al., 2011, Calvert et al., 2011). More recent observations of large reductions in the fibro-fatty tissue component measured with serial Virtual Histology™ (VH)-IVUS following long-term high-intensity statin therapy (Puri et al., 2014), and significant reductions in coronary lipid measured with serial near-infrared spectroscopy following short-term high-intensity statin therapy (Kini et al., 2013), suggests that the lipidic content of coronary atheroma might represent an equally important and modifiable tissue substrate. Moreover, a recent study VH-IVUS study undertaken within culprit coronary lesions (>70% angiographic stenosis severity) of patients prior to percutaneous coronary intervention found that fibrofatty plaque volume independently associated with future cardiovascular events (Kim et al., 2013). Our findings thus outline a mechanistic link between epicardial segments demonstrating reduced NO bioavailability and greater amounts of both lipidic and necrotic core tissue. These findings are consistent with necrotic core tissue being a substrate for active inflammation and oxidative stress (Naghavi et al., 2003), with such pro-atherogenic processes being previously demonstrated both in animal models (Pendyala et al., 2009) and within individuals demonstrating coronary endothelial dysfunction (Lavi et al., 2008). In addition, our findings of an association between a greater extent of fibrotic plaque and segmental

vasodilatation appears consistent with the proposition that enhanced collagen expression, at the extent of lower content of inflammatory infiltrate, may exert a stabilizing effect on the arterial wall (Aikawa et al., 1998).

Clinical complications of atherosclerosis commonly arise within arterial segments originally harboring non-obstructive atheroma. The Providing Regional Observations to Study Predictors of Events in the Coronary Tree (PROSPECT) study outlined the importance of non-culprit segment pathology, whereby half of all incident clinical events following 3.4 years of clinical follow-up were attributed to coronary segments remote to the original culprit lesion, particularly those containing greater amounts of necrotic core tissue (Stone et al., 2011). Similarly, coronary spasm following IC acetyl choline provocation occurs in 50% of non-culprit coronary vessels respectively following acute coronary syndrome (Ong et al., 2008); findings that were prognostic of major adverse cardiovascular events after nearly 4 years of follow-up (Wakabayashi et al., 2008). More recently, an alteration of plaque morphology with evidence of macrophage extravasation was observed in atherosclerotic coronary plaques of rabbits following infusion of spasmogens *in vivo* (Shiomi et al., 2013). These collective observations, in addition to the present analysis, suggest that abnormal epicardial vasoreactivity and atheroma composition are likely features of coronary instability and possible heightened clinical risk in the setting of an acute coronary syndrome.

The present findings may have future clinical implications beyond simply their mechanistic associations. While IVUS is invasive and thus not applicable for use a

primary preventive cohort, emerging data utilizing non-invasive coronary imaging similarly associates coronary atheroma burden, measured semi-quantitatively, with future cardiac events in non-obstructive coronaries of individuals with both stable (Lin et al., 2011) and acute coronary syndromes (Kristensen et al., 2011). However prospective trials testing formally this approach against current models of clinical risk-stratification are currently lacking. Nevertheless, there is an ongoing need to develop the non-invasive assessment of coronary atherosclerosis beyond simply measuring its volume, and the described association between atheroma composition and epicardial vasoreactivity provides further rationale for this approach. Indeed, a combined non-invasive structural and functional epicardial assessment was recently undertaken by Hays et al. using coronary magnetic resonance imaging (Hays et al., 2010). When refined, a combined technique may hold further potential for better risk-stratifying the coronary tree across large populations at varying risk for future coronary events.

Asides from high-reported accuracies of both VH and iMAP for reporting atheroma composition *in vivo* (Nair et al., 2002, Sathyanarayana et al., 2009), there are a number of pros and cons of each commercially available algorithm that are beyond the scope of detailed discussion in this manuscript (Shin et al., 2011, Katouzian et al., 2012). A common limitation however, is the occurrence of horizontal bias incurred from gating the RF acquisition signal to the R-wave. This makes equal sampling of RF images during a defined coronary segment, and subsequent precise frame-matching of coronary segments during serial IVUS analysis difficult due to heart rate variability at differing time points (Puri et al., 2011). We utilized a custom-modified IVUS console which provided RF-IVUS data every 4 imaging frames (7.5 iMAP frames per second).

This enabled tissue composition to be available at constant 67 micron intervals during an automated transducer pullback speed of 0.5 mm/sec, such that each 5 mm coronary segment contained the same degree of RF tissue sampling. Furthermore, our methodological approach involved imaging of whole, matched, contiguous, non-overlapping epicardial segments (a median of 40 mm per patient), enabling an unbiased direct volumetric appraisal of lumen response in reference to underlying plaque composition. This averted the need for additional angiographic co-registration of lumen response to the RF-IVUS data (Lavi et al., 2009).

Several limitations of this study should be noted. This study was conducted in non-culprit vessels of patients with NSTEMI. Hence, the findings cannot be extrapolated to culprit vessels containing more critical stenoses. However Kim et al. recently described an association between higher degrees of fibrofatty volume in severe lesions of culprit vessels undergoing percutaneous coronary intervention (Kim et al., 2013). Moreover, the possibility of severe spasm and vessel dissection would render such an invasive IC provocation and imaging protocol unethical to be conducted across critical stenoses in patients with stable or acute coronary syndromes. It is unknown whether similar conclusions would have arisen had a VH-IVUS algorithm been used in the present study, as systematic differences in reporting atheroma composition between VH and iMAP have been demonstrated in humans *in vivo* (Shin et al., 2011). It is however reassuring that in stable patients with non-critical left anterior descending coronary artery disease, similar associations to those found in the present analysis were reported between VH-IVUS-derived atheroma composition and segmental epicardial vasoreactivity following IC acetyl choline provocation (Lavi et al., 2009), in addition to

the clinical findings of Kim et al (Kim et al., 2013). Direct vasodilator responses to intracoronary nitroglycerin injection were not evaluated. This would have allowed us to test if smooth muscle cell dysfunction, rather than impairment in NO-dependent function, contributed to blunted vessel wall reactivity in a number of segments. Salbutamol, however, has minimal direct smooth muscle cell dilating properties, as shown in a prior validation study (Puri et al., 2012b). Due to the protocol's invasive nature involving a higher-risk patient cohort than traditionally targeted for intracoronary provocation, only those patients that were medically stabilized and pain free were eligible for inclusion, as study protocol mandated halting of beta-blockers and infusional nitrates for 24 hours and 12 hours respectively prior to a coronary angiography. This could have resulted in a degree of selection bias. However this was critical so as to not subject patients to unnecessary coronary spasm as whilst also ensuring a correct appraisal of NO-dependent behavior of the epicardial coronary tree in such patients. The volumes of lipidic and necrotic plaque per 5 mm epicardial segment are fairly modest, and it is unclear if measurement of these plaque components across small segments will find clinical utility. Rather, quantification of these components across the entire conduit segment would seem more likely to yield greater prognostic utility.

CONCLUSIONS

In conclusion, the present study outlines novel associations between epicardial atheroma composition and corresponding segmental endothelium-dependent vasomotor reactivity *in vivo* in patients with NSTEMI. Greater amounts of lipid-rich and necrotic core tissue were found in segments displaying endothelial dysfunction, whereas a

greater extent of fibrotic tissue was noted in segments with preserved vasomotor reactivity. The observed link between plaque composition and vessel reactivity could provide a basis for better assessing plaque vulnerability in systemically vulnerable individuals.

Table 1 Clinical, biochemical and angiographic characteristics

Variable	**NSTEMI patients** **N = 23 patients**
Age (yrs)	59±12
Male, n (%)	19 (83)
*Smoker, n (%)	15 (65)
Diabetes, n (%)	6 (26)
Hypertension, n (%)	16 (70)
LDL-C (mg/dL)	104±35
HDL-C (mg/dL)	35±11
Triglycerides (mg/dL)	97 (89,133)
hsCRP (µg/dL)	4.0 (2.2,12)
Statin use	13 (59)
Troponin T (ng/mL)	1.7±3.6
Non-culprit study artery LAD, n (%) LCx, n (%) RCA, n (%)	 11 (48) 9 (39) 3 (13)
Segments per patient	8 (7, 10)

Data expressed as mean±SD or median and interquartile range when appropriate
*Definition of smoking was taken as current or within 4 weeks
LDL-C, low-density lipoprotein cholesterol; HDL-C, high-density lipoprotein cholesterol
hsCRP, high sensitivity C-reactive protein
LAD, left anterior descending artery; LCx, left circumflex artery; RCA, right coronary artery
PAV, percent atheroma volume; TAV, total atheroma volume; SLV, segmental lumen volume; EEM, external elastic membrane

Table 2: Segmental grey-scale and tissue compositional data at baseline and according to pattern of coronary vasomotor response

Parameter	**All segments**	**Change in SLV**		**P-value**
		Constriction	**Dilation**	
	N = 187	**N = 78**	**N = 109**	
Baseline SLV (mm^3)	38.9±14.9	40.7±1.7	37.5±1.4	0.15
†% change SLV (%)	0.7±4.6	-3.1±2.8	3.4±3.5	<0.001
Within-group p-value	*N/A*	*<0.001*	*<0.001*	
†Change in SLV (mm^3)	2.7±12.3	-7.4±6.0	10.0±10.4	<0.001
Within-group p-value	*N/A*	*<0.001*	*<0.001*	
PAV (%)	40.2±12.0	42.5±1.4	38.6±1.1	0.029
EEM (mm^3)	66.3±23.1	72.5±2.6	61.9±2.2	0.002
Necrotic (%)	16.4±10.3	18.3±1.2	14.9±0.98	0.029
Fibrotic (%)	73.5±13.4	71.0±1.6	75.6±1.3	0.026
Lipidic (%)	8.5±4.0	9.2±0.45	7.9±0.37	0.039
Calcific (%)	1.5±1.8	1.50±0.21	1.58±0.18	0.72

Baseline data expressed as mean ± SD or median and interquartile range when appropriate

†Changes in segmental lumen volumes (SLV) are expressed as least squares means ± SE, following controlling for baseline SLV, and using mixed-effects modeling to account for repeated measures per patient

PAV, percent atheroma volume; TAV, total atheroma volume; SLV, segmental lumen volume; EEM, external elastic membrane

Table 3: Correlations between segmental coronary vasomotor response and underlying tissue composition

Tissue component	Absolute Δ SLV (mm^3)		Percent Δ SLV (%)	
	R (95% CI)	P-value	R (95%CI)	P-value
Necrotic	-0.21 (-0.35, -0.06)	0.006	-0.23 (-0.38, -0.088)	0.002
Fibrotic	0.21 (0.061, 0.35)	0.006	0.23 (0.089, 0.38)	0.002
Lipidic	-0.19 (-0.34, -0.044)	0.01	-0.23 (-0.37, -0.081)	0.002
Calcific	-0.04 (-0.19, 0.11)	0.60	0.001 (-0.15, 0.15)	0.99

R-values (95% CI) represent Spearman correlation coefficients
Tissue components expressed as % of plaque burden per coronary segment
Δ = change

Table 4: Multivariable predictors of segmental coronary vasomotion (any change in SLV) and segmental coronary vasoconstriction (change in SLV ≤0)

Plaque parameter	Change in SLV			Vasoconstriction		
	β coefficient ± SE	P-value	AIC	β coefficient ± SE	P-value	QIC
PAV	-0.037±0.03	0.19	1086.5	0.027±0.02	0.094	240.9
Necrotic	-1.4±0.55	0.011	1022.5	0.66±0.30	0.027	230.2
Fibrotic	3.9±1.7	0.027	1021.8	-1.83±0.98	0.062	231.7
Lipidic	-2.2±0.93	0.019	1022.4	1.2±0.51	0.023	229.5
Calcific	-0.32±0.32	0.33	1004.1	0.17±0.16	0.29	231.1

All tissue components (except PAV) are log-transformed, and these are expressed as a % of total plaque burden per coronary segment

AIC = Aikake Information Criteria. QIC = Quasi-likelihood Information Criteria. PAV = percent atheroma volume; SLV = segmental lumen volume

Model adjusted for baseline SLV, age, smoking and (log)hsCRP

FIGURE LEGENDS

Figure 1

[A] Grey scale intravascular ultrasound image of a non-culprit epicardial segment. **[B]** Corresponding iMAP image. The four tissue subtypes are shown. Yellow (lipidic), green (fibrotic), magenta (necrotic core), blue (calcific). The variations of each color (i.e. darker yellow speckle) signify variable levels of tissue confidence of spectral similarity (24).

Figure 2

Segmental volumetric lumen and plaque analysis with intravascular ultrasound (IVUS). Automated IVUS pullback enabled the overall long imaged epicardial section to be divided into 5 mm segments (denoted by yellow lines on longitudinal view). Within each segment, plaque and lumen volumes were calculated upon sequential frames spaced 1 mm apart (red lines), each containing radiofrequency (iMAP) tissue compositional data, numbered 1-6 (cross-sectional views).

Figure 3

Segmental epicardial vasomotor response according to tissue composition. Panel A depicts a representative frame from an epicardial segment with predominant fibrotic tissue composition. Panel B shows the corresponding grey scale image of panel A. Following intracoronary salbutamol provocation, this matched frame (panel C) showed a 7.5% degree of vasodilatation in lumen area (LA). Panel D depicts a representative frame from an epicardial segment with comparatively less fibrotic, yet greater amounts of necrotic core and lipidic tissue. Panel E shows the corresponding grey scale image of

panel D. Following intracoronary salbutamol provocation, this matched frame (panel F) showed a 4.7 % degree of vasoconstriction.

Figure 1: Grey scale and corresponding radiofrequency (iMAP) intravascular ultrasound

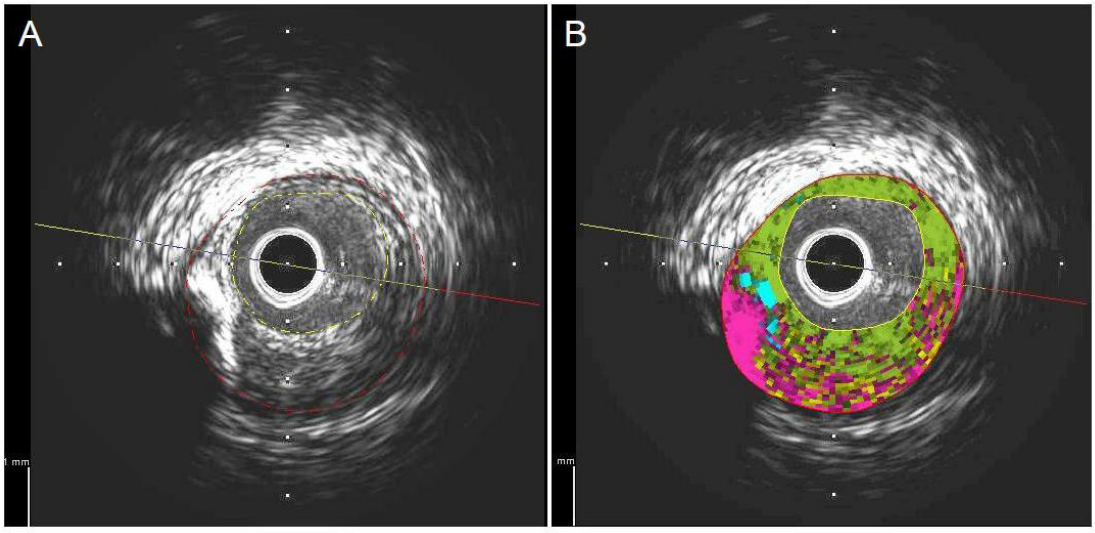

Figure 2: Segmental volumetric lumen and plaque analysis with radiofrequency intravascular ultrasound

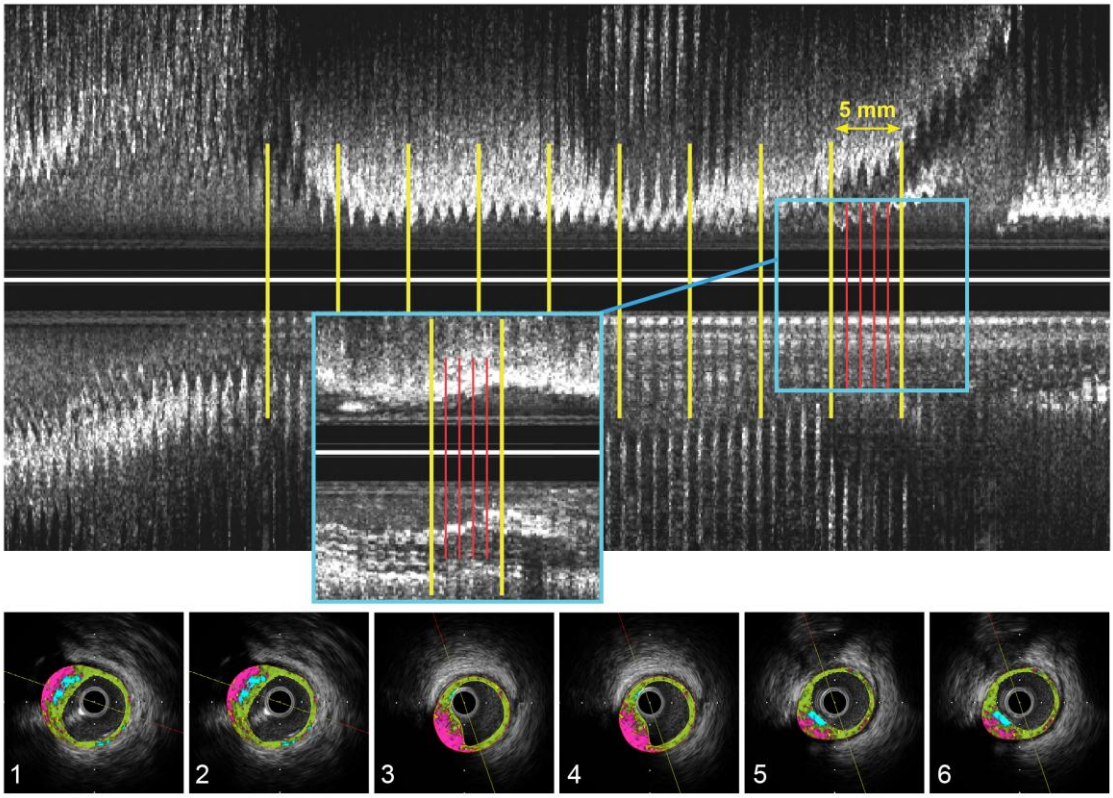

Figure 3: Segmental epicardial vasomotor response according to tissue composition

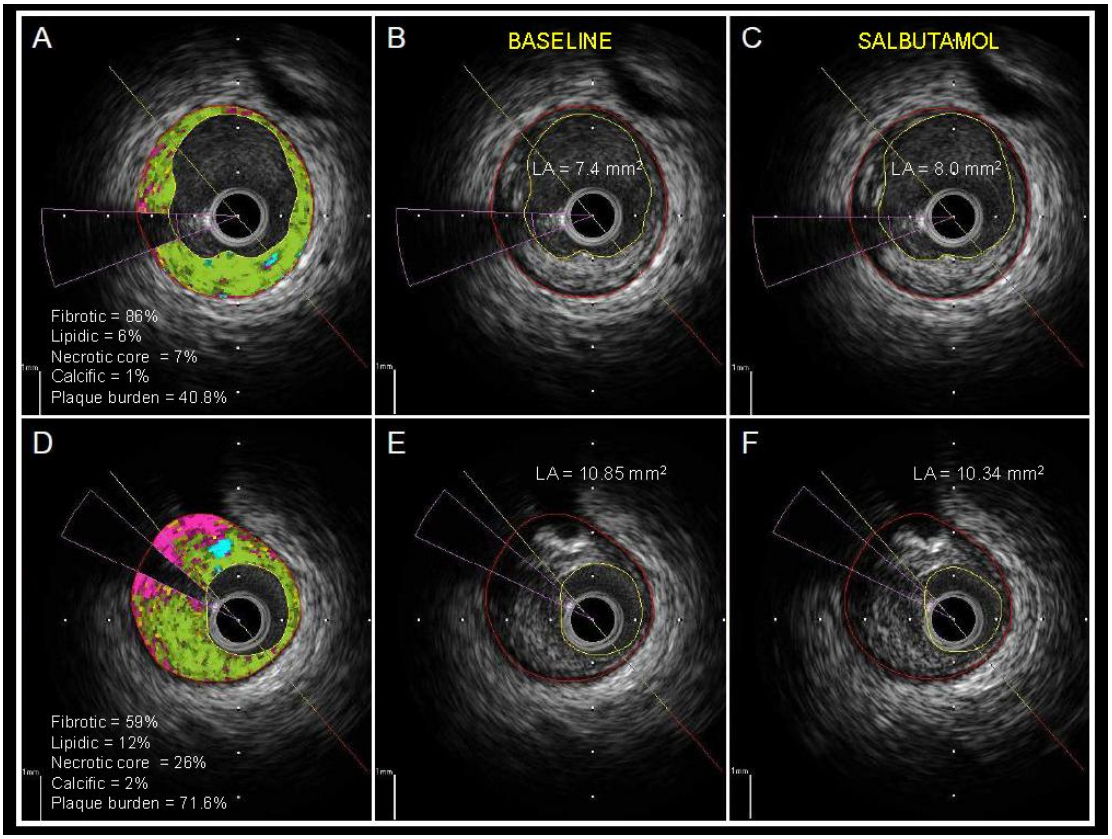

Author contributions:

Dr Rishi Puri – Study design, patient recruitment, data collection, analysis, preparation of manuscript

Professor Stephen Nicholls - Correction and critical review of manuscript

Mrs Danielle Brennan – Analysis, correction and critical review of manuscript

Ms Jordan Andrews - Analysis, correction and critical review of manuscript

Dr Gary Liew – Cath lab procedures, analysis, correction and critical review of manuscript

Dr Adam Nelson - Correction and critical review of manuscript

Mr Angelo Carbone – Record keeping, data collection, critical review of manuscript

Ms Barbara Copus – Cath lab procedures, critical review of manuscript

Professor Samir R. Kapadia - Correction and critical review of manuscript

Professor E. Murat Tuzcu - Correction and critical review of manuscript

Professor John Beltrame – Supervision, correction and critical review of manuscript

Professor Stephen Worthley – Supervision, cath lab procedures, critical review of manuscript

Associate Professor Matthew Worthley – Primary Supervision, study design, cath lab procedures, correction and critical review of manuscript

I hereby give permission for this original manuscript to be included in this thesis submission:

Dr Rishi Puri

Professor Stephen J. Nicholls

Mrs Danielle M. Brennan

Ms Jordan Andrews

Dr. Gary Y. Liew

Mr Angelo Carbone

Ms Barbara Copus

Dr Adam J. Nelson

Professor Samir R. Kapadia

Professor E. Murat Tuzcu

Professor John F. Beltrame

Professor Stephen G. Worthley

Associate Professor Matthew I. Worthley

CHAPTER 7: CORONARY ARTERY WALL SHEAR STRESS IS ASSOCIATED WITH ENDOTHELIAL DYSFUNCTION AND EXPANSIVE ARTERIAL REMODELING IN PATIENTS WITH CORONARY ARTERY DISEASE

Adapted from PURI, R., LEONG, D.P., NICHOLLS, S.J., LIEW, G.Y., NELSON, A.J., CARBONE, A., COPUS, B., WONG, D.T., BELTRAME, J.F., WORTHLEY, S.G., WORTHLEY, M.I. 2013. Coronary artery wall shear stress is associated with endothelial dysfunction and expansive arterial remodeling in patients with coronary artery disease. *EuroIntervention* 2014 [Epub ahead of print Jan 15]

Key words: Wall shear stress; Endothelial function; IVUS; Salbutamol; Atherosclerosis; Remodeling

Puri, R., Leong, D.P., Nicholls, S.J., Liew, G.Y., Nelson, A.J., Carbone, A., Copus, B., Wong, D.T. Beltrame, J.F., Worthley, S.G. & Worthley, M.I. (2013) Coronary artery wall shear stress is associated with endothelial dysfunction and expansive arterial remodeling in patients with coronary artery disease.
EuroIntervention, (in print)

Author contributions:

Dr Rishi Puri – Study design, patient recruitment, analysis, preparation of manuscript

Professor Stephen Nicholls - Correction and critical review of manuscript

Dr Darryl Leong – Analysis, correction and critical review of manuscript

Dr Gary Liew – Cath lab procedures, analysis, correction and critical review of manuscript

Dr Adam Nelson - Correction and critical review of manuscript

Dr Dennis Wong - Correction and critical review of manuscript

Mr Angelo Carbone – Record keeping, critical review of manuscript

Ms Barbara Copus – Cath lab procedures, critical review of manuscript

Professor John Beltrame – Supervision, correction and critical review of manuscript

Professor Stephen Worthley – Supervision, cath lab procedures, critical review of manuscript

Associate Professor Matthew Worthley – Primary Supervision, study design, cath lab procedures, correction and critical review of manuscript

I hereby give permission for this published original manuscript to be included in this thesis submission:

Dr Rishi Puri

Professor Stephen J. Nicholls

Dr. Gary Y. Liew

Dr Darryl P. Leong

Mr Angelo Carbone

Ms Barbara Copus

Dr Adam J. Nelson

Dr Dennis T. Wong

Professor John F. Beltrame

Professor Stephen G. Worthley

Associate Professor Matthew I. Worthley

CHAPTER 8: LEFT MAIN CORONARY ARTERIAL ENDOTHELIAL FUNCTION AND HETEROGENOUS SEGMENTAL EPICARDIAL VASOMOTOR REACTIVITY IN VIVO: INSIGHTS FROM INTRAVASCULAR ULTRASONOGRAPHY

Adapted from PURI, R., NICHOLLS, S.J., BRENNAN, D.M., ANDREWS, J., KING, K.L., LIEW, G.Y., CARBONE, A., COPUS, B., NELSON, A.J., KAPADIA, S.R., TUZCU, E.M., BELTRAME, J.F., WORTHLEY, S.G., WORTHLEY, M.I. 2013. Left main coronary arterial endothelial function and heterogenous segmental epicardial vasomotor reactivity in vivo: insights from intravascular ultrasonography. *Eur Heart J Cardiovasc Imaging* 2014 [Accepted In Press]

Key words: Left main coronary artery; Endothelial function; IVUS; Salbutamol

ABSTRACT

Aims: While the relationship between epicardial coronary vasomotor reactivity and cardiovascular events is well established, this observation has yet to be evaluated within the left main coronary artery (LMCA) in humans *in vivo*. Our aims were to test the endothelium-dependent vasomotor properties of the LMCA, and to compare these responses to downstream epicardial segments.

Methods and results: Thirty patients referred for coronary angiography underwent intracoronary salbutamol provocation during intravascular ultrasound imaging within a non-critically diseased, left-sided conduit vessel. Macrovascular vasomotor response [change in average lumen area at baseline and following 5 mins of 0.30 mcg/min IC salbutamol] and percent atheroma volume (PAV) were evaluated in 30 LMCA, 42 proximal, 109 mid and 132 distal epicardial coronary segments. In comparison with all other segments, the LMCA had the greatest lumen and vessel areas ($p<0.001$), yet the proximal epicardial segments contained the greatest PAV ($p<0.02$). The mid and distal epicardial segments displayed significant endothelium-dependent vasodilatation from baseline ($p=0.002$, $p<0.001$), however the proximal epicardial and LMCA segments did not ($p=0.20$, $p=0.46$). Significant segmental vasomotor heterogeneity was noted in all 30 patients, with opposing vasomotor responses between adjacent LMCA and epicardial segments. Across all segments, baseline LA inversely correlated with the % change in LA ($r = -0.16$, $p=0.0005$).

Conclusions: Endothelium-dependent vasomotor reactivity is heterogenous within the conduit coronary system. Vascular dynamic responses were less prominent in the larger

caliber LMCA and proximal epicardial segments. This may in part relate to higher shear stress in smaller, distal segments, yet also may explain the propensity for culprit plaques to cluster proximally.

Atherosclerosis is a diffuse, systemic disease, driven by a host of endogenous and environmental risk factors. Yet its complications invariably result from a culmination of processes promoting accelerated disease progression, localized regions of disease instability and subsequent thrombo-embolic complications (Naghavi et al., 2003). Endothelial dysfunction is characterized by the reduced bioavailability of nitric oxide (NO) and a resultant impairment of a number of NO-mediated vasomotor, anti-thrombotic and anti-atherosclerotic effects (Quyyumi et al., 1997a); a key component of which includes plaque stabilization (Celermajer et al., 1994). Segmental vasoconstriction may play a synergistic role in mediating acute plaque events, and is implicated not only in the progression of disease (Ross and Glomset, 1973, Yoon et al., 2013), but possibly also plaque erosion and rupture (Bogaty et al., 1994, Lerman and Zeiher, 2005). Although thoroughly investigated within the epicardial and coronary microvasculature in humans *in vivo* (Flammer et al., 2012), a direct evaluation of left main coronary artery (LMCA) endothelium-dependent vasomotor reactivity has not been previously reported in humans. A mechanistic understanding of these factors in this segment is of obvious importance, as the consequences of LMCA disease and occlusion can be sudden and catastrophic.

We recently reported a novel imaging approach of direct intracoronary stimulation during coronary intravascular ultrasonography (IVUS) (Puri et al., 2012b). This enabled volumetric appraisals of lumen response and plaque burden in contiguous, non-overlapping whole epicardial coronary segments across large sections of the coronary tree *in vivo,* enabling the validation of intracoronary salbutamol (and thus selective coronary β_2-adrenoreceptor stimulation) as an epicardial and coronary

microvascular endothelium-dependent vasomotor stimulus (Flammer et al., 2012). We further elucidated that the degree of segmental epicardial vasomotor reactivity per unit of underlying plaque volume remained constant irrespective of the nature of clinical presentation [non-ST segment elevation myocardial infarction (NSTEMI) vs. stable, non-critical coronary disease] (Puri et al., 2013a). Given that this invasive protocol involved infusing IC salbutamol via the coronary guiding catheter placed within the ostium of the left (or right) coronary arteries, the direct stimulation and subsequent IVUS imaging of whole, matched LMCA segments was possible. We thus chose to assess the nature and extent of LMCA vasomotor reactivity in humans *in vivo*. We tested the hypothesis that conduit vasomotor reactivity across the LMCA and downstream epicardial segments may be heterogenous, with a variation in the structure-function relationship of segments across the coronary tree.

METHODS

Study subjects

Forty-seven patients (aged ≥18 yrs) referred for a clinically indicated coronary angiogram were initially recruited for a previous study that assessed the relationship between coronary atheroma volume and segmental epicardial endothelium-dependent vasomotor reactivity in subjects with stable, minimal angiographic disease versus those with NSTEMI (Puri et al., 2013a). The present *post hoc* analysis pooled data from 30 of the original 47 patients, representing the individuals only the individuals undergoing invasive assessment of their left coronary system (with available analyzable, matched LMCA images), thus enabling a specific interrogation of their LMCA segment. There were 4 additional patients in whom adequate sampling/matching of LMCA frames was

deemed technically inadequate by the Core Lab, and the present analysis does not include those individuals. The chosen vessel for IC provocation and imaging in this group of patients was invariably the longest vessel (left anterior descending or left circumflex) containing numerous side-branches (for ease of anatomic matching) and minimal tortuosity, for more stable IVUS imaging. Of these 30 patients who underwent left sided coronary imaging, 13 patients presented with stable (troponin T negative), minimally detectable (<30% visual angiographic stenosis) coronary disease throughout the entire epicardial tree, whereas 17 patients presented with chest discomfort in concert with a significant elevation in troponin T with/without ECG changes. In these NSTEMI patients, the invasive research protocol was performed in a non-critically diseased (<30% angiographic stenosis), non-culprit ('study') vessel, prior to percutaneous coronary intervention within the culprit vessel, adopting the same angiographic inclusion/exclusion criteria for selection of the study vessel as the stable, near-normal cohort. Following informed consent, vasoactive medications were held for at least 24 hrs prior to the invasive study. All procedures were performed in the morning prior to an overnight fast. Exclusion criteria included significant valvular heart disease, left ventricular dysfunction (ejection fraction ≤40%), prior percutaneous or surgical revascularization, acute coronary syndrome within the preceding 4 weeks (in the near normal cohort), known coronary spasm, severe obstructive lung disease, creatinine clearance ≤60 mL/min, β-blocker use in the preceding 24 hrs, or the use of short or long acting β_2 agonists within the previous 12 hrs. This study was approved by the Royal Adelaide Hospital Human Research Ethics Committee.

Cardiac catheterization and intravascular imaging protocols

Coronary angiography was performed via a standard 6-French technique. Intravenous heparin (70 IU/kg) was administered. A 0.014-inch coronary guide wire was placed into the study vessel within its mid-segment away from major side-branches. This wire was also used to deliver a 2.5-French 40-MHz Atlantic Pro IVUS catheter (Boston Scientific, Natick, MA, USA) into the study artery. This was undertaken without pre-treatment with IC nitroglycerin. If percutaneous coronary intervention was to be performed to a culprit lesion, this was done immediately following the invasive research protocol. All IC infusions were administered through an infusion pump at 2 mL/min via the coronary guiding catheter for a period of 5 minutes. Following 3 minutes of IC infusion (of either vehicle solution or salbutamol), the IVUS catheter was then moved from within the guiding catheter into the distal conduit vessel and images were acquired during automated catheter withdrawal at 0.5 mm/sec, during which time the infusions continued. Towards the end of the IVUS pullback, care was taken to minimally disengage the guiding catheter in order to image the ostial LMCA-aortic junction. Our previous validation study showed that repeated, consecutive, IC vehicle infusions over 5 minutes during IC instrumentation with IVUS has no significant impact on changes in lumen measurements over time (Puri et al., 2012b). The IVUS images were recorded on a DVD for off-line analysis.

Coronary infusion and endothelial function testing protocols

The infusion protocols performed for validating IC salbutamol as an endothelium-dependent coronary vasomotor stimulus were previously described in detail (Barbato et al., 2005, Puri et al., 2012b). The rationale for choosing IC salbutamol over IC acetyl choline (ACh) in patients undergoing repeated IVUS-imaging without pre-treatment

with IC nitroglycerin related to a concern regarding the possibility of inducing clinically significant coronary spasm with an ACh-based protocol, particularly involving the LMCA segment. We chose salbutamol as our endothelium-dependent vasodilator as a series of *in vivo* human observations had proven coronary β_2-adrenoreceptor stimulation resulted in nitric-oxide (NO)-mediated peripheral and coronary arterial vasomotor responses (Dawes et al., 1997, Wilkinson et al., 2002, Barbato et al., 2005, Barbato, 2009, Puri et al., 2012b). This analysis comprised of the differences in lumen dimensions obtained following baseline vehicle infusion (IC 5% dextrose) and following a 5 minute infusion of IC salbutamol at the 0.30 μg/min dose.

Data acquisition and analysis

Analysis of IVUS data was performed by the Atherosclerosis Imaging Core Laboratory, Cleveland Clinic, according to prior experience and published guidelines (Mintz et al., 2001, Nicholls et al., 2010). Technicians were blinded to clinical details and imaging sequence. Proximal and distal fiduciary markers (anatomical side-branches) were chosen to define the overall region of vessel to be analyzed, as well as for segment matching. Cross-sectional images were selected every 30 frames (0.5 mm apart). Frames that precluded complete lumen or vessel wall planimetry were excluded from analysis, as were segments that involved branch points. Each IVUS pullback of the epicardial vessel was divided into 5 mm epicardial segments comprising of 11 frames taken at 10 evenly spaced cross-sectional (0.5 mm) intervals (Figure 1). Due to variations in the length of the LMCA segment across the cohort, the entire LMCA segment was analyzed, providing a minimum of 2 mm (5 consecutive frames) of matched LMCA segment could be analyzed. The non-LMCA (or epicardial) segments

were divided according to their proximal, mid or distal location (Figure 2). For the left anterior descending artery (LAD), segments between the LAD ostium until the first major septal branch or first diagonal branch (whichever came first) were considered 'proximal.' Segments between the first septal (or first diagonal) branch until the second diagonal branch were considered 'mid.' All segments distal to the second diagonal branch were considered 'distal.' For the left circumflex artery (LCx), segments between the LCx ostium until the first obtuse marginal branch were considered 'proximal.' Segments positioned between the first and second obtuse marginal were considered 'mid.' All segments distal to the second obtuse marginal branch were considered 'distal' (Figure 2).

Given the proposed segmental heterogeneity of coronary vasomotor reactivity (el-Tamimi et al., 1994, Penny et al., 1995, Tousoulis et al., 1996, Lavi et al., 2009), each segment was thus analyzed separately as an individual entity, with appropriately utilized statistical methods. Matching frames of anatomical side-branches from the baseline and post-salbutamol stimulation IVUS runs were co-registered to ensure accurate segment matching between runs. Leading edges of the lumen and external elastic membrane (EEM) were manually planimetered. Segmental plaque burden was calculated as the average plaque area (area between EEM and lumen-plaque interface), as well as percent atheroma volume (PAV) (Nicholls et al., 2010):

$$\mathbf{PAV = \sum [(EEM_{area} - Lumen_{area}) / \sum EEM_{area}] \; X \; 100}$$

Segmental lumen dimensions were expressed as average lumen areas, taken as the average of all lumen areas of each frame analyzed per segment. Segmental eccentricity

indices (EI) were determined by calculating the average of all EI's of each analyzable frame within a coronary segment (EI= ratio of maximal to minimal plaque thickness). All measurements were performed by 2 analysts blinded to the specific infusion sequence. Intra- and inter-observer variability analysis was performed following planimetry of lumen and plaque areas from 20 randomly selected IVUS frames by two-independent observers and by one observer at two time points separated by 1 week.

Observer variability

For coronary lumen measurements, the intra-observer coefficient of variation was 1.1%, and inter-observer coefficient of variation was 2.6%. For plaque measurements, the intra-observer coefficient of variation was 1.8%, and the inter-observer coefficient of variation was 3.8%.

Statistical analysis

Data are expressed as mean ± standard deviation (SD) or median and 25^{th} and 75^{th} percentiles, as appropriate, for continuous data. Categorical data are presented as a percent of non-missing data. Spearman correlation coefficients were used to describe the correlation between plaque burden and endothelial function. Ultrasonic characteristics are compared across segment type using Student's t-test for normally distributed data and Wilcoxon rank-sum for non-normally distributed data. Absolute change and percent change in lumen area (LA) are summarized as least-squared means (LSmeans) from a mixed model analysis with adjustment for the baseline LA measurement and the presence of an acute coronary syndrome (versus stable coronary

syndrome) at presentation. All analyses were performed used SAS version 9.2 (SAS Institute, Cary, NC). P values <0.05 are considered statistically significant.

RESULTS

Clinical, angiographic and hemodynamic data

Table 1 describes clinical, biochemical and angiographic characteristics of the patient group. Mean age was 58±12 years and 70% of the population were male, 63% smokers, 17% had diabetes, and 50% hypertensive. Mean fasting low-density lipoprotein cholesterol (LDL-C) was 109±35mg/dL, high-density lipoprotein cholesterol was 39±13 mg/dL, and the median high-sensitivity C-Reactive protein level was 3 mg/L. The median LMCA length was 6.5 (2.5, 8.5) mm. The LAD was interrogated 70% of the time.

Intracoronary salbutamol (0.30 μg/min for 5 minutes) resulted in no significant change in heart rate or blood pressure from baseline (Puri et al., 2012b, Puri et al., 2013a). None of the 30 patients reported side effects during the invasive protocol.

Ultrasonic characteristics and vasomotor reactivity according to segment type

Table 2 and Figure 3 describes the overall ultrasonic characteristics of segments at baseline and following IC stimulation, as well as according to segment type (LMCA vs. LAD vs. LCx) and location (proximal vs. mid vs. distal). Overall, compared with the proximal (n=42), mid (n=109) and distal (n=132) epicardial segments, the LMCA segment (n=30) had significantly larger lumen area (LA) ($p<0.001$ for any differences across segments), EEM area ($p<0.001$ for any differences across segments), and average plaque area ($p<0.001$ for any differences across segments). However, compared with

the epicardial segments, the LMCA had significantly smaller PAV ($p=0.02$ for any differences across segments) and eccentricity indices ($p<0.001$ for any differences across segments). Following IC salbutamol provocation, the LMCA and proximal epicardial segments underwent modest changes in LA (absolute change in LA: $p=0.87$; % change in LA: $p=0.16$) from baseline. However, significant endothelium-dependent vasodilatation from baseline was noted in the mid (absolute change in LA: $p=0.085$; % change in LA: $p=0.0017$) and distal (absolute change in LA: $p<0.001$; % change in LA: $p<0.001$) epicardial segments.

During specific interrogation of the LAD, the LMCA segment had a significantly larger EEM, LA and average plaque area than the proximal, mid and distal LAD segments. The LMCA segment also contained the least eccentric plaque compared with the proximal, mid and distal LAD segments ($p<0.001$ for any statistical differences across all groups). Following IC salbutamol provocation, the LMCA and proximal LAD segments underwent modest, non-significant changes in LA (absolute change in LA: $p=0.18$; % change in LA: $p=0.65$) from baseline. However, significant endothelium-dependent vasodilatation from baseline was noted in the mid (absolute change in LA: $p=0.023$; % change in LA: $p=0.002$) and distal (absolute change in LA: $p<0.001$; % change in LA: $p<0.001$) LAD segments.

Compared with data from the LAD, a similar pattern of plaque, vessel and baseline lumen characteristics was found during LCx interrogation. The LMCA segment had a significantly larger EEM and LA than the proximal, mid and distal LCx segments ($p<0.001$ for any statistical differences across all groups for all described

parameters). Again (and owing to the larger overall size of the LMCA segment), while the average plaque area of the LMCA segment was greater compared with epicardial LCx segments ($p<0.001$ for differences across groups), PAV of the LMCA was the smallest in comparison with PAV of the epicardial LCx segments ($p=0.068$ for any statistical differences across all groups). Akin to observations from the LAD, the LMCA segment also contained the least eccentric plaque compared with the proximal, mid and distal LCx segments ($p<0.001$ for any statistical differences across all groups). Following IC salbutamol provocation, LMCA segments demonstrated significant endothelium-dependent vasodilatation (absolute change in LA: $p=0.013$; % change in LA: $p=0.024$) from baseline. On the other hand, all of the epicardial LCx segments (proximal, mid and distal) demonstrated modest, non-significant changes in LA, with a tendency towards vasoconstriction.

Correlations between plaque burden and endothelial function according to segment

Table 3 describes Spearman correlation coefficients for relationships between PAV and changes in lumen areas (absolute and % change). No significant correlations were noted between baseline PAV and vasomotor reactivity in the LMCA segment. A trend towards an inverse correlation between PAV and vasomotor reactivity was evident proximal and mid epicardial coronary segments. Significant inverse correlations were noted between PAV and changes in LA in the distal epicardial segments.

Heterogeneity of segmental coronary endothelial function

Figure 4 illustrates the per-patient heterogeneity of segmental coronary vasomotor reactivity across all LMCA and epicardial segments. This pictorially demonstrates the

marked variation in vasomotor response between adjacent epicardial segments, as well as opposing responses of the LMCA and epicardial segments, in virtually all 30 patients.

Given the known physiological interactions between baseline vessel size, flow, and endothelial function (Pyke and Tschakovsky, 2005), which is thought to be mediated by wall shear stress (WSS), we assessed the relationship between baseline segmental LA and stimulated lumen responses (% change in baseline LA). There was a significant relationship between baseline LA and % change in LA (Spearman r = -0.17, p=0.0005) (Figure 5).

DISCUSSION

The present analysis is the first to describe the endothelium-dependent vasomotor reactivity of the LMCA segment in humans *in vivo,* with direct comparisons of the structure and function of downstream LAD and LCx epicardial segments. These results demonstrate that although the LMCA segment differs in size and structure compared with the downstream epicardial vasculature, NO-dependent vasomotor reactivity was measurable following direct provocation with the selective β_2-adrenoreceptor agonist, salbutamol. With the higher image resolution obtained with IVUS, accurate quantification of segmental lumen responses in relation to underlying plaque volume and topography was obtained, providing a unique insight into the vast heterogeneity of the structure-function relationship of the conduit (LMCA and epicardial) coronary system.

Segmental heterogeneity of epicardial (but not LMCA) vasomotor responses has been previously described using coronary angiography (el-Tamimi et al., 1994, Penny et al., 1995, Tousoulis et al., 1996). These studies utilized sub-selective IC ACh injections into a proximal portion of an epicardial vessel, by-passing the LMCA. By measuring lumen responses of all measurable contiguous segments distal to the infusion catheter, Penny et al. further highlighted opposing segmental vasomotor responses within the same coronary segment following differing doses of IC ACh (Penny et al., 1995). Kato et al. observed IC ACh and bradykinin to elicit opposing vasomotor responses within the same segment (Kato et al., 1997). Seminal studies of coronary endothelial function found significant associations between the presence of endothelial dysfunction and incident cardiovascular events (Schachinger et al., 2000, Suwaidi et al., 2000, Halcox et al., 2002). Similarly, many small scale mechanistic studies demonstrated associations between various risk factors, biomarkers and plaque phenotype with the presence of epicardial endothelial dysfunction (Lavi et al., 2009, Flammer et al., 2012). Yet common to most of these studies was the assessment of only a focalized (2-3 mm length) segment of conduit vessel, and thus a limited representation of the coronary tree. Evaluating responses along the entire length of imaged epicardial conduit, as undertaken in the present analysis and as initially proposed by Penny et al. (Penny et al., 1995), overcomes selection bias, and has important implications for future evaluation of coronary vasomotor reactivity (Puri et al., 2012c).

In the present analysis, the demonstration of a greater tendency of more distally located conduit segments to display endothelium-dependent vasodilatation could be a result of an increasing proximal-to-distal gradient of NO bioavailability along the

epicardial coronary vasculature. Alternatively, coronary arterioles and myocardial resistance vessels are thought to contain up to a five-fold greater density of endothelial β-adrenoreceptors compared with upstream epicardial segments (Barbato, 2009). A likely explanation for the blunted vasomotor response in the LMCA and proximal epicardial segments relates to the significant microvascular vasodilatation and subsequent augmentation of coronary blood flow following IC salbutamol. This is likely to have resulted in an upstream flow-mediated effect (Barbato et al., 2005, Puri et al., 2012b). However, the demonstration of an inverse relationship between baseline LA and segmental vasomotor reactivity in the present analysis is consistent with the known physiological associations between vessel size, flow and the degree of NO-mediated response (Pyke and Tschakovsky, 2005). Regional WSS is believed to be the stimulus for flow-mediated NO-dependent responses, which is invariably greater in smaller sized segments. This may explain the tendency for the larger caliber LMCA and proximal epicardial segments to demonstrate less vasomotor reactivity. Indeed, diminished responses to IC ACh have also previously been described in the proximal compared with mid-distal epicardial coronary vasculature (Simaitis et al., 2004). Furthermore, with the topography and enhanced image resolution of IVUS, we observed a predilection for plaque to accumulate in greater amounts within the LMCA and proximal epicardial segments, compared with distal epicardial segments. Collectively, these observations may help explain why culprit lesions for myocardial infarction more commonly locate in the proximal epicardial coronary tree (Hong et al., 2005, Geske et al., 2010, Toutouzas et al., 2012).

The presence of segmental variation of endothelium-dependent vasomotor reactivity may relate to the variable nature of disease progression along the coronary tree. Opposing serial responses of the LMCA arterial wall to a range of established anti-atherosclerotic therapies was recently described, compared with the corresponding epicardial segment (Puri et al., 2013c). Associations between the baseline burden of LMCA plaque, its rate of progression and constrictive remodeling with incident clinical events were also elucidated. These observations were noted in a sample of 340 patients enrolled in serial IVUS trials. Similar associations between plaque burden and disease progression have been described in the non-LMCA coronary tree, albeit in populations requiring a much larger sample size to demonstrate this association (Nicholls et al., 2010, Puri et al., 2013b). This suggests that pathophysiological characteristics intrinsic to the LMCA may be a more sensitive marker of the overall behavior of the conduit coronary vasculature, possibly better reflecting coronary risk.

The coronary vasculature forms the substrate for a majority of mortal and non-mortal cardiovascular events, and there is difficulty in extrapolating surrogate measures of disease burden and vessel function from the peripheral circulation to the coronary tree. The larger dimensions of the LMCA segment compared to its distal tributaries, enables non-invasive LMCA imaging as a possible means of risk stratifying at-risk patients for incident coronary events. This approach would also be applicable to a far broader patient population than invasive coronary imaging technologies. As a proof-of-concept, cardiac magnetic resonance imaging was successful in non-invasively demonstrating epicardial coronary vasomotor reactivity following isometric handgrip (Hays et al., 2010). Further studies are required to determine the reproducibility of these

findings, as well as standardizing the methodology for non-invasively assessing coronary structure and function, prior to a large-scale, prospective appraisal of its prognostic capacity. Given that larger caliber vessels typically demonstrate less vasomotor reactivity, from a practical viewpoint therefore, the present analysis suggests that a specific functional assessment of the LMCA segment may prove difficult to quantify non-invasively, or with an imaging modality with lesser resolution than IVUS. As such, the LMCA segment perhaps remains more attractive for structural plaque imaging, whereas the epicardial tree is able to be assessed both structurally and functionally along most of its length. The heterogeneity of segmental epicardial vascular responses coupled with the prognostic utility of both plaque burden and vasomotor reactivity, highlights the need to develop imaging strategies that improve our ability to better identify individuals at greatest risk of their sentinel cardiovascular event.

A number of caveats of the present analysis warrant further consideration. Precise mechanisms underlying the apparent progressive gradient of greater vasomotor reactivity, occurring distally along the conduit vessel, were not ascertained from this study. Part of this reasoning however, may relate to inherent differences in structural components of the arterial wall along the coronary tree. Given its proximity to the aorta, the ostial portion of the LMCA is likely subject to vastly different wall shear stress conditions than the remainder of the coronary system. The proximal LMCA is also known to harbor greater amounts of smooth muscle cells, and lacks surrounding adventitia. The density of smooth muscle cells is also thought to lessen distally along the coronary tree (Bergelson and Tommaso, 1995). The behavior of the LCx also seems

to differ from observations from within the LAD. This may simply relate to a smaller number of LCx vessels/segments examined in our analysis, or because of the differing amounts of salbutamol that could have reached each epicardial vessel based upon blood flow division/diversion at the LAD-LCx bifurcation following infusion into the LMCA. However, the blunted NO-dependent vasomotor capacity of the entire LCx system is consistent with the prior demonstration of plaque rupture found along the entire length of LCx vessel, compared with the greater predilection for accumulating within the proximal portion of the LAD (Hong et al., 2005). More recently, an autopsy study revealed the LCx to harbor more thin-capped fibroatheromas compared with the LAD and RCA (Bhanvadia et al., 2013). Collectively, these observations suggest that structural and functional features of plaque vulnerability may be harbored over proportionally greater lengths of the LCx artery compared with the LAD, although this requires further investigation. Plaque composition was not assessed in this analysis, which might have provided added mechanistic insight into the variable nature of plaque vulnerability along the coronary tree, yet is itself not without certain limitations (Thim et al., 2010, Falk and Wilensky, 2012). Bifurcating segments were purposely not evaluated, due to difficulties in assessing lumen dimensions across these regions. Direct vasodilator responses to intracoronary nitroglycerin injection were not evaluated. This would have allowed us to test if smooth muscle cell dysfunction, rather than impairment in NO-dependent function, contributed to blunted vessel wall reactivity in a number of segments. Salbutamol, however, has minimal direct smooth muscle cell dilating properties, as shown in a prior validation study (Puri et al., 2012b).

In conclusion, the present analysis achieved its objectives of highlighting, for the first time in man, the endothelium-dependent vasomotor reactivity of the LMCA segment and its relationship to its tributary branches. Heterogenous and opposing vascular responses between adjacent coronary segments was observed, along with an apparent gradient of NO-dependent segmental responses along the epicardial coronary tree, which may in turn be shear stress related. These mechanistic observations provide support for the proximal clustering of culprit plaque in patients presenting with acute coronary syndromes. Such findings have broad implications for improving imaging methodologies required to advance the field of coronary imaging into clinical practice, with the ultimate aim of better stratifying coronary risk.

Table 1: Clinical and biochemical

Variable	**N = 30 patients**
Age (yrs)	58±12
Male, n (%)	21 (70)
*Smoker, n (%)	19 (63)
Diabetes, n (%)	5 (17)
Hypertension, n (%)	15 (50)
Stable CAD, n (%)	13 (43)
ACS, n (%)	17 (57)
LDL-C (mg/dL)	109±35
HDL-C (mg/dL)	39±13
Triglycerides (mg/dL)	97 (53,115)
hsCRP (mg/L)	3.0 (1.5,6.3)
Troponin T (ng/mL)	0.2 (0.1, 1.0)
LMCA length (mm)	6.5 (2.5, 8.5)
Non-culprit study artery	
LAD, n (%)	21 (70)
LCx, n (%)	9 (30)

Data expressed as mean±SD or median and interquartile range when appropriate
*Definition of smoking was taken as current or within 4 weeks
ACS: acute coronary syndrome; CAD: coronary artery disease; HDL-C: high-density lipoprotein cholesterol; LDL-C: low-density lipoprotein cholesterol; hsCRP, high sensitivity C-reactive protein; LAD, left anterior descending artery; LCx, left circumflex artery

Table 2: Ultrasonic characteristics and segmental vascular reactivity

Variable	**LMCA**	**ALL EPICARDIAL SEGMENTS**			**P-value***
		PROX	**MID**	**DISTAL**	
	N=30	**N=42**	**N=109**	**N=132**	
Average LA (mm^2)	15.2±3.9	10.1±4.4	9.2±3.7	7.2±2.7	<0.001
Average plaque area (mm^2)	6.6 (5.5, 8.5)	5.9 (4.7, 8.4)	5.4 (3.4, 7.4)	3.5 (2.3, 5.8)	<0.001
PAV (%)	32.6±8.0	41.2±15	37.5±13	35.2±13	0.02
Average EEM area (mm^2)	21 (19, 26)	17 (13, 19)	15 (11, 18)	11 (8, 14)	<0.001
EI	3.2 (2.9, 3.9)	5.5 (3.7, 8.3)	5.7 (3.8, 8.9)	4.7 (3.5, 8.5)	<0.001
# Change in LA (mm^2) *Within segment p-value*	-0.04±0.22 *(0.87)*	0.15±0.16 *(0.35)*	0.17±0.10 *(0.085)*	0.32±0.10 *(<0.001)*	0.53
# % change in LA *Within segment p-value*	3.7±2.6 *(0.16)*	1.5±2.0 *(0.45)*	2.9±1.2 *(0.0017)*	4.5±1.1 *(<0.001)*	0.53
	N=21	**LEFT ANTERIOR DESCENDING** **N=36**	**N=80**	**N=92**	
Average LA (mm^2)	15.2±4.1	10.5±4.6	9.6±4.0	7.2±2.9	<0.001
Average plaque area (mm^2)	6.5 (5.4, 8.1)	5.6 (4.5, 8.2)	5.2 (3.3, 6.9)	3.3 (1.9, 5.5)	<0.001
PAV (%)	32.2±8.1	40.4±16	35.7±14	33.3±14	0.051
Average EEM area (mm^2)	20 (19, 27)	17 (13, 20)	15 (11, 18)	10 (8, 13)	<0.001
EI	3.2 (2.6, 3.5)	5.5 (4.0, 8.8)	6.5 (4.3, 9.3)	5.4 (3.6, 9.3)	<0.001
# Change in LA (mm^2) *Within segment p-value*	0.36±0.26 *(0.18)*	0.19±0.18 *(0.31)*	0.28±0.12 *(0.023)*	0.49±0.12 *(<0.001)*	0.05
# % change in LA *Within segment p-value*	1.4±3.2 *(0.65)*	2.0±2.2 *(0.37)*	4.4±1.4 *(0.002)*	6.6±1.4 *(<0.001)*	0.29
	LMCA **N=9**	**LEFT CIRCUMFLEX** **N=6**	**N=29**	**N=40**	
Average LA (mm^2)	15.1±3.7	7.9±1.3	8.2±2.6	7.2±2.4	<0.001
Average plaque area (mm^2)	6.7 (5.9, 8.5)	6.3 (4.9, 9.0)	6.2 (4.5, 7.8)	4.1 (2.9, 6.9)	<0.001
PAV (%)	33.7±8.1	45.5±5.5	42.3±10	39.4±10	0.068

Average EEM area (mm^2)	23 (20, 25)	14 (13, 17)	14 (11, 18)	12 (8, 16)	<0.001
EI	3.4 (3.0, 4.1)	6.1 (3.5, 6.9)	4.7 (3.2, 7.7)	4.1 (3.1, 5.0)	0.39
[#]Change in LA (mm^2) *Within segment p-value*	1.0±0.39 *(0.013)*	-0.14±0.36 *(0.69)*	-0.13±0.16 *(0.42)*	-0.13±0.15 *(0.40)*	0.074
[#] % change in LA *Within segment p-value*	10.5±4.6 *(0.024)*	-1.9±4.2 *(0.66)*	-1.6±1.9 *(0.41)*	-0.24±1.7 *(0.89)*	0.12

*Represents level of significance across any type of segment

PAV = percent atheroma volume; EEM = external elastic membrane; EI = eccentricity index

Changes in LA are in response to IC salbutamol

[#]Least squares means from a mixed model adjusting for baseline measurements

Table 3: Correlations between plaque burden and endothelial function according to segment

Plaque measure	Change in Lumen Area	
	% change	Absolute change
LMCA PAV	r = 0.15, p = 0.42	r = 0.14 , p = 0.48
Prox epicardial PAV	r = -0.22, p = 0.17	r = -0.37 , p = 0.018
Mid epicardial PAV	r = -0.14, p =0.14	r = -0.18 , p = 0.06
Distal epicardial PAV	r = -0.17, p = 0.047	r = -0.30, p = 0.0006

FIGURE LEGEND

Figure 1: Segmental volumetric lumen & plaque analysis with IVUS

IVUS pullback divided into 5-mm segments (denoted by red lines on longitudinal view). Within each segment, plaque and lumen volumes were calculated upon sequential numbered frames spaced 0.5 mm apart, numbered 1-10 (cross-sectional views) (Adapted from Puri R et al., Eur Heart J 2012;33:495-504)

Figure 2: Segmentation of the LMCA and epicardial coronary tree

For the left anterior descending artery (LAD), segments between the LAD ostium until the first major septal branch (S1) or first diagonal branch (D1) (whichever came first) were considered 'proximal.' Segments between S1 (or D1) until the second diagonal branch (D2) were considered 'mid.' All segments distal to D2 branch were considered 'distal.' For the left circumflex artery (LCx), segments between the LCx ostium until the first obtuse marginal branch (OM1) were considered 'proximal.' Segments positioned between OM1 and second obtuse marginal (OM2) were considered 'mid.' All segments distal OM2 were considered 'distal'

Figure 3: Lumen areas pre- and post intracoronary salbutamol across the LMCA, LAD and LCx segments

Figure 4: Heterogeneity of segmental conduit endothelial-dependent vasomotor reactivity

In almost all patients, there was discordance in the direction of vasomotor response between the LMCA and epicardial segments, as well as marked heterogeneity within each individual between adjacent epicardial segments

Figure 5: Relationship between baseline segmental lumen area and % change in LA following IC salbutamol

Linear regression line demonstrating a significant inverse relationship between baseline segmental lumen area (LA) and the % change in LA following IC salbutamol provocation

Figure 1

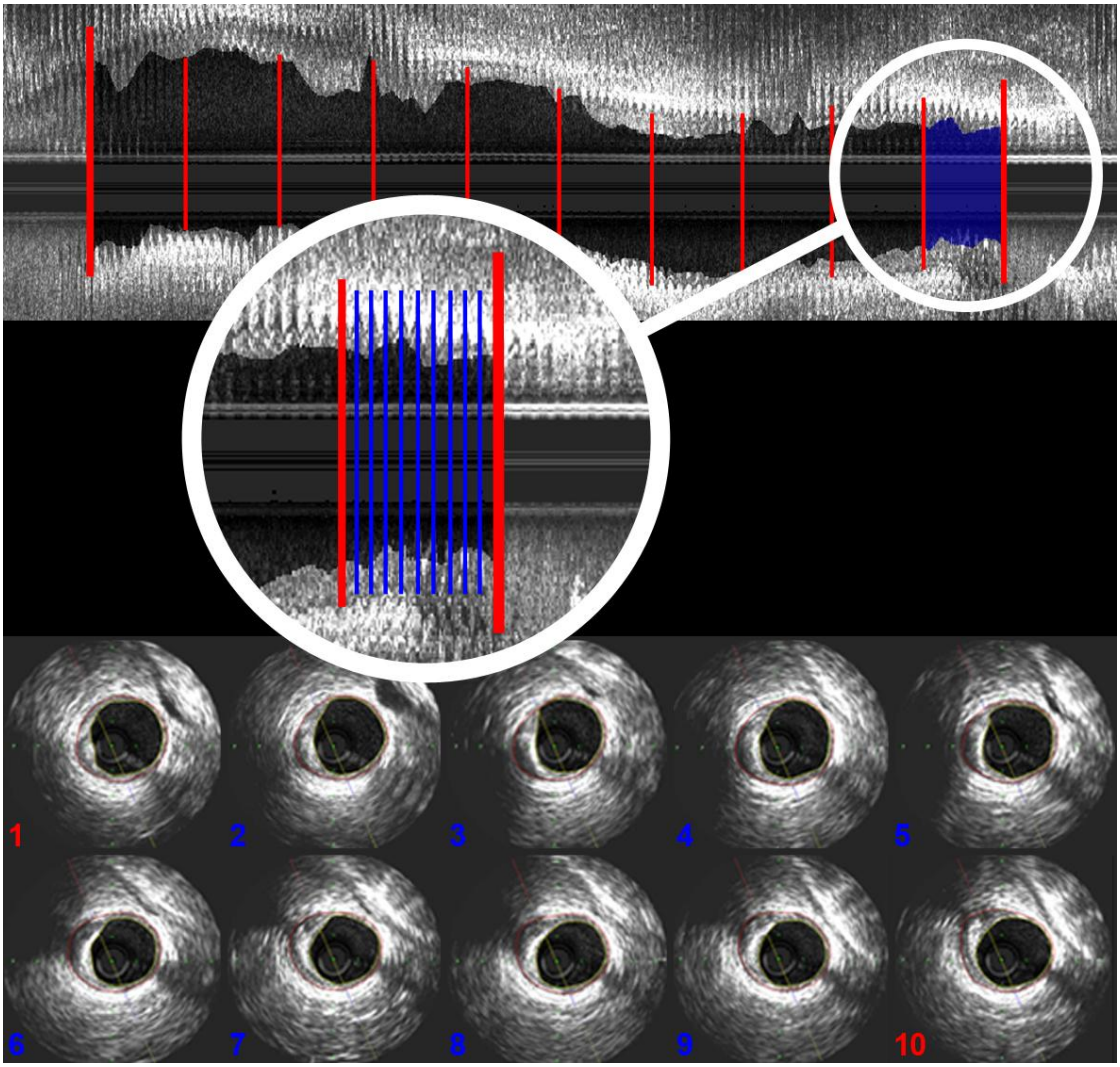

Figure 2

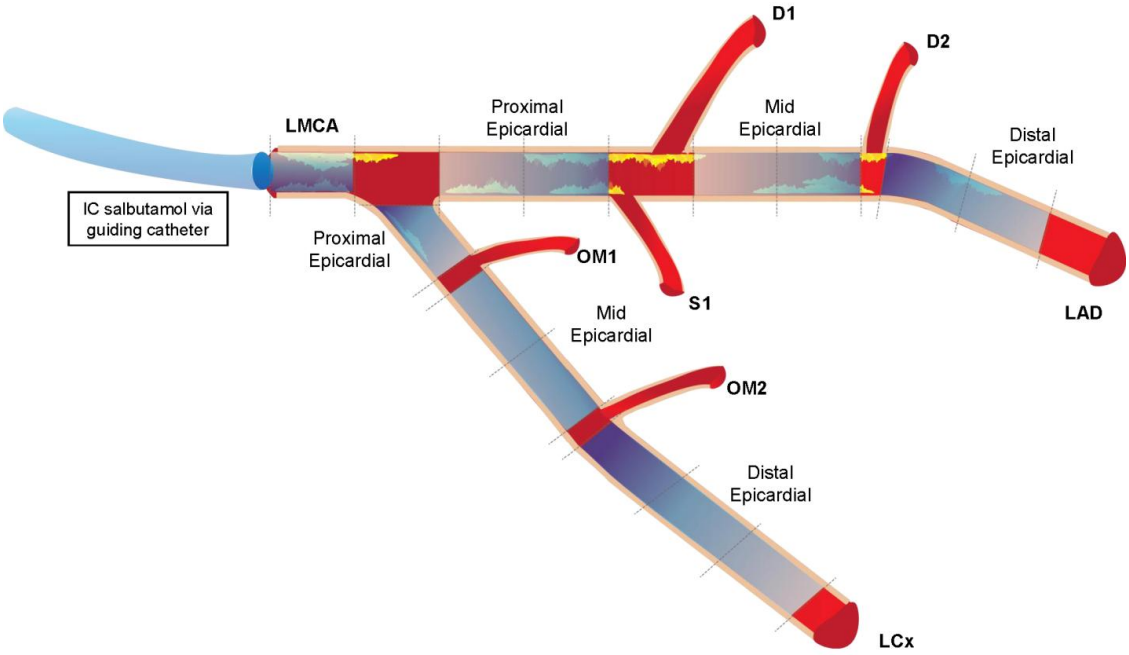
D1
D2
LMCA
Proximal Epicardial
Mid Epicardial
Distal Epicardial
IC salbutamol via guiding catheter
Proximal Epicardial
OM1
S1
Mid Epicardial
LAD
OM2
Distal Epicardial
LCx

Figure 3

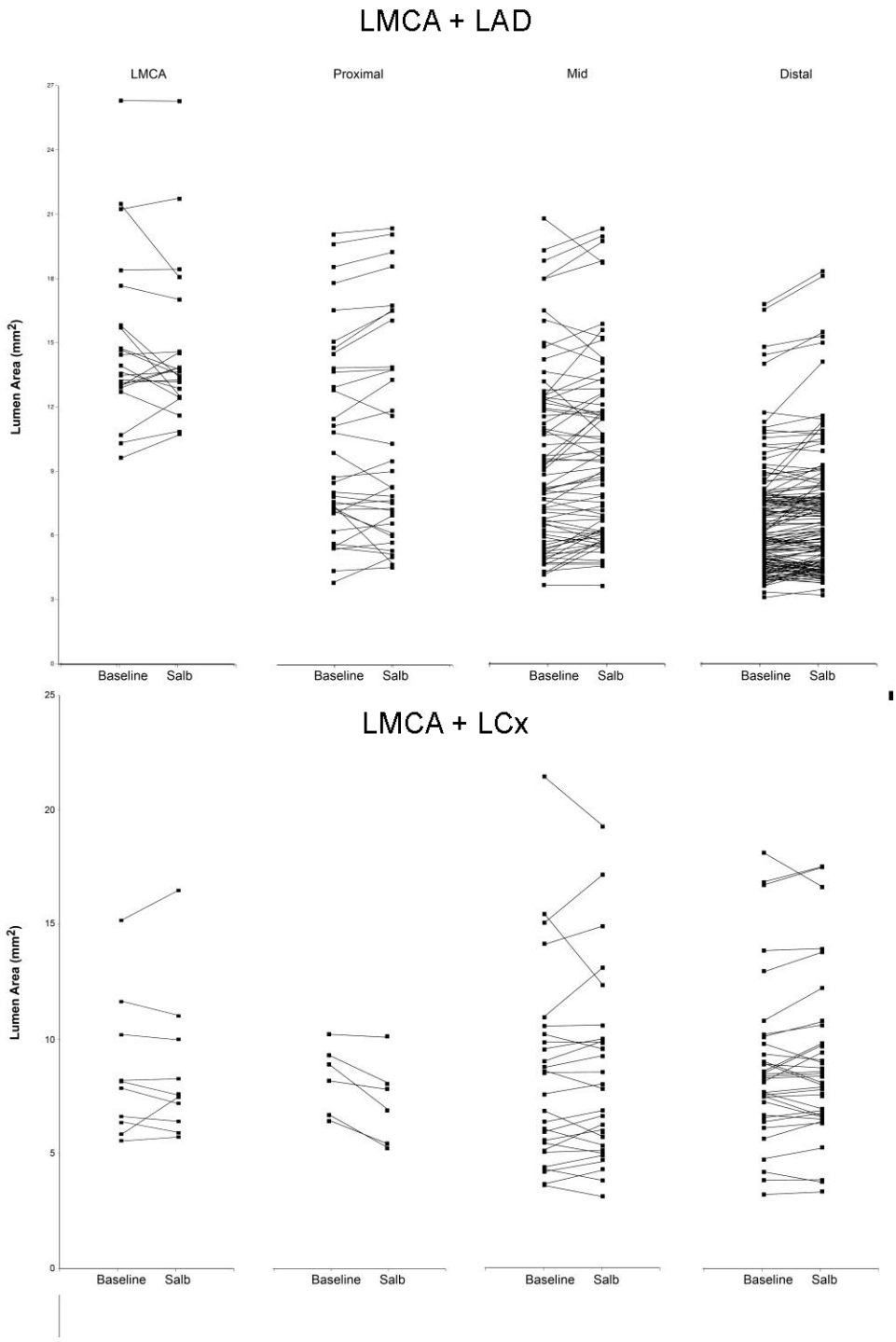
LMCA + LAD
LMCA
Proximal
Mid
Distal
Lumen Area (mm²)
Baseline
Salb
LMCA + LCx

Figure 4

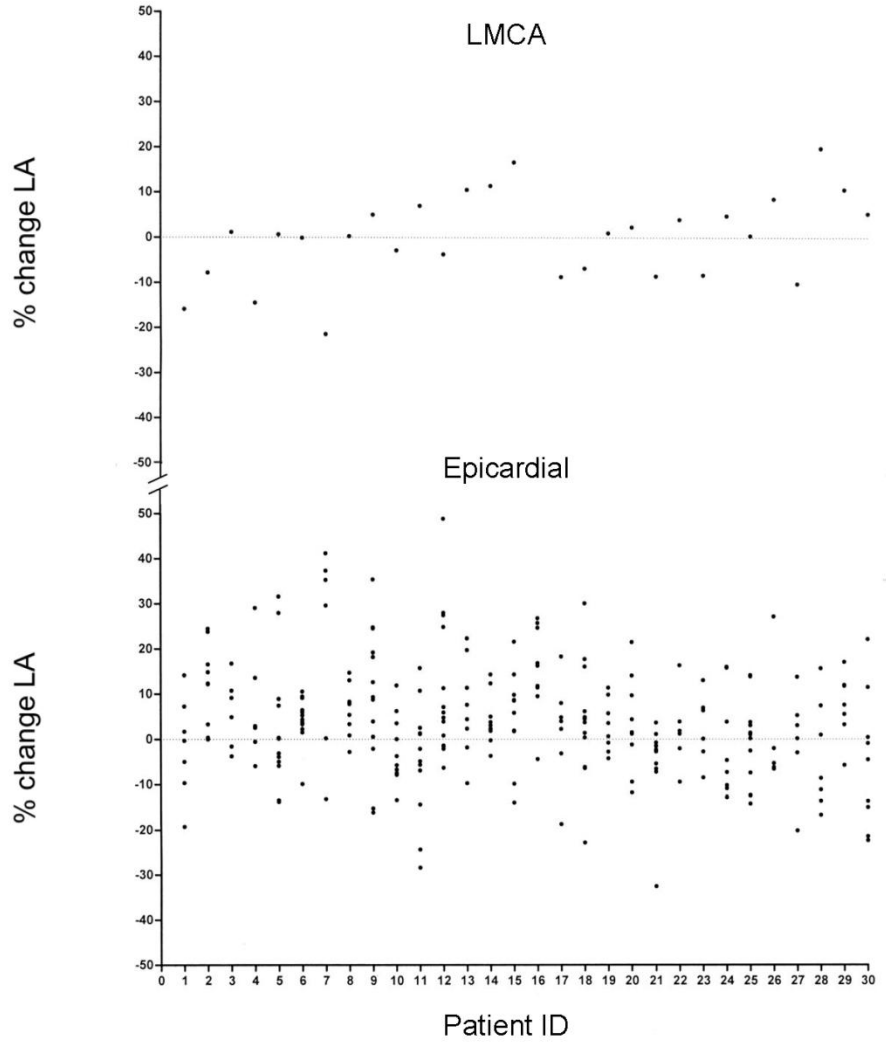

Figure 5

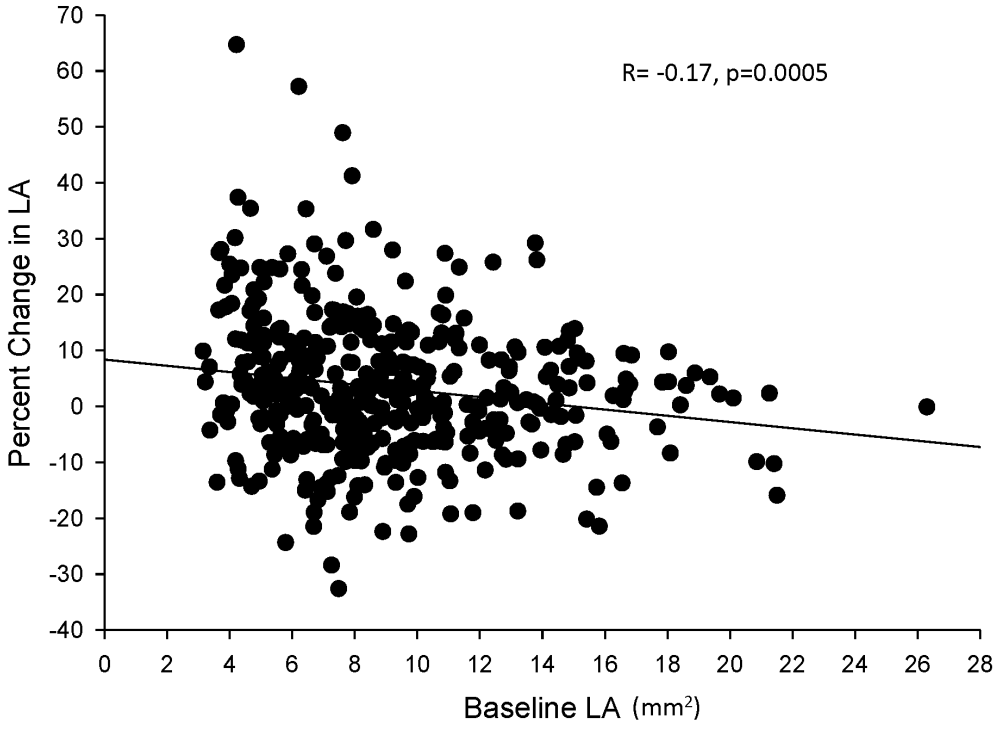
R= -0.17, p=0.0005
Percent Change in LA
Baseline LA (mm²)
70
60
50
40
30
20
10
0
-10
-20
-30
-40
0
2
4
6
8
10
12
14
16
18
20
22
24
26
28

Author contributions:

Dr Rishi Puri – Study design, patient recruitment, analysis, preparation of manuscript

Professor Stephen Nicholls - Correction and critical review of manuscript

Mrs Danielle Brennan – Analysis, correction and critical review of manuscript

Ms Jordan Andrews - Analysis, correction and critical review of manuscript

Mrs Karilane King - Analysis, correction and critical review of manuscript

Dr Gary Liew – Cath lab procedures, analysis, correction and critical review of manuscript

Dr Adam Nelson - Correction and critical review of manuscript

Mr Angelo Carbone – Record keeping, critical review of manuscript

Ms Barbara Copus – Cath lab procedures, critical review of manuscript

Professor Samir Kapadia - Correction and critical review of manuscript

Professor E. Murat Tuzcu - Correction and critical review of manuscript

Professor John Beltrame – Supervision, correction and critical review of manuscript

Professor Stephen Worthley – Supervision, cath lab procedures, critical review of manuscript

Associate Professor Matthew Worthley – Primary Supervision, study design, cath lab procedures, correction and critical review of manuscript

I hereby give permission for this original manuscript to be included in this thesis submission:

Dr Rishi Puri Professor Stephen J. Nicholls

Dr. Gary Y. Liew

Mr Angelo Carbone

Ms Barbara Copus

Dr Adam J. Nelson

Professor Samir R. Kapadia

Professor E. Murat Tuzcu

Mrs Danielle M. Brennan

Professor John F. Beltrame

Ms Jordan Andrews

Mrs Karilane L. King

Professor Stephen G. Worthley

Associate Professor Matthew I. Worthley

CHAPTER 9: VARIATIONS IN HUMAN CORONARY LUMEN DIMENSIONS MEASURED *IN VIVO*: QUANTITATIVE COMPARISONS BETWEEN INTRAVASCULAR ULTRASOUND, FOURIER-DOMAIN OPTICAL COHERENCE TOMOGRAPHY AND THREE DIMENSIONAL QUANTITATIVE CORONARY ANGIOGRAPHY

Adapted from PURI, R., NELSON, A.J., LIEW, G.Y., NICHOLLS, S.J., CARBONE, A., WONG, D.T., HARVEY, J.E., UNO, K., COPUS, B., LEONG, D.P., BELTRAME, J.F., WORTHLEY, S.G., WORTHLEY, M.I. 2012. Variations in coronary lumen dimensions measured in vivo. *JACC Cardiovasc Imaging*. 5(1):123-4

Key words: intravascular ultrasound (IVUS), optical coherence tomography (OCT), lumen dimensions

Abbreviations:

IVUS: Intravascular ultrasound

FD-OCT: Frequency domain optical coherence tomography

3D-QCA: Three dimensional quantitative coronary angiography

LD: Lumen diameter

LA: Lumen area

PAV: Percent atheroma volume

PCI: Percutaneous coronary intervention

ABSTRACT

Objective: To evaluate systematic differences of *in vivo* human coronary lumen dimensions measured within multiple coronary segments utilizing multi-modality invasive coronary imaging tools.

Background: As the use of multiple invasive coronary imaging modalities becomes more common, a better understanding of the inherent differences in *in vivo* quantitative coronary lumen measurements within coronary segments of varying size and plaque burden between different imaging modalities is required.

Methods: Ten patients with non-critical coronary disease underwent IVUS, Fourier-domain (FD)-OCT and 3D-QCA imaging. Coronary segments 4mm in length (n=80) were defined. Measured lumen dimensions [mean lumen diameters (LD), lumen areas (LA)] were compared with each imaging modality, with IVUS-derived plaque burden measurements also undertaken. Segments were stratified according to IVUS-derived segmental LD and LA as small (LD <2.75mm, LA <5mm^2), moderate (LD 2.75-4mm, LA 5-9 mm^2) or large (LD >4mm, LA >9 mm^2) respectively.

Results: Corresponding lumen measurements on IVUS were significantly larger than those acquired by FD-OCT (differences in LD 7%, p<0.0001 and LA 13%, p<0.0001). Such differences were greater in small segments compared to moderate and large sized segments [LA (small, moderate, large): 24%, 9.1%, 12%; p=0.002 small vs. moderate, p=0.03 small vs. large; LD (small, moderate, large): 11%, 5.3%, 5.9%, p=0.08 small vs. moderate, p=0.06 small vs. large], with no influence of plaque burden upon these differences. The 3D-QCA derived LA measurements were significantly smaller compared to IVUS (41%, p< 0.0001) and FD-OCT (29%, p<0.0001).

Conclusions: For the same *in vivo* coronary segment, measured lumen dimensions were significantly greater with IVUS compared to FD-OCT and 3D-QCA. These findings were significantly magnified within smaller coronary segments. Until further validation studies are conducted, specific cut-off values validated with IVUS should not be arbitrarily translated into the OCT hemisphere for clinical decision making.

Optical coherence tomography (OCT) is rapidly emerging as an exciting intravascular imaging modality that uses processed backscattered reflections of infrared light to generate real-time tomographic images. The light-tissue interaction allows for a vastly superior axial and lateral resolution than contemporary intravascular ultrasound (IVUS) technologies. This superior near-field resolution comes at the expense of limited tissue penetration and subsequent far-field imaging capabilities. The more recent widespread availability of the non-occlusive Fourier-domain imaging (FD-OCT) platform has considerably reduced procedural time, and increased safety (Imola et al., 2010, Prati et al., 2007).

Intravascular ultrasonography is still considered the 'gold-standard' technique for coronary imaging, whereby the ability to image through blood for visualizing the entire vessel wall provides a consistent method of providing accurate quantitative measurements of vessel and plaque dimensions in a variety of clinical and research scenarios (Sipahi et al., 2006, Nicholls et al., 2007a). A number of specific cut-off measurements of lumen dimensions have been validated with IVUS for the assessment of indeterminate coronary lesions and furthermore this imaging modality has revolutionized the interventional cardiologists understanding of appropriate balloon and stent expansion. Although limited in its ability to quantify plaque burden, OCT offers a sharp, precise evaluation of the lumen-intima border, theoretically allowing a superior accuracy compared to IVUS-based lumen evaluation, particularly for evaluating optimal stent deployment and apposition. Despite a previous study describing OCT to consistently underestimate lumen dimensions compared to IVUS in a limited number of *ex vivo* and *in vivo* samples (Gonzalo et al., 2009a), there is a paucity a data comparing

contemporary versions of each technology within the *in vivo* human coronary setting. Therefore, prior to the declaration of OCT as a potential new 'gold-standard' for *in vivo* coronary lumen-based imaging, a comprehensive understanding of the relative differences of lumen measurements between each modality is required. This will be important for the interpretation of a number of current and future trials which are employing both IVUS and OCT for assessing the baseline and lumen response to a variety of local and systemic therapies, as well as for current and future clinical decision making during percutaneous coronary intervention (PCI).

The chief aim of this study was to utilize state-of-the-art multi-modality invasive coronary imaging techniques to assess potential inter-modality differences in measured *in vivo* coronary lumen dimensions across a broad range of coronary segments stratified according to size and plaque burden.

METHODS

Study subjects

This study enrolled 10 consecutive patients (aged ≥18 years) electively referred to the Royal Adelaide Hospital cardiac catheterization laboratories for the investigation of chest pain. Informed consent was obtained prior to the procedure. Patients with prior percutaneous or surgical revascularization, recent acute coronary syndrome, systolic heart failure (LVEF ≤35%), severe valvular heart disease or a creatinine clearance ≤60 mL/min were excluded. Only patients with non-obstructive coronary disease (≤70% stenoses) in all 3 native vessels were included, with the target vessel needing to have

angiographic stenosis ≤50% to be included. This study was approved by the Royal Adelaide Hospital Human Research Ethics Committee.

Catheterization, IVUS and FD-OCT imaging protocols

Coronary angiography was performed via a standard 6 French technique. A 6 French guiding catheter was placed into the coronary ostium. Intravenous heparin (70 IU/kg) was administered for the research protocol. Intravascular ultrasound was performed using a high-frequency rotational catheter (either 40MHz Atlantis® SR Pro catheter, Boston Scientific, Natick, MA, USA, or 45MHz Revolution® catheter, Volcano Therapeutics, Rancho Cordova, CA, USA) in each patient at an automated pullback speed of 0.5 mm/s, and was performed prior to FD-OCT imaging. All IVUS imaged were saved and recorded on a DVD for off-line analysis.

Fourier domain-based OCT image acquisition was performed immediately following IVUS acquisition within the same vessel. The C7-XR OCT system (using the 2.7 Fr C7 Dragonfly™ Imaging Catheter, LightLab Inc., Westford, MA, USA) was used, whereby angiographic contrast media was injected through the guiding catheter via an injection pump (settings: 14 mL volume contrast, 4mL/s, 300 psi per OCT run) to achieve effective intracoronary clearance of blood for optimal image acquisition. At an automated pullback speed of 20 mm/s, each pullback recorded 54 mm of coronary artery over a 2-3 second period. Prior to the commencement of imaging, the Z-offset was adjusted for appropriate image calibration for accurate image measurements offline. Images were saved and recorded on a DVD for off-line analysis.

Data analysis and segment matching

All IVUS and FD-OCT data was analyzed using echoPlaque 3.0.60 (Indec Systems, Santa Clara, CA, USA). For each run, the common most distal and proximal fiduciary markers (anatomical side-branches) were chosen from corresponding IVUS and OCT pullbacks in order to define the region of vessel to be analyzed. For IVUS imaging, cross-sectional images were selected every 30 frames (0.5 mm) apart. Coronary lumen and the external elastic membrane were traced by manual planimetry upon each selected IVUS frame, to enable the calculation of average lumen areas and plaque burden within each segment. Plaque burden was calculated as percent atheroma volume (PAV) within each segment (Nicholls et al., 2007a). Briefly, the leading edges of the lumen and EEM were traced by manual planimetry. Plaque area was defined as the area occupied between these leading edges. The PAV within each coronary segment was calculated as the proportion of the entire vessel cross-sectional area (of the respective coronary segment) occupied by atherosclerotic plaque. For OCT imaging, cross-sectional images were selected every 2nd frame (0.4 mm) apart. Each IVUS and OCT run was precisely divided into pre-defined consecutive 4 mm segments, comprising of 9 cross-sectional IVUS frames (with 8 x 0.5 mm intervals) and 11 cross-sectional OCT frames (with 10 x 0.4 mm intervals). Each segment was therefore analyzed separately. Using MIB software (Indec Medical Systems, Santa Clara, CA, USA), the corresponding IVUS and OCT pullbacks (with numbered frames) were simultaneously played in order to accurately frame match anatomical fiduciary markers between each run. This technique ensured that precisely the same arterial segments were consistently analyzed between each IVUS and OCT run per patient. The leading edges of the lumen were traced by

manual planimetry. Only cross sectional images deemed acceptable for complete lumen tracing (frames that contained a complete lumen circumference) were included. Within each segment, the average lumen area (LA) and mean lumen diameter (LD) were calculated from each analyzable frame (Figure 1).

Three-dimensional QCA was performed offline using 3D reconstruction software (Paieon Medical, Rosh Ha'ayin, Israel). The contrast-filled non-tapered part of the guiding catheter was used to calibrate pixel size. The 2 best orthogonal views of the entire segment of vessel to be analyzed were used for 3D-QCA reconstructions. The same proximal and distal anatomical fiduciary markers were identified from the coronary angiogram in 2 selected views which were at least 30^{o} orthogonal to each other. Following the identification of the centre of the lumen, the software generated a 3D representation of the arterial lumen. Representative LA's were obtained from each interval step of the cursor, and subsequently matched to represent each pre-defined 4 mm coronary segment. Similar to IVUS and OCT measurements, the average 3D-QCA derived LA was calculated per segment (Figure 2).

Segmental lumen and plaque measurements were further categorized according to lumen size and plaque burden. Small coronary segments (LD <2.75mm) were defined according to a common and clinically accepted cut-off (Ardissino et al., 2004, Biondi-Zoccai et al.). From a LA perspective, other than an IVUS-derived minimum LA of 4 mm^2 within the epicardial coronary tree, considered to be a good correlate of lesion hemodynamic significance (Sipahi et al., 2006), there are no universally accepted criteria of grading coronary vessel size. For this reason, we arbitrarily chose an LA of

<5mm^2 as the cut-off mark for a 'small' vessel. Classification of lumen diameters were thus made according to the following criteria: 'small' segments had LD <2.75 mm; 'medium' segments had LD 2.75-5 mm; 'large' segments had LD >5 mm. Similarly, classification of LA's were made according to the following criteria: 'small' segments had LA <5 mm^2; 'medium' segments had LA 5-9 mm^2; 'large' segments had LA >9 mm^2. Similarly, segment classification according to baseline plaque burden was simply categorized according to tertiles of plaque burden.

Statistical analysis

Continuous variables are expressed as mean ± SD, and categorical data are expressed as number or frequencies of occurrence. Normality of data was determined using the D'Agostino Pearson test. Spearman's correlation was performed for non-parametric data. Linear regression and Bland-Altman plots were used to compare measurements by IVUS, OCT and 3D-QCA. Paired t-test (or Wilcoxon matched-pairs signed rank test for non-Gaussian distributed data) was used to assess for significant differences between each imaging modality. The relative differences between segmental measurements were calculated, and defined as the absolute difference divided by the average of both measurements (Gonzalo et al., 2009a). Statistical analysis was performed using GraphPad Prism (version 5.01, GraphPad Software, La Jolla, CA, USA). A two-tailed P value of < 0.05 was considered significant.

RESULTS

Clinical, procedural and vessel characteristics

Clinical and segment characteristics are described in Tables 1 and 2 respectively. The imaging research protocol was completed in all patients without incident. A total of 80 (4 mm) coronary segments were evaluated in 10 coronary arteries. Segments were stratified according to lumen dimensions (LD and LA), as well as by plaque burden (PAV) (Table 2).

IVUS vs. FD-OCT comparisons (of lumen area and diameter measurements)

There was a good agreement between IVUS and OCT measurements of LD and LA (Figure 3). The mean LD of all segments (irrespective of vessel size or plaque burden) measured with IVUS was 3.37±0.76 mm, compared with the corresponding mean LD measured by OCT as 3.07±0.70 mm ($p < 0.0001$), with a mean relative difference between IVUS and OCT of 6.8%. The mean lumen area (LA) of all segments with IVUS was 9.35±4.1 mm^2, compared with a corresponding mean LA on OCT as 7.79±3.3 mm^2 ($p < 0.0001$), with a mean relative difference of 13.1%.

IVUS vs. FD-OCT lumen comparisons: influence of vessel size

Small coronary segments had a mean LD and LA of 2.2±0.48 mm and 3.8±0.9 mm^2 respectively; medium coronary segments had a mean LD and LA of 3.3±0.84 mm and 7.5±1.0 mm^2 respectively; and large coronary segments had mean LD and LA of 4.4±1.1 mm and 12.9±3.0 mm^2 respectively (Table 2). Corresponding measurements of LD and LA measured with OCT were: small segments LD 1.92±0.32 mm, LA 3.1±0.97 mm^2 respectively; medium segments LD 3.11±0.44 mm, LA 6.89±1.34 mm^2

respectively; large segments LD 4.01±0.35 mm, LA 10.75±2.36 mm^2 respectively. The mean relative differences between IVUS and OCT for LD measurements in small, moderate and large sized segments were 11%, 5.3%,and 5.9% respectively (p=0.08 for small vs. moderate, p=0.057 for small vs. large). The mean relative differences between IVUS and OCT for LA measurements in small, medium and large segments were 24%, 9.1% and 12% respectively (p=0.002 for small vs. moderate, p=0.032 for small vs. large) (Figure 4).

IVUS vs. FD-OCT lumen comparisons: influence of plaque burden

Segments were stratified according to segmental plaque burden (PAV) within in each coronary segment. Segments were then analyzed according to tertiles of plaque burden (Table 2). The mean relative differences between IVUS and OCT for LA in tertiles 1, 2 and 3 of plaque burden were 11%, 16% and 13% respectively (p=0.67 for T1 vs. T2, p=0.87 for T1 vs. T3). The mean relative differences between IVUS and OCT for LD in tertiles 1, 2 and 3 of plaque burden were 5.5%, 7.9% and 6.4% respectively (p=0.68 for T1 vs. T2, p=0.80 for T1 vs. T3). Plaque burden was thus found to have no significant influence upon measured differences of LD and LA between IVUS and FD-OCT.

Comparison between 3D-QCA measurements and IVUS/FD-OCT measurements

There was satisfactory agreement between LA derived by 3D-QCA compared with IVUS and OCT (Figure 5). The mean LA of all segments obtained with 3D-QCA was 6.30±3.27 mm^2 ($p < 0.0001$ compared with both IVUS and OCT). The mean relative difference of LA measured with 3D-QCA and IVUS was 41.5%, compared with 28.9% with 3D-QCA and OCT ($p = 0.012$) (Figure 6).

DISCUSSION

This is the first human *in vivo* study to evaluate the systematic variation of measured coronary lumen dimensions within multiple coronary segments imaged with a state-of-the-art FD-OCT system, high-frequency rotational IVUS systems and 3D-QCA software. We highlight consistently larger LD and LA measurements obtained with IVUS compared to OCT across all segments, with a further significant reduction in these luminal measurements when measured with 3D-QCA. We also show that the relative differences in lumen measurements between IVUS and OCT appear to be greater within smaller coronary segments. This finding was not influenced by plaque burden.

Differences in lumen measurements between IVUS and FD-OCT

Previous reports have shown IVUS to produce larger lumen dimensions than OCT during *ex vivo* and *in vivo* coronary imaging (Gonzalo et al., 2009a, Yamaguchi et al., 2008). However these observations were made with a previous generation OCT imaging system that used an occlusive technique to displace blood from the coronary lumen (Yamaguchi et al., 2008). This technique is known to result in a drop in intracoronary pressure distal to the site of balloon occlusion, resulting in a degree of lumen collapse. The study by Gonzalo et al. also utilized a 20MHz steady state IVUS catheter (Eagle Eye,® Volcano Therapeutics, Rancho Cordova, CA, USA) to compare against OCT measurements (Gonzalo et al., 2009a), which results in poorer near-field spatial resolution than comparative 40MHz or 45MHz IVUS catheters, further contributing towards the relative overestimation of lumen dimensions compared to OCT. Our study is therefore the first to use the latest OFDI OCT imaging system with a rapid pullback

speed (20 mm/sec) along with significantly higher resolution (40MHz and 45MHz) rotational IVUS catheters to compare the inter-modality agreement of coronary lumen dimensions in a multiple in vivo human coronary arterial segments. Our results indicate that despite the use of a non-occlusive FD-OCT system, IVUS still results in significantly larger relative LD (7%) and LA (13%) measurements respectively. Similarly, despite the use of higher resolution IVUS and superior OCT capabilities than prior studies, IVUS consistently produced LD and LA measurements that were 11% and 24% relatively greater in small coronary segments respectively. These observations highlight the limited axial/spatial resolution images produced with IVUS, accentuated within small vessels, whereby difficulties may arise with differentiating luminal blood speckling from intimal tissue or motion artifacts. It would also appear that such differences are unaffected by the burden of atherosclerosis, further highlighting the importance of lumen dimensions rather than vessel dimensions in determining the nature of such *in vivo* measurements.

It is known that LA measurements may vary according to the cardiac cycle by up to 8% (Ge et al., 1994), and therefore ECG-gating of coronary images measured with IVUS would be required to factor in the issue of coronary compliance influencing lumen dimensions. As OCT images are not gated to the cardiac cycle, it has been previously suggested that this discrepancy in image gating between both modalities may account for the observed differences between IVUS and OCT measurements. However, even though our IVUS images were ECG-gated, we selected IVUS frames at exactly 0.5 mm apart. Our methodology ensured the selection of 9 consecutive IVUS frames to represent lumen dimensions of each 4 mm segment. This technique would be expected

to result in the random sampling of an equal number of systolic and diastolic-gated frames per segment, which should not significantly affect the nature of our IVUS measurements

Differences in lumen measurements obtained with 3D-QCA and IVUS/FD-OCT

Densitometric and edge-detection techniques of 2D angiographic images have consistently produced smaller lumen dimensions than measured with IVUS (von Birgelen et al., 1996). There has been considerable interest in the use of (the recently available) commercial 3D-QCA systems. Such systems have been designed for a number of clinical and research applications in interventional cardiology, ranging from potentially more accurate assessment of vessel dimensions in complex, eccentric and bifurcation lesions during PCI, to its use for advanced computational fluid dynamics processing for evaluation of *in vivo* shear stress patterns within the coronary vasculature. Although widespread experience with 3D-QCA is still limited, there are currently a number of conflicting observations regarding the accuracy of this technology. It has been shown that despite showing overall statistical agreement in measurements, 3D-QCA significantly underestimated actual plexiglass phantom diameter values *in vivo* compared to a traditionally used 2D-QCA system (Tsuchida et al., 2007). Furthermore, there were significant differences in measurements between 2 commercially available 3D-QCA systems when evaluating pre-defined plexiglass phantom dimensions *in vivo* (Ramcharitar et al., 2008). Although recent comparisons between 3D-QCA and IVUS for evaluating lesion length have shown good agreement (Tu et al.), to date there has been no data comparing 3D-QCA dimensions against those obtained with contemporary intravascular imaging modalities in humans *in vivo*. Our

data is the first to show that although LA's derived from 3D-QCA analysis correlates with corresponding LA's obtained with IVUS and OCT, 3D-QCA tends to significantly underestimate LA's by 40% and 29% respectively. Furthermore, we found that although significant differences exist between measured lumen dimensions with 3D-QCA compared to both intravascular imaging modalities, LA's measured with OCT were significantly closer to angiographic values than those obtained by IVUS. It is likely that coronary angiography will probably undergo dramatic changes in the future, whereby 3D-QCA projections of coronary segments will be immediately derived and simultaneously projected for view alongside many other component coronary imaging modalities including IVUS, OCT and multi-slice computed tomography coronary angiography in the cardiac catheterization laboratory. As the utility of such imaging modalities during PCI is likely to be complementary, our data suggest the importance of understanding the limitations and degrees of agreement of each of these current imaging modalities *in vivo*.

Clinical implications

Intravascular ultrasound has evolved as an effective clinical tool in interventional cardiology for the further evaluation of angiographic intermediate lesions (including ambiguous left main coronary lesions), for guidance of PCI and for assessing complications of PCI. Although currently lacking a defined clinical role, the recent rapid rise of OCT use coupled with evolving studies utilizing OCT, may unearth an important clinical niche. At present, the unsurpassed resolution of the lumen/intima interface seen with OCT will mean that it will continue to be utilized for the *in vivo* assessment of novel coronary stent platforms in a variety of clinical/research trial

settings. Until OCT-derived coronary lumen measurements are validated and adopted for clinical decision making, the current finding of significant differences in between IVUS and OCT measurements suggests these imaging modalities are not entirely interchangeable for current clinical decision making. Although newly developed hybrid IVUS/OCT catheters will ultimately enable a simultaneous, and highly accurate assessment of lumen and vessel characteristics, the challenge will be to incorporate such data appropriately into daily clinical practice (Li et al., 2010b).

Limitations

Our data is limited to the *in vivo* evaluation of coronary segments that do not contain angiographically significant stenoses. As such, our observations cannot strictly be applied to segments containing critical lesions. Understanding that the greatest differences between these imaging modalities were observed within coronary segments with small luminal dimensions, it is possible that the significant differences we observed between imaging modalities may be even greater in significantly stenosed segments. In addition, our data cannot be applied within stented coronary segments. Of note, a prior study did not find significant differences in lumen volumes within stented porcine coronary segments when assessed with IVUS and the occlusion technique of OCT (Kawase et al., 2005).

CONCLUSION

Coronary lumen dimensions measured by IVUS are larger than comparative segments measured with OCT, with differences further exemplified in smaller coronary segments. This finding is not related to underlying plaque burden. Furthermore, 3D-QCA

significantly underestimates coronary dimensions compared with IVUS and OCT. Until further validation studies are conducted across broader patient, vessel and lesion subsets, specific lumen-based cut-off values validated with IVUS should not be arbitrarily translated into the OCT hemisphere.

TABLE 1: Clinical characteristics

	Entire cohort n=10
	61 ± 10
Age, years	
Male, n	7
Medications, n	
Aspirin	6
Statin	3
ACEI/ARB	3
Calcium channel blocker	1
Beta-blocker	0
Lipids, mg/dL	
Total cholesterol	183 ± 43
TGL	79 ± 40
HDL	51 ± 13
LDL	116 ± 35
hsCRP, mg/L	5.1 ±8.4
Artery Investigated, n	
LAD	8
LCx	1
RCA	1

ACEI = angiotensin converting enzyme inhibitor; ARB = angiotensin receptor blocker; HDL = high-density lipoprotein; TGL = triglycerides; LAD = left anterior descending artery; LCx = left circumflex artery; LDL = low-density lipoprotein; RCA = right coronary artery

TABLE 2: Segment characteristics

	Entire cohort n=80
Plaque burden	
Tertile 1, n	26
PAV	19.9 ± 5.2
Tertile 2, n	27
PAV	33.6 ± 4.8
Tertile 3, n	26
PAV	51.1 ± 6.4
Segment size (by IVUS-derived LD)	
Small (LD <2.75 mm), n	17
LD	2.2 ± 0.48
Medium (LD 2.75-4 mm), n	46
LD	3.3 ± 0.84
Large (LD >4 mm), n	17
LD	4.4 ± 1.1
Segment size (by IVUS-derived LA)	
Small (LA <5 mm^2), n	13
LA	3.8 ± 0.9
Medium (LA 5-9 mm^2), n	31
LA	7.5 ± 1.0
Large (LA >9 mm^2), n	36
LA	12.9 ± 3.0

Values are mean ± SD; PAV = percent atheroma volume; LD = lumen diameter; LA = lumen area

FIGURE 1: Segmental analysis of coronary lumen dimensions with IVUS and OCT

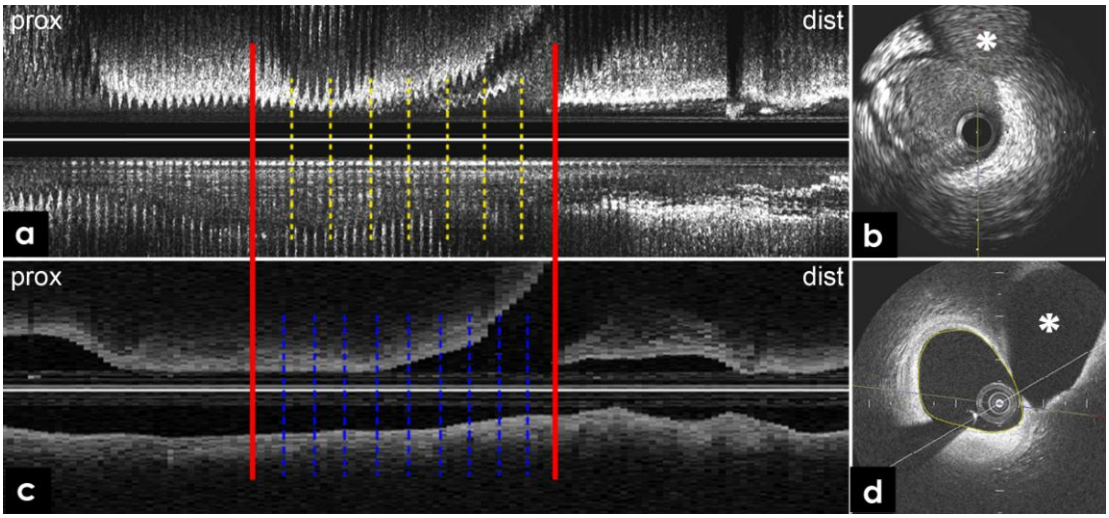

Corresponding horizontal views of IVUS (a) and OCT (c) imaging of the same coronary segment. Start frames (cross-sectional views) of IVUS and OCT shown in (b) and (d) respectively illustrating distal fiducial markers (white asterix). For IVUS, 9 consecutive cross sectional frames (yellow dotted lines, spaced at 0.5 mm intervals), and for OCT 11 consecutive cross sectional frames (blue dotted lines, spaced at 0.4 mm intervals) were traced to depict each 4 mm coronary segment.

FIGURE 2: Segmental analysis via 3D-QCA

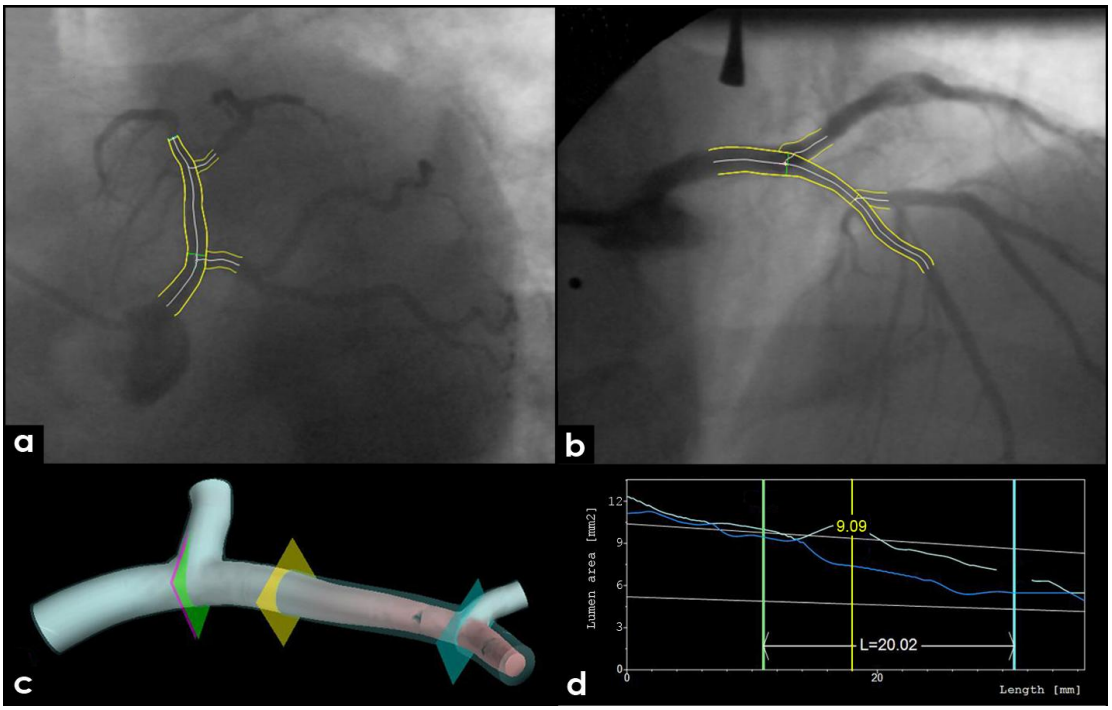

(a)Left anterior caudal and (b) cranial views of the left coronary system outlining the 3D reconstruction of the segment of the left anterior descending artery between 2 fiduciary branches, as shown in (c). The representative lumen area (yellow line) along each step of this highlighted segment was taken within each 4 mm segment, as shown in (d).

FIGURE 3: Lumen measurements in all segments with IVUS and OCT

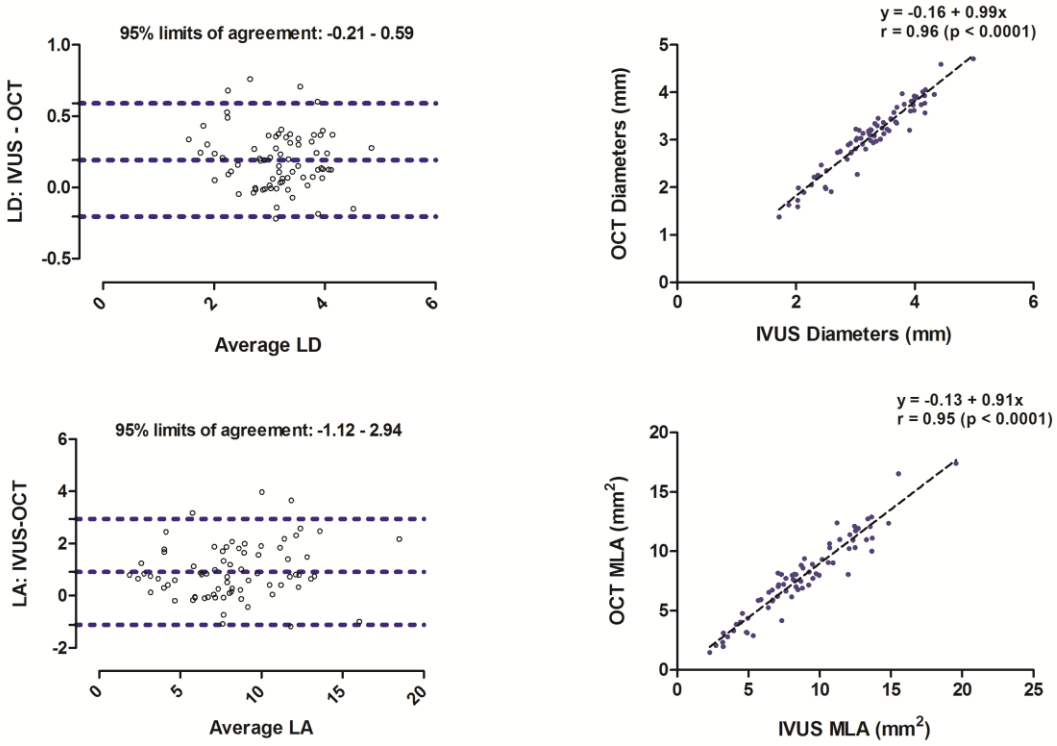

Bland-Altman plots and linear regression graphs showing the degrees of agreement and correlation of lumen diameters and lumen areas between IVUS and OCT.

FIGURE 4: Comparisons of lumen measurements between IVUS and OCT according to segment size

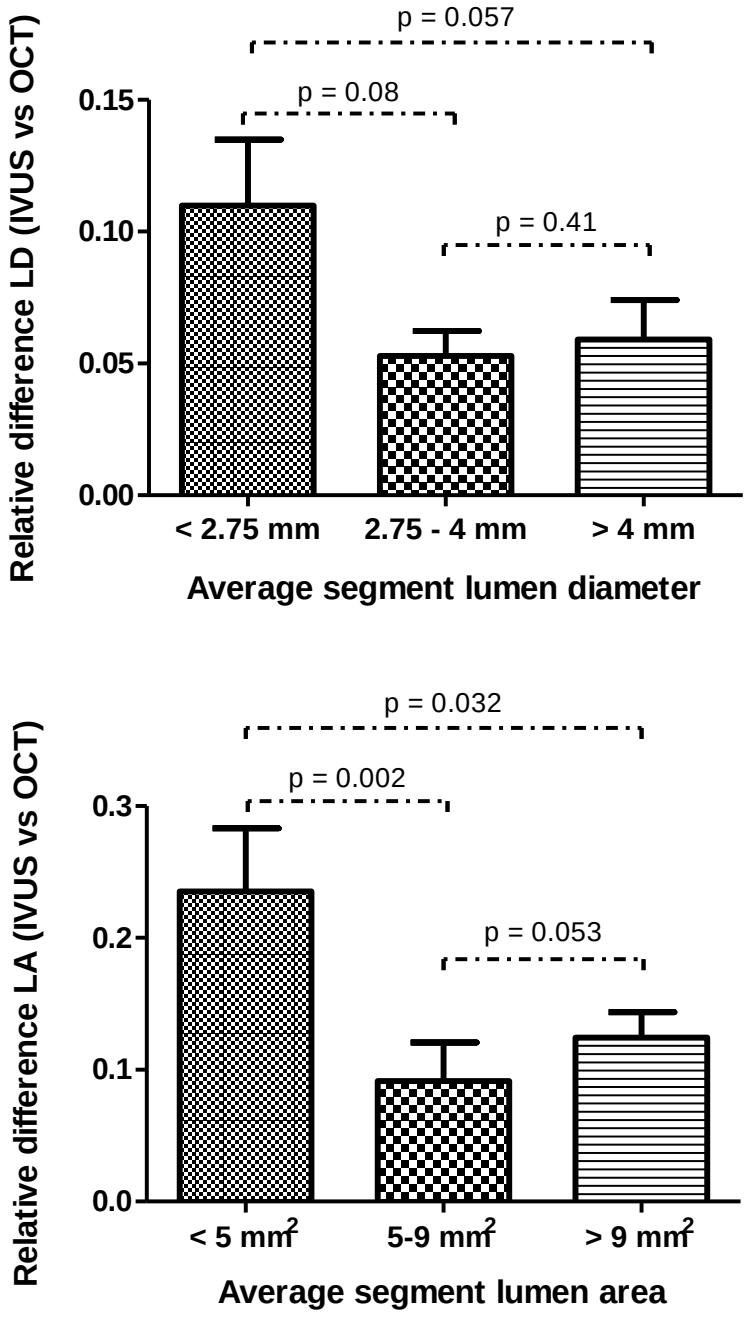

There are strong trends suggesting that the observed differences in LD measurements between IVUS and OCT are greater within small coronary segments. There are

significant inter-modality differences between LA measurements in small vs. large coronary segments

FIGURE 5: Comparisons of lumen area measurements between 3D-QCA and IVUS/OCT

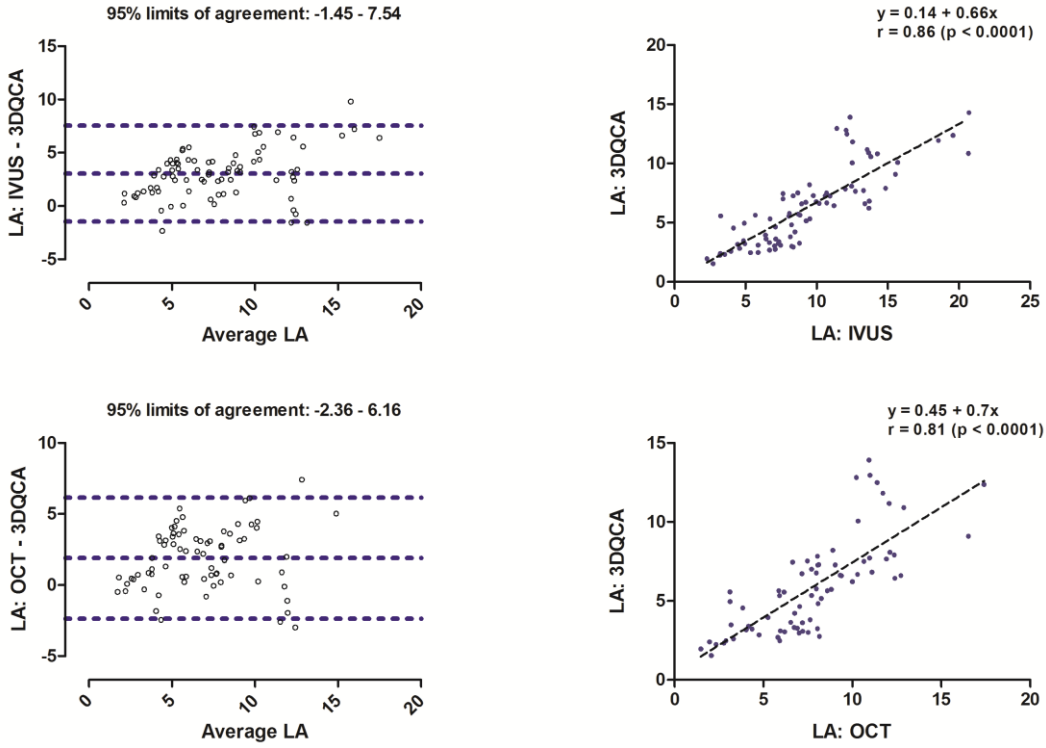

Bland-Altman plots and linear regression graphs showing the degree of agreement and correlation of lumen areas between 3D-QCA and IVUS/OCT.

FIGURE 6: Relative differences in LA measurements between IVUS and OCT with 3D-QCA

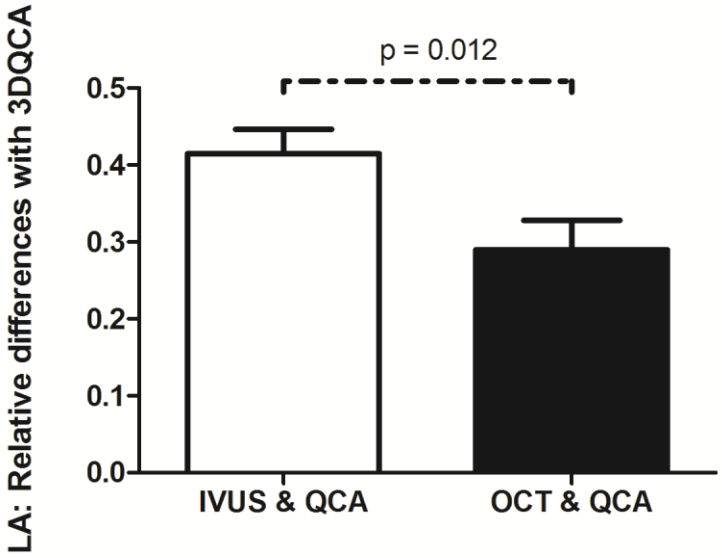

Despite 3D-QCA consistently showing significantly smaller LA compared with IVUS and OCT overall, the relative difference is significantly smaller between 3D-QCA and OCT than compared to 3D-QCA and IVUS.

Author contributions:

Dr Rishi Puri – Study design, patient recruitment, analysis, preparation of manuscript

Professor Stephen Nicholls - Correction and critical review of manuscript

Dr Darryl Leong – Analysis, correction and critical review of manuscript

Dr Gary Liew – Cath lab procedures, analysis, correction and critical review of manuscript

Dr Adam Nelson - Critical review of manuscript

Dr Kiyoko Uno – Analysis, critical review of manuscript

Dr James Harvey - Analysis, critical review of manuscript

Mr Angelo Carbone – Record keeping, critical review of manuscript

Ms Barbara Copus – Cath lab procedures, critical review of manuscript

Professor John Beltrame – Supervision, correction and critical review of manuscript

Professor Stephen Worthley – Supervision, cath lab procedures, critical review of manuscript

Associate Professor Matthew Worthley – Primary Supervision, study design, cath lab procedures, correction and critical review of manuscript

I hereby give permission for this original manuscript to be included in this thesis submission:

Dr Rishi Puri Dr Adam Nelson

Professor Stephen J. Nicholls

Dr Gary Y. Liew

Mr Angelo Carbone

Dr Darryl P. Leong

Dr Kiyoko Uno

Dr James E. Harvey

Mrs Barbara Copus

Dr Dennis T. Wong

Professor John F. Beltrame

Professor Stephen G. Worthley

Associate Professor Matthew I. Worthley

CHAPTER 10: CONCLUSIONS AND FUTURE DIRECTIONS

Utilizing a novel technique of coronary IVUS imaging during IC provocation, we established the novel finding of nitric oxide (NO)-dependent properties of coronary β_2-adrenoreceptor stimulation in epicardial human coronary arteries *in vivo*. This in turn allowed us to characterize of a number of fundamental relationships between human coronary atheroma and segmental vasomotor reactivity *in vivo,* summarized below:

- Coronary atheroma volume correlates inversely with segmental endothelium-dependent vasomotor function, independent of the presence of systemic risk factors for coronary artery disease. Plaque burden appeared to contribute most to segmental endothelium-dependent epicardial vasomotion

- The above relationship between coronary atheroma volume and segmental coronary vasomotor reactivity holds constant, per unit of plaque measure, irrespective of the nature of clinical presentation (stable, angiographically minimal coronary disease vs. non ST-segment elevation myocardial infarction)

- Subclinical systemic inflammation (plasma high-sensitivity C-reactive protein levels $\geq$2 mg/L) interact with greater volumes of coronary atheroma, to mediate epicardial vasomotor reactivity

- Independent of the presence of risk factors for coronary artery disease, high-sensitivity C-reactive protein levels and coronary atheroma volume, greater amounts of lipidic and necrotic core plaque more likely associate with segmental epicardial endothelial dysfunction (vasoconstriction), whereas greater degrees of

fibrotic plaque more likely associate with the tendency for epicardial vasodilatation

- In the setting of stable, non-critical coronary disease, segmental wall shear stress (WSS) values correlate directly with the magnitude of NO-dependent epicardial vasomotion, and indirectly to the segmental arterial remodeling index. Coronary segments with low WSS values and high plaque volume displayed expansive coronary remodeling and epicardial vasoconstriction

- Epicardial vasomotor reactivity is heterogenous, with adjacent segments within the same coronary artery displaying opposing vasomotor function. The human left main coronary artery (LMCA) and proximal epicardial segments display the least degree of vasomotion, compared with the mid-distal epicardial segments. This may relate to the larger lumen areas of the LMCA and proximal segments, likely harboring the lowest WSS, and therefore a reduced stimulus for NO-dependent coronary vasomotion

- A newer light-based intracoronary imaging technology (fourier domain optical coherence tomography, or FD-OCT) systematically provides lower lumen area measurements than IVUS, with such differences appearing greater within smaller-sized coronary segments. This suggests that specific lumen-based cut-off values validated with IVUS should not be arbitrarily translated into the OCT hemisphere

These findings have a number of possible clinical implications. Collectively, these results highlight the potential for coronary imaging to be prospectively tested as a complementary means of coronary risk stratification. Although the invasiveness (and superior resolution) of our imaging and stimulation protocol enabled us to elucidate a number of novel mechanistic insights *in vivo*, non-invasive coronary imaging however is best positioned to evaluate both coronary atheroma volume and endothelium-dependent function in a broader patient cohort. Prospective studies utilizing invasive coronary imaging have demonstrated prognostic associations between endothelial dysfunction and future cardiovascular events, and the prognostic utility of coronary plaque volume has also been demonstrated using both invasive and non-invasive coronary imaging. Our findings hint at the suggestion that vasoconstricting, disease-laden epicardial coronary segments, particularly those lipid or necrotic core-rich segments, may be more prone towards causing a coronary event. Therefore a combined approach of assessing plaque volume and composition, in addition to coronary vasomotor reactivity may have additional prognostic yield. This conjecture will however, require formal prospective evaluation. Such an approach would seem applicable to those with established coronary disease, as well as many at-risk individuals without established coronary disease. Our observations of an interaction between subclinical systemic inflammation and greater amounts of plaque in mediating vasomotor reactivity suggests that future attempts at coronary risk-stratification using coronary imaging could be undertaken in combination with both established and novel systemic risk factors.

Although baseline coronary WSS predicts plaque progression and future coronary events, it's offline computation using finite element analysis, computational fluid dynamics and multi-modality image co-registration is cumbersome, expensive and time consuming. This poses limitations to its current use and applicability in daily clinical practice. Utilizing IVUS as the sole imaging modality, albeit with known assumptions and limitations, the methodology we adopted for WSS calculations (modified from previous attempts utilizing angiography) proved to be a simple, yet effective means of identifying mechanistic relationships with NO-dependent function and coronary arterial remodeling. The methods of WSS calculation in our study are easy to obtain, with the potential for prompt automated offline analysis and prospective evaluation.

The marked heterogeneity of epicardial vasomotor responses, including the behavior of the left main coronary arterial (LMCA) segment *in vivo*, suggests that future attempts at assessing epicardial coronary vasomotor reactivity should include the assessment of multiple, contiguous segments rather than sub-selecting single points of interest.

Future research

Current strategies for assessing cardiovascular risk lack the specificity for accurately predicting myocardial infarction and coronary-related death. Moreover, established risk-calculators possess a number of inherent limitations. Coronary imaging therefore is well positioned to improve the prognostic yield for coronary risk-stratification, via directly

assessing the substrate for myocardial infarction. Future research priorities should therefore encompass the following:

Non-invasive coronary imaging

- Improving the resolution of non-invasive coronary imaging modalities (computed tomography and magnetic resonance imaging) to more accurately assess coronary atheroma volume and composition

- Akin to guidelines released by the American College of Cardiology/American Heart Association for performing plaque analysis following coronary intravascular ultrasound (IVUS) imaging, similar guidelines should be developed for the non-invasive assessment of coronary atheroma. Such guidelines should not only stimulate concordance amongst the imaging community and dedicated Core Laboratories for measuring coronary atheroma non-invasively, but also pave the way for large-scale prospective natural history studies assessing the prognostic utility of coronary atheroma volume in a variety of patient subsets

- It would seem prudent to simultaneously investigate strategies of non-invasively assessing both coronary atheroma volume and endothelial function, and to design large-scale natural history studies that formally assess the prognostic utility of simply assessing coronary atheroma volume vs. coronary vasomotor reactivity vs. simultaneously assessing both coronary atheroma volume and vasomotor reactivity

Invasive coronary imaging

Although the future of coronary atheroma imaging for risk-stratification on a population scale lies within the realm of non-invasive imaging technologies, the physical proximity of imaging technologies to actual coronary atheroma *in vivo* is likely to continue to position various next-generation invasive imaging technologies (such as intravascular molecular imaging) at the forefront of atherosclerosis research. This would involve:

- Improving the capacity of current-generation IVUS platforms for optimizing both near- and far-field imaging resolution, and testing the feasibility of dual-modality/hybrid coronary imaging catheters

- Large-scale natural history studies assessing the prognostic utility of some of the newer-generation coronary imaging technologies, such as optical coherence tomography and near-infrared spectroscopy

- Improving the validation of plaque compositional imaging, and formally investigating if plaque composition imaging provides incremental prognostic benefit over simply measuring the total volume of plaque

- Designing and conducting a natural history study that tests the hypothesis that the baseline extent of segmental epicardial vasomotor reactivity, is a marker for local disease progression

Although a major focus of the presented series of studies in this thesis involves the atheroma structure-vessel function relationship of the epicardial coronary tree, the coronary microcirculation plays a critical role in mediating the upstream nature of

disease. Indeed, those individuals with impaired coronary microvascular reserve are also at greater risk for future events. Hence, the overriding challenge facing the cardiology community is to develop imaging protocols (both invasive and non-invasive) that reliably assess the integrity of the coronary circulation in its entirety, rather than focusing on individual entities such as atheroma composition or isolated regions of vasoreactivity. As Aristotle said, "*The whole is always greater than the sum of its parts*."

BIBLIOGRAPHY

1983. Coronary artery surgery study (CASS): a randomized trial of coronary artery bypass surgery. Survival data. *Circulation,* 68**,** 939-50.

2011a. Biomarker and Imaging Study to assess the ability of high doses rosuvastatin to decrease artherosclerosis in coronary arteries. *http://www.trialregister.nl/trialreg/admin/rctview.asp?TC=2872*.

2011b. Coronary Assessment by Near-infrared of Atherosclerotic Rupture-prone Yellow. *http://clinicaltrials.gov/ct2/show/NCT01268319?term=CANARY&rank=1*.

2011c. The Stabilization of Atherosclerotic Plaque by Initiation of Darapladib Therapy Trial (STABILITY). *http://clinicaltrials.gov/ct2/show/NCT00799903*.

AIKAWA, M., RABKIN, E., OKADA, Y., VOGLIC, S. J., CLINTON, S. K., BRINCKERHOFF, C. E., SUKHOVA, G. K. & LIBBY, P. 1998. Lipid lowering by diet reduces matrix metalloproteinase activity and increases collagen content of rabbit atheroma: a potential mechanism of lesion stabilization. *Circulation,* 97**,** 2433-44.

AMBROSE, J. A., TANNENBAUM, M. A., ALEXOPOULOS, D., HJEMDAHL-MONSEN, C. E., LEAVY, J., WEISS, M., BORRICO, S., GORLIN, R. & FUSTER, V. 1988. Angiographic progression of coronary artery disease and the development of myocardial infarction. *J Am Coll Cardiol,* 12**,** 56-62.

ANDERSON, T. J., WORTHLEY, M. I., GOODHART, D. M. & CURTIS, M. J. 2005. Relation of Basal coronary nitric oxide activity to the burden of atherosclerosis. *Am J Cardiol,* 95**,** 1170-4.

APTECAR, E., TEIGER, E., DUPOUY, P., BENVENUTI, C., KERN, M. J., WOSCOBOINIK, J., SEDIAME, S., PERNES, J. M., CASTAIGNE, A., LOISANCE, D. & DUBOIS-RANDE, J. L. 2000. Effects of bradykinin on coronary blood flow and vasomotion in transplant patients. *J Am Coll Cardiol,* 35**,** 1607-15.

ARDISSINO, D., CAVALLINI, C., BRAMUCCI, E., INDOLFI, C., MARZOCCHI, A., MANARI, A., ANGELONI, G., CAROSIO, G., BONIZZONI, E., COLUSSO, S., REPETTO, M. & MERLINI, P. A. 2004. Sirolimus-eluting vs uncoated stents for prevention of restenosis in small coronary arteries: a randomized trial. *JAMA,* 292**,** 2727-34.

BALLANTYNE, C. M. 1998. Clinical trial endpoints: angiograms, events, and plaque instability. *Am J Cardiol,* 82**,** 5M-11M.

BARBATO, E. 2009. Role of adrenergic receptors in human coronary vasomotion. *Heart,* 95**,** 603-8.

BARBATO, E., PISCIONE, F., BARTUNEK, J., GALASSO, G., CIRILLO, P., DE LUCA, G., IACCARINO, G., DE BRUYNE, B., CHIARIELLO, M. & WIJNS, W. 2005. Role of beta2 adrenergic receptors in human atherosclerotic coronary arteries. *Circulation,* 111**,** 288-94.

BARLIS, P., REGAR, E., SERRUYS, P. W., DIMOPOULOS, K., VAN DER GIESSEN, W. J., VAN GEUNS, R. J., FERRANTE, G., WANDEL, S., WINDECKER, S., VAN ES, G. A., EERDMANS, P., JUNI, P. & DI MARIO, C. 2010. An optical coherence tomography study of a biodegradable vs. durable

polymer-coated limus-eluting stent: a LEADERS trial sub-study. *Eur Heart J,* 31**,** 165-76.

BAUMGART, D., HAUDE, M., GORGE, G., LIU, F., GE, J., GROSSE-EGGEBRECHT, C., ERBEL, R. & HEUSCH, G. 1999. Augmented alpha-adrenergic constriction of atherosclerotic human coronary arteries. *Circulation,* 99**,** 2090-7.

BAYTURAN, O., KAPADIA, S., NICHOLLS, S. J., TUZCU, E. M., SHAO, M., UNO, K., SHREEVATSA, A., LAVOIE, A. J., WOLSKI, K., SCHOENHAGEN, P. & NISSEN, S. E. 2010. Clinical predictors of plaque progression despite very low levels of low-density lipoprotein cholesterol. *J Am Coll Cardiol,* 55**,** 2736-42.

BEA, M. L., GHALEH, B., GIUDICELLI, J. F. & BERDEAUX, A. 1994. Lack of importance of NO in beta-adrenoceptor-mediated relaxation of large epicardial canine coronary arteries. *Br J Pharmacol,* 111**,** 981-2.

BENSON, T. J., NEREM, R. M. & PEDLEY, T. J. 1980. Assessment of wall shear stress in arteries, applied to the coronary circulation. *Cardiovascular Research,* 14**,** 568-76.

BERGELSON, B. A. & TOMMASO, C. L. 1995. Left main coronary artery disease: assessment, diagnosis, and therapy. *Am Heart J,* 129**,** 350-9.

BHANVADIA, V. M., DESAI, N. J. & AGARWAL, N. M. 2013. Study of coronary atherosclerosis by modified american heart association classification of atherosclerosis-an autopsy study. *J Clin Diagn Res,* 7**,** 2494-7.

BIONDI-ZOCCAI, G., MORETTI, C., ABBATE, A. & SHEIBAN, I. Percutaneous coronary intervention for small vessel coronary artery disease. *Cardiovasc Revasc Med,* 11**,** 189-98.

BOGATY, P., HACKETT, D., DAVIES, G. & MASERI, A. 1994. Vasoreactivity of the culprit lesion in unstable angina. *Circulation,* 90**,** 5-11.

BRAUN, O. O. & INSEL, P. A. 2009. The best "model system" for human (coronary arteries) is human. *J Am Coll Cardiol,* 54**,** 1146-8.

BRUGGINK, J. L., MEERWALDT, R., VAN DAM, G. M., LEFRANDT, J. D., SLART, R. H., TIO, R. A., SMIT, A. J. & ZEEBREGTS, C. J. 2010. Spectroscopy to improve identification of vulnerable plaques in cardiovascular disease. *Int J Cardiovasc Imaging,* 26**,** 111-9.

BUCHI, M. & JENNI, R. 1998. Measurement of flow velocity in the coronary circulation: requirements and pitfalls. *Semin Interv Cardiol,* 3**,** 45-50.

BURKE, A. P., FARB, A., MALCOM, G. T., LIANG, Y. H., SMIALEK, J. & VIRMANI, R. 1997. Coronary risk factors and plaque morphology in men with coronary disease who died suddenly. *N Engl J Med,* 336**,** 1276-82.

BUSCHMAN, H. P., MOTZ, J. T., DEINUM, G., ROMER, T. J., FITZMAURICE, M., KRAMER, J. R., VAN DER LAARSE, A., BRUSCHKE, A. V. & FELD, M. S. 2001. Diagnosis of human coronary atherosclerosis by morphology-based Raman spectroscopy. *Cardiovasc Pathol,* 10**,** 59-68.

CALVERT, P. A., OBAID, D. R., O'SULLIVAN, M., SHAPIRO, L. M., MCNAB, D., DENSEM, C. G., SCHOFIELD, P. M., BRAGANZA, D., CLARKE, S. C., RAY, K. K., WEST, N. E. & BENNETT, M. R. 2011. Association between

IVUS findings and adverse outcomes in patients with coronary artery disease: the VIVA (VH-IVUS in Vulnerable Atherosclerosis) Study. *JACC. Cardiovascular imaging,* 4**,** 894-901.

CANNON, C. P., BRINDIS, R. G., CHAITMAN, B. R., COHEN, D. J., CROSS, J. T., JR., DROZDA, J. P., JR., FESMIRE, F. M., FINTEL, D. J., FONAROW, G. C., FOX, K. A., GRAY, D. T., HARRINGTON, R. A., HICKS, K. A., HOLLANDER, J. E., KRUMHOLZ, H., LABARTHE, D. R., LONG, J. B., MASCETTE, A. M., MEYER, C., PETERSON, E. D., RADFORD, M. J., ROE, M. T., RICHMANN, J. B., SELKER, H. P., SHAHIAN, D. M., SHAW, R. E., SPRENGER, S., SWOR, R., UNDERBERG, J. A., VAN DE WERF, F., WEINER, B. H. & WEINTRAUB, W. S. 2013. 2013 ACCF/AHA key data elements and definitions for measuring the clinical management and outcomes of patients with acute coronary syndromes and coronary artery disease: a report of the American College of Cardiology Foundation/American Heart Association Task Force on clinical data standards (writing committee to develop acute coronary syndromes and coronary artery disease clinical data standards). *J Am Coll Cardiol,* 61**,** 992-1025.

CASSIS, L. A. & LODDER, R. A. 1993. Near-IR imaging of atheromas in living arterial tissue. *Anal Chem,* 65**,** 1247-56.

CELERMAJER, D. S. 1997. Endothelial dysfunction: does it matter? Is it reversible? *J Am Coll Cardiol,* 30**,** 325-33.

CELERMAJER, D. S., SORENSEN, K. E., BULL, C., ROBINSON, J. & DEANFIELD, J. E. 1994. Endothelium-dependent dilation in the systemic

arteries of asymptomatic subjects relates to coronary risk factors and their interaction. *J Am Coll Cardiol,* 24**,** 1468-74.

CHATZIZISIS, Y. S., COSKUN, A. U., JONAS, M., EDELMAN, E. R., FELDMAN, C. L. & STONE, P. H. 2007. Role of endothelial shear stress in the natural history of coronary atherosclerosis and vascular remodeling: molecular, cellular, and vascular behavior. *J Am Coll Cardiol,* 49**,** 2379-93.

CHEN, S. L., KAN, J., ZHANG, J. J., HU, Z. Y. & XU, T. 2012a. Hemodynamic change in wall shear stress in patients with coronary bifurcation lesions treated by double kissing crush or single-stent technique. *Chin Med J,* 125**,** 1720-6.

CHEN, S. L., XU, T., ZHANG, J. J., YE, F., HU, Z. Y., TIAN, N. L., ZHANG, Y. J., KOTANI, J. & ZHANG, J. X. 2012b. Angioscopy study from a large patient population comparing sirolimus-eluting stent with biodegradable versus durable polymer. *Catheter Cardiovasc Interv,* 80**,** 420-8.

CHEN, S. L., YE, F., ZHANG, J. J., TIAN, N. L., LIU, Z. Z., SANTOSO, T., ZHOU, Y. J., JIANG, T. M., WEN, S. Y. & KWAN, T. W. 2012c. Intravascular ultrasound-guided systematic two-stent techniques for coronary bifurcation lesions and reduced late stent thrombosis. *Catheter Cardiovasc Interv*.

CLAESSEN, B. E., MEHRAN, R., MINTZ, G. S., WEISZ, G., LEON, M. B., DOGAN, O., DE RIBAMAR COSTA, J., JR., STONE, G. W., APOSTOLIDOU, I., MORALES, A., CHANTZIARA, V., SYROS, G., SANIDAS, E., XU, K., TIJSSEN, J. G., HENRIQUES, J. P., PIEK, J. J., MOSES, J. W., MAEHARA, A. & DANGAS, G. D. 2011. Impact of intravascular ultrasound imaging on

early and late clinical outcomes following percutaneous coronary intervention with drug-eluting stents. *JACC. Cardiovascular interventions,* 4**,** 974-81.

COATS, A. J. & SHEWAN, L. G. 2011. Statement on authorship and publishing ethics in the International Journal of Cardiology. *Int J Cardiol,* 153**,** 239-40.

COLOMBO, A., HALL, P., NAKAMURA, S., ALMAGOR, Y., MAIELLO, L., MARTINI, G., GAGLIONE, A., GOLDBERG, S. L. & TOBIS, J. M. 1995. Intracoronary stenting without anticoagulation accomplished with intravascular ultrasound guidance. *Circulation,* 91**,** 1676-88.

COOK, S., WENAWESER, P., TOGNI, M., BILLINGER, M., MORGER, C., SEILER, C., VOGEL, R., HESS, O., MEIER, B. & WINDECKER, S. 2007. Incomplete stent apposition and very late stent thrombosis after drug-eluting stent implantation. *Circulation,* 115**,** 2426-34.

COSKUN, A. U., YEGHIAZARIANS, Y., KINLAY, S., CLARK, M. E., ILEGBUSI, O. J., WAHLE, A., SONKA, M., POPMA, J. J., KUNTZ, R. E., FELDMAN, C. L. & STONE, P. H. 2003. Reproducibility of coronary lumen, plaque, and vessel wall reconstruction and of endothelial shear stress measurements in vivo in humans. *Catheter Cardiovasc Interv,* 60**,** 67-78.

CRISBY, M., NORDIN-FREDRIKSSON, G., SHAH, P. K., YANO, J., ZHU, J. & NILSSON, J. 2001. Pravastatin treatment increases collagen content and decreases lipid content, inflammation, metalloproteinases, and cell death in human carotid plaques: implications for plaque stabilization. *Circulation,* 103**,** 926-33.

DAVIES, M. J. & THOMAS, A. 1984. Thrombosis and acute coronary-artery lesions in sudden cardiac ischemic death. *N Engl J Med,* 310**,** 1137-40.

DAWES, M., CHOWIENCZYK, P. J. & RITTER, J. M. 1997. Effects of inhibition of the L-arginine/nitric oxide pathway on vasodilation caused by beta-adrenergic agonists in human forearm. *Circulation,* 95**,** 2293-7.

DE KORTE, C. L., VAN DER STEEN, A. F., CESPEDES, E. I. & PASTERKAMP, G. 1998. Intravascular ultrasound elastography in human arteries: initial experience in vitro. *Ultrasound Med Biol,* 24**,** 401-8.

DEWOOD, M. A., SPORES, J., NOTSKE, R., MOUSER, L. T., BURROUGHS, R., GOLDEN, M. S. & LANG, H. T. 1980. Prevalence of total coronary occlusion during the early hours of transmural myocardial infarction. *N Engl J Med,* 303**,** 897-902.

DISHY, V., SOFOWORA, G. G., XIE, H. G., KIM, R. B., BYRNE, D. W., STEIN, C. M. & WOOD, A. J. 2001. The effect of common polymorphisms of the beta2-adrenergic receptor on agonist-mediated vascular desensitization. *N Engl J Med,* 345**,** 1030-5.

DORIOT, P. A., DORSAZ, P. A., DORSAZ, L., DE BENEDETTI, E., CHATELAIN, P. & DELAFONTAINE, P. 2000. In-vivo measurements of wall shear stress in human coronary arteries. *Coronary Artery Disease,* 11**,** 495-502.

DREXLER, H., ZEIHER, A. M., WOLLSCHLAGER, H., MEINERTZ, T., JUST, H. & BONZEL, T. 1989. Flow-dependent coronary artery dilatation in humans. *Circulation,* 80**,** 466-74.

EISEN, H. J., TUZCU, E. M., DORENT, R., KOBASHIGAWA, J., MANCINI, D., VALANTINE-VON KAEPPLER, H. A., STARLING, R. C., SORENSEN, K., HUMMEL, M., LIND, J. M., ABEYWICKRAMA, K. H. & BERNHARDT, P. 2003. Everolimus for the prevention of allograft rejection and vasculopathy in cardiac-transplant recipients. *N Engl J Med,* 349**,** 847-58.

EL-TAMIMI, H., MANSOUR, M., WARGOVICH, T. J., HILL, J. A., KERENSKY, R. A., CONTI, C. R. & PEPINE, C. J. 1994. Constrictor and dilator responses to intracoronary acetylcholine in adjacent segments of the same coronary artery in patients with coronary artery disease. Endothelial function revisited. *Circulation,* 89**,** 45-51.

FALK, E., SHAH, P. K. & FUSTER, V. 1995. Coronary plaque disruption. *Circulation,* 92**,** 657-71.

FALK, E. & WILENSKY, R. L. 2012. Prediction of coronary events by intravascular imaging. *JACC Cardiovasc Imaging,* 5**,** S38-41.

FAROUQUE, H. M. & MEREDITH, I. T. 2001. The assessment of endothelial function in humans. *Coron Artery Dis,* 12**,** 445-54.

FEARON, W. F., BORNSCHEIN, B., TONINO, P. A., GOTHE, R. M., BRUYNE, B. D., PIJLS, N. H. & SIEBERT, U. 2010. Economic evaluation of fractional flow reserve-guided percutaneous coronary intervention in patients with multivessel disease. *Circulation,* 122**,** 2545-50.

FERRANTE, G., PRESBITERO, P., WHITBOURN, R. & BARLIS, P. 2013. Current applications of optical coherence tomography for coronary intervention. *Int J Cardiol,* 165**,** 7-16.

FERRO, A., QUEEN, L. R., PRIEST, R. M., XU, B., RITTER, J. M., POSTON, L. & WARD, J. P. 1999. Activation of nitric oxide synthase by beta 2-adrenoceptors in human umbilical vein endothelium in vitro. *Br J Pharmacol,* 126**,** 1872-80.

FINN, A. V., JONER, M., NAKAZAWA, G., KOLODGIE, F., NEWELL, J., JOHN, M. C., GOLD, H. K. & VIRMANI, R. 2007. Pathological correlates of late drug-eluting stent thrombosis: strut coverage as a marker of endothelialization. *Circulation,* 115**,** 2435-41.

FINN, A. V., NAKANO, M., NARULA, J., KOLODGIE, F. D. & VIRMANI, R. 2010. Concept of vulnerable/unstable plaque. *Arterioscler Thromb Vasc Biol,* 30**,** 1282-92.

FLAMMER, A. J., ANDERSON, T., CELERMAJER, D. S., CREAGER, M. A., DEANFIELD, J., GANZ, P., HAMBURG, N. M., LUSCHER, T. F., SHECHTER, M., TADDEI, S., VITA, J. A. & LERMAN, A. 2012. The assessment of endothelial function: from research into clinical practice. *Circulation,* 126**,** 753-67.

FOIN, N., VICECONTE, N., CHAN, P. H., LINDSAY, A. C., KRAMS, R. & DI MARIO, C. 2011. Jailed side branches: fate of unapposed struts studied with 3D frequency-domain optical coherence tomography. *J Cardiovasc Med (Hagerstown),* 12**,** 581-2.

FOLTS, J. D., CROWELL, E. B., JR. & ROWE, G. G. 1976. Platelet aggregation in partially obstructed vessels and its elimination with aspirin. *Circulation,* 54**,** 365-70.

FUJII, K., KOBAYASHI, Y., MINTZ, G. S., TAKEBAYASHI, H., DANGAS, G., MOUSSA, I., MEHRAN, R., LANSKY, A. J., KREPS, E., COLLINS, M., COLOMBO, A., STONE, G. W., LEON, M. B. & MOSES, J. W. 2003. Intravascular ultrasound assessment of ulcerated ruptured plaques: a comparison of culprit and nonculprit lesions of patients with acute coronary syndromes and lesions in patients without acute coronary syndromes. *Circulation,* 108**,** 2473-8.

FUJII, K., MINTZ, G. S., CARLIER, S. G., COSTA, J. R., JR., KIMURA, M., SANO, K., TANAKA, K., COSTA, R. A., LUI, J., STONE, G. W., MOSES, J. W. & LEON, M. B. 2006. Intravascular ultrasound profile analysis of ruptured coronary plaques. *Am J Cardiol,* 98**,** 429-35.

FURCHGOTT, R. F. & ZAWADZKI, J. V. 1980. The obligatory role of endothelial cells in the relaxation of arterial smooth muscle by acetylcholine. *Nature,* 288**,** 373-6.

GAMBILLARA, V., CHAMBAZ, C., MONTORZI, G., ROY, S., STERGIOPULOS, N. & SILACCI, P. 2006. Plaque-prone hemodynamics impair endothelial function in pig carotid arteries. *Am J Physiol Heart Circ Physiol,* 290**,** H2320-8.

GARCIA-CARDENA, G., COMANDER, J. I., BLACKMAN, B. R., ANDERSON, K. R. & GIMBRONE, M. A. 2001. Mechanosensitive endothelial gene expression profiles: scripts for the role of hemodynamics in atherogenesis? *Annals of the New York Academy of Sciences,* 947**,** 1-6.

GARDINER, S. M., KEMP, P. A. & BENNETT, T. 1991. Effects of NG-nitro-L-arginine methyl ester on vasodilator responses to acetylcholine, 5'-N-

ethylcarboxamidoadenosine or salbutamol in conscious rats. *Br J Pharmacol,* 103**,** 1725-32.

GARDNER, C. M., TAN, H., HULL, E. L., LISAUSKAS, J. B., SUM, S. T., MEESE, T. M., JIANG, C., MADDEN, S. P., CAPLAN, J. D., BURKE, A. P., VIRMANI, R., GOLDSTEIN, J. & MULLER, J. E. 2008. Detection of lipid core coronary plaques in autopsy specimens with a novel catheter-based near-infrared spectroscopy system. *JACC Cardiovasc Imaging,* 1**,** 638-48.

GE, J., ERBEL, R., GERBER, T., GORGE, G., KOCH, L., HAUDE, M. & MEYER, J. 1994. Intravascular ultrasound imaging of angiographically normal coronary arteries: a prospective study in vivo. *Br Heart J,* 71**,** 572-8.

GESKE, J. B., EDWARDS, W. D., MACDONALD, R. J. & HOLMES, D. R., JR. 2010. Location of coronary culprit lesions at autopsy in 41 nondiabetic patients with acute myocardial infarction. *Am J Forensic Med Pathol,* 31**,** 213-7.

GIBSON, C. M., DIAZ, L., KANDARPA, K., SACKS, F. M., PASTERNAK, R. C., SANDOR, T., FELDMAN, C. & STONE, P. H. 1993. Relation of vessel wall shear stress to atherosclerosis progression in human coronary arteries. *Arterioscler Thromb,* 13**,** 310-5.

GIJSEN, F. J., OORTMAN, R. M., WENTZEL, J. J., SCHUURBIERS, J. C., TANABE, K., DEGERTEKIN, M., LIGTHART, J. M., THURY, A., DE FEYTER, P. J., SERRUYS, P. W. & SLAGER, C. J. 2003. Usefulness of shear stress pattern in predicting neointima distribution in sirolimus-eluting stents in coronary arteries. *Am J Cardiol,* 92**,** 1325-8.

GLAGOV, S., WEISENBERG, E., ZARINS, C. K., STANKUNAVICIUS, R. & KOLETTIS, G. J. 1987. Compensatory enlargement of human atherosclerotic coronary arteries. *N Engl J Med,* 316**,** 1371-5.

GOERTZ, D. E., FRIJLINK, M. E., TEMPEL, D., BHAGWANDAS, V., GISOLF, A., KRAMS, R., DE JONG, N. & VAN DER STEEN, A. F. 2007. Subharmonic contrast intravascular ultrasound for vasa vasorum imaging. *Ultrasound Med Biol,* 33**,** 1859-72.

GOLDSTEIN, J. A., DEMETRIOU, D., GRINES, C. L., PICA, M., SHOUKFEH, M. & O'NEILL, W. W. 2000. Multiple complex coronary plaques in patients with acute myocardial infarction. *N Engl J Med,* 343**,** 915-22.

GOLDSTEIN, J. A., MAINI, B., DIXON, S. R., BRILAKIS, E. S., GRINES, C. L., RIZIK, D. G., POWERS, E. R., STEINBERG, D. H., SHUNK, K. A., WEISZ, G., MORENO, P. R., KINI, A., SHARMA, S. K., HENDRICKS, M. J., SUM, S. T., MADDEN, S. P., MULLER, J. E., STONE, G. W. & KERN, M. J. 2011. Detection of lipid-core plaques by intracoronary near-infrared spectroscopy identifies high risk of periprocedural myocardial infarction. *Circ Cardiovasc Interv,* 4**,** 429-37.

GONZALO, N., SERRUYS, P. W., GARCIA-GARCIA, H. M., VAN SOEST, G., OKAMURA, T., LIGTHART, J., KNAAPEN, M., VERHEYE, S., BRUINING, N. & REGAR, E. 2009a. Quantitative ex vivo and in vivo comparison of lumen dimensions measured by optical coherence tomography and intravascular ultrasound in human coronary arteries. *Rev Esp Cardiol,* 62**,** 615-24.

GONZALO, N., SERRUYS, P. W., OKAMURA, T., SHEN, Z. J., ONUMA, Y., GARCIA-GARCIA, H. M., SARNO, G., SCHULTZ, C., VAN GEUNS, R. J., LIGTHART, J. & REGAR, E. 2009b. Optical coherence tomography assessment of the acute effects of stent implantation on the vessel wall: a systematic quantitative approach. *Heart,* 95**,** 1913-9.

GRAIER, W. F., KUKOVETZ, W. R. & GROSCHNER, K. 1993. Cyclic AMP enhances agonist-induced Ca2+ entry into endothelial cells by activation of potassium channels and membrane hyperpolarization. *Biochem J,* 291 (Pt 1)**,** 263-7.

GRAVES, J. & POSTON, L. 1993. Beta-adrenoceptor agonist mediated relaxation of rat isolated resistance arteries: a role for the endothelium and nitric oxide. *Br J Pharmacol,* 108**,** 631-7.

GRAY, D. W. & MARSHALL, I. 1992. Novel signal transduction pathway mediating endothelium-dependent beta-adrenoceptor vasorelaxation in rat thoracic aorta. *Br J Pharmacol,* 107**,** 684-90.

HABARA, M., NASU, K., TERASHIMA, M., KANEDA, H., YOKOTA, D., KO, E., ITO, T., KURITA, T., TANAKA, N., KIMURA, M., KINOSHITA, Y., TSUCHIKANE, E., ASAKURA, K., ASAKURA, Y., KATOH, O. & SUZUKI, T. 2012. Impact of frequency-domain optical coherence tomography guidance for optimal coronary stent implantation in comparison with intravascular ultrasound guidance. *Circ Cardiovasc Intv,* 5**,** 193-201.

HALCOX, J. P., SCHENKE, W. H., ZALOS, G., MINCEMOYER, R., PRASAD, A., WACLAWIW, M. A., NOUR, K. R. & QUYYUMI, A. A. 2002. Prognostic value of coronary vascular endothelial dysfunction. *Circulation,* 106**,** 653-8.

HAMILTON, A. J., HUANG, S. L., WARNICK, D., RABBAT, M., KANE, B., NAGARAJ, A., KLEGERMAN, M. & MCPHERSON, D. D. 2004. Intravascular ultrasound molecular imaging of atheroma components in vivo. *J Am Coll Cardiol,* 43**,** 453-60.

HASSOON, M., DE BELDER, A., SAHA, M. & HILDICK-SMITH, D. 2011. Changing the coronary bifurcation angles after stenting procedures: the relevance to the technique and unfavorable outcome (Three-dimensional analysis). *Minerva Cardioangiol,* 59**,** 309-19.

HAUSMANN, D., ERBEL, R., ALIBELLI-CHEMARIN, M. J., BOKSCH, W., CARACCIOLO, E., COHN, J. M., CULP, S. C., DANIEL, W. G., DE SCHEERDER, I., DIMARIO, C. & ET AL. 1995. The safety of intracoronary ultrasound. A multicenter survey of 2207 examinations. *Circulation,* 91**,** 623-30.

HAYS, A. G., HIRSCH, G. A., KELLE, S., GERSTENBLITH, G., WEISS, R. G. & STUBER, M. 2010. Noninvasive visualization of coronary artery endothelial function in healthy subjects and in patients with coronary artery disease. *J Am Coll Cardiol,* 56**,** 1657-65.

HEO, J. H., BRUGALETTA, S., GARCIA-GARCIA, H. M., GOMEZ-LARA, J., LIGTHART, J. M., WITBERG, K., MAGRO, M., SHIN, E. S. & SERRUYS, P. W. 2014. Reproducibility of intravascular ultrasound iMAP for radiofrequency

data analysis: Implications for design of longitudinal studies. *Catheter Cardiovasc Interv,* 83**,** E233-42.

HERRICK, J. B. 1983. Landmark article (JAMA 1912). Clinical features of sudden obstruction of the coronary arteries. By James B. Herrick. *JAMA,* 250**,** 1757-65.

HERRMANN, J., KASKI, J. C. & LERMAN, A. 2012. Coronary microvascular dysfunction in the clinical setting: from mystery to reality. *Eur Heart J,* 33**,** 2771-83.

HEUSCH, G., BAUMGART, D., CAMICI, P., CHILIAN, W., GREGORINI, L., HESS, O., INDOLFI, C. & RIMOLDI, O. 2000. Alpha-adrenergic coronary vasoconstriction and myocardial ischemia in humans. *Circulation,* 101**,** 689-94.

HOLLENBERG, S. M., TAMBURRO, P., JOHNSON, M. R., BURNS, D. E., SPOKAS, D., COSTANZO, M. R., PARRILLO, J. E. & KLEIN, L. W. 1999. Simultaneous intracoronary ultrasound and Doppler flow studies distinguish flow-mediated from receptor-mediated endothelial responses. *Catheter Cardiovasc Interv,* 46**,** 282-8.

HONG, M. K., MINTZ, G. S., LEE, C. W., KIM, Y. H., LEE, S. W., SONG, J. M., HAN, K. H., KANG, D. H., SONG, J. K., KIM, J. J., PARK, S. W. & PARK, S. J. 2004. Comparison of coronary plaque rupture between stable angina and acute myocardial infarction: a three-vessel intravascular ultrasound study in 235 patients. *Circulation,* 110**,** 928-33.

HONG, M. K., MINTZ, G. S., LEE, C. W., LEE, B. K., YANG, T. H., KIM, Y. H., SONG, J. M., HAN, K. H., KANG, D. H., CHEONG, S. S., SONG, J. K., KIM, J. J., PARK, S. W. & PARK, S. J. 2005. The site of plaque rupture in native

coronary arteries: a three-vessel intravascular ultrasound analysis. *J Am Coll Cardiol,* 46**,** 261-5.

HONG, M. K., MINTZ, G. S., LEE, C. W., LEE, J. W., PARK, J. H., PARK, D. W., LEE, S. W., KIM, Y. H., CHEONG, S. S., KIM, J. J., PARK, S. W. & PARK, S. J. 2008. A three-vessel virtual histology intravascular ultrasound analysis of frequency and distribution of thin-cap fibroatheromas in patients with acute coronary syndrome or stable angina pectoris. *Am J Cardiol,* 101**,** 568-72.

IMOLA, F., MALLUS, M. T., RAMAZZOTTI, V., MANZOLI, A., PAPPALARDO, A., DI GIORGIO, A., ALBERTUCCI, M. & PRATI, F. 2010. Safety and feasibility of frequency domain optical coherence tomography to guide decision making in percutaneous coronary intervention. *EuroIntervention,* 6**,** 575-81.

JANG, I. K., TEARNEY, G. J., MACNEILL, B., TAKANO, M., MOSELEWSKI, F., IFTIMA, N., SHISHKOV, M., HOUSER, S., ARETZ, H. T., HALPERN, E. F. & BOUMA, B. E. 2005. In vivo characterization of coronary atherosclerotic plaque by use of optical coherence tomography. *Circulation,* 111**,** 1551-5.

JAROSS, W., NEUMEISTER, V., LATTKE, P. & SCHUH, D. 1999. Determination of cholesterol in atherosclerotic plaques using near infrared diffuse reflection spectroscopy. *Atherosclerosis,* 147**,** 327-37.

JENSEN, B. C., SWIGART, P. M., LADEN, M. E., DEMARCO, T., HOOPES, C. & SIMPSON, P. C. 2009. The alpha-1D Is the predominant alpha-1-adrenergic receptor subtype in human epicardial coronary arteries. *J Am Coll Cardiol,* 54**,** 1137-45.

JEREMIAS, A., SPIES, C., HERITY, N. A., POMERANTSEV, E., YOCK, P. G., FITZGERALD, P. J. & YEUNG, A. C. 2000. Coronary artery compliance and adaptive vessel remodelling in patients with stable and unstable coronary artery disease. *Heart,* 84**,** 314-9.

JONER, M., FINN, A. V., FARB, A., MONT, E. K., KOLODGIE, F. D., LADICH, E., KUTYS, R., SKORIJA, K., GOLD, H. K. & VIRMANI, R. 2006. Pathology of drug-eluting stents in humans: delayed healing and late thrombotic risk. *J Am Coll Cardiol,* 48**,** 193-202.

KAPADIA, S. R., NISSEN, S. E. & TUZCU, E. M. 1999. Impact of intravascular ultrasound in understanding transplant coronary artery disease. *Curr Opin Cardiol,* 14**,** 140-50.

KATO, M., SHIODE, N., YAMAGATA, T., MATSUURA, H. & KAJIYAMA, G. 1997. Coronary segmental responses to acetylcholine and bradykinin in patients with atherosclerotic risk factors. *Am J Cardiol,* 80**,** 751-5.

KATOUZIAN, A., ANGELINI, E. D., CARLIER, S. G., SURI, J. S., NAVAB, N. & LAINE, A. F. 2012. A state-of-the-art review on segmentation algorithms in intravascular ultrasound (IVUS) images. *IEEE Trans Inf Technol Biomed,* 16**,** 823-34.

KATZ, I. M., SHAUGHNESSY, E. J. & CRESS, B. B. 1995. A technical problem in the calculation of laminar flow near irregular surfaces described by sampled geometric data. *Journal of Biomechanics,* 28**,** 461-4.

KAUFMANN, B. A. 2009. Ultrasound molecular imaging of atherosclerosis. *Cardiovasc Res,* 83**,** 617-25.

KAWASAKI, M., BOUMA, B. E., BRESSNER, J., HOUSER, S. L., NADKARNI, S. K., MACNEILL, B. D., JANG, I. K., FUJIWARA, H. & TEARNEY, G. J. 2006. Diagnostic accuracy of optical coherence tomography and integrated backscatter intravascular ultrasound images for tissue characterization of human coronary plaques. *J Am Coll Cardiol,* 48**,** 81-8.

KAWASAKI, M., TAKATSU, H., NODA, T., ITO, Y., KUNISHIMA, A., ARAI, M., NISHIGAKI, K., TAKEMURA, G., MORITA, N., MINATOGUCHI, S. & FUJIWARA, H. 2001. Noninvasive quantitative tissue characterization and two-dimensional color-coded map of human atherosclerotic lesions using ultrasound integrated backscatter: comparison between histology and integrated backscatter images. *J Am Coll Cardiol,* 38**,** 486-92.

KAWASE, Y., HOSHINO, K., YONEYAMA, R., MCGREGOR, J., HAJJAR, R. J., JANG, I. K. & HAYASE, M. 2005. In vivo volumetric analysis of coronary stent using optical coherence tomography with a novel balloon occlusion-flushing catheter: a comparison with intravascular ultrasound. *Ultrasound Med Biol,* 31**,** 1343-9.

KIM, J. S., HONG, M. K., KO, Y. G., CHOI, D., YOON, J. H., CHOI, S. H., HAHN, J. Y., GWON, H. C., JEONG, M. H., KIM, H. S., SEONG, I. W., YANG, J. Y., RHA, S. W., TAHK, S. J., SEUNG, K. B., PARK, S. J. & JANG, Y. 2011. Impact of intravascular ultrasound guidance on long-term clinical outcomes in patients treated with drug-eluting stent for bifurcation lesions: data from a Korean multicenter bifurcation registry. *Am Heart J,* 161**,** 180-7.

KIM, K. H., KIM, W. H., PARK, H. W., SONG, I. G., YANG, D. J., SEO, Y. H., YUK, H. B., PARK, Y. H., KWON, T. G., RIHAL, C. S., LERMAN, A., LEE, M. S. & BAE, J. H. 2013. Impact of plaque composition on long-term clinical outcomes in patients with coronary artery occlusive disease. *Korean Circ J,* 43**,** 377-83.

KIM, Y. H., PARK, S. W., HONG, M. K., PARK, D. W., PARK, K. M., LEE, B. K., SONG, J. M., HAN, K. H., LEE, C. W., KANG, D. H., SONG, J. K., KIM, J. J. & PARK, S. J. 2006. Comparison of simple and complex stenting techniques in the treatment of unprotected left main coronary artery bifurcation stenosis. *Am J Cardiol,* 97**,** 1597-601.

KINI, A. S., BABER, U., KOVACIC, J. C., LIMAYE, A., ALI, Z. A., SWEENY, J., MAEHARA, A., MEHRAN, R., DANGAS, G., MINTZ, G. S., FUSTER, V., NARULA, J., SHARMA, S. K. & MORENO, P. R. 2013. Changes in Plaque Lipid Content After Short-Term Intensive Versus Standard Statin Therapy: The YELLOW Trial (Reduction in Yellow Plaque by Aggressive Lipid-Lowering Therapy). *J Am Coll Cardiol,* 62**,** 21-9.

KOBASHIGAWA, J. A., TOBIS, J. M., STARLING, R. C., TUZCU, E. M., SMITH, A. L., VALANTINE, H. A., YEUNG, A. C., MEHRA, M. R., ANZAI, H., OESER, B. T., ABEYWICKRAMA, K. H., MURPHY, J. & CRETIN, N. 2005. Multicenter intravascular ultrasound validation study among heart transplant recipients: outcomes after five years. *J Am Coll Cardiol,* 45**,** 1532-7.

KOLODGIE, F. D., GOLD, H. K., BURKE, A. P., FOWLER, D. R., KRUTH, H. S., WEBER, D. K., FARB, A., GUERRERO, L. J., HAYASE, M., KUTYS, R.,

NARULA, J., FINN, A. V. & VIRMANI, R. 2003. Intraplaque hemorrhage and progression of coronary atheroma. *N Engl J Med,* 349**,** 2316-25.

KOLODGIE, F. D., VIRMANI, R., BURKE, A. P., FARB, A., WEBER, D. K., KUTYS, R., FINN, A. V. & GOLD, H. K. 2004. Pathologic assessment of the vulnerable human coronary plaque. *Heart,* 90**,** 1385-91.

KOSKINAS, K. C., FELDMAN, C. L., CHATZIZISIS, Y. S., COSKUN, A. U., JONAS, M., MAYNARD, C., BAKER, A. B., PAPAFAKLIS, M. I., EDELMAN, E. R. & STONE, P. H. 2010. Natural history of experimental coronary atherosclerosis and vascular remodeling in relation to endothelial shear stress: a serial, in vivo intravascular ultrasound study. *Circulation,* 121**,** 2092-101.

KRAMS, R., WENTZEL, J. J., OOMEN, J. A., VINKE, R., SCHUURBIERS, J. C., DE FEYTER, P. J., SERRUYS, P. W. & SLAGER, C. J. 1997. Evaluation of endothelial shear stress and 3D geometry as factors determining the development of atherosclerosis and remodeling in human coronary arteries in vivo. Combining 3D reconstruction from angiography and IVUS (ANGUS) with computational fluid dynamics. *Arterioscler Thromb Vasc Biol,* 17**,** 2061-5.

KRISTENSEN, T. S., KOFOED, K. F., KUHL, J. T., NIELSEN, W. B., NIELSEN, M. B. & KELBAEK, H. 2011. Prognostic implications of nonobstructive coronary plaques in patients with non-ST-segment elevation myocardial infarction: a multidetector computed tomography study. *J Am Coll Cardiol,* 58**,** 502-9.

KUBO, T., IMANISHI, T., KASHIWAGI, M., IKEJIMA, H., TSUJIOKA, H., KUROI, A., ISHIBASHI, K., KOMUKAI, K., TANIMOTO, T., INO, Y., KITABATA,

H., TAKARADA, S., TANAKA, A., MIZUKOSHI, M. & AKASAKA, T. 2010a. Multiple coronary lesion instability in patients with acute myocardial infarction as determined by optical coherence tomography. *Am J Cardiol,* 105**,** 318-22.

KUBO, T., IMANISHI, T., TAKARADA, S., KUROI, A., UENO, S., YAMANO, T., TANIMOTO, T., MATSUO, Y., MASHO, T., KITABATA, H., TSUDA, K., TOMOBUCHI, Y. & AKASAKA, T. 2007. Assessment of culprit lesion morphology in acute myocardial infarction: ability of optical coherence tomography compared with intravascular ultrasound and coronary angioscopy. *J Am Coll Cardiol,* 50**,** 933-9.

KUBO, T., MAEHARA, A., MINTZ, G. S., DOI, H., TSUJITA, K., CHOI, S. Y., KATOH, O., NASU, K., KOENIG, A., PIEPER, M., ROGERS, J. H., WIJNS, W., BOSE, D., MARGOLIS, M. P., MOSES, J. W., STONE, G. W. & LEON, M. B. 2010b. The dynamic nature of coronary artery lesion morphology assessed by serial virtual histology intravascular ultrasound tissue characterization. *J Am Coll Cardiol,* 55**,** 1590-7.

LAM, C. F., PETERSON, T. E., RICHARDSON, D. M., CROATT, A. J., D'USCIO, L. V., NATH, K. A. & KATUSIC, Z. S. 2006. Increased blood flow causes coordinated upregulation of arterial eNOS and biosynthesis of tetrahydrobiopterin. *Am J Physiol Heart Circ Physiol,* 290**,** H786-93.

LAUFS, U., LA FATA, V., PLUTZKY, J. & LIAO, J. K. 1998. Upregulation of endothelial nitric oxide synthase by HMG CoA reductase inhibitors. *Circulation,* 97**,** 1129-35.

LAVI, S., BAE, J. H., RIHAL, C. S., PRASAD, A., BARSNESS, G. W., LENNON, R. J., HOLMES, D. R., JR. & LERMAN, A. 2009. Segmental coronary endothelial dysfunction in patients with minimal atherosclerosis is associated with necrotic core plaques. *Heart,* 95**,** 1525-30.

LAVI, S., PRASAD, A., YANG, E. H., MATHEW, V., SIMARI, R. D., RIHAL, C. S., LERMAN, L. O. & LERMAN, A. 2007. Smoking is associated with epicardial coronary endothelial dysfunction and elevated white blood cell count in patients with chest pain and early coronary artery disease. *Circulation,* 115**,** 2621-7.

LAVI, S., YANG, E. H., PRASAD, A., MATHEW, V., BARSNESS, G. W., RIHAL, C. S., LERMAN, L. O. & LERMAN, A. 2008. The interaction between coronary endothelial dysfunction, local oxidative stress, and endogenous nitric oxide in humans. *Hypertension,* 51**,** 127-33.

LEON, M. B. How to improve upon the left main cohort results from SYNTAX. 8th Annual Chronic Total Occlusion and Left Main Coronary Intervention Summit, February 14-16, 2011 February 14-16, 2011 New York City, NY, USA.

LERMAN, A. & ZEIHER, A. M. 2005. Endothelial function: cardiac events. *Circulation,* 111**,** 363-8.

LI, Q. X., FU, Q. Q., SHI, S. W., WANG, Y. F., XIE, J. J., YU, X., CHENG, X. & LIAO, Y. H. 2010a. Relationship between plasma inflammatory markers and plaque fibrous cap thickness determined by intravascular optical coherence tomography. *Heart,* 96**,** 196-201.

LI, X., YIN, J., HU, C., ZHOU, Q., SHUNG, K. K. & CHEN, Z. 2010b. High-resolution coregistered intravascular imaging with integrated ultrasound and optical coherence tomography probe. *Appl Phys Lett,* 97**,** 133702.

LIBBY, P. 2013. Mechanisms of acute coronary syndromes and their implications for therapy. *N Engl J Med,* 368**,** 2004-13.

LIBBY, P. & AIKAWA, M. 2003. Mechanisms of plaque stabilization with statins. *Am J Cardiol,* 91**,** 4B-8B.

LIN, F. Y., SHAW, L. J., DUNNING, A. M., LABOUNTY, T. M., CHOI, J. H., WEINSAFT, J. W., KODURU, S., GOMEZ, M. J., DELAGO, A. J., CALLISTER, T. Q., BERMAN, D. S. & MIN, J. K. 2011. Mortality risk in symptomatic patients with nonobstructive coronary artery disease: a prospective 2-center study of 2,583 patients undergoing 64-detector row coronary computed tomographic angiography. *J Am Coll Cardiol,* 58**,** 510-9.

LINDNER, J. R. 2009. Contrast ultrasound molecular imaging: harnessing the power of bubbles. *Cardiovasc Res,* 83**,** 615-6.

LUDMER, P. L., SELWYN, A. P., SHOOK, T. L., WAYNE, R. R., MUDGE, G. H., ALEXANDER, R. W. & GANZ, P. 1986. Paradoxical vasoconstriction induced by acetylcholine in atherosclerotic coronary arteries. *N Engl J Med,* 315**,** 1046-51.

MACDONALD, P. S., DUBBIN, P. N. & DUSTING, G. J. 1987. Beta-adrenoceptors on endothelial cells do not influence release of relaxing factor in dog coronary arteries. *Clin Exp Pharmacol Physiol,* 14**,** 525-34.

MACNEILL, B. D., JANG, I. K., BOUMA, B. E., IFTIMIA, N., TAKANO, M., YABUSHITA, H., SHISHKOV, M., KAUFFMAN, C. R., HOUSER, S. L., ARETZ, H. T., DEJOSEPH, D., HALPERN, E. F. & TEARNEY, G. J. 2004. Focal and multi-focal plaque macrophage distributions in patients with acute and stable presentations of coronary artery disease. *J Am Coll Cardiol,* 44**,** 972-9.

MADJID, M., WILLERSON, J. T. & CASSCELLS, S. W. 2006. Intracoronary thermography for detection of high-risk vulnerable plaques. *J Am Coll Cardiol,* 47**,** C80-5.

MAEHARA, A., MINTZ, G. S., BUI, A. B., WALTER, O. R., CASTAGNA, M. T., CANOS, D., PICHARD, A. D., SATLER, L. F., WAKSMAN, R., SUDDATH, W. O., LAIRD, J. R., JR., KENT, K. M. & WEISSMAN, N. J. 2002. Morphologic and angiographic features of coronary plaque rupture detected by intravascular ultrasound. *J Am Coll Cardiol,* 40**,** 904-10.

MAJMUDAR, N. G., ANUMBA, D., ROBSON, S. C. & FORD, G. A. 1999. Contribution of nitric oxide to beta2-adrenoceptor mediated vasodilatation in human forearm arterial vasculature. *Br J Clin Pharmacol,* 47**,** 173-7.

MANFRINI, O., MONT, E., LEONE, O., ARBUSTINI, E., EUSEBI, V., VIRMANI, R. & BUGIARDINI, R. 2006. Sources of error and interpretation of plaque morphology by optical coherence tomography. *Am J Cardiol,* 98**,** 156-9.

MANGINAS, A., VOUDRIS, V., PAVLIDES, G., KARATASAKIS, G., ATHANASSOPOULOS, G. & COKKINOS, D. V. 1998. Effect of plaque burden on coronary vasoreactivity in early atherosclerosis. *Am J Cardiol,* 81**,** 401-6.

MASERI, A., BELTRAME, J. F. & SHIMOKAWA, H. 2009. Role of coronary vasoconstriction in ischemic heart disease and search for novel therapeutic targets. *Circ J,* 73**,** 394-403.

MCFADDEN, E. P., CLARKE, J. G., DAVIES, G. J., KASKI, J. C., HAIDER, A. W. & MASERI, A. 1991. Effect of intracoronary serotonin on coronary vessels in patients with stable angina and patients with variant angina. *N Engl J Med,* 324**,** 648-54.

MCPHERSON, J. A., MAEHARA, A., WEISZ, G., MINTZ, G. S., CRISTEA, E., MEHRAN, R., FOSTER, M., VERHEYE, S., RABBANI, L., XU, K., FAHY, M., TEMPLIN, B., ZHANG, Z., LANSKY, A. J., DE BRUYNE, B., SERRUYS, P. W. & STONE, G. W. 2012. Residual plaque burden in patients with acute coronary syndromes after successful percutaneous coronary intervention. *JACC. Cardiovascular imaging,* 5**,** S76-85.

MINTZ, G. S., NISSEN, S. E., ANDERSON, W. D., BAILEY, S. R., ERBEL, R., FITZGERALD, P. J., PINTO, F. J., ROSENFIELD, K., SIEGEL, R. J., TUZCU, E. M. & YOCK, P. G. 2001. American College of Cardiology Clinical Expert Consensus Document on Standards for Acquisition, Measurement and Reporting of Intravascular Ultrasound Studies (IVUS). A report of the American College of Cardiology Task Force on Clinical Expert Consensus Documents. *J Am Coll Cardiol,* 37**,** 1478-92.

MINTZ, G. S., PAINTER, J. A., PICHARD, A. D., KENT, K. M., SATLER, L. F., POPMA, J. J., CHUANG, Y. C., BUCHER, T. A., SOKOLOWICZ, L. E. & LEON, M. B. 1995. Atherosclerosis in angiographically "normal" coronary

artery reference segments: an intravascular ultrasound study with clinical correlations. *J Am Coll Cardiol,* 25**,** 1479-85.

MINTZ, G. S., PICHARD, A. D., KOVACH, J. A., KENT, K. M., SATLER, L. F., JAVIER, S. P., POPMA, J. J. & LEON, M. B. 1994. Impact of preintervention intravascular ultrasound imaging on transcatheter treatment strategies in coronary artery disease. *Am J Cardiol,* 73**,** 423-30.

MINTZ, G. S., POPMA, J. J., PICHARD, A. D., KENT, K. M., SATLER, L. F., CHUANG, Y. C., DEFALCO, R. A. & LEON, M. B. 1996. Limitations of angiography in the assessment of plaque distribution in coronary artery disease: a systematic study of target lesion eccentricity in 1446 lesions. *Circulation,* 93**,** 924-31.

MIYATA, N., YAMAURA, H., TSUCHIDA, K. & OTOMO, S. 1992. Effects of CD-349 and 8-BrcGMP on isoproterenol-induced relaxation in rabbit aorta precontracted with endothelin-1. *Am J Physiol,* 263**,** H1113-8.

MOLENAAR, P., MALTA, E., JONES, C. R., BUXTON, B. F. & SUMMERS, R. J. 1988. Autoradiographic localization and function of beta-adrenoceptors on the human internal mammary artery and saphenous vein. *Br J Pharmacol,* 95**,** 225-33.

MOORE, S. 1973. Thromboatherosclerosis in normolipemic rabbits. A result of continued endothelial damage. *Lab Invest,* 29**,** 478-87.

MORENO, P. R., PURUSHOTHAMAN, K. R., SIROL, M., LEVY, A. P. & FUSTER, V. 2006. Neovascularization in human atherosclerosis. *Circulation,* 113**,** 2245-52.

MUELLER, C., HODGSON, J. M., SCHINDLER, C., PERRUCHOUD, A. P., ROSKAMM, H. & BUETTNER, H. J. 2003. Cost-effectiveness of intracoronary ultrasound for percutaneous coronary interventions. *Am J Cardiol,* 91**,** 143-7.

MULLER, J. E., TOFLER, G. H. & STONE, P. H. 1989. Circadian variation and triggers of onset of acute cardiovascular disease. *Circulation,* 79**,** 733-43.

NAGHAVI, M., LIBBY, P., FALK, E., CASSCELLS, S. W., LITOVSKY, S., RUMBERGER, J., BADIMON, J. J., STEFANADIS, C., MORENO, P., PASTERKAMP, G., FAYAD, Z., STONE, P. H., WAXMAN, S., RAGGI, P., MADJID, M., ZARRABI, A., BURKE, A., YUAN, C., FITZGERALD, P. J., SISCOVICK, D. S., DE KORTE, C. L., AIKAWA, M., JUHANI AIRAKSINEN, K. E., ASSMANN, G., BECKER, C. R., CHESEBRO, J. H., FARB, A., GALIS, Z. S., JACKSON, C., JANG, I. K., KOENIG, W., LODDER, R. A., MARCH, K., DEMIROVIC, J., NAVAB, M., PRIORI, S. G., REKHTER, M. D., BAHR, R., GRUNDY, S. M., MEHRAN, R., COLOMBO, A., BOERWINKLE, E., BALLANTYNE, C., INSULL, W., JR., SCHWARTZ, R. S., VOGEL, R., SERRUYS, P. W., HANSSON, G. K., FAXON, D. P., KAUL, S., DREXLER, H., GREENLAND, P., MULLER, J. E., VIRMANI, R., RIDKER, P. M., ZIPES, D. P., SHAH, P. K. & WILLERSON, J. T. 2003. From vulnerable plaque to vulnerable patient: a call for new definitions and risk assessment strategies: Part I. *Circulation,* 108**,** 1664-72.

NAIR, A., KUBAN, B. D., OBUCHOWSKI, N. & VINCE, D. G. 2001. Assessing spectral algorithms to predict atherosclerotic plaque composition with

normalized and raw intravascular ultrasound data. *Ultrasound Med Biol,* 27**,** 1319-31.

NAIR, A., KUBAN, B. D., TUZCU, E. M., SCHOENHAGEN, P., NISSEN, S. E. & VINCE, D. G. 2002. Coronary plaque classification with intravascular ultrasound radiofrequency data analysis. *Circulation,* 106**,** 2200-6.

NAIR, A., MARGOLIS, M. P., KUBAN, B. D. & VINCE, D. G. 2007. Automated coronary plaque characterisation with intravascular ultrasound backscatter: ex vivo validation. *EuroIntervention,* 3**,** 113-20.

NAM, D., NI, C. W., REZVAN, A., SUO, J., BUDZYN, K., LLANOS, A., HARRISON, D., GIDDENS, D. & JO, H. 2009. Partial carotid ligation is a model of acutely induced disturbed flow, leading to rapid endothelial dysfunction and atherosclerosis. *Am J Physiol Heart Circ Physiol,* 297**,** H1535-43.

NAZEMI, J. H. & BRENNAN, J. F. 2009. Lipid concentrations in human coronary artery determined with high wavenumber Raman shifted light. *J Biomed Opt,* 14**,** 034009.

NEWMAN, C. M., MASERI, A., HACKETT, D. R., EL-TAMIMI, H. M. & DAVIES, G. J. 1990. Response of angiographically normal and atherosclerotic left anterior descending coronary arteries to acetylcholine. *Am J Cardiol,* 66**,** 1070-6.

NICHOLLS, S. J., ANDREWS, J. & MOON, K. W. 2007a. Exploring the natural history of atherosclerosis with intravascular ultrasound. *Expert Rev Cardiovasc Ther,* 5**,** 295-306.

NICHOLLS, S. J., BALLANTYNE, C. M., BARTER, P. J., CHAPMAN, M. J., ERBEL, R. M., LIBBY, P., RAICHLEN, J. S., UNO, K., BORGMAN, M., WOLSKI, K. & NISSEN, S. E. 2011. Effect of two intensive statin regimens on progression of coronary disease. *N Engl J Med,* 365**,** 2078-87.

NICHOLLS SJ, H. A., BRENNAN DM, KALIDINDI SR, MOON K, TUZCU EM, NISSEN SE 2007. Baseline and Changes in Atheroma Volume Predict Clinical Outcome in Patients with Coronary Artery Disease: Insights from ILLUSTRATE. *Circulation,* 116.

NICHOLLS, S. J., HSU, A., WOLSKI, K., HU, B., BAYTURAN, O., LAVOIE, A., UNO, K., TUZCU, E. M. & NISSEN, S. E. 2010. Intravascular ultrasound-derived measures of coronary atherosclerotic plaque burden and clinical outcome. *J Am Coll Cardiol,* 55**,** 2399-407.

NICHOLLS, S. J., TUZCU, E. M., KALIDINDI, S., WOLSKI, K., MOON, K. W., SIPAHI, I., SCHOENHAGEN, P. & NISSEN, S. E. 2008. Effect of diabetes on progression of coronary atherosclerosis and arterial remodeling: a pooled analysis of 5 intravascular ultrasound trials. *J Am Coll Cardiol,* 52**,** 255-62.

NICHOLLS, S. J., TUZCU, E. M., SIPAHI, I., GRASSO, A. W., SCHOENHAGEN, P., HU, T., WOLSKI, K., CROWE, T., DESAI, M. Y., HAZEN, S. L., KAPADIA, S. R. & NISSEN, S. E. 2007b. Statins, high-density lipoprotein cholesterol, and regression of coronary atherosclerosis. *JAMA,* 297**,** 499-508.

NICHOLLS, S. J., TUZCU, E. M., SIPAHI, I., SCHOENHAGEN, P. & NISSEN, S. E. 2006. Intravascular ultrasound in cardiovascular medicine. *Circulation,* 114**,** e55-9.

NISHIMURA, R. A., LERMAN, A., CHESEBRO, J. H., ILSTRUP, D. M., HODGE, D. O., HIGANO, S. T., HOLMES, D. R., JR. & TAJIK, A. J. 1995. Epicardial vasomotor responses to acetylcholine are not predicted by coronary atherosclerosis as assessed by intracoronary ultrasound. *J Am Coll Cardiol,* 26**,** 41-9.

NISSEN, S. E., NICHOLLS, S. J., SIPAHI, I., LIBBY, P., RAICHLEN, J. S., BALLANTYNE, C. M., DAVIGNON, J., ERBEL, R., FRUCHART, J. C., TARDIF, J. C., SCHOENHAGEN, P., CROWE, T., CAIN, V., WOLSKI, K., GOORMASTIC, M. & TUZCU, E. M. 2006a. Effect of very high-intensity statin therapy on regression of coronary atherosclerosis: the ASTEROID trial. *JAMA,* 295**,** 1556-65.

NISSEN, S. E., NICHOLLS, S. J., WOLSKI, K., NESTO, R., KUPFER, S., PEREZ, A., JURE, H., DE LAROCHELLIERE, R., STANILOAE, C. S., MAVROMATIS, K., SAW, J., HU, B., LINCOFF, A. M. & TUZCU, E. M. 2008. Comparison of pioglitazone vs glimepiride on progression of coronary atherosclerosis in patients with type 2 diabetes: the PERISCOPE randomized controlled trial. *JAMA,* 299**,** 1561-73.

NISSEN, S. E., TARDIF, J. C., NICHOLLS, S. J., REVKIN, J. H., SHEAR, C. L., DUGGAN, W. T., RUZYLLO, W., BACHINSKY, W. B., LASALA, G. P. & TUZCU, E. M. 2007. Effect of torcetrapib on the progression of coronary atherosclerosis. *N Engl J Med,* 356**,** 1304-16.

NISSEN, S. E., TSUNODA, T., TUZCU, E. M., SCHOENHAGEN, P., COOPER, C. J., YASIN, M., EATON, G. M., LAUER, M. A., SHELDON, W. S., GRINES,

C. L., HALPERN, S., CROWE, T., BLANKENSHIP, J. C. & KERENSKY, R. 2003. Effect of recombinant ApoA-I Milano on coronary atherosclerosis in patients with acute coronary syndromes: a randomized controlled trial. *JAMA,* 290**,** 2292-300.

NISSEN, S. E., TUZCU, E. M., BREWER, H. B., SIPAHI, I., NICHOLLS, S. J., GANZ, P., SCHOENHAGEN, P., WATERS, D. D., PEPINE, C. J., CROWE, T. D., DAVIDSON, M. H., DEANFIELD, J. E., WISNIEWSKI, L. M., HANYOK, J. J., KASSALOW, L. M. & INVESTIGATORS, A. I. A. T. E. 2006b. Effect of ACAT inhibition on the progression of coronary atherosclerosis. *N Engl J Med,* 354**,** 1253-63.

NISSEN, S. E., TUZCU, E. M., LIBBY, P., THOMPSON, P. D., GHALI, M., GARZA, D., BERMAN, L., SHI, H., BUEBENDORF, E. & TOPOL, E. J. 2004a. Effect of antihypertensive agents on cardiovascular events in patients with coronary disease and normal blood pressure: the CAMELOT study: a randomized controlled trial. *JAMA,* 292**,** 2217-25.

NISSEN, S. E., TUZCU, E. M., SCHOENHAGEN, P., BROWN, B. G., GANZ, P., VOGEL, R. A., CROWE, T., HOWARD, G., COOPER, C. J., BRODIE, B., GRINES, C. L. & DEMARIA, A. N. 2004b. Effect of intensive compared with moderate lipid-lowering therapy on progression of coronary atherosclerosis: a randomized controlled trial. *JAMA,* 291**,** 1071-80.

NISSEN, S. E., TUZCU, E. M., SCHOENHAGEN, P., CROWE, T., SASIELA, W. J., TSAI, J., ORAZEM, J., MAGORIEN, R. D., O'SHAUGHNESSY, C. & GANZ,

P. 2005. Statin therapy, LDL cholesterol, C-reactive protein, and coronary artery disease. *N Engl J Med,* 352**,** 29-38.

O'DONOGHUE, M. L., BRAUNWALD, E., WHITE, H. D., SERRUYS, P., STEG, P. G., HOCHMAN, J., MAGGIONI, A. P., BODE, C., WEAVER, D., JOHNSON, J. L., CICCONETTI, G., LUKAS, M. A., TARKA, E. & CANNON, C. P. 2011. Study design and rationale for the Stabilization of pLaques usIng Darapladib-Thrombolysis in Myocardial Infarction (SOLID-TIMI 52) trial in patients after an acute coronary syndrome. *Am Heart J,* 162**,** 613-619 e1.

OKAMURA, T., ONUMA, Y., GARCIA-GARCIA, H. M., REGAR, E., WYKRZYKOWSKA, J. J., KOOLEN, J., THUESEN, L., WINDECKER, S., WHITBOURN, R., MCCLEAN, D. R., ORMISTON, J. A. & SERRUYS, P. W. 2010. 3-Dimensional optical coherence tomography assessment of jailed side branches by bioresorbable vascular scaffolds: a proposal for classification. *JACC. Cardiovascular interventions,* 3**,** 836-44.

OKAZAKI, S., YOKOYAMA, T., MIYAUCHI, K., SHIMADA, K., KURATA, T., SATO, H. & DAIDA, H. 2004. Early statin treatment in patients with acute coronary syndrome: demonstration of the beneficial effect on atherosclerotic lesions by serial volumetric intravascular ultrasound analysis during half a year after coronary event: the ESTABLISH Study. *Circulation,* 110**,** 1061-8.

OKUBO, M., KAWASAKI, M., ISHIHARA, Y., TAKEYAMA, U., YASUDA, S., KUBOTA, T., TANAKA, S., YAMAKI, T., OJIO, S., NISHIGAKI, K., TAKEMURA, G., SAIO, M., TAKAMI, T., FUJIWARA, H. & MINATOGUCHI, S. 2008. Tissue characterization of coronary plaques:

comparison of integrated backscatter intravascular ultrasound with virtual histology intravascular ultrasound. *Circ J,* 72**,** 1631-9.

ONG, P., ATHANASIADIS, A., HILL, S., VOGELSBERG, H., VOEHRINGER, M. & SECHTEM, U. 2008. Coronary artery spasm as a frequent cause of acute coronary syndrome: The CASPAR (Coronary Artery Spasm in Patients With Acute Coronary Syndrome) Study. *J Am Coll Cardiol,* 52**,** 523-7.

PARENT, R., AL-OBAIDI, M. & LAVALLEE, M. 1993. Nitric oxide formation contributes to beta-adrenergic dilation of resistance coronary vessels in conscious dogs. *Circ Res,* 73**,** 241-51.

PARK, S. J., KIM, Y. H., PARK, D. W., LEE, S. W., KIM, W. J., SUH, J., YUN, S. C., LEE, C. W., HONG, M. K., LEE, J. H. & PARK, S. W. 2009. Impact of intravascular ultrasound guidance on long-term mortality in stenting for unprotected left main coronary artery stenosis. *Circ Cardiovasc Interv,* 2**,** 167-77.

PENDYALA, L. K., LI, J., SHINKE, T., GEVA, S., YIN, X., CHEN, J. P., KING, S. B., 3RD, ROBINSON, K. A., CHRONOS, N. A. & HOU, D. 2009. Endothelium-dependent vasomotor dysfunction in pig coronary arteries with Paclitaxel-eluting stents is associated with inflammation and oxidative stress. *JACC Cardiovasc Interv,* 2**,** 253-62.

PENNY, W. F., BEN-YEHUDA, O., KUROE, K., LONG, J., BOND, A., BHARGAVA, V., PETERSON, J. F., MCDANIEL, M., JULIANO, J., WITZTUM, J. L., ROSS, J., JR. & PETERSON, K. L. 2001. Improvement of coronary artery endothelial dysfunction with lipid-lowering therapy:

heterogeneity of segmental response and correlation with plasma-oxidized low density lipoprotein. *J Am Coll Cardiol,* 37**,** 766-74.

PENNY, W. F., ROCKMAN, H., LONG, J., BHARGAVA, V., CARRIGAN, K., IBRIHAM, A., SHABETAI, R., ROSS, J., JR. & PETERSON, K. L. 1995. Heterogeneity of vasomotor response to acetylcholine along the human coronary artery. *J Am Coll Cardiol,* 25**,** 1046-55.

PHINIKARIDOU, A., HUA, N., PHAM, T. & HAMILTON, J. A. 2013. Regions of low endothelial shear stress colocalize with positive vascular remodeling and atherosclerotic plaque disruption: an in vivo magnetic resonance imaging study. *Circ Cardiovasc Imaging,* 6**,** 302-10.

PORTER, T. R., SEARS, T., XIE, F., MICHELS, A., MATA, J., WELSH, D. & SHURMUR, S. 1993. Intravascular ultrasound study of angiographically mildly diseased coronary arteries. *J Am Coll Cardiol,* 22**,** 1858-65.

PRATI, F., CERA, M., RAMAZZOTTI, V., IMOLA, F., GIUDICE, R. & ALBERTUCCI, M. 2007. Safety and feasibility of a new non-occlusive technique for facilitated intracoronary optical coherence tomography (OCT) acquisition in various clinical and anatomical scenarios. *EuroIntervention,* 3**,** 365-70.

PRATI, F., DI VITO, L., BIONDI-ZOCCAI, G., OCCHIPINTI, M., LA MANNA, A., TAMBURINO, C., BURZOTTA, F., TRANI, C., PORTO, I., RAMAZZOTTI, V., IMOLA, F., MANZOLI, A., MATERIA, L., CREMONESI, A. & ALBERTUCCI, M. 2012. Angiography alone versus angiography plus optical coherence tomography to guide decision-making during percutaneous coronary

intervention: the Centro per la Lotta contro l'Infarto-Optimisation of Percutaneous Coronary Intervention (CLI-OPCI) study. *EuroIntervention,* 8**,** 823-9.

PRATI, F., REGAR, E., MINTZ, G. S., ARBUSTINI, E., DI MARIO, C., JANG, I. K., AKASAKA, T., COSTA, M., GUAGLIUMI, G., GRUBE, E., OZAKI, Y., PINTO, F. & SERRUYS, P. W. 2010. Expert review document on methodology, terminology, and clinical applications of optical coherence tomography: physical principles, methodology of image acquisition, and clinical application for assessment of coronary arteries and atherosclerosis. *Eur Heart J,* 31**,** 401-15.

PURI, R., KAPADIA, S. R., NICHOLLS, S. J., HARVEY, J. E., KATAOKA, Y. & TUZCU, E. M. 2012a. Optimizing outcomes during left main percutaneous coronary intervention with intravascular ultrasound and fractional flow reserve: the current state of evidence. *JACC Cardiovasc Interv,* 5**,** 697-707.

PURI, R., LIBBY, P., NISSEN, S. E., WOLSKI, K., BALLANTYNE, C. M., BARTER, P. J., CHAPMAN, M. J., ERBEL, R., RAICHLEN, J. S., UNO, K., KATAOKA, Y., TUZCU, E. M. & NICHOLLS, S. J. 2014. Long-term effects of maximally intensive statin therapy on changes in coronary atheroma composition: insights from SATURN. *Eur Heart J Cardiovasc Imaging,* 15**,** 380-8.

PURI, R., LIEW, G. Y., NICHOLLS, S. J., NELSON, A. J., LEONG, D. P., CARBONE, A., COPUS, B., WONG, D. T., BELTRAME, J. F., WORTHLEY, S. G. & WORTHLEY, M. I. 2012b. Coronary beta2-adrenoreceptors mediate

endothelium-dependent vasoreactivity in humans: novel insights from an in vivo intravascular ultrasound study. *Eur Heart J,* 33**,** 495-504.

PURI, R., NICHOLLS, S. J., NISSEN, S. E., BRENNAN, D. M., ANDREWS, J., LIEW, G. Y., NELSON, A. J., CARBONE, A., COPUS, B., TUZCU, E. M., BELTRAME, J. F., WORTHLEY, S. G. & WORTHLEY, M. I. 2013a. Coronary endothelium-dependent vasoreactivity and atheroma volume in subjects with stable, minimal angiographic disease versus non-ST-segment-elevation myocardial infarction: an intravascular ultrasound study. *Circ Cardiovasc Imaging,* 6**,** 674-82.

PURI, R., NISSEN, S. E., SHAO, M., BALLANTYNE, C. M., BARTER, P. J., CHAPMAN, M. J., ERBEL, R., LIBBY, P., RAICHLEN, J. S., UNO, K., KATAOKA, Y. & NICHOLLS, S. J. 2013b. Coronary atheroma volume and cardiovascular events during maximally intensive statin therapy. *Eur Heart J,* 34**,** 3182-90.

PURI, R., ONG, P., KATAOKA, Y., KAPADIA, S. R., TUZCU, E. M., NICHOLLS, S. J. & WORTHLEY, M. I. 2012c. "Framing" the vessel: the critical importance of volumetric analysis during serial intravascular imaging studies. *J Am Coll Cardiol,* 59**,** 1038-9.

PURI, R., WOLSKI, K., UNO, K., KATAOKA, Y., KING, K. L., CROWE, T. D., KAPADIA, S. R., TUZCU, E. M., NISSEN, S. E. & NICHOLLS, S. J. 2013c. Left main coronary atherosclerosis progression, constrictive remodeling, and clinical events. *JACC Cardiovasc Interv,* 6**,** 29-35.

PURI, R., WORTHLEY, M. I. & NICHOLLS, S. J. 2011. Intravascular imaging of vulnerable coronary plaque: current and future concepts. *Nat Rev Cardiol,* 8**,** 131-9.

PYKE, K. E. & TSCHAKOVSKY, M. E. 2005. The relationship between shear stress and flow-mediated dilatation: implications for the assessment of endothelial function. *J Physiol,* 568**,** 357-69.

QUYYUMI, A. A., DAKAK, N., MULCAHY, D., ANDREWS, N. P., HUSAIN, S., PANZA, J. A. & CANNON, R. O., 3RD 1997a. Nitric oxide activity in the atherosclerotic human coronary circulation. *J Am Coll Cardiol,* 29**,** 308-17.

QUYYUMI, A. A., MULCAHY, D., ANDREWS, N. P., HUSAIN, S., PANZA, J. A. & CANNON, R. O., 3RD 1997b. Coronary vascular nitric oxide activity in hypertension and hypercholesterolemia. Comparison of acetylcholine and substance P. *Circulation,* 95**,** 104-10.

RÄBER, L. & RADU, M. D. 2012. Optimising cardiovascular outcomes using optical coherence tomography-guided percutaneous coronary interventions. *EuroIntervention,* 8**,** 765-771.

RADU, M. D. & FALK, E. 2012. In search of vulnerable features of coronary plaques with optical coherence tomography: is it time to rethink the current methodological concepts? *Eur Heart J,* 33**,** 9-12.

RAFFEL, O. C., TEARNEY, G. J., GAUTHIER, D. D., HALPERN, E. F., BOUMA, B. E. & JANG, I. K. 2007. Relationship between a systemic inflammatory marker, plaque inflammation, and plaque characteristics determined by intravascular optical coherence tomography. *Arterioscler Thromb Vasc Biol,* 27**,** 1820-7.

RAMCHARITAR, S., DAEMAN, J., PATTERSON, M., VAN GUENS, R. J., BOERSMA, E., SERRUYS, P. W. & VAN DER GIESSEN, W. J. 2008. First direct in vivo comparison of two commercially available three-dimensional quantitative coronary angiography systems. *Catheter Cardiovasc Interv,* 71**,** 44-50.

REDDY, K. G., NAIR, R. N., SHEEHAN, H. M. & HODGSON, J. M. 1994. Evidence that selective endothelial dysfunction may occur in the absence of angiographic or ultrasound atherosclerosis in patients with risk factors for atherosclerosis. *J Am Coll Cardiol,* 23**,** 833-43.

RENEMAN, R. S., ARTS, T. & HOEKS, A. P. 2006. Wall shear stress--an important determinant of endothelial cell function and structure--in the arterial system in vivo. Discrepancies with theory. *Journal of Vascular Research,* 43**,** 251-69.

RIDKER, P. M., DANIELSON, E., FONSECA, F. A., GENEST, J., GOTTO, A. M., JR., KASTELEIN, J. J., KOENIG, W., LIBBY, P., LORENZATTI, A. J., MACFADYEN, J. G., NORDESTGAARD, B. G., SHEPHERD, J., WILLERSON, J. T. & GLYNN, R. J. 2008. Rosuvastatin to prevent vascular events in men and women with elevated C-reactive protein. *N Engl J Med,* 359**,** 2195-207.

RIDKER, P. M., KASTELEIN, J. J., GENEST, J. & KOENIG, W. 2013. C-reactive protein and cholesterol are equally strong predictors of cardiovascular risk and both are important for quality clinical care. *Eur Heart J,* 34**,** 1258-61.

RILEY, R. F., DON, C. W., POWELL, W., MAYNARD, C. & DEAN, L. S. 2011. Trends in coronary revascularization in the United States from 2001 to 2009:

recent declines in percutaneous coronary intervention volumes. *Circ Cardiovasc Qual Outcomes,* 4**,** 193-7.

RIOUFOL, G., FINET, G., GINON, I., ANDRE-FOUET, X., ROSSI, R., VIALLE, E., DESJOYAUX, E., CONVERT, G., HURET, J. F. & TABIB, A. 2002. Multiple atherosclerotic plaque rupture in acute coronary syndrome: a three-vessel intravascular ultrasound study. *Circulation,* 106**,** 804-8.

RODRIGUEZ-GRANILLO, G. A., GARCIA-GARCIA, H. M., MC FADDEN, E. P., VALGIMIGLI, M., AOKI, J., DE FEYTER, P. & SERRUYS, P. W. 2005. In vivo intravascular ultrasound-derived thin-cap fibroatheroma detection using ultrasound radiofrequency data analysis. *J Am Coll Cardiol,* 46**,** 2038-42.

ROGER, V. L., GO, A. S., LLOYD-JONES, D. M., BENJAMIN, E. J., BERRY, J. D., BORDEN, W. B., BRAVATA, D. M., DAI, S., FORD, E. S., FOX, C. S., FULLERTON, H. J., GILLESPIE, C., HAILPERN, S. M., HEIT, J. A., HOWARD, V. J., KISSELA, B. M., KITTNER, S. J., LACKLAND, D. T., LICHTMAN, J. H., LISABETH, L. D., MAKUC, D. M., MARCUS, G. M., MARELLI, A., MATCHAR, D. B., MOY, C. S., MOZAFFARIAN, D., MUSSOLINO, M. E., NICHOL, G., PAYNTER, N. P., SOLIMAN, E. Z., SORLIE, P. D., SOTOODEHNIA, N., TURAN, T. N., VIRANI, S. S., WONG, N. D., WOO, D. & TURNER, M. B. 2012. Heart disease and stroke statistics--2012 update: a report from the American Heart Association. *Circulation,* 125**,** e2-e220.

ROMER, T. J., BRENNAN, J. F., 3RD, PUPPELS, G. J., ZWINDERMAN, A. H., VAN DUINEN, S. G., VAN DER LAARSE, A., VAN DER STEEN, A. F.,

BOM, N. A. & BRUSCHKE, A. V. 2000. Intravascular ultrasound combined with Raman spectroscopy to localize and quantify cholesterol and calcium salts in atherosclerotic coronary arteries. *Arterioscler Thromb Vasc Biol,* 20**,** 478-83.

ROSS, R. & GLOMSET, J. A. 1973. Atherosclerosis and the arterial smooth muscle cell: Proliferation of smooth muscle is a key event in the genesis of the lesions of atherosclerosis. *Science,* 180**,** 1332-9.

ROY, P., STEINBERG, D. H., SUSHINSKY, S. J., OKABE, T., PINTO SLOTTOW, T. L., KANESHIGE, K., XUE, Z., SATLER, L. F., KENT, K. M., SUDDATH, W. O., PICHARD, A. D., WEISSMAN, N. J., LINDSAY, J. & WAKSMAN, R. 2008. The potential clinical utility of intravascular ultrasound guidance in patients undergoing percutaneous coronary intervention with drug-eluting stents. *Eur Heart J,* 29**,** 1851-7.

RUBANYI, G. & VANHOUTTE, P. M. 1985. Endothelium-removal decreases relaxations of canine coronary arteries caused by beta-adrenergic agonists and adenosine. *J Cardiovasc Pharmacol,* 7**,** 139-44.

RZESZUTKO, L., LEGUTKO, J., KALUZA, G. L., WIZIMIRSKI, M., RICHTER, A., CHYRCHEL, M., HEBA, G., DUBIEL, J. S. & DUDEK, D. 2006. Assessment of culprit plaque temperature by intracoronary thermography appears inconclusive in patients with acute coronary syndromes. *Arteriosclerosis, Thrombosis, and Vascular Biology,* 26**,** 1889-94.

SAMADY, H., ESHTEHARDI, P., MCDANIEL, M. C., SUO, J., DHAWAN, S. S., MAYNARD, C., TIMMINS, L. H., QUYYUMI, A. A. & GIDDENS, D. P. 2011. Coronary artery wall shear stress is associated with progression and

transformation of atherosclerotic plaque and arterial remodeling in patients with coronary artery disease. *Circulation,* 124**,** 779-88.

SATHYANARAYANA, S., CARLIER, S., LI, W. & THOMAS, L. 2009. Characterisation of atherosclerotic plaque by spectral similarity of radiofrequency intravascular ultrasound signals. *EuroIntervention,* 5**,** 133-9.

SAWADA, T., SHITE, J., SHINKE, T., TANINO, Y., OGASAWARA, D., KAWAMORI, H., KATO, H., MIYOSHI, N., YOSHINO, N. & HIRATA, K. 2008. Very late thrombosis of sirolimus-eluting stent due to late malapposition: serial observations with optical coherence tomography. *J Cardiol,* 52**,** 290-5.

SCHAAR, J. A., MULLER, J. E., FALK, E., VIRMANI, R., FUSTER, V., SERRUYS, P. W., COLOMBO, A., STEFANADIS, C., WARD CASSCELLS, S., MORENO, P. R., MASERI, A. & VAN DER STEEN, A. F. 2004a. Terminology for high-risk and vulnerable coronary artery plaques. Report of a meeting on the vulnerable plaque, June 17 and 18, 2003, Santorini, Greece. *Eur Heart J,* 25**,** 1077-82.

SCHAAR, J. A., REGAR, E., MASTIK, F., MCFADDEN, E. P., SAIA, F., DISCO, C., DE KORTE, C. L., DE FEYTER, P. J., VAN DER STEEN, A. F. & SERRUYS, P. W. 2004b. Incidence of high-strain patterns in human coronary arteries: assessment with three-dimensional intravascular palpography and correlation with clinical presentation. *Circulation,* 109**,** 2716-9.

SCHACHINGER, V., BRITTEN, M. B. & ZEIHER, A. M. 2000. Prognostic impact of coronary vasodilator dysfunction on adverse long-term outcome of coronary heart disease. *Circulation,* 101**,** 1899-906.

SCHACHINGER, V. & ZEIHER, A. M. 1995. Quantitative assessment of coronary vasoreactivity in humans in vivo. Importance of baseline vasomotor tone in atherosclerosis. *Circulation,* 92**,** 2087-94.

SCHARTL, M., BOCKSCH, W., KOSCHYK, D. H., VOELKER, W., KARSCH, K. R., KREUZER, J., HAUSMANN, D., BECKMANN, S. & GROSS, M. 2001. Use of intravascular ultrasound to compare effects of different strategies of lipid-lowering therapy on plaque volume and composition in patients with coronary artery disease. *Circulation,* 104**,** 387-92.

SCHINDLER, T. H., NITZSCHE, E. U., OLSCHEWSKI, M., MAGOSAKI, N., MIX, M., PRIOR, J. O., FACTA, A. D., SOLZBACH, U., JUST, H. & SCHELBERT, H. R. 2004. Chronic inflammation and impaired coronary vasoreactivity in patients with coronary risk factors. *Circulation,* 110**,** 1069-75.

SCHOENHAGEN, P., VINCE, D. G., ZIADA, K. M., KAPADIA, S. R., LAUER, M. A., CROWE, T. D., NISSEN, S. E. & TUZCU, E. M. 2002. Relation of matrix-metalloproteinase 3 found in coronary lesion samples retrieved by directional coronary atherectomy to intravascular ultrasound observations on coronary remodeling. *Am J Cardiol,* 89**,** 1354-9.

SCHOENHAGEN, P., ZIADA, K. M., KAPADIA, S. R., CROWE, T. D., NISSEN, S. E. & TUZCU, E. M. 2000. Extent and direction of arterial remodeling in stable versus unstable coronary syndromes : an intravascular ultrasound study. *Circulation,* 101**,** 598-603.

SCHOENHAGEN, P., ZIADA, K. M., VINCE, D. G., NISSEN, S. E. & TUZCU, E. M. 2001. Arterial remodeling and coronary artery disease: the concept of "dilated" versus "obstructive" coronary atherosclerosis. *J Am Coll Cardiol,* 38**,** 297-306.

SEDDON, M., MELIKIAN, N., DWORAKOWSKI, R., SHABEEH, H., JIANG, B., BYRNE, J., CASADEI, B., CHOWIENCZYK, P. & SHAH, A. M. 2009. Effects of neuronal nitric oxide synthase on human coronary artery diameter and blood flow in vivo. *Circulation,* 119**,** 2656-62.

SERRUYS, P. W. 2010. Study of Near Infrared Spectroscopy (NIRS) and Intravascular Ultrasound (IVUS) Combination Coronary Catheter (SAVOIR) http://www.clinicaltrials.gov/ct2/show/NCT00901446.

SERRUYS, P. W., GARCIA-GARCIA, H. M., BUSZMAN, P., ERNE, P., VERHEYE, S., ASCHERMANN, M., DUCKERS, H., BLEIE, O., DUDEK, D., BOTKER, H. E., VON BIRGELEN, C., D'AMICO, D., HUTCHINSON, T., ZAMBANINI, A., MASTIK, F., VAN ES, G. A., VAN DER STEEN, A. F., VINCE, D. G., GANZ, P., HAMM, C. W., WIJNS, W. & ZALEWSKI, A. 2008. Effects of the direct lipoprotein-associated phospholipase A(2) inhibitor darapladib on human coronary atherosclerotic plaque. *Circulation,* 118**,** 1172-82.

SERRUYS, P. W., ORMISTON, J. A., ONUMA, Y., REGAR, E., GONZALO, N., GARCIA-GARCIA, H. M., NIEMAN, K., BRUINING, N., DORANGE, C., MIQUEL-HEBERT, K., VELDHOF, S., WEBSTER, M., THUESEN, L. & DUDEK, D. 2009. A bioabsorbable everolimus-eluting coronary stent system

(ABSORB): 2-year outcomes and results from multiple imaging methods. *Lancet,* 373**,** 897-910.

SHIN, E. S., GARCIA-GARCIA, H. M., LIGTHART, J. M., WITBERG, K., SCHULTZ, C., VAN DER STEEN, A. F. & SERRUYS, P. W. 2011. In vivo findings of tissue characteristics using iMap IVUS and Virtual Histology IVUS. *EuroIntervention,* 6**,** 1017-9.

SHIOMI, M., ISHIDA, T., KOBAYASHI, T., NITTA, N., SONODA, A., YAMADA, S., KOIKE, T., KUNIYOSHI, N., MURATA, K., HIRATA, K., ITO, T. & LIBBY, P. 2013. Vasospasm of Atherosclerotic Coronary Arteries Precipitates Acute Ischemic Myocardial Damage in Myocardial Infarction–Prone Strain of the Watanabe Heritable Hyperlipidemic Rabbits. *Arterioscler Thromb Vasc Biol***,** 33, 2518-2523.

SIMAITIS, A., LAUCEVICIUS, A. & JARASUNIENE, D. 2004. Contribution of risk factors to endothelial dysfunction of coronary arteries with minimal lesions. *Seminars in Cardiology,* 10**,** 33-36.

SIPAHI, I., NICHOLLS, S. J. & TUZCU, E. M. 2006. Intravascular ultrasound in the current percutaneous coronary intervention era. *Cardiol Clin,* 24**,** 163-73, v.

SLAGER, C. J., WENTZEL, J. J., SCHUURBIERS, J. C., OOMEN, J. A., KLOET, J., KRAMS, R., VON BIRGELEN, C., VAN DER GIESSEN, W. J., SERRUYS, P. W. & DE FEYTER, P. J. 2000. True 3-dimensional reconstruction of coronary arteries in patients by fusion of angiography and IVUS (ANGUS) and its quantitative validation. *Circulation,* 102**,** 511-6.

SMITS, P. C., PASTERKAMP, G., DE JAEGERE, P. P., DE FEYTER, P. J. & BORST, C. 1999. Angioscopic complex lesions are predominantly compensatory enlarged: an angioscopy and intracoronary ultrasound study. *Cardiovasc Res,* 41**,** 458-64.

SOULIS, J. V., GIANNOGLOU, G. D., CHATZIZISIS, Y. S., FARMAKIS, T. M., GIANNAKOULAS, G. A., PARCHARIDIS, G. E. & LOURIDAS, G. E. 2006. Spatial and phasic oscillation of non-Newtonian wall shear stress in human left coronary artery bifurcation: an insight to atherogenesis. *Coronary Artery Disease,* 17**,** 351-8.

STEIN, C. M., NELSON, R., DEEGAN, R., HE, H., INAGAMI, T., FRAZER, M., BADR, K. F., WOOD, M. & WOOD, A. J. 1995. Tachyphylaxis of human forearm vascular responses does not occur rapidly after exposure to isoproterenol. *Hypertension,* 25**,** 1294-300.

STEINBERG, D. 1987. Lipoproteins and the pathogenesis of atherosclerosis. *Circulation,* 76**,** 508-14.

STONE, G. W. 2009. Providing Regional Observations to Study Predictors of Events in the Coronary Tree - the PROSPECT trial. *Transcatheter Cardiovascular Therapeutics conference (San Francisco).*

STONE, G. W., MAEHARA, A., LANSKY, A. J., DE BRUYNE, B., CRISTEA, E., MINTZ, G. S., MEHRAN, R., MCPHERSON, J., FARHAT, N., MARSO, S. P., PARISE, H., TEMPLIN, B., WHITE, R., ZHANG, Z. & SERRUYS, P. W. 2011. A prospective natural-history study of coronary atherosclerosis. *N Engl J Med,* 364**,** 226-35.

STONE, P. H., COSKUN, A. U., KINLAY, S., POPMA, J. J., SONKA, M., WAHLE, A., YEGHIAZARIANS, Y., MAYNARD, C., KUNTZ, R. E. & FELDMAN, C. L. 2007. Regions of low endothelial shear stress are the sites where coronary plaque progresses and vascular remodelling occurs in humans: an in vivo serial study. *European Heart Journal,* 28**,** 705-10.

STONE, P. H., SAITO, S., TAKAHASHI, S., MAKITA, Y., NAKAMURA, S., KAWASAKI, T., TAKAHASHI, A., KATSUKI, T., NAMIKI, A., HIROHATA, A., MATSUMURA, T., YAMAZAKI, S., YOKOI, H., TANAKA, S., OTSUJI, S., YOSHIMACHI, F., HONYE, J., HARWOOD, D., REITMAN, M., COSKUN, A. U., PAPAFAKLIS, M. I. & FELDMAN, C. L. 2012. Prediction of Progression of Coronary Artery Disease and Clinical Outcomes Using Vascular Profiling of Endothelial Shear Stress and Arterial Plaque Characteristics: The PREDICTION Study. *Circulation,* 126**,** 172-181.

SUN, D., HUANG, A., MITAL, S., KICHUK, M. R., MARBOE, C. C., ADDONIZIO, L. J., MICHLER, R. E., KOLLER, A., HINTZE, T. H. & KALEY, G. 2002. Norepinephrine elicits beta2-receptor-mediated dilation of isolated human coronary arterioles. *Circulation,* 106**,** 550-5.

SUWAIDI, J. A., HAMASAKI, S., HIGANO, S. T., NISHIMURA, R. A., HOLMES, D. R., JR. & LERMAN, A. 2000. Long-term follow-up of patients with mild coronary artery disease and endothelial dysfunction. *Circulation,* 101**,** 948-54.

TAKANO, M., MIZUNO, K., OKAMATSU, K., YOKOYAMA, S., OHBA, T. & SAKAI, S. 2001a. Mechanical and structural characteristics of vulnerable

plaques: analysis by coronary angioscopy and intravascular ultrasound. *J Am Coll Cardiol,* 38**,** 99-104.

TAKANO, M., MIZUNO, K., OKAMATSU, K., YOKOYAMA, S., OHBA, T. & SAKAI, S. 2001b. Mechanical and structural characteristics of vulnerable plaques: analysis by coronary angioscopy and intravascular ultrasound. *Journal of the American College of Cardiology,* 38**,** 99-104.

TAKANO, M., MIZUNO, K., YOKOYAMA, S., SEIMIYA, K., ISHIBASHI, F., OKAMATSU, K. & UEMURA, R. 2003. Changes in coronary plaque color and morphology by lipid-lowering therapy with atorvastatin: serial evaluation by coronary angioscopy. *Journal of the American College of Cardiology,* 42**,** 680-6.

TAKARADA, S., IMANISHI, T., KUBO, T., TANIMOTO, T., KITABATA, H., NAKAMURA, N., TANAKA, A., MIZUKOSHI, M. & AKASAKA, T. 2009. Effect of statin therapy on coronary fibrous-cap thickness in patients with acute coronary syndrome: assessment by optical coherence tomography study. *Atherosclerosis,* 202**,** 491-7.

TANAKA, A., IMANISHI, T., KITABATA, H., KUBO, T., TAKARADA, S., TANIMOTO, T., KUROI, A., TSUJIOKA, H., IKEJIMA, H., UENO, S., KATAIWA, H., OKOUCHI, K., KASHIWAGHI, M., MATSUMOTO, H., TAKEMOTO, K., NAKAMURA, N., HIRATA, K., MIZUKOSHI, M. & AKASAKA, T. 2008. Morphology of exertion-triggered plaque rupture in patients with acute coronary syndrome: an optical coherence tomography study. *Circulation,* 118**,** 2368-73.

TARDIF, J. C., GREGOIRE, J., L'ALLIER, P. L., ANDERSON, T. J., BERTRAND, O., REEVES, F., TITLE, L. M., ALFONSO, F., SCHAMPAERT, E., HASSAN, A., MCLAIN, R., PRESSLER, M. L., IBRAHIM, R., LESPERANCE, J., BLUE, J., HEINONEN, T. & RODES-CABAU, J. 2004. Effects of the acyl coenzyme A:cholesterol acyltransferase inhibitor avasimibe on human atherosclerotic lesions. *Circulation,* 110**,** 3372-7.

TARDIF, J. C., GREGOIRE, J., L'ALLIER, P. L., IBRAHIM, R., LESPERANCE, J., HEINONEN, T. M., KOUZ, S., BERRY, C., BASSER, R., LAVOIE, M. A., GUERTIN, M. C. & RODES-CABAU, J. 2007. Effects of reconstituted high-density lipoprotein infusions on coronary atherosclerosis: a randomized controlled trial. *JAMA,* 297**,** 1675-82.

TEARNEY, G. J., YABUSHITA, H., HOUSER, S. L., ARETZ, H. T., JANG, I. K., SCHLENDORF, K. H., KAUFFMAN, C. R., SHISHKOV, M., HALPERN, E. F. & BOUMA, B. E. 2003. Quantification of macrophage content in atherosclerotic plaques by optical coherence tomography. *Circulation,* 107**,** 113-9.

THIEME, T., WERNECKE, K. D., MEYER, R., BRANDENSTEIN, E., HABEDANK, D., HINZ, A., FELIX, S. B., BAUMANN, G. & KLEBER, F. X. 1996. Angioscopic evaluation of atherosclerotic plaques: validation by histomorphologic analysis and association with stable and unstable coronary syndromes. *J Am Coll Cardiol,* 28**,** 1-6.

THIM, T., HAGENSEN, M. K., WALLACE-BRADLEY, D., GRANADA, J. F., KALUZA, G. L., DROUET, L., PAASKE, W. P., BOTKER, H. E. & FALK, E.

2010. Unreliable assessment of necrotic core by virtual histology intravascular ultrasound in porcine coronary artery disease. *Circ Cardiovasc Imaging,* 3**,** 384-91.

TOMAI, F., CREA, F., GASPARDONE, A., VERSACI, F., GHINI, A. S., CHIARIELLO, L. & GIOFFRE, P. A. 2001. Unstable angina and elevated c-reactive protein levels predict enhanced vasoreactivity of the culprit lesion. *Circulation,* 104**,** 1471-6.

TOPOL, E. J. & NISSEN, S. E. 1995. Our preoccupation with coronary luminology. The dissociation between clinical and angiographic findings in ischemic heart disease. *Circulation,* 92**,** 2333-42.

TOUSOULIS, D., DAVIES, G., LEFROY, D. C., HAIDER, A. W. & CRAKE, T. 1996. Variable coronary vasomotor responses to acetylcholine in patients with normal coronary arteriograms: evidence for localised endothelial dysfunction. *Heart,* 75**,** 261-6.

TOUTOUZAS, K., KARANASOS, A., RIGA, M., TSIAMIS, E., SYNETOS, A., MICHELONGONA, A., PAPANIKOLAOU, A., TRIANTAFYLLOU, G., TSIOUFIS, C. & STEFANADIS, C. 2012. Optical coherence tomography assessment of the spatial distribution of culprit ruptured plaques and thin-cap fibroatheromas in acute coronary syndrome. *EuroIntervention,* 8**,** 477-85.

TOYOSHIMA, H., NASA, Y., HASHIZUME, Y., KOSEKI, Y., ISAYAMA, Y., KOHSAKA, Y., YAMADA, T. & TAKEO, S. 1998. Modulation of cAMP-mediated vasorelaxation by endothelial nitric oxide and basal cGMP in vascular smooth muscle. *J Cardiovasc Pharmacol,* 32**,** 543-51.

TSUCHIDA, K., VAN DER GIESSEN, W. J., PATTERSON, M., TANIMOTO, S., GARCIA-GARCIA, H. M., REGAR, E., LIGTHART, J. M., MAUGENEST, A. M., MAATRIJK, G., WENTZEL, J. J. & SERRUYS, P. W. 2007. In vivo validation of a novel three-dimensional quantitative coronary angiography system (CardiOp-B): comparison with a conventional two-dimensional system (CAAS II) and with special reference to optical coherence tomography. *EuroIntervention,* 3**,** 100-8.

TU, S., HUANG, Z., KONING, G., CUI, K. & REIBER, J. H. A novel three-dimensional quantitative coronary angiography system: In-vivo comparison with intravascular ultrasound for assessing arterial segment length. *Catheter Cardiovasc Interv,* 76**,** 291-8.

TU, S., JING, J., HOLM, N. R., ONSEA, K., ZHANG, T., ADRIAENSSENS, T., DUBOIS, C., DESMET, W., THUESEN, L., CHEN, Y. & REIBER, J. H. 2012. In vivo assessment of bifurcation optimal viewing angles and bifurcation angles by three-dimensional (3D) quantitative coronary angiography. *Int J Cardiovasc Imaging,* 28**,** 1617-25.

UEDA, Y., OHTANI, T., SHIMIZU, M., HIRAYAMA, A. & KODAMA, K. 2004. Assessment of plaque vulnerability by angioscopic classification of plaque color. *American Heart Journal,* 148**,** 333-5.

VAN'T VEER, M., PIJLS, N. H., AARNOUDSE, W., KOOLEN, J. J. & VAN DE VOSSE, F. N. 2006. Evaluation of the haemodynamic characteristics of drug-eluting stents at implantation and at follow-up. *European Heart Journal,* 27**,** 1811-7.

VAN MIEGHEM, C. A., MCFADDEN, E. P., DE FEYTER, P. J., BRUINING, N., SCHAAR, J. A., MOLLET, N. R., CADEMARTIRI, F., GOEDHART, D., DE WINTER, S., GRANILLO, G. R., VALGIMIGLI, M., MASTIK, F., VAN DER STEEN, A. F., VAN DER GIESSEN, W. J., SIANOS, G., BACKX, B., MOREL, M. A., VAN ES, G. A., ZALEWSKI, A. & SERRUYS, P. W. 2006. Noninvasive detection of subclinical coronary atherosclerosis coupled with assessment of changes in plaque characteristics using novel invasive imaging modalities: the Integrated Biomarker and Imaging Study (IBIS). *J Am Coll Cardiol,* 47**,** 1134-42.

VAN SOEST, G., REGAR, E., GODERIE, T. P., GONZALO, N., KOLJENOVIC, S., VAN LEENDERS, G. J., SERRUYS, P. W. & VAN DER STEEN, A. F. 2011. Pitfalls in plaque characterization by OCT: image artifacts in native coronary arteries. *JACC. Cardiovascular imaging,* 4**,** 810-3.

VARNAVA, A. M., MILLS, P. G. & DAVIES, M. J. 2002. Relationship between coronary artery remodeling and plaque vulnerability. *Circulation,* 105**,** 939-43.

VAVURANAKIS, M., KAKADIARIS, I. A., O'MALLEY, S. M., PAPAIOANNOU, T. G., SANIDAS, E. A., NAGHAVI, M., CARLIER, S., TOUSOULIS, D. & STEFANADIS, C. 2008. A new method for assessment of plaque vulnerability based on vasa vasorum imaging, by using contrast-enhanced intravascular ultrasound and differential image analysis. *Int J Cardiol,* 130**,** 23-9.

VERHEYE, S., DE MEYER, G. R., KRAMS, R., KOCKX, M. M., VAN DAMME, L. C., MOUSAVI GOURABI, B., KNAAPEN, M. W., VAN LANGENHOVE, G.

& SERRUYS, P. W. 2004. Intravascular thermography: Immediate functional and morphological vascular findings. *Eur Heart J,* 25**,** 158-65.

VERHEYE, S., DE MEYER, G. R., VAN LANGENHOVE, G., KNAAPEN, M. W. & KOCKX, M. M. 2002. In vivo temperature heterogeneity of atherosclerotic plaques is determined by plaque composition. *Circulation,* 105**,** 1596-601.

VITA, J. A., TREASURE, C. B., NABEL, E. G., MCLENACHAN, J. M., FISH, R. D., YEUNG, A. C., VEKSHTEIN, V. I., SELWYN, A. P. & GANZ, P. 1990. Coronary vasomotor response to acetylcholine relates to risk factors for coronary artery disease. *Circulation,* 81**,** 491-7.

VON BIRGELEN, C., HARTMANN, M., MINTZ, G. S., BAUMGART, D., SCHMERMUND, A. & ERBEL, R. 2003. Relation between progression and regression of atherosclerotic left main coronary artery disease and serum cholesterol levels as assessed with serial long-term (> or =12 months) follow-up intravascular ultrasound. *Circulation,* 108**,** 2757-62.

VON BIRGELEN, C., KUTRYK, M. J., GIL, R., OZAKI, Y., DI MARIO, C., ROELANDT, J. R., DE FEYTER, P. J. & SERRUYS, P. W. 1996. Quantification of the minimal luminal cross-sectional area after coronary stenting by two- and three-dimensional intravascular ultrasound versus edge detection and videodensitometry. *Am J Cardiol,* 78**,** 520-5.

VORPAHL, M., NAKANO, M. & VIRMANI, R. 2010. Small black holes in optical frequency domain imaging matches intravascular neoangiogenesis formation in histology. *Eur Heart J,* 31**,** 1889.

WAKABAYASHI, K., SUZUKI, H., HONDA, Y., WAKATSUKI, D., KAWACHI, K., OTA, K., KOBA, S., SHIMIZU, N., ASANO, F., SATO, T. & TAKEYAMA, Y. 2008. Provoked coronary spasm predicts adverse outcome in patients with acute myocardial infarction: a novel predictor of prognosis after acute myocardial infarction. *J Am Coll Cardiol,* 52**,** 518-22.

WAKSMAN, R., TORGUSON, R., KENT, K. M., PICHARD, A. D., SUDDATH, W. O., SATLER, L. F., MARTIN, B. D., PERLMAN, T. J., MALTAIS, J. A., WEISSMAN, N. J., FITZGERALD, P. J. & BREWER, H. B., JR. 2010. A first-in-man, randomized, placebo-controlled study to evaluate the safety and feasibility of autologous delipidated high-density lipoprotein plasma infusions in patients with acute coronary syndrome. *J Am Coll Cardiol,* 55**,** 2727-35.

WAXMAN, S., DIXON, S. R., L'ALLIER, P., MOSES, J. W., PETERSEN, J. L., CUTLIP, D., TARDIF, J. C., NESTO, R. W., MULLER, J. E., HENDRICKS, M. J., SUM, S. T., GARDNER, C. M., GOLDSTEIN, J. A., STONE, G. W. & KRUCOFF, M. W. 2009. In vivo validation of a catheter-based near-infrared spectroscopy system for detection of lipid core coronary plaques: initial results of the SPECTACL study. *JACC Cardiovasc Imaging,* 2**,** 858-68.

WENTZEL, J. J., KRAMS, R., SCHUURBIERS, J. C., OOMEN, J. A., KLOET, J., VAN DER GIESSEN, W. J., SERRUYS, P. W. & SLAGER, C. J. 2001. Relationship between neointimal thickness and shear stress after Wallstent implantation in human coronary arteries. *Circulation,* 103**,** 1740-5.

WHALEN, E. J., JOHNSON, A. K. & LEWIS, S. J. 2000. Beta-adrenoceptor dysfunction after inhibition of NO synthesis. *Hypertension,* 36**,** 376-82.

WICKLINE SA, M. J., RECCHIA D 1994. Beyond intravascular imaging: Quantitative ultrasonic tissue characterization of vascular pathology. *IEEE Ultrasonics Symp,* 3**,** 1589-1597.

WILKINSON, I. B., HALL, I. R., MACCALLUM, H., MACKENZIE, I. S., MCENIERY, C. M., VAN DER AREND, B. J., SHU, Y. E., MACKAY, L. S., WEBB, D. J. & COCKCROFT, J. R. 2002. Pulse-wave analysis: clinical evaluation of a noninvasive, widely applicable method for assessing endothelial function. *Arterioscler Thromb Vasc Biol,* 22**,** 147-52.

WILLIAMS, K. J. & TABAS, I. 1995. The response-to-retention hypothesis of early atherogenesis. *Arterioscler Thromb Vasc Biol,* 15**,** 551-61.

YAMAGUCHI, T., TERASHIMA, M., AKASAKA, T., HAYASHI, T., MIZUNO, K., MURAMATSU, T., NAKAMURA, M., NAKAMURA, S., SAITO, S., TAKANO, M., TAKAYAMA, T., YOSHIKAWA, J. & SUZUKI, T. 2008. Safety and feasibility of an intravascular optical coherence tomography image wire system in the clinical setting. *Am J Cardiol,* 101**,** 562-7.

YEUNG, A. C., VEKSHTEIN, V. I., KRANTZ, D. S., VITA, J. A., RYAN, T. J., JR., GANZ, P. & SELWYN, A. P. 1991. The effect of atherosclerosis on the vasomotor response of coronary arteries to mental stress. *N Engl J Med,* 325**,** 1551-6.

YOON, M. H., RERIANI, M., MARIO, G., RIHAL, C., GULATI, R., LENNON, R., TILFORD, J. M., LERMAN, L. O. & LERMAN, A. 2013. Long-term endothelin receptor antagonism attenuates coronary plaque progression in patients with early atherosclerosis. *Int J Cardiol,* 168**,** 1316-21.

YUAN, S., RONEY, C. A., WIERWILLE, J., CHEN, C. W., XU, B., GRIFFITHS, G., JIANG, J., MA, H., CABLE, A., SUMMERS, R. M. & CHEN, Y. 2010. Co-registered optical coherence tomography and fluorescence molecular imaging for simultaneous morphological and molecular imaging. *Phys Med Biol,* 55**,** 191-206.

ZEIHER, A. M., DREXLER, H., WOLLSCHLAEGER, H., SAURBIER, B. & JUST, H. 1989. Coronary vasomotion in response to sympathetic stimulation in humans: importance of the functional integrity of the endothelium. *J Am Coll Cardiol,* 14**,** 1181-90.

ZEIHER, A. M., DREXLER, H., WOLLSCHLAGER, H. & JUST, H. 1991a. Endothelial dysfunction of the coronary microvasculature is associated with coronary blood flow regulation in patients with early atherosclerosis. *Circulation,* 84**,** 1984-92.

ZEIHER, A. M., DREXLER, H., WOLLSCHLAGER, H. & JUST, H. 1991b. Modulation of coronary vasomotor tone in humans. Progressive endothelial dysfunction with different early stages of coronary atherosclerosis. *Circulation,* 83**,** 391-401.

ZEIHER, A. M., GOEBEL, H., SCHACHINGER, V. & IHLING, C. 1995. Tissue endothelin-1 immunoreactivity in the active coronary atherosclerotic plaque. A clue to the mechanism of increased vasoreactivity of the culprit lesion in unstable angina. *Circulation,* 91**,** 941-7.

ZEIHER, A. M., SCHACHLINGER, V., HOHNLOSER, S. H., SAURBIER, B. & JUST, H. 1994. Coronary atherosclerotic wall thickening and vascular reactivity

in humans. Elevated high-density lipoprotein levels ameliorate abnormal vasoconstriction in early atherosclerosis. *Circulation,* 89**,** 2525-32.

ZHANG, Y., FAROOQ, V., GARCIA-GARCIA, H. M., BOURANTAS, C. V., TIAN, N., DONG, S., LI, M., YANG, S., SERRUYS, P. W. & CHEN, S. L. 2012. Comparison of intravascular ultrasound versus angiography-guided drug-eluting stent implantation: a meta-analysis of one randomised trial and ten observational studies involving 19,619 patients. *EuroIntervention,* 8**,** 855-65.